DEVELOPMENT AND APPLICATION OF CHEMICALLY MODIFIED ELECTRODES FOR ANALYSIS

A thesis

Submitted for the degree

of

Doctor of Philosophy in Chemistry

at the

University of Canterbury

By

Shuanghua Xu

1992

To my wife, parents and family

Acknowledgements

My sincere and grateful thanks are extended to my supervisors, Dr. H. K. J. Powell and Dr. A. J. Downard, for their supervision, support, enthusiasm, knowledge, and guidance throughout this period of study. I also thank Dr. C. Freeman for his kind help in my study.

I would like to thank the academic staff and technical staff of the Chemistry Department of the University for their help and assistance.

I wish to express my thanks to my fellow students, James, Jane and Alisa, for helpful discussions and advice, particularly on the computational aspect of this work.

Special thanks are also due to Kip, Alison, David and Wendy due to kind donations of blood samples for Mg determination in my research.

The New Zealand University Grants Committee is especially thanked for the award of a Post-Graduate Scholarship.

Finally, my thanks go to my wife, parents and family for all their help, encouragement and support.

CONTENTS

CHAPTER TWO: EXPERIMENTAL

CHAPTER THREE: VOLTAMMETRIC METHODS USING POLYMER MODIFIED ELECTRODES

CHAPTER FOUR: VOLTAMMETRIC METHODS USING DIP COATING ELECTRODES

CHAPTER FIVE: VOLTAMMETRIC METHODS USING CHEMICALLY MODIFIED GRAPHITE POWDER ELECTRODES

ABSTRACT

This thesis presents a study on development and application of chemically modified electrodes (CMEs) for analysis, especially for analysis of aluminium(III). A parallel study involved flow injection analysis with indirect amperometric detection.

The electrochemistry was studied for several electroactive ligands which bind strongly to aluminium(III). The effect of pH on redox behaviour was investigated. The complex formation between aluminium(III) and these ligands was examined under different conditions such as pH, electrolyte and temperature. For quantitative determination of aluminium(III), either the increase in peak height due to the redox processes of the formed aluminium(III)-ligand complex, or the decrease of the peak height for free ligand redox processes, was used.

Several CMEs were prepared using polymer coatings, chemisorption and by mixing ligand into the electrode material.

The use of CMEs consisting of charged polymers for preconcentration of analytes was investigated. The accumulation of aluminium(III) in polyxylylviologen coated electrodes as anionic phenolic complexes was studied. The measurement of aluminium(III)-(4-nitrocatechol) complexes which have an overall negative charge resulted in a sensitive method for analysis of aluminium(III).

A 1,2-dihydroxyanthraquinone(alizarin)-modified graphite electrode was used in the voltammetric determination of aluminium(III). Alizarin was immobilised on a solid electrode by chemisorption. The electrode was applied in determination of

exchangeable aluminium(III) in soils. This provided a simple, rapid method for monitoring aluminium in the environment.

Ligands mixed into electrode materials (carbon paste and graphite epoxy) were studied. Graphite epoxy modified with 4-nitrocatechol showed good results for the determination of aluminium(III).

In CME studies, it was found that the loss of ligand from CMEs due to irreversible oxidation of ligand and other reasons limits electrodes to single-use.

The method for determination of aluminium(III) by adsorptive stripping voltammetry of its SVRS complex was modified by room temperature reaction at a higher pH, followed by accumulation in acidified solution. This method provided good results with high sensitivity and reproducibility and significantly shorter analysis time.

Aluminium(III) was determined in a flow injection system involving the formation of the aluminium(III)-1,2-dihydroxyanthraquinone-3-sulphonic acid (DASA) complex and amperometric measurement of excess DASA at +0.50 V on a gold electrode. Electrode fouling by adsorption of ligand oxidation products was minimized by use of a double pumping system and cathodic/anodic voltage cycling. The method was applied to soil extracts.

A simple flow system for magnesium(II) determination in natural waters and serum was developed. This involved complexation of magnesium(II) with the redox active ligand eriochrome black T (EBT). Analysis of human blood serum samples was effected by two methods: (1) direct injection of serum after dilution and (2) after dialysis to effect separation of magnesium(II) from acidified serum in the flow system. Electrode fouling by adsorption of EBT oxidation products and

serum in the flow system was minimized by use of several surfactants and a dialyzer.

CHAPTER ONE

INTRODUCTION

1.1. ENVIRONMENTAL SIGNIFICANCE OF ALUMINIUM

Aluminium is the most abundant metallic element in the earth's crust and is widely distributed; it accounts for approximately 8.8% of the total crustal mass. It is found in all soils and natural waters, and is present in biological systems.

In the past decade, the importance of aluminium and its biological impact on man and his environment has become more and more apparent. Aluminium is not considered an essential trace element for animal life. Yet, it is an important element in that a large number of artifacts to which humans are exposed are made of aluminium metal. Also great quantities of aluminium compounds are consumed or used by the population for various clinical or cosmetic purposes.

With widespread public interest in the effects of acidic deposition on terrestrial ecosystems, the chemistry of aluminium in soils and natural waters has emerged as a scientific problem of critical importance. Chemists, especially environmental chemists, have responded to this public concern. Recently, a marked increase in the geochemical mobility of aluminium has been noted in many watersheds affected by acid precipitation.

Interest in a possible biological function of aluminium continues to increase. The question has been raised whether aluminium is retained in the body in amounts significant enough to result in toxicity. It was initially assumed that aluminium is not harmful because it is an

abundant element and largely present in non-reactive forms. But this reasoning is not necessarily valid since silicon is also an abundant element yet silicosis is a serious disease[1]. Now people have a greater understanding of this problem. It has been realized that there are several main effects arising from aluminium in our environment[2].

1.1.1. Effects of aluminium on plants

It has long been recognized that toxicity of aluminium to plants is a major growth-limiting factor in acid soils. In strongly acidic soils aluminium toxicity may decrease plant growth simply because aluminosilicate or aluminium oxide solubility increases markedly as the pH decreases. Root growth into the more acid subsoil materials is inhibited by both physical and chemical factors. The chemical factor most responsible for poor root growth has been identified as excess soluble aluminium[3]. When plants suffer aluminium toxicity, the first measurable effect is generally a reduced root growth. The signs first appear in the tip of the main roots where cell division and elongation are restricted. Root tips turn brown, become stunted and sometimes necrotic[4]. After these effects the colour of the lower leaves turns yellow and finally reddish-brown, however the growth inhibition is most marked in roots[5].

It is found that aluminium can also accumulate in plant tissue. Aluminium taken up by roots is mainly retained in the mucilage layer on the root tip surface[6] and in the walls of the epidermis and cortex cells[7]. The root cells, and the mucilage produced by them, have a high cation exchange capacity and would readily immobilize cationic species. However once these sites are blocked, and providing there is no physical hindrance, this would pave the way for subsequent species (Al^{3+}) to find their way to the meristematic cells. For example,

aluminium is rapidly and strongly adsorbed by barley roots and cell walls[8]; mitotic inhibition is complete within 6 to 8 hours[9].

1.1.2. Effects of aluminium on fish

An increased level of aluminium in acidified natural waters is a primary cause of fish death from damage to gill epithelia and loss of osmoregulatory capacity. It is realized that as in animals, aluminium seems to have its primary effect on enzyme systems important for the uptake of nutrients. Now it is known that in acidic water (pH 4.6 - 5.3) low levels of labile aluminium (between 25-75 μg/L) are toxic[10]. Also aluminium toxicity depends on both the aluminium concentration and the aqueous aluminium species that prevail. For various life stages and species of fresh water fish survival is correlated inversely with the concentration of labile (inorganic) monomeric aluminium and with pH[11].

An aluminium-induced ion loss (Na^+, K^+) reflects both an increased outflux and a decreased influx of ions. The effect on influx is probably caused by a reduced activity of gill enzymes. The effect on outflux is considered to reflect modifications on opening of the tight junctions of the paracellular channels. The ameliorating effect of calcium on aluminium response is by tightening of the junctions, thereby preventing the passive loss of ions.

Fish exposed to acidic aluminium-rich waters will accumulate aluminium on the gill surface[11]. The precipitation and accumulation is due to the negative charge of the mucus caused by sialic acid residues. The gill also serves as an excretion organ for ammonium (NH_4^+). At low pH and high aluminium concentrations, the reduced blood pH (acidosis) and increased CO_2 levels (hypercapnia) will interfere with the formation of ammonia from ammonium; thus more is excreted as

NH_4^+. At the interface between mucus and water, the ammonium will be transformed to ammonia, changing the pH and thus enhancing precipitation of aluminium at the gill surface.

Increased mucus layer will serve to increase the diffusion distance for O_2 and CO_2 between the water and blood. This can lead to a decreased oxygen tension in the arterial blood, reduced hemoglobin oxygenation and pH, and an increased blood CO_2 and blood lactate. At low pH, the increased mucus layer will reduce the rate of ion loss. At high concentrations of H^+ and aluminium, the primary cause of mortality might thus be respiratory rather than osmoregulatory failure[12].

1.1.3. Effects of aluminium on human and terrestrial animals

From medical research it is known that under certain conditions aluminium causes severe disturbance, especially in the mineral balance and nervous system, mostly in connection with renal failure. In the last decade an increasing number of human as well as animal studies have been conducted, both *in vivo* and *in vitro*, and these reveal several physiological and biochemical implications of aluminium[13].

Aluminium in water has received increased attention, not only in relation to toxicity to aqueous organisms but also in relation to drinking water and health. There has been increasing evidence in recent years indicating that aluminium is involved in human metabolism and disease. Aluminium plays an important role in encephalopathy[14], renal diseases and osteodystrophy[15] observed in patients treated by haemodialysis. It has been established that if aluminium is present in dialyzing water used for patients with renal failure, it may penetrate into the blood and accumulate in the bone tissue and brain. In the latter case the resulting encephalopathy bears a strong resemblence to Alzheimer's disease.

It has also been reported that intake of aluminium-containing antacids in combination with citric acid enhances aluminium-uptake due to the formation of lipid soluble $[Al(citrate)]^0$ in the gut. The findings of Nyholm indicate that increased aluminium concentrations in streams and waters may cause aluminium accumulation in terrestrial animals eating prey originated from contaminated water[16].

It is discovered that aluminium in the brain is localised in neurons bearing neurofibrillary tangles and as aluminosilicates at the core of senile plaques. It is reported that the aluminium content in spinal cord and brain, as well as the pathological changes, are comparable to those from human and animal studies where aluminium has been associated with disorders in the central nervous system. The neurons with aluminium accumulation in dense tangles and interactions with several biochemical reactions, have been well documented from both human and animal studies.

The complex mechanism by which aluminium induces osteomalecia is not yet fully understood. The presence of aluminium in bone marrow is associated with reduced apatite deposition. Both from *in vivo* and *in vitro* studies aluminium is reported to accumulate in the calcification front of bones, inhibiting calcium phosphate precipitation by some physical chemical action. Aluminium may also interfere with biochemical reactions as well as cell reactions important in the mineralisation processes[17].

Two types of mechanism are generally responsible for reducing exposure to risk of aluminium toxicity in biological systems. The first of these is a series of adaptations which prevent aluminium from passing outer cell barriers, and the second makes use of high-affinity macromolecular binding which renders the metal biologically unavailable[18].

1.2. COMPLEX FORMATION BY ALUMINIUM(III)

The aqueous aluminium ion is the "hardest" of the trivalent ions commonly found in biological systems and the environment. Its effective ionic radius of 0.54 Å is considerably smaller than for other commonly encountered trivalent metal ions such as Fe^{3+} (0.64 Å). The free aqueous aluminium ion, Al^{3+}, is coordinated by six water molecules in an octahedral configuration and can be represented by the formula $Al(H_2O)_6^{3+}$.

Because of its small ionic radius, aluminium polarizes solvated water molecules very strongly, giving rise to several hydrolytic species (hydroxo complexes) such as the monomers $Al(OH)_2^+$ and $AlOH^{2+}$, and a series of polymers. These monomers and Al^{3+} have generally been regarded as the toxic forms of aluminium in aqueous systems.

Donor groups which are effective in binding aluminium in aqueous solution include F^-, oxyanions, and organic ligands containing -COOH, alkyl-OH and aryl-OH groupings. These donors all compete effectively with hydroxide ion in neutral or weakly acid solution. Aluminium fluoro, sulphato, phosphato and organic complexes are described here.

1.2.1. Inorganic ligands

Fluoro complexes

The fluoride ion is small and isoelectronic with OH^-. The binding of fluoride to aluminium while quite strong, is however considerably weaker than that of hydroxide ion. This difference is due to the polarity of the hydroxide ion, whereby its negative charge is directed toward the electron acceptor, whereas the fluoride ion is symmetrical. Thus

the metal ion sees less negative charge density with fluoride binding than it does with hydroxide coordination. However it forms inner-sphere complexes with the aluminium ion in weakly acidic solution up to the maximum of octahedral coordination (AlF_6^{3-}). The fluoro and hydroxo complexes represent the strongest inorganic ion associations with aluminium in natural waters. The aqueous fluoride stability constants are shown in Table 1.1.

Sulphato complexes

Although the complexing of aluminium with sulphate is significantly weaker than with fluoride, it is strong enough to have an effect on conductance and spectroscopic measurements of aluminium sulphate solutions. Aluminium-sulphate associations have been reported as ion pairs, outer-sphere complexes, and inner-sphere complexes. Such variable speciation is a common characteristic for many aqueous polyvalent metal-sulphate associations. The distribution of these three forms is strongly temperature-dependent[19]. Table 1.1 gives the equilibrium constants of these complexes.

Phosphato complexes

Aqueous systems involving aluminium-phosphate interactions are notoriously difficult to characterize experimentally because of low solubility of aluminium phosphates; as a result complex formation has not often been studied. Langmuir[20] investigated these reactions:

$$Al^{3+} + H_2PO_4^- = AlH_2PO_4^{2+} \qquad \text{and}$$

$$Al^{3+} + HPO_4^{2-} = AlHPO_4^+$$

and obtained stability constant values (log K) of 3.1 and 7.4, respectively.

Table 1.1 Fluoro[21] and sulphato[22] reactions of aluminium

Reaction No.	Equilibrium Reaction	log β
1	$Al^{3+} + F^- = AlF^{2+}$	7.01
2	$Al^{3+} + 2\ F^- = AlF_2^+$	12.75
3	$Al^{3+} + 3\ F^- = AlF_3^0$	17.02
4	$Al^{3+} + 4\ F^- = AlF_4^-$	19.72
5	$Al^{3+} + 5\ F^- = AlF_5^{2-}$	20.91
6	$Al^{3+} + 6\ F^- = AlF_6^{3-}$	20.86
7	$Al^{3+} + SO_4^{2-} = AlSO_4^+$	3.20
8	$Al^{3+} + 2\ SO_4^{2-} = Al(SO_4)_2^-$	5.10
9	$2\ Al^{3+} + 3\ SO_4^{2-} = Al_2(SO_4)_3^0$	-1.88

1.2.2. Organic ligands

Organically complexed forms of aluminium are generally thought to have little phytotoxicity. Many organic ligands have sufficient affinity for aluminium to form complexes stable enough to (i) resist aluminium's strong hydrolytic tendencies and (ii) exist at high dilution in environmental systems. These ligands are generally multidentate and contain arrangements of several donor groups involving hard oxygen donors.

Aluminium complexation occurs predominantly with oxygen-containing functional groups; ligands containing nitrogen donors

generally form weak complexes with aluminium. Hence the ligands which will be important in governing aluminium speciation are those containing carboxyl (aliphatic or aromatic) and hydroxyl groups (either phenolic, enolic, or aliphatic).

The following are some of the groups which are most frequently present in organic ligands found to be effective in binding aluminium in aqueous solution. They are presented in order of decreasing "hardness", which is also the order of decreasing metal ion affinity. The numerical values indicate the approximate log β for proton dissociation

Monodentate donor groups:

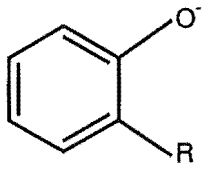

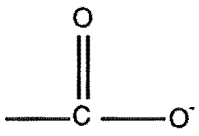

Alkoxide > - 14 Phenoxide - 12 Carboxylate - 4

The following are some of the more frequently encountered bidentate moieties containing these oxygen donor groups. They are found in both natural and synthetic ligands which are effective for aluminium complexation.

Bidentate combinations:

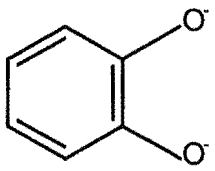

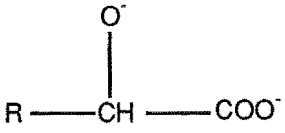

Catecholate - 22 Hydroxy carboxylic acid - 18

Two main groups of ligands, carboxyl and phenolic, are effective complexors in different pH ranges. The $-COO^-$ group is less basic and forms less stable complexes; complex formation dominates at low pH, with OH- substitution occurring around neutral pH. In contrast the more basic phenolate group competes more strongly against OH^- but remains protonated at low pH. The latter is effective in more basic solution.

Several groups of ligands based on these structural units have widespread use in analytical chemistry. For example; catecholates: 1,2-dihydroxy-anthraquinone-3-sulphonic acid (DASA) and alizarin; polycarboxylic acids: citric acid; diphenol-azo: solochrome violet RS (SVRS), pyrocatechol violet (PCV); mixed phenol-carboxylic: salicylic acid, chrome azurol S (CAS).

Table 1.2 contains examples of equilibrium constants for formation of the aluminium complexes of ligands with the functional groups of interest. A variety of ligands is selected so that the complexes listed represent a considerable variation of structural types and a wide range of stabilities.

The stability constants given correspond to reaction of the aquo metal ion with the most basic form of the ligand as indicated by equation (1):

$$Al^{3+} + mL^{n-} = AlL_m^{(3-mn)+} \qquad (1)$$

for m=1 $$K_1 = \frac{[AlL^{(3-n)+}]}{[Al^{3+}]\,[L^{n-}]}$$

for m>1 $$\beta_m = \frac{[AlL_m^{(3-mn)+}]}{[Al^{3+}]\,[L^{n-}]^m}$$

Table 1.2 Aluminium-organic formation constants[23]

ligands	log K(or log β)
I. Monocarboxylic Acids	
Methanoic acid, HCO_2H	
K_1	0.56
β2	1.76
II. Dicarboxylic Acids	
Ethanedioic acid (oxalic acid),	
K_1	6.1
β2	11.1
β3	15.1
III. Tricarboxylic Acids	
2-Hydroxypropane-1,2,3-tricarboxylic acid (citric acid),	
K_1	7.98
$ML = M(H_{-1}L) + H$	-3.31
$M(H_{-1}L) = M(OH)(H_{-1}L) + H$	-6.23
$3\ M + 3\ L = M_3(OH)(H_{-1}L)_3 + 4\ H^+$	14.43
IV. Monohydroxy Phenols	
2-Hydroxybenzoic acid (salicylic acid),	
K_1	14.5
β2	23.2
β3	29.8

V. Dihydroxy phenols

1,2-Dihydroxybenzene (catechol),

K_1	16.1
β2	29.1
β3	37.8

VI. Trihydroxy phenols

1,2,3-Trihydroxybenzene (pyrogallol),

K_1	14.3
β2	27.8
β3	39.7

VII. Azo-napthols

1-(2-hydroxy-5-sulfophenylazo)-2-napthol (solochrome violet R),

K_1	18.4
β2	31.6

VIII. Amino Acids

l-Aminobutanedioic acid (aspartic acid),

K_1	16.29
β2	30.69
β3	42.19

IX. Azine-phenol

7-Iodo-8-hydroxyquinoline-5-sulfonic acid (ferron),

K_1	7.6
β2	14.7
β3	20.3

1.3. HYDROLYSIS REACTIONS OF ALUMINIUM

Like many other cations, aluminium hydrolyses to form solutions of monomeric and polymeric hydroxide complexes. However, some of the reactions in solution are quite slow at room temperature and may involve the formation of colloidal species. Moreover, metastable precipitates can form and redissolve slowly, the character of the precipitate and the rate of these reactions depending on the precise conditions of the hydrolysis.

The identification of the stable hydrolysis products of aluminium has been difficult, not only because of slow reactions in solution and interference from transient and permanent precipitation, but also because at least one of the stable species in solution is a large polymeric ion which is difficult to characterize exactly. The mononuclear species $AlOH^{2+}$, $Al(OH)_2^+$, $Al(OH)_3^0(aq)$ and $Al(OH)_4^-$ form rapidly and reversibly. The first of these, $AlOH^{2+}$, appears above pH 3 but is dominant only in dilute solutions; the last, $Al(OH)_4^-$, is responsible for the solubility of aluminium hydroxide in alkaline solutions.

Relative molar concentrations of hydrolysed aluminium species as a function of pH and at a total analytical concentration of 1.00×10^{-6} M, are illustrated in Figure 1.1[24]. The concentration of the complex $Al(OH)_3$ is plotted as a soluble (supersaturated) complex. Equilibruim data for the stable hydrolysis products of aluminium in dilute solution are summarized in Table 1.3.

Table 1.3. Hydrolysis reactions of aluminium[25]

Reaction No.	Equilibrium Reaction	log *β
monomers		
1	$Al^{3+} + H_2O = AlOH^{2+} + H^+$	-5.02
2	$Al^{3+} + 2\ H_2O = Al(OH)_2^+ + 2\ H^+$	-9.30
3	$Al^{3+} + 3\ H_2O = Al(OH)_3^0 + 3\ H^+$	-14.99
4	$Al^{3+} + 4\ H_2O = Al(OH)_4^- + 4\ H^+$	-23.33
polymer		
5	$2\ Al^{3+} + 2\ H_2O = Al_2(OH)_2^{4+} + 2\ H^+$	-7.69
6	$3\ Al^{3+} + 5\ H_2O = Al_3(OH)_5^{4+} + 5\ H^+$	-13.57
7	$13\ Al^{3+} + 28\ H_2O$ $= [AlO_4Al_{12}(OH)_{24}(H_2O)_{12}]^{7+} + 32\ H^+$	-109.2

In addition to the monomers there is evidence for formation of polymers, $Al_3(OH)_4^{5+}$ and $Al_p(OH)_q$ (p ca.13), in more concentrated solution. There is strong evidence for the existence of the larger polymer. But definitive assignment of its stoichiometry is difficult because it appears in a very small pH range (5.0-5.2) in dilute solution before precipitation of $Al(OH)_3$ occurs. Least squares analyses of solution equilibrium data indicate that (p,q) values ranging from (5, 12) to (14, 34) are equally probable. However weight is given to the (13, 32) assignment, log *β = -109.2, because the $Al_{13}O_4(OH)_{24}^{7+}$ cation has been charactered by X-ray analysis of basic aluminium sulphates and selenates.

The $Al_{13}(OH)_{32}^{7+}$ species[26], sometimes written as the partially dehydrated form $Al_{13}O_4(OH)_{24}^{7+}$ (Figure. 1.2), dominates the solution equilibrium from pH 5 to 8 in more concentrated solution as indicated in Figure 1.3[24].

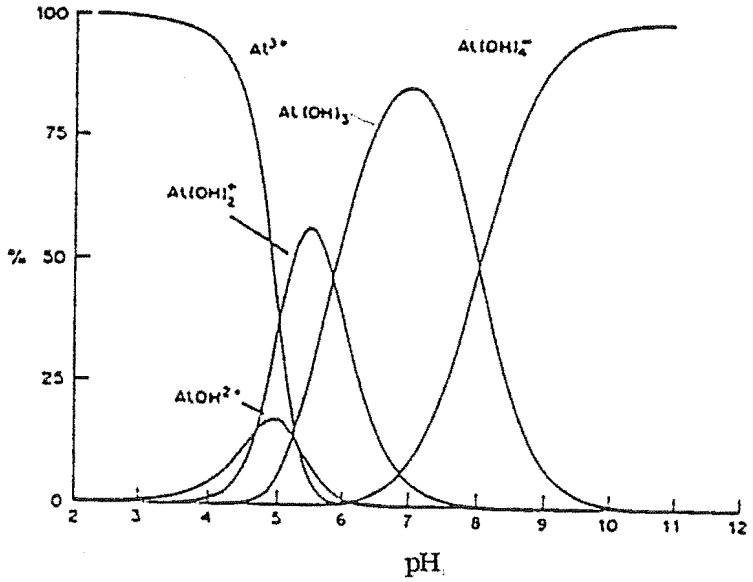

Figure 1.1 Relative molar concentrations of hydrolytic species formed from the aquo aluminium(III) ion as a function of -log [H^+]. Total analytical concentration of aluminium(III) species is 1.00×10^{-6} M. The concentration of $Al(OH)_3$ is plotted as a supersaturated solution. T = 25 °C; μ = 0.100 M.

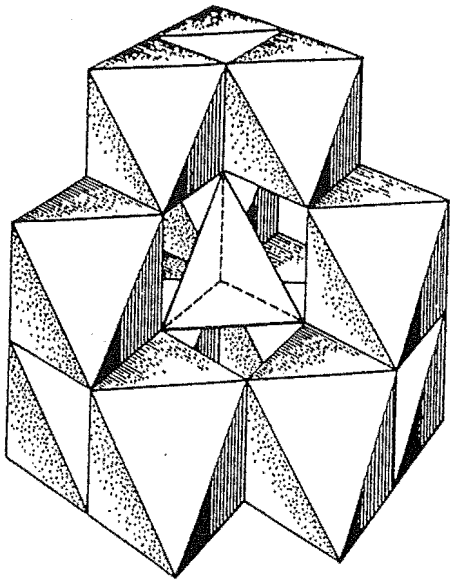

Figure 1.2 Representation of the $[AlO_4Al_{12}(OH)_{24}(H_2O)_{12}]^{7+}$ polymeric species, demonstrating the tetrahedrally coordinated aluminium at the centre of the cage-like structure comprising 12 octahedrally coordinated aluminium atoms joined by common edges.

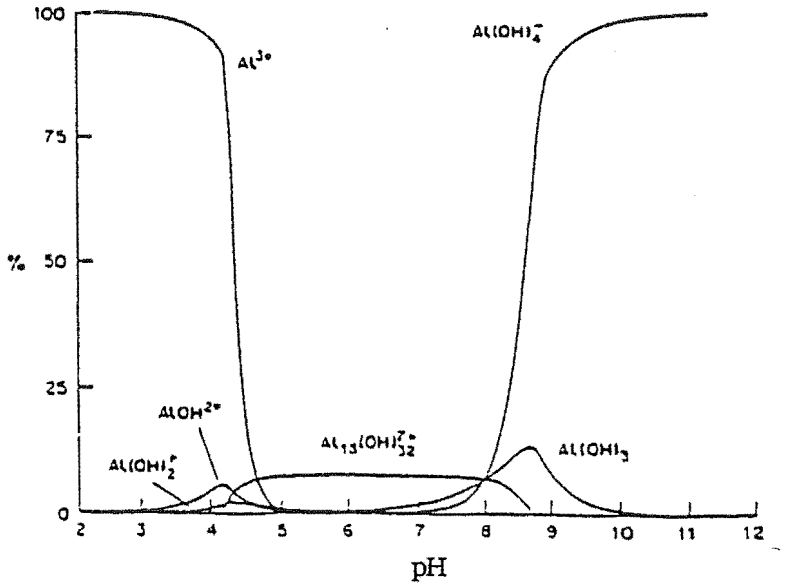

Figure 1.3 Relative molar concentrations of hydrolytic species formed from the aquo aluminium(III) ion as a function of -log $[H^+]$. Total analytical concentration of aluminium(III) species is 1.00×10^{-3} M. The molar concentration of $Al_{13}(OH)_{32}$ constitutes 98.8% of the aluminium(III) present for pH 5-8. The concentration of $Al(OH)_3$ is plotted as a supersaturated solution. T = 25 °C; μ = 0.100 M.

1.4. ELECTROCHEMISTRY OF ALUMINIUM

1.4.1. Standard potential

Aluminium belongs to that group of metals which have very negative electrode potentials and before passivation evolve hydrogen on contact with most aqueous electrolytes. The hydrogen evolution reaction and formation of a nonconducting oxide or amorphous hydroxide layer make the experimental determination of the standard potential of aluminium difficult. Very early experimental attempts to place aluminium in the electrochemical series were made by Heyrovsky[27] who carried out an extensive investigation of the electrode potentials of aluminium in aqueous solution. Using aluminium amalgam and working in $AlCl_3$ solutions, he found a value of -1.337 V vs NHE (at 25 °C) for the standard potential of aluminium. He attributed this electrode potential to the reaction

$$Al + 3OH^- = Al(OH)_3 + 3e^-$$

Since then a number of workers have studied the standard potential of aluminium. There are some minor differences among them. Malachesky[28] has summarized the available experimental data as follows. Hagyard and Earl measured a potential of -1.65 V vs NHE for the oxide-free aluminium electrodes in 0.00033 M $AlCl_3$ (+ 1 M KCl) from which a value of -1.58 V can be calculated for the standard potential of aluminium. In basic solution, Plumb and Swain observed that at pH < 12.4 the electrode potential data corresponded to an aluminium/aluminate ion couple with

E (V vs SCE) = 0.5099 + 0.0197 log aluminate ion + 0.1182 pH

At pH > 12.4, a change in the potential-determining reaction apparently occurred with the potential data described by the empirical relationship

E (V vs SCE) = 0.962 + 0.0788 pH

Table 1.4 presents the electrode potential data for aluminium as calculated from thermodynamic data by de Bethune and Lound.

Table 1.4 Standard electrode potentials for aluminium

Electrode reaction	E^o (V vs NHE)
$Al^{3+} + 3e^- = Al$	-1.662
$AlF_6^{3-} + 3e^- = Al + 6F^-$	-2.069
$H_2AlO_3^- + H_2O + 3e^- = Al + 4OH^-$	-2.33
$Al(OH)_3 + 3e^- = Al + 3OH^-$	-2.30

1.4.2. The direct electrochemical determination of aluminium(III)

The direct polarographic determination of aluminium(III) presents difficulties because it is reduced at very negative potentials, yielding an irreversible wave distorted by the hydrogen evolution current. The first reported study of the polarographic behaviour of the aluminium ion is attributed to Prajzler[29] who observed a reduction wave due to aluminium in 0.05 N $BaCl_2$ at - 1.75 V vs SCE. Cyclic

voltammetry of aluminium(III) reveals a cathodic current peak which, under certain conditions, is proportional to aluminium(III) concentration[30]. No oxidation peak can be observed and there is evidence that the reduction process is associated with adsorption phenomena. It was found that the aluminium reduction peak potential is a function of the starting potential, aluminium(III) concentration, and composition of the solution (salt concentration, pH, and buffer concentration).

In the presence of complexing agents such as fluoride, oxalate, citrate, and tartrate, at amounts equivalent to the aluminium ion concentration, significant changes occur in the aluminium polarographic wave. Galova and Szmerkova[31] examined the polarographic behaviour of aluminium in the presence of fluoride, tartrate, and citrate. As the complexing anion/aluminium concentration ratio is increased, the $E_{1/2}$ values shift to more negative potentials. The $E_{1/2}$ values are also dependent on the concentration of the complex. Little or no shift occurs in the $E_{1/2}$ of the citrate complex, while the shift of the $E_{1/2}$ of the 1 : 6 fluoride complex is quite marked.

1.4.3. The indirect electrochemical determination of aluminium(III)

Indirect methods exist for the polarographic determination of aluminium. One example involves the *o*, *o*'-dihydroxyazo dyes which form chelates with aluminium, the half wave potentials of which are more negative than those of the dye itself. Willard and Dean[32] developed the first successful indirect method for the polarographic determination of aluminium. Using Solochrome Violet RS (SVRS), they observed that in the presence of aluminium, the normal reduction wave of the organic dye split up into two discrete waves. The SVRS-aluminium complex was reduced at a potential 0.2 V more negative

than the SVRS itself. The total height of the two steps was equal to that of the dye alone, with the height of the second wave proportional to the aluminium concentration. Subsequently several other *o*, *o*'-dihydroxyazo dyes (for example Superchrome Garnet Y[33]), pyrocatechol violet (PCV)[34] and 1,2-dihydroxy-anthraquinone-3-sulphonic acid (DASA)[35] have been used for the indirect determination of aluminium. The electrochemistry of these classes of organic ligands will be introduced in the following sections.

1.5. ELECTROCHEMISTRY OF *o*-DIHYDROXYARYL COMPOUNDS

Stable complexes are formed between aluminium and *o*-dihydroxyaryls. The electrochemistry of benzene-1,2-diol (catechol) and its derivatives, the simplest *o*-dihydroxyaryls has been well-studied.

Many workers have shown that *o*- and *p*-dihydroxyaryls can be oxidized electrochemically to *o*- and *p*-quinones, respectively. Generally, in aqueous solution, the oxidation of catechol, and its derivatives, involves the oxidation of the 1,2-dihydroxy grouping to the *o*-quinone. The oxidation reaction involves the loss of two electrons and two protons.

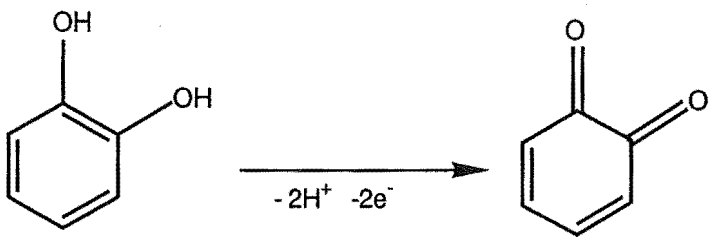

1.5.1 Effect of pH on oxidation potential of *o*-dihydroxyaryls

The effect of pH on $E_{1/2}$ for a dihydroxyaryl is very significant. In general, $E_{1/2}$ values decrease in going from acid to basic solutions.

Oxidation of an *o*-dihydroxyaryl might, by analogy with *p*-dihydroxyaryls, involve any of the species shown in the "nine member square scheme"[36].

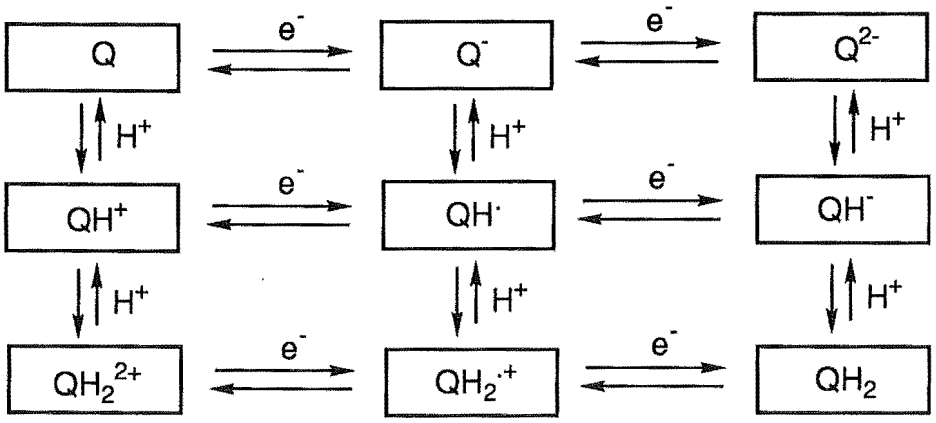

The particular species involved depend on pK_a values and solution pH, but for benzene-1,2-diol and its derivatives, detailed experimental studies have been limited to the pH range where the reaction is represented by

$$Q + 2\ H^+ + 2\ e^- = QH_2$$

Under these conditions

$$E = E^o + \frac{0.059}{2} \log\frac{[Q]}{[QH_2]} + \frac{0.059}{2} \log [H^+]^2$$

$$= E^o + \frac{0.059}{2} \log\frac{[Q]}{[QH_2]} - 0.059\ pH$$

At the half-wave potential, $[Q] = [QH_2]$

$E_{1/2} = E^o - 0.059\ pH$

For an electrochemically reversible system, half-wave potentials, $E_{1/2}$, are a good approximation to equilibrium potentials[37], and so a plot of $E_{1/2}$ against pH gives an equilibrium line with a theoretical slope of -59 mV per pH unit.

Doskocil[38] has investigated $E_{1/2}$ values for benzene-1,2-diol and 4-methylbenzene-1,2-diol at a dropping mercury electrode in aqueous solutions as a function of pH. His results were fitted to a line of -59 mV per pH unit over the pH range 4-8. Ritchie and co-workers[39] used cyclic voltammetry at a gold electrode to examine the pH-dependent electrochemistry of a series of substituted benzene-1,2-diols. Plots of $E_{1/2}$ against pH for benzene-1,2-diol, 4-ethylbenzene-1,2-diol and methyl-3,4-dihydroxybenzoic acid are presented in Figure 1.4. As can be seen from the Figure, the experimental points for the ethyl and benzoate derivatives lie on straight lines whose slopes are close to -59 mV per pH unit. For benzene-1,2-diol below pH 5.0, data fit a line with slope -59 mV per pH unit, but above pH 5 the slope is only -43 mV per pH unit. The reason for this behaviour is not known.

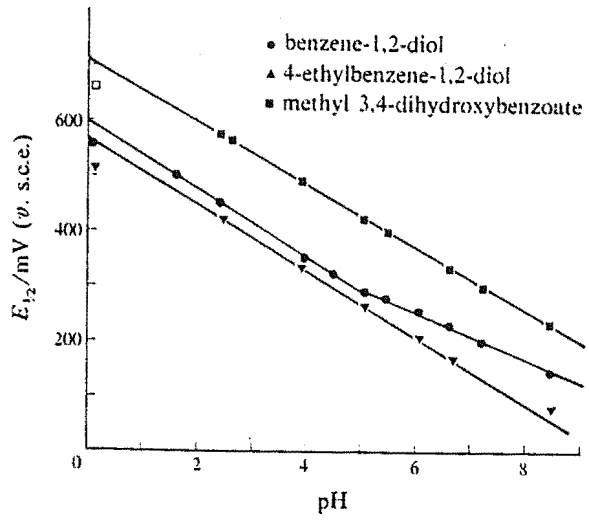

Figure 1.4. Plots of $E_{1/2}$ against pH for benzene-1,2-diol, 4-ethylbenzene-1,2-diol and methyl-3,4-dihydroxybenzoate.

At lower pH values, protonation of the quinone may occur. Thus Ritchie et al.[39] found that the $E_{1/2}$ value at pH 0.05 for each compound was not collinear with the other experimental points and attributed this to the reaction

$$QH^+ + H^+ + 2e^- = QH_2$$

This would give a slope of -30 mV per pH unit on the $E_{1/2}$ vs pH diagram.

At higher pH values, ionisation of the hydroquinone may occur. For example

$$Q + H^+ + 2e^- = QH^-$$

Again this would give a slope of -30 mV per pH unit. However, measurements in this pH region are complicated by the instability of the quinone.

1.5.2. The mechanism of oxidation of *o*-dihydroxyaryls in aqueous solution

The overall two-electron, two-proton process shown above occurs by a series of one-electron and one-proton transfers at the electrode. Details of the microscopic pathway are difficult to obtain and are expected to depend on pK_a values of a particular species and solution pH. Wightman and co-workers[40] have made a careful study of some substitued catechols at neutral pH. For 4-methylcatechol, 3,4-

dihydroxyphenylacetic acid and 3,4-dihydroxybenzylamine the reaction pathway was determined to be:

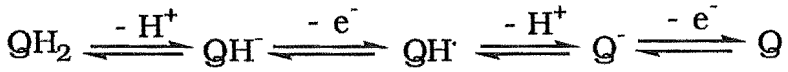

1.5.3. Effect of pH on the kinetics

In general, for the electrode process

$$Q + 2H^+ + 2e^- = QH_2$$

the rate of the redox reaction decreases with increasing pH. Thus, using a rotating disc method, Bailey et al.[41] observed that as the pH was increased, the shape of the polarization curve became increasingly irreversible. This suggests that the oxidation rate depends on the proton concentration.

In cyclic voltammetry[39], the peak-to-peak potential separation (ΔE_p) decreased with decreasing pH, again indicating that the oxidation rate depends on the proton concentration. In accord with this, Wightman's study[40] of the microscopic reaction pathway for some substituted catechols revealed pH dependent heterogeneous rate constants for the individual one-electron steps.

1.5.4. Reactivity of *o*-quinones

Electrooxidation of a dihydroxyaryl gives a quinone which may be very reactive and able to undergo a variety of further reactions. The first possibility is the reaction of the *o*-quinone with water.

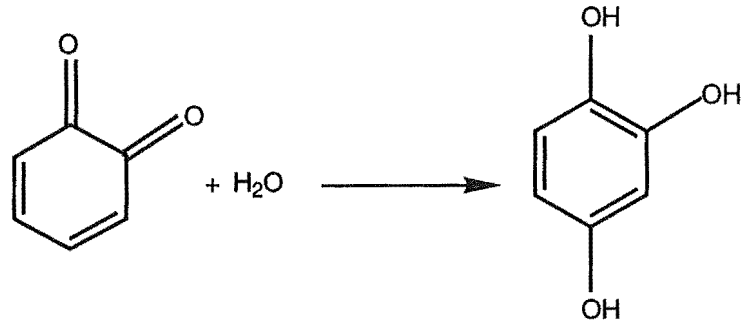

Because a *p*-quinone is formed when 1,2,4-trihydroxybenzene is oxidized, trihydroxybenzene is easier to oxidize than catechol. Thus, reaction will occur when the trihydroxybenzene is formed

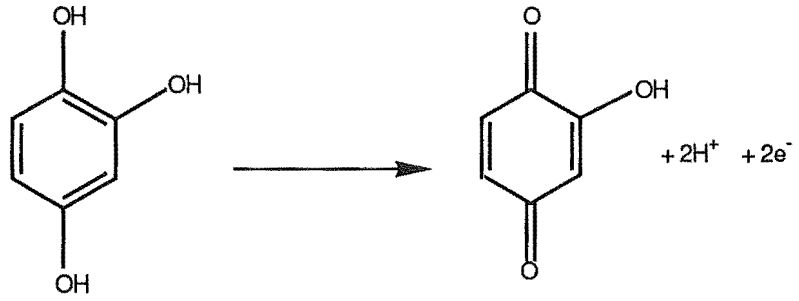

This species may then undergo a polymerization reaction.

A second reaction pathway is reaction of the *o*-quinone with the starting material,

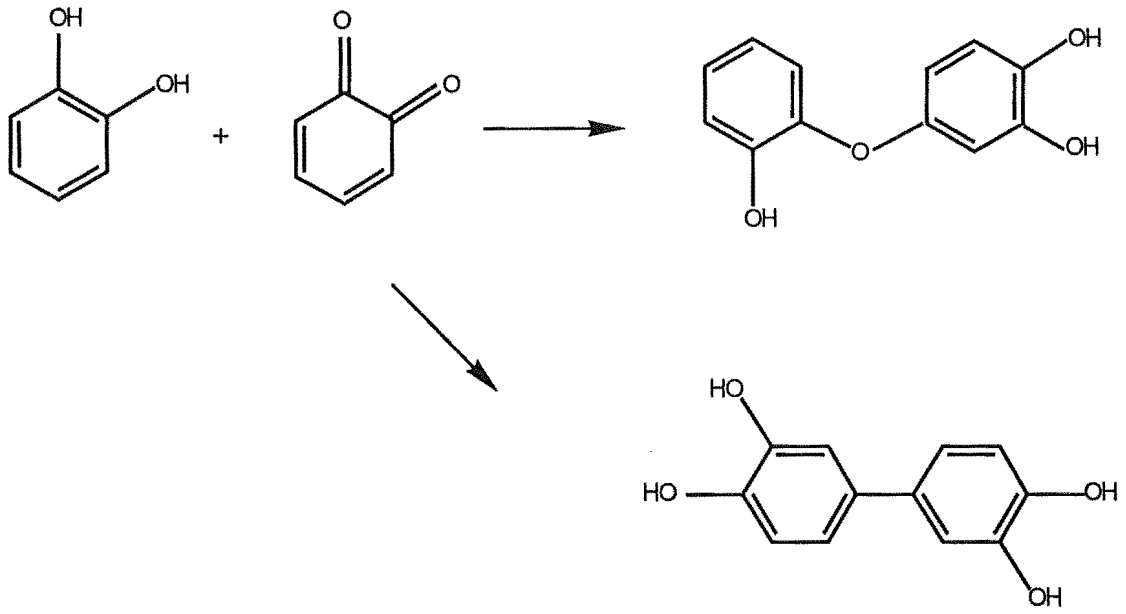

Both of these products can be further oxidized to form *o*-quinones. In the above reaction, the reactive phenol may also be one of the anionic forms of catechol, which is formed by the acid dissociation reaction. The coupling reaction may also occur by way of a semiquinone intermediate. Ryan et al.[42] studied the oxidation of substituted catechols using cyclic voltammetry, chronoamperometry, rotating ring-disk voltammetry, and coulometry. They found that over a wide pH range the *o*-quinones are attacked by the various anionic forms of the *o*-dihydroxyaryl to form a diphenyl ether. The reactions are fast on the electrochemical timescale. Ritchie and co-worker[39] examined the stability of substituted quinones using cyclic voltammetry. The ratio of cathodic peak current to anodic peak current (at 100 mV/s) was measured as a function of pH and for benzene-1,2-diol, 4-ethylbenzene-1,2-diol and methyl 3,4-dihydroxybenzoate, the ratio became less than unity above a certain critical pH (6.7, 8.5 and 4.0 respectively). The order of stability of the quinone was 4-ethylbenzene-1,2-diol > benzene-1,2-diol > methyl 3,4-dihydroxybenzoate. The reaction was assumed to be a coupling reaction.

Finally, Adams and co-workers[43] have shown that 4-methyl-*o*-benzoquinone can react with nucleophiles such as ammonia, chloride, and sulphhydryl compounds to form the addition products.

1.5.5. Effect of substituents on the oxidation potential of *o*-dihydroxyaryls

$E_{1/2}$ values for dihydroxyaryls are strongly dependent on the kind, number, and position of substituents. Electron-donating substituents (OH, OMe, OAc, NR_2, alkyl, aryl, etc.) shift $E_{1/2}$ toward more negative potentials (which makes the dihydroxyaryl more easily oxidized). This effect is greatest for the ortho substituents. Conversely, electron-withdrawing substituents (halogen, NO_2, COOR, COR, etc.) shift $E_{1/2}$ toward more positive values.

1.6. ELECTROCHEMISTRY OF AZO COMPOUNDS

The ability of certain *o*, *o*'-dihydroxyazo dyes to form discrete polarographic reduction waves in the presence of metal ions has long been recognised, and *o*, *o*'-dihydroxyazo dyes have been used to determine a wide range of metals. The electrochemistry of azo groups has been well-studied.

Electrochemically, the azoxy, azo and hydrazo groups are closely related as shown in the equation[44]. These steps usually occur as two- or four-electron transfers and the reversibility of a particular step will depend on the experimental conditions.

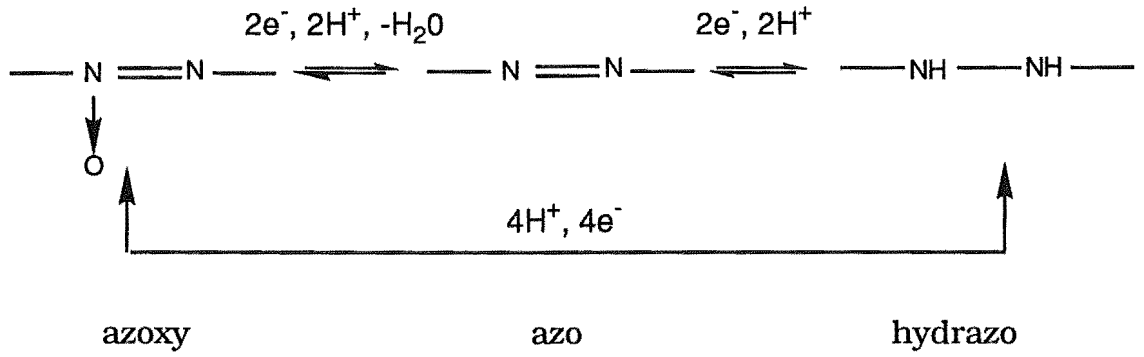

As the equation indicates, the electrochemistry of any one of these groups may involve one or both of the other two.

1.6.1. Redox chemistry of azoxy compounds

The reduction of azoxy compounds in aqueous ethanol mixtures occurs in a single four-electron step[45]. The half-wave potential for the reduction depends on the solvent composition and on the pH of the solution, becoming more negative as the pH and/or the ethanol concentration increase. This move to more negative reduction potentials is consistent with the decrease in proton availability as the pH increases and the decrease in concentration of the azoxybenzene which reduces the reversibility of the electrode reaction.

The reduction of azoxy compounds in aqueous methanol containing a range of phenols and carboxylic acids was studied by Holleck[46]. A two-stage process mechanism was proposed as follows:

(1)

(2)

where AH is the solvent (water or methanol) and A^- the conjugate base (OH^- or CH_3O^-).

The electrochemistry of substituted azoxy compounds is generally similar to that of the parent one when the substituent groups are not themselves electroactive. However, the presence of electroactive substituents, particularly in the 2 position, may greatly modify the electrochemistry.

1.6.2. Redox chemistry of azo compounds

In general, azo compounds undergo the following two-electron reduction at the dropping mercury electrode.

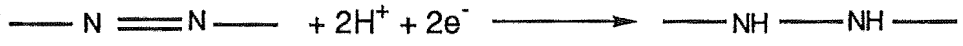

Although the overall reaction is quite straightforward, the polarographic behaviour of these compounds commonly shows that the electroreduction reactions are very complex[47]. The half-wave potentials are found to be dependent on the concentration of the azo compound, solvent composition, the presence of surfactants and the pH of the solution. If the reaction is assumed to be reversible, the shape of the polarographic wave will be described by the Nernst equation and the half-wave potential at 25 ^{o} C is given by

$$E_{1/2} = E^{o} - \frac{0.059q}{n} pH$$

where q and n are the number of protons and electrons, respectively, involved in the electrode reaction. Since q = n = 2 for the reaction the half-wave potential for the reduction of azo compounds should change by -59 mV for every unit increase in the pH of the solution.

The polarography of several azo compounds has been investigated by Florence[48]. The electron attracting or releasing ability of the substituents is related to their effect on the half wave potentials and limiting currents. The results show that only strongly electron-releasing groups such as hydroxy and amino cause the electrode reaction to involve more than two electrons. Thus, Laitinen and Kneip[49] investigated the polarographic behaviour of *p*-dimethylaminoazobenzene and showed that the number of electrons involved in the reduction is pH-dependent. At pH <9.5 the step height corresponded to four electrons, and at pH 13.5 to approximately three. Controlled potential coulometric reduction of this dye at a large stirred mercury pool cathode led to n values of four in both acid and alkaline media. It is proposed that an unstable hydrazo intermediate is involved in the reduction of this compound.

1.6.3. Redox chemistry of hydrazo compounds

Since hydrazo compounds are the immediate products of the reduction of azo and azoxy compounds in protolytic solvents, the electro-oxidation of hydrazo compounds is usually the reverse of the electro-reduction of azo compounds[50].

Generally, hydrazo compounds are much more unstable than azo or azoxy compounds and as a result, their reduction to the amines

commonly involves a combination of chemical auto-oxidation-reduction steps and electron exchange reactions.

1.7. ELECTROCHEMISTRY OF METAL-LIGAND COMPLEXES

Since Willard and Dean first used a di-*o*-hydroxyazo dye for the polarographic determination of aluminium, SVRS and similar electroactive ligands have been used for the polarographic determination of thorium and zirconium[51], gallium and indium[52], uranium[53] and some lanthanides[47]. These analytical applications have prompted studies aimed at investigating the origin of a discrete metal-ligand complex wave.

1.7.1. Effect of complex formation on the half-wave potential shift

Several theories have been proposed to explain why the metal complex of an electroactive ligand is reduced at a more negative potential than the uncomplexed ligand. Florence[54] summarised the theories:

(1) The effect is due to stabilization of one of the geometrical isomers of the dye as suggested by Willard and Dean[32]. But this explanation can be discounted on structural grounds. It has been found that the *cis* isomer is more easily reduced than the *trans* form. For the metal-ligand complex it would have to be assumed that the *cis* isomer is the

form stabilized, yet the complex is more difficult to reduce than free ligand. Thus the *cis-trans* explanation is unsatisfactory. Also, the magnitude of the half-wave potential shift ($\Delta E_{1/2}$) of the ligand on complexing with a metal is not constant, but shows a wide variation with metal ion present. If isomer-stabilization were the explanation, $\Delta E_{1/2}$-values would be independent of the nature of the metal ion.

(2) The shift in $E_{1/2}$-values is based on the "rigidity" of the metal-dye complex[55]. In support of this theory, Dean and Bryan showed that a correlation existed between $\Delta E_{1/2}$ and ionic radius of the metal ion. However, other workers using more accurate $\Delta E_{1/2}$-values have found that there is no apparent correlation between $\Delta E_{1/2}$ and ionic radius.

(3) The half-wave potential shift is caused by metal-ligand chelate formation with the electroactive group involved in the coordination. The $\Delta E_{1/2}$-values should then be related to the relevant metal-ligand stability constants[56] and several workers have demonstrated such a relationship for metal-ligand systems which exhibit simple complexation equilibria.

Based on this latter proposal, Shiu and Harrison[57] have recently derived a general equation for the shift in half wave potential for ligand reduction on complexation with a metal. The general equation is applicable to systems where more than one protonated form of the ligand can form a complex, and the complexes can also exist in various states of protonation. the complexation reaction of metal, M, with the ligand, LH_N, can be written for different stoichiometries as

$$M + x\ LH_N = M(LH_{N-q})_x + qxH^+$$

$$x = (0, 1, \cdots, X)$$

where N is the total number of acid sites on the ligand L, X is the highest order of complexation and q is the number of protons displaced on formation of a given complex stoichiometry.

Under conditions of excess metal ion, they analyzed the effect of the formal concentration of M and LH_N on shifts in the half wave potential, $\Delta E_{1/2}$, upon complex formation. When only one protonated form of the free ligand and of the complex are significant, and only the one-to-one complex is dominant for the oxidised ligand-metal complex, the general equation can be simplified as

$$\Delta E_{1/2} = \frac{-RT}{nF} \ln \frac{1 + \beta^{ox}_{N-i,j} \alpha^{ox}_{i} [M]}{\sum_{j}^{1/x} \beta^{R}_{N+n-i',j} \alpha^{R}_{i'} [M]^{j}}$$

R, T and F have their usual meanings and activity cofficients are assumed to be unity. The index *i* is given by *i*=1 to N for the oxidised form of the ligand and *i'* is defined in the same manner for the reduced form of the ligand. The index *j* is given by *j* = 0, 1, 1/2, 1/3, · · · 1/X. The term $\beta^{ox}_{N-i,j}$, the overall pseudo formation constant for the *j*th complex with the *i* deprotonated form of the oxidised ligand is given by the equation. The term $\beta^{R}_{N+n-i',j}$ is the overall pseudo formation constant for the *j*th complex with the *i'* deprotonated form of the reduced ligand. The terms α^{ox}_{i} and $\alpha^{R}_{i'}$ are the fractions of the *i*th and *i'*th deprotonated forms of the oxidised ligand and reduced ligand derivatives, respectively. These terms are sensitive to pH but when *i*=*i'*, each term shows the same dependence on pH and the ratio is pH-independent. When *i*≠*i'*, $\Delta E_{1/2}$ will show pH-dependency. Hence, at constant pH or when *i*=*i'*, the expression shows that $\Delta E_{1/2}$ will be constant if the stoichiometry is the same for both oxidised and reduced forms of the complex and both terms in [M] in the numerator and

denominator are large relative to unity. In this case the shift in $E_{1/2}$ is controlled by the stability constants for the oxidised and reduced complexes.

On other hand, a change in stoichiometry on reduction of the complex will lead to $\Delta E_{1/2}$ dependence on metal ion concentration. Assuming that only one complex stoichiometry is important for each oxidation state and the coordination number changes from *j* to p on reduction, the $\Delta E_{1/2}$ is given by

$$\Delta E_{1/2} = \frac{-RT}{NF} \left\{ \ln \frac{\beta_{N-i,j} \alpha_{i}^{ox}}{\beta_{N+n-i',p} \alpha_{i'}^{R}} + (j - p) \ln [M] \right\}$$

This treatment has been applied successfully to the determination of the stoichiometry of the complexes formed between La^{3+} and both alizarin red S and alizarin complexone following reduction of the quinone ligand[58]. At constant pH, $\Delta E_{1/2}$ was found to be independent of metal ion concentration indicating that the reduced as well as the oxidised forms of the ligands form one-to-one complexes.

Earlier, Florence[54] carried out a similar study of the Ni^{2+}-SVRS complex. In the azo form, SVRS forms a one-to-one complex with Ni^{2+} and $\Delta E_{1/2}$ for reduction was found to be independent of metal ion concentration and pH. From these observations it was concluded that there is no change in stoichiometry following the redox reaction.

1.8. SCOPE OF THIS WORK

Chemically modified electrodes (CMEs) are electrodes which are deliberately coated with a chemical reagent to alter their chemical or electrochemical characteristics[59,60,61]. CMEs have received a great deal of attention since their inception about 20 years ago. Since they offer an inherently high sensitivity, and good selectivity may be achieved by correct choice of modifier and control of electrode potential, CMEs are very well suited to electroanalytical applications. Further, the modifier may protect the electrode surface from interferences, thereby improving reproducibility and lifetime.

The goal of this work was the development and application of CMEs for quantitative inorganic analysis with emphasis on analysis of metals which are not easy to determine by other direct electrochemical methods. Analysis of aluminium(III) was the main research objective. The primary approach was to use aluminium-specific redox active ligands, either in solution or incorporated in CMEs, as a method for indirect electrochemical analysis of aluminium. The most appropriate electrochemical techniques (such as cyclic voltammetry, differential pulse voltammetry or amperometry) were established for analysis of aluminium(III) using different soluble complexes or CMEs.

Initially the electrochemistry was studied for several appropriate electroactive ligands which were known to bind strongly to aluminium(III). The effect of pH on the oxidation and reduction potentials was investigated in some detail. The complex formation between aluminium and these ligands was examined under different conditions such as pH, electrolyte and temperature. Optimization of the potential shift on complexation, $\Delta E_{1/2}$, was particularly emphasized in the investigation. The increase in peak height due to the redox

processes of the formed aluminium-ligand complex, or the decrease of the peak height for free ligand redox processes, was used to determine aluminium(III).

Several methods were investigated for the preparation of CMEs incorporating ligands. Polymer films were coated on the electrode using different methods such as drop coating (polyxylylviologen (PXV)) and electrochemically assisted coating (polypyrrole (PPy)). Glassy carbon electrodes modified with PPy and incorporating ligands were readily obtained by electropolymerization of solutions of pyrrole containing the ligands as electrolytes. Electrodes modified by films of PXV were shown to incorporate a variety of anionic (eg. sulphonated) ligands by ion-exchange. Ligand incorporation by use of composite graphite powder/ion exchanger electrodes and graphite epoxy/ligand electrodes were also investigated.

The use of CMEs consisting of charged polymers for preconcentration of analytes was also investigated. The accumulation of aluminium(III) in these electrodes as anionic phenolic complexes was studied.

PXV coated electrodes were studied for preconcentration using their ion-exchange property. Thus, the measurement of aluminium-(4-nitrocatechol) complexes which have an overall negative charge was studied. A sensitive method for analysis of aluminium was achieved.

CMEs developed in this work were used for analysis of aluminium(III). A 1,2-dihydroxyanthraquinone(alizarin)-modified graphite electrode was used in the voltammetric determination of aluminium(III). Alizarin, an electroactive complexing ligand, was incorporated on a solid electrode by chemisorption. The electrode was applied in determination of exchangeable aluminium(III) in soils. This provided a simple, rapid method for monitoring aluminium in the environment.

Also the CMEs were evaluated on the basis of factors such as durability, stability, ease of fabrication and detection limits. Fundamental studies included investigations of the rate and extent of reactions of the ligands with the metals in the CMEs as a function of solution conditions and the properties of the electrode coating. These enabled optimization of CME performance.

As part of a programme to develop amperometric methods for measurement of aluminium(III) in environmental samples, the oxidation reactions of free and aluminium bound ligands at solid electrodes in a flow system (FIA) were studied. This approach has the advantage of automated solution handling, which replaces manual operations like pipetting, mixing, and separating, and results in a drastic reduction in the volumes of sample and reagent solutions that are required, with no loss of reproducibility. The flow system is able to control volumes, mixing patterns, and residence times exactly. Also in a flow system electrode activity can be maintained, despite fouling by adsorbed redox products, by techniques such as voltage pulsing. An amperometric FIA method for aluminium(III) was developed based on the ligand DASA. Electrode fouling by absorption of ligand oxidation products in flow systems was studied. A double pumping system and cathodic/anodic voltage cycling were used to reactivate the gold electrode surface.

Like aluminium(III), magnesium(II) is reduced at very negative potentials, therefore an indirect method of electrochemical analysis is necessary. The electrochemistry of the electroactive ligand Eriochrome Black-T (EBT) and EBT-Mg(II) was investigated by cyclic voltammetry and hydrodynamic voltammetry with particular reference to the oxidation processes involved. A simple flow system for magnesium(II) determination in natural waters and serum was developed. The optimum conditions were established for highest

percent formation of Mg-EBT. Conditions for minimum interference by Ca(II) were determined on the basis of speciation calculations for the EBT/OH^-/Ca(II)/Mg(II) system. Ca(II) and Fe(III) interference were controlled by pH and addition of masking agents. Electrode fouling by adsorption of EBT oxidation products and serum in the flow system was studied. Several surfactants and a dialyzer which resolved the electrode fouling problem were used in the flow system. The use of polymer films Poly(3-methylthiophene) (P3-MT) and PPY to minimize the electrode fouling was also studied.

The SVRS-aluminium system has proved to be a useful method for analysis of aluminium by adsorption voltammetry. However the requirement for heating to form the complex (90 ^oC, 10 minutes) is a disadvantage. After making a survey of the complex formation under different conditions a modified method was developed. The heating step was replaced by allowing the aluminium reaction with SVRS to occur at a higher pH, followed by accumulation in acidified solution. It also provided good results with high sensitivity and reproducibility.

CHAPTER TWO

EXPERIMENTAL

2.1. INSTRUMENTATION

2.1.1. Electrochemistry

Cyclic voltammograms (CVs) were obtained using: (1) a PAR 173 potentiostat coupled to a PAR 175 universal programmer and a Graphtec WX 1200 recorder and (2) a PAR 173 potentiostat and a home-built sweep generator with either a Graphtec WX 1200 or a PAR RE 0074 XY recorder.

Differential pulse voltammograms (DPVs) were measured with: (1) a PAR 174 polarographic analyzer and a PAR 0092 recorder and (2) a PAR 384B polarographic analyzer.

A home-built integrator was used to measure the charge passed during controlled potential electrolysis and polymerisation experiments.

2.1.2. pH meters

Solution pH was measured by using either a Digital Testmeter or an HI 8424 Portable Microprocessor pH meter.

Before measurements pH electrodes were calibrated using standard buffer solutions.

2.1.3. Spectrophotometry

Atomic absorption spectrometry (AAS)

AAS measurements were made using a Varian AA-1475 Series Atomic Absorption Spectrometer.

Visible absorption spectra

Spectrophotometric measurements were made using a Varian Superscan 3 Spectrophotometer.

2.2. ELECTRODES AND CELLS

A standard PAR pyrex three-electrode cell was used in differential pulse polarographic and cathodic stripping voltammetric measurements. It consisted of a mercury drop working electrode, a platinum wire counter electrode and a Ag/AgCl (saturated KCl) reference electrode. Laboratory-built three-electrode 10-mL (for glassy carbon working electrode) and 15-mL (for graphite and carbon paste working electrodes) glass cells were also used in differential pulse voltammetric and cyclic voltammetric measurements. They consisted of the CME (or glassy carbon electrode, graphite, carbon paste electrode) as working electrode, a platinum wire counter electrode and a saturated calomel reference electrode (SCE).

2.2.1. SCE reference electrode

Home-made saturated calomel electrodes were used as reference electrodes. Their design is shown in Figure 2.1. For some experiments the SCE was placed in a compartment containing buffer and separated from the analyte solution by a Vycor tip.

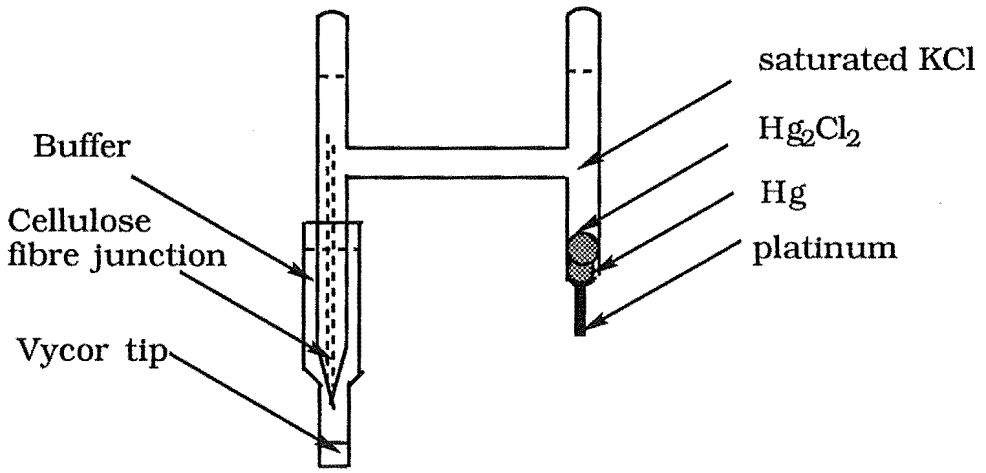

Figure 2.1. Diagram of SCE reference electrode

2.2.2. Carbon electrodes

Preparation of the electrodes

Glassy carbon electrodes (GCE) were made in the following manner. A 0.5 cm length of glassy carbon rod (0.3 cm diameter; Atomergic Chemetals, VC-10) was sealed in a Teflon rod (0.7 cm diameter). Electrode contact with the glassy carbon was effected with a central copper rod.

Graphite electrodes were made in the following manner. A high-density graphite rod (PAR G0091) (0.6 cm diameter) was sealed in a Teflon rod (1.2 cm diameter). Electrical connection to the electrode was made by using a few drops of mercury and a copper wire.

Treatment of the electrodes

Newly fabricated carbon electrodes were polished metallographically to a mirror-like finish using polishing papers followed by 9, 6, 3 then 1 μm diamond paste. The electrodes were washed with acetone (BDH, Analar) followed by washing with doubly distilled water, then dried with filter paper. Between measurements, the electrode was briefly polished with 1 μm diamond paste, rinsed with acetone and doubly distilled water and dried on filter-paper. For measurements requiring high sensitivity, the electrodes were sonicated for 5 minutes in doubly-distilled water.

2.3. GLASSWARE

All glassware was "B" grade and was cleaned as follows. It was soaked in dilute Analar HNO_3 solution (about 10%) for at least 24 hours, followed by washing with doubly distilled water then soaking in 1% Aristar HNO_3 solution for 24 hours. It was kept soaking in doubly distilled water until use.

In order to avoid contamination by metal ions, a special glass spoon was used in all chemical weighing

2.4. REAGENTS AND PREPARATION OF SOLUTIONS

2.4.1.Reagents

(1) 1,2-dihydroxyanthraquinone-3-sulphonic acid (DASA), tiron, catechol, eriochrome black T (EBT), 1,2-naphthoquinone-4-sulphonate, 1,2-naphthoquinone, 1,2-diaminoethane, triton X-100 (iso-octylphenoxypolyethoxyethanol), and ethyleneglycol-bis(ß-aminoethylether) N,N,N',N'-tetra-acetic acid (EGTA) (all reagent grade) and triethanolamine (Analar) were obtained from BDH.

(2) Alizarin (Riedel-de Haen) was purified by sublimation, followed by recrystallization from ethanol.

(3) The provided sample of fulvic acid was isolated from a gley podzol B_h horizon by the XAD-7 pyrophosphate method described by Gregor and Powell[62].

(4) The tannin was isolated from Chinese quince (*Chaenomeles chinensis*) and supplied by L. J. Porter.

(5) 4-nitrocatechol and albumin (98 - 99%) and pyrocatechol violet (PCV) (all from Sigma) were used as supplied.

(6) Hostapur SAS93 was kindly supplied by Hoechst (New Zealand) Ltd.

(8) Solochrome violet RS (SVRS) (the stated purity is 60%), pyrrole (98%) and 3-methylthiophene (3-MT) (99%) (all from Aldrich) were used as received.

2.4.2. Preparation of solutions

All solutions were prepared in doubly distilled water or Milli-Q deionized water (resistance 18 MΩ).

Standard buffer solutions

Four primary reference standard buffers were used in pairs to calibrate the pH meter (Glass/calomel electrode pair). All solids were BDH, Analar.

(1) Tetroxalate standard buffer (0.05 M, pH = 1.679): 6.305 g $KH_3(C_2O_4)\cdot 2H_2O$ (dried at 60 °C) was dissolved in 500 mL doubly distilled water.

(2) Phthalate standard buffer (0.05 M, pH = 4.005): 5.060 g $KOOCC_6H_4COOH$ (dried at 110 °C) was dissolved in 500 mL doubly distilled water.

(3) Phosphate (1:1) standard buffer (0.025 M, pH = 6.863): 1.694 g KH_2PO_4 and 1.767 g Na_2HPO_4 (both dried at 40 °C) was dissolved in 500 mL doubly distilled water.

(4) Borax standard buffer (0.01 M, pH = 9.183): 1.900 g $Na_2B_4O_7\cdot 10H_2O$ (dried in room temperature desiccator) was dissolved in 500 mL doubly distilled water.

Electrolytes

Three types of buffer solutions were used as electrolytes.

(1) 0.1 M sodium acetate (Peking reagent AR) - acetic acid (BDH, Analar). pH of solutions was changed from 4.0 to 6.0 by changing the ratio of sodium acetate and acetic acid.

(2) 0.1 M ammonium acetate (M&B, AR) - ammonia (BDH, Analar). pH of solutions was changed from 6.5 to 8.0 by changing the ratio of ammonium acetate and ammonia.

(3) 0.1 M ammonium chloride (Koch-Light, AR) - ammonia (BDH, Analar). pH of solutions was changed from 8.0 to 10.0 by changing the ratio of ammonium chloride and ammonia.

Metal solutions

(1) Aluminium(III) standards were prepared from an acidified (pH 3) stock solution of $KAl(SO_4)_2 \cdot 12H_2O$ (1×10^{-3} M) (BDH, Analar).

(2) Magnesium standards were prepared from $MgSO_4 \cdot 7H_2O$ (BDH, Analar).

(3) Iron(III) standards were prepared from an acidified (1×10^{-3} M in 0.05 M HCl) stock solution of $FeCl_3 \cdot 6H_2O$ (Fisons, AR).

(4) Copper standards were prepared from $Cu(NO_3)_2 \cdot 3H_2O$ (BDH, Analar).

(5) Zinc standards were prepared from $ZnSO_4 \cdot 7H_2O$ (BDH, Analar).

(6) Lead standards were prepared from $Pb(NO_3)_2$ (BDH, Analar).

Ligand solutions

Ligand solutions were prepared with milli-Q water or doubly distilled water. SVRS and DASA solutions (2×10^{-4} M) were prepared daily by dissolving SVRS and DASA in water. EBT solution (5×10^{-5} M) was prepared by dissolving EBT in water and kept in a refrigerator (this solution was stable for up to one week).

2.5. SAMPLES

2.5.1. Water samples

Water samples were provided by DSIR (NZ) Chemistry Division who performed independent analyses for Mg (AAS), Fe (AAS), Al (FIA; eriochrome cyanine R) and PO_4^{3-} (FIA). The samples were selected to provide a wide range of concentrations for Mg, Ca and Fe (0.6 - 5.2, 1.3 - 134 and <0.1 - 2.9 ppm respectively).

2.5.2. Serum samples

Blood was taken in heparinised tubes, chilled (4 °C) and centrifuged within 2 hours of collection; the serum was removed from the erythrocytes and stored at 4 °C.

2.5.3. Soil samples

Soil samples were obtained from DSIR (NZ) Land Resources. To determine exchangeable aluminium(III) soil samples (1.0 g) were extracted with 1.0 M potassium chloride solution (10 mL) by the rapid (5 minute) extraction method[63] followed by filtration and centrifugation.

2.6. CLEAN ROOM

All ultra trace analyses were made in a class 100 room. In the clean room, overshoes, lint-free lab coat and cap were worn. Disposable gloves were worn for most operations on samples and solutions.

2.7. SPECIATION CALCULATIONS

Speciation calculations were performed with the program SIAS[64]. Protonation and metal-ligand stability constants used were literature values, as cited.

CHAPTER THREE

VOLTAMMETRIC METHODS USING POLYMER MODIFIED ELECTRODES

3.1. INTRODUCTION

In attempts to enhance the sensitivity or selectivity of voltammetric methods, electrodes modified with thin films of polymeric materials have attracted increasing interest in recent years. There are two main types of polymers used as electrode coatings: conducting polymers and nonconducting polymers.

Conducting polymers are a class of new materials that have electronic conductivity. A structural characteristic of conducting organic polymers is the conjugation of the chain-linked electroactive units, i.e. the monomers interact via a π-electron system. Polyacetylene was made in the mid-1970s[65] and was the first reported conducting polymer. Since then a number of other conducting polymers have been synthesized. The most important polymers are polyacetylene (PA)[66], polypyrrole (PPy)[67], polythiophene (PTh)[68] and polyaniline (PANI)[69] whose structures are shown in Figure 3.1. When the conducting polymers are reduced they are nonconducting. When these films are oxidized they show electrical conductivity and are positively charged (for example, PPy has one positive charge per three pyrrole rings[70]). To maintain charge neutrality counteranions must be associated with the oxidised polymers. These conducting polymers can be readily prepared either by chemical or electrochemical polymerization from a monomer solution containing an electrolyte salt[71]. Hence, conducting

polymers provide a convenient means of preparing new chemically active electrodes.

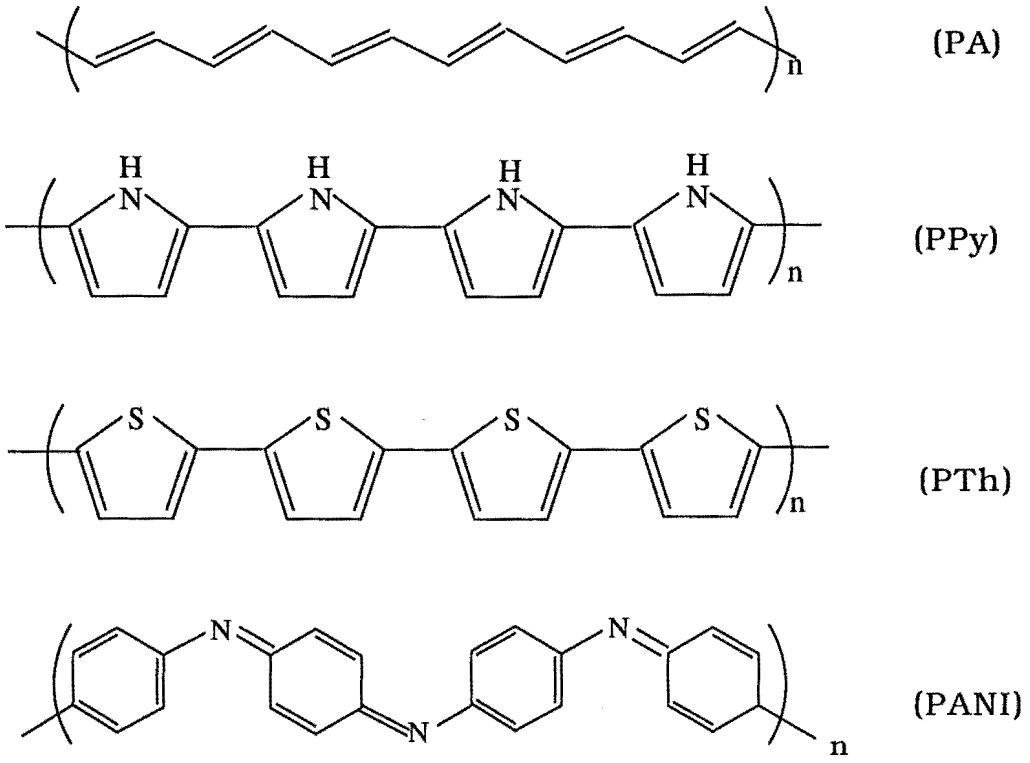

Figure 3.1. Structure of the conducting polymers

Nonconducting polymers include redox polymers in which the redox centre is part of the polymer backbone or a pendant group and ion-exchange polymers in which the redox active component is a counterion to a poly-ionic (anionic or cationic) polymer. Examples of nonconducting polymers are the cationic polymers quaternized polyvinylpyridine (QPVP) and polyxylylviologen (PXV), and the anionic polymers polystyrene sulphonate and the perfluoro sulphonated material, Nafion.

The use of electrodes modified with polymeric coatings has some major advantages in analysis. Film coatings are applied in order to incorporate redox-mediators which may react with analytes in

solution[72, 73], to concentrate analytes before the actual electrochemical measurement[74-77] or to create a selective barrier for certain classes of compounds in the solution[78-80].

Work described in this Chapter is based on the use of polymer modified electrodes to accumulate aluminium(III)-ligand complexes. It was expected that pre-concentration of complexed aluminium(III) on the coated electrodes would lead to greater sensitivity in the analysis of aluminium(III). Both nonconducting ion-exchange polymers and conducting polymers which can concentrate anions as countercharges were studied. Two approaches were used for the determination of aluminium(III).

In the first method, electroactive ligands which have a high affinity for aluminium(III) were incorporated by ion exchange into a cationic polymer film. The electrode with the polymer/ligand coating was then exposed to the aluminium(III) solution and its electrochemical response recorded. Abruña has used similar methods for the determination of copper and calcium[81,82]. For copper determination, 2,9-dimethyl sulphonated bathophenanthroline was incorporated by ion exchange into electrode films of both quaternized vinylpyridine vinylferrocene copolymer and $[Ru(v\text{-}bpy)_3]^{2+}$ (v-bpy is 4-vinyl-4'-methyl-2,2'-bipyridine). Cu(I) was accumulated into the films by contact with an aqueous solution and the concentration of copper was determined by the current for the oxidation of Cu(I). For calcium determination, antipyrylazo III was incorporated by ion exchange into an electrode film of viologen polymer. Ca(II) was complexed with antipyrylazo III in the film during electrode soaking in the Ca(II) solution and the concentration of Ca(II) was measured by the decrease in the current for the oxidation of antipyrylazo III.

For both of these methods, after accumulation of the metal from aqueous solution, the modified electrode was transferred to an organic solvent for electrochemical analysis.

In the second method for the determination of aluminium(III) in this work, pre-formed aluminium(III)-ligand complexes with high stability constants were incorporated by ion exchange into a cationic polymer. Similar work has been done in this area by Wallace and Riley[83] who used an electrode modified with a protonated poly(4-vinyl-pyridine) film to preconcentrate and determine gold(III) in the form of $[AuCl_4]^-$. In another example, Wallace and his co-workers used an electrode modified with an oxidised poly(3-methylthiophene) film to preconcentrate Cr(VI) oxyanions[84]. Using a similar method, lanthanum(III) has been determined at a QPVP coated electrode after a lanthanum(III)-DASA complex, formed at pH 9.2, was incorporated into the QPVP film by ion exchange[58].

The determination of aluminium(III) at polymer modified electrodes requires the use of an electroactive ligand. Suitable ligands must form complexes of high stability with aluminium(III) and there must be a change in the electrochemistry of the ligand in the presence of aluminium(III).

Ligands chosen for the initial survey included those which have been used to determine aluminium(III) at mercury electrodes. Solochrome violet RS (SVRS) has been investigated by many workers for polarographic determination of aluminium(III) in acetate buffers, pH 4.5 - 5.5[32, 85-89]. Under these conditions, the reduction wave of the complex appears at approximately -0.5 V vs SCE, 0.2 V more negative than the reduction wave of the free ligand. Using cathodic stripping voltammetry (CSV) at mercury, Wang reported peaks at -0.49 V and -0.61 V vs Ag/AgCl for the aluminium(III)-SVRS system[88]. A reduction of SVRS occurred at $E_{1/2}$ = -0.455 V at the pyrolytic graphite

electrode[127]. The oxidation wave of the aluminium(III)-SVRS complex, at $E_{1/2}$ = +0.88 V vs SCE, has also been used to determine aluminium(III) using a pyrolytic graphite electrode. Cyclic voltammetry showed that the height of the complex wave and the decrease in height of the free dye wave at $E_{1/2}$ = +0.53 V are proportional to the aluminium(III) concentration. All of the these procedures required heating of the solutions to increase the rate of reaction of aluminium(III) with SVRS.

Aluminium(III) has also been determined by CSV of its 1,2-dihydroxyanthraquinone-3-sulphonate (DASA) complex on the hanging mercury drop electrode[35]. Using the conditions of a BES (N,N'-bis-(2-hydroxyethyl)-2-aminoethane sulphonic acid) buffer, pH 7.1, and an adsorption potential of -0.90 V, a peak due to the aluminium(III)-DASA complex appeared at -1.17 V vs Ag/AgCl.

Linear scan voltammetry (LSV) was used for the determination of aluminium(III) after adsorptive accumulation of the pyrocatechol violet (PCV) complex in a triethanolamine/perchloric acid electrolyte, pH 6.5, at a mercury electrode[34]. Scanning in a negative direction after adsorption gave a current peak at -0.70 V (vs Ag/AgCl) for reduction of adsorbed PCV and a peak at -0.90 V for reduction of the adsorbed aluminium(III)-PCV complex.

A cyclic voltammetric study of 4,5-dihydroxy-1,3-benzenedisulphonic acid (tiron) at pH 2.5 in the presence and absence of aluminium(III) has been reported[90]. Tiron yields an oxidation peak at ca. 0.70 V and reduction peak at ca. 0.25 V vs Ag/AgCl on glassy carbon. The metal-tiron complexes yield oxidation peaks more positive than the ligand itself. The peak height and peak potential of tiron and its complexes are changed with the pH of the supporting electrolyte. In the reported study, M^{n+}-tiron complexes (M^{n+} = Al(III), Fe(III), Os(III)

and Ti(IV)) were separated by chromatography and determined amperometrically at +1.2 V vs SCE.

Other ligands chosen for the electrochemical survey were chrome azurol S (CAS)[91] and chromotrope 2R (Ch-2R) which are reagents for the spectrophotometric determination of aluminium(III), and 1,2-dihydroxynaphthalene-4-sulphonate (1,2-DHNS) for which complexation equilibria with aluminium(III) have been studied[92,93]. Catechol forms stable aluminium(III) complexes according to stability constant data, and the electrochemical behaviour of aluminium(III)-catechol solutions was examined. Finally, 2,3-dihydroxynaphthalene-6-sulphonate (2,3-DHNS) and 4-nitrocatechol, which incorporate the *o*-dihydroxy group and are also expected to form stable aluminium(III) complexes, were investigated. Figure 3.2 shows the structures of these ligands and Table 3.1 shows the stability constants of these ligands with H^+ and Al^{3+}.

1,2-dihydroxyanthraquinone-3-sulphonate (DASA):

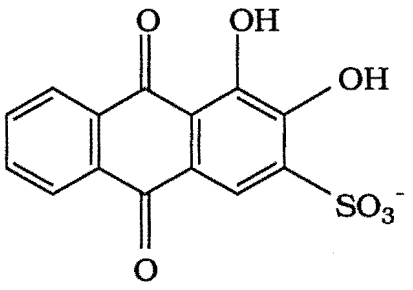

Solochrome violet RS (SVRS):

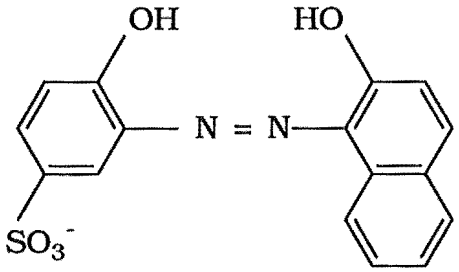

Chrome azurol S (CAS)

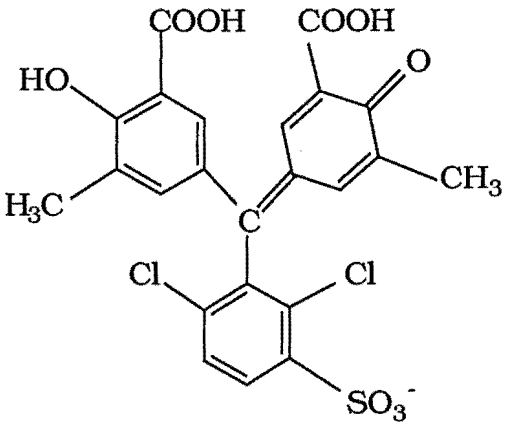

Pyrocatechol violet (PCV)

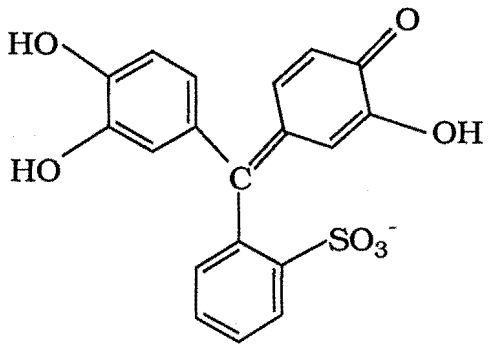

Chromotrope 2R (Ch-2R)

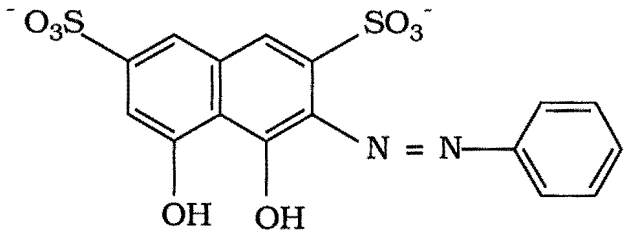

1,2-dihydroxynaphthalene-4-sulphonate (1,2-DHNS):

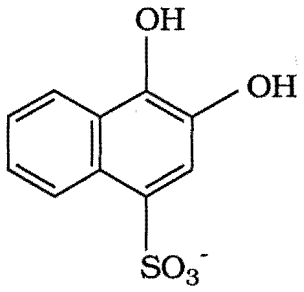

2,3-dihydroxynaphthalene-6-sulphonate (2,3-DHNS):

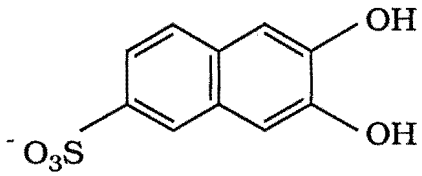

Catechol:

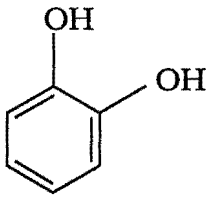

4,5-dihydroxy-1,3-benzene-disulphonate (tiron):

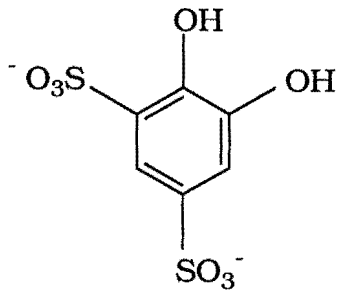

4-nitrocatechol (4-Ncat):

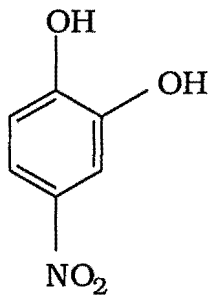

Figure 3.2. Structure of the ligands

Table 3.1. Stability constants of the ligands with H^+ and Al^{3+}

ligand	Metal	Log of equilibrium constant			Ref.
SVRS	H^+	K_1 13.04	K_2 7.03		94
	Al^{3+}	K_1 18.4	K_2 13.2		94
DASA	H^+	K_1 11.01	K_2 6.07		94
	Al^{3+}	K_1 11.31	K_2 6.06		94
1,2-DHNS	H^+	K_1 12.60	K_2 7.80		92, 93
	Al^{3+}	K_1 15.06	K_2 12.62		92, 93
Ch-2R	H^+	K_1 9.19			94
	Al^{3+}	K_1 18.41			94
CAS	H^+	K_1 11.8	K_2 4.7	K_3 2.3	94
	Al^{3+}	$K[Al^{3+} + 2HL^{3-} = Al(HL)_2^{3-}]$ 6.82			94
PCV	H^+	K_1 11.82	K_2 9.94	K_3 7.90	94
	Al^{3+}	K_1 25.12	K_2 22.27	K_3 20.74	94
catechol	H^+	K_1 13.00	K_2 9.32		94
	Al^{3+}	K_1 16.9	K_2 13.6	K_3 8.9	94
tiron	H^+	K_1 12.6	K_2 7.68		94
	Al^{3+}	K_1 16.7	K_2 13.6	K_3 9.7	94
4-Ncat	H^+	K_1 10.71	K_2 6.86		94

3.2. EXPERIMENTAL

Cyclic voltammetry was carried out by using a PAR 173 potentiostat, in conjunction with a PAR 175 universal programmer and a Graphtec WX 1200 recorder. The polymerisation charge data were collected with a integrator. A standard three-electrode 10 mL cell was used, consisting of glassy carbon electrode or PXV or PPy/ligand coated CME as working electrode, a platinum wire counter electrode and a saturated calomel reference electrode (SCE) which was placed in a compartment containing buffer and separated from the analyte solution by a Vycor tip.

Synthesis and purification of polyxylylviogen

Polyxylylviologen (PXV) was prepared by reacting equimolar amounts of 4,4'-bipyridyl (Aldrich) and α,α'-dichloro-*p*-xylene (Aldrich) in 5% concentration in dry acetonitrile at room temperature for 18 hours. The product precipitates out as the Cl^- salt[95].

Poly-(4,4'-dipyridyl-*p*-xylene) dichloride, $(PXV)Cl_2$, was dissolved in a small volume of water and a saturated solution of KPF_6 was added dropwise. The PF_6^- salt precipitated out. Part of this was retained and the remainder was dissolved in CH_3CN and was reprecipitated as the Cl^- salt by adding an CH_3CN solution of tetraethylammonium chloride. The polymeric viologen dichloride was then characterized by 'H NMR (300 MHz D_20) which gave a similar result to that reported by Greager and Fox[101].

Synthesis of 1,2-dihydroxynaphthalene-4-sulphonate

1,2-dihydroxynaphthalene-4-sulphonate (1,2-DHNS) was synthesized by electrochemical reduction of potassium 1,2-naphthoquinone-4-sulphonate (KQ). The reduction was performed coulometrically at 0.0 V (vs. SCE) and followed with a charge integrating meter. The solution containing KQ (0.5 M) and $HClO_4$ (0.1 M) was placed in the cell shown in Figure 3.3 and the solution was deoxygenated with nitrogen and electrolyzed while continuing the N_2 bubbing. The current was measured as a function of time. The current decreased exponentially with time, and when it reached 1% of its initial value, the charge passed corresponded to 97% reduction.

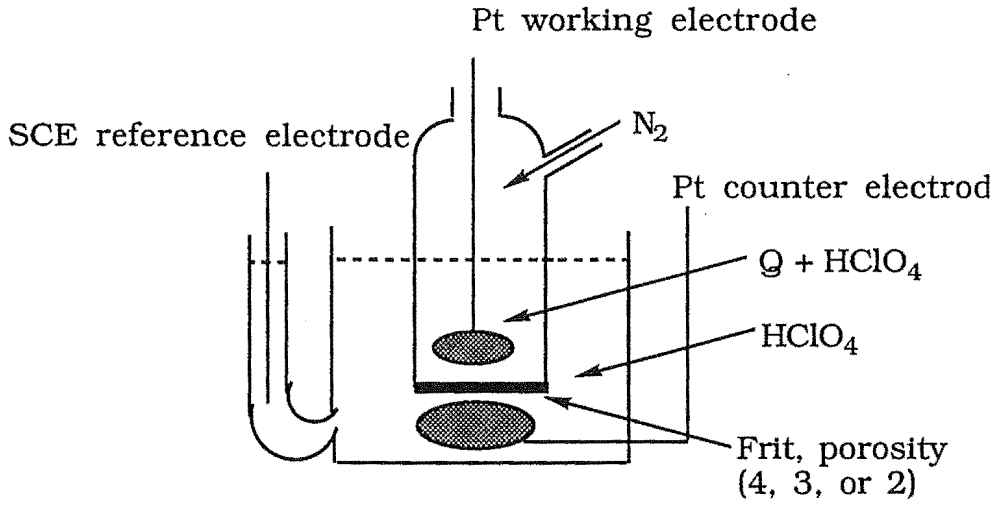

Figure 3.3. Diagram of cell used in the synthesis of 1,2-dihydroxynaphthalene-4-sulphonate.

3.3. SURVEY OF POSSIBLE REDOX ACTIVE LIGANDS FOR ALUMINIUM(III)

The electrochemistry of the ligands and their aluminium(III) complexes was examined using cyclic voltammetry at a glassy carbon electrode and the results are summarised in Table 3.2. In the discussion below, electrode processes are described as reversible or irreversible on the basis of the chemical stability of the redox forms.

Generally, the pH and buffer used were those found by other workers to optimise the electrochemical response or to optimise the formation of aluminium(III)-ligand complexes.

Table 3.2 (continued)

ligand	concentration (M)	buffer	pH	scan rate (mV s^{-1})	oxidation E_p^a (V vs SCE)	E_p^c	$E_{1/2}$	reduction E_p^c (V vs SCE)	E_p^a	$E_{1/2}$	with added Al(III) [Al(III)] (M)	oxidation E_p^a (V vs SCE)	
1,2-DHNS	1×10^{-3}	NaAc-HAc	5.0	100	0.33	-0.08	c				3×10^{-4}		b
2,3-DHNS	1×10^{-3}	NaAc-HAc	4.5	100	0.58	0.50	c				2×10^{-4}		b
	1×10^{-3}	NH_4Ac	7.0	100	0.45	0.40	c				2×10^{-4}		b
	1×10^{-3}	NH_4Cl-NH_3	8.6	100	0.36	0.30	c				2×10^{-4}		b
PCV	1×10^{-3}	NaAc-HAc	4.5	50	0.38			-0.62	-0.55	-0.59	2×10^{-4}	b	0.66
	1×10^{-3}	NH_4Ac	6.5	50	0.25			-0.75	-0.69	-0.72	2×10^{-4}	b	0.66
catechol	1×10^{-3}	NaAc-HAc	4.5	50	0.50	0.25	c						
		NH_4Cl-NH_3	8.9	50	0.11	-0.05	c				2×10^{-4}		0.29
tiron	1×10^{-3}	NH_4Cl-NH_3	8.5	50	0.26	0.20	c				1×10^{-4}		0.58
4-Ncat	2×10^{-4}	NH_4Cl-NH_3	8.5	50	0.27	0.20	c				1×10^{-5}		0.55

a. 0.1 M Tetra-n-butylammonium perchlorate. b. No shift in potential observed with added aluminium(III). c. $i_p^a/i_p^c >> 1$

Table 3.2. The electrochemistry of the ligands and their aluminium(III) complexes at glassy carbon

ligand	concentration (M)	buffer	pH	scan rate ($mV\ s^{-1}$)	oxidation E_p^a (V vs SCE)	oxidation E_p^c (V vs SCE)	oxidation $E_{1/2}$ (V vs SCE)	reduction E_p^c (V vs SCE)	reduction E_p^a (V vs SCE)	reduction $E_{1/2}$ (V vs SCE)	with added Al(III) [Al(III)] (M)	with added Al(III) reduction E_p^c (V vs SCE)	with added Al(III) oxidation E_p^a (V vs SCE)
SVRS	1×10^{-3}	NaAc-HAc	4.5	100	0.57			-0.50			3×10^{-4}	-0.79	0.92
	5×10^{-4}	NH_4Cl-NH_3	8.5	100	0.26			-0.66			1×10^{-4}	b	0.76
DASA	1×10^{-3}	NaAc-HAc	4.5	100	0.55			-0.42	-0.37	-0.40	3×10^{-4}	b	0.88
		NH_4Cl-NH_3	8.6	100	0.25			-0.70	-0.65	-0.68	3×10^{-4}	b	0.80
alizarin	5×10^{-3}	(DMF + TBAP)[a]		100	0.29	0.22	c	-0.65					
CAS	1×10^{-3}	NaAc-HAc	4.5	100				-0.50	-0.30	-0.40	3×10^{-4}	b	
Ch-2R	1×10^{-3}	NaAc-HAc	4.4	100				-0.59			3×10^{-4}	b	

3.3.1. Solochrome Voilet RS (SVRS)

Figure 3.4 shows the cyclic voltammograms of SVRS and SVRS with added aluminium(III) at pH 4.5, acetate buffer. On addition of aluminium(III), with heating to 60 °C for 5 minutes, there is a decrease in the ligand reduction and oxidation peaks and the appearance of new peaks due to reduction and oxidation of the complex.

The ligand reduction process involves the azo group as mentioned in Chapter One. Oxidation of SVRS may involve formation of an azoxy derivative, however formation of a quinoid structure cannot be discounted[96]. Aluminium(III) coordinates to the azo and *o,o'*-dihydroxy groups and hence the shift in peak potentials is related to the stoichiometries and stability constants of the complexes with each redox form of SVRS.

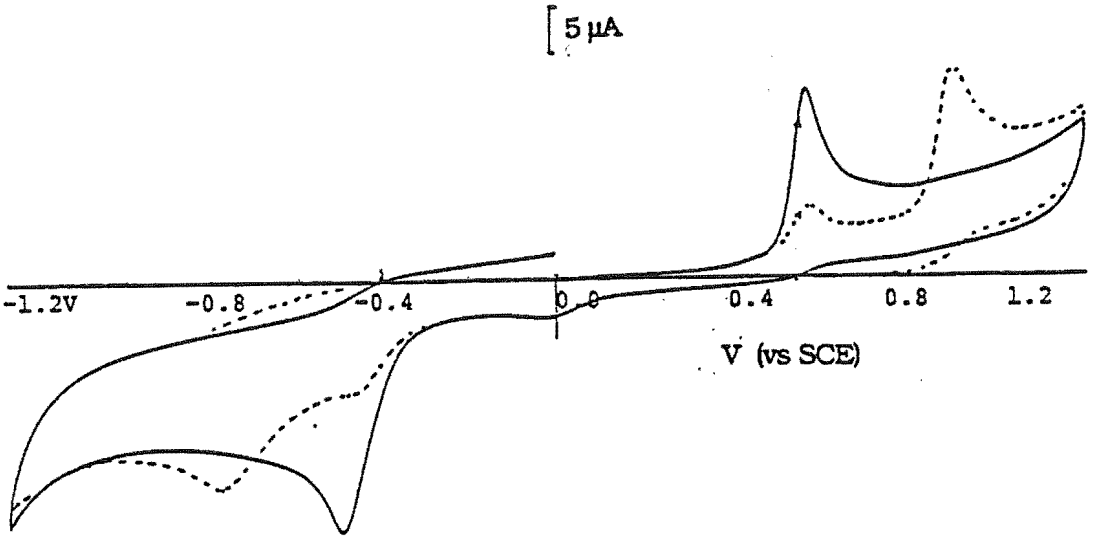

Figure 3.4. Cyclic voltammograms (100 mV s^{-1}) of SVRS (1 x 10^{-3} M) in sodium acetate-acetic acid buffer, pH 4.5, at glassy carbon: (solid line) absence of aluminium(III) and (dashed line) 1 x 10^{-4} M aluminium(III).

3.3.2. 1,2-dihydroxyanthraquinone-3-sulphonate (DASA)

Figure 3.5. shows cyclic voltammograms for DASA and its aluminium(III) complex in pH 4.5 acetate buffer. On addition of aluminium(III) there is a decrease in the current for the reduction process but no new peak due to the reduction of aluminium(III)-DASA complex. The reduction process is described by:

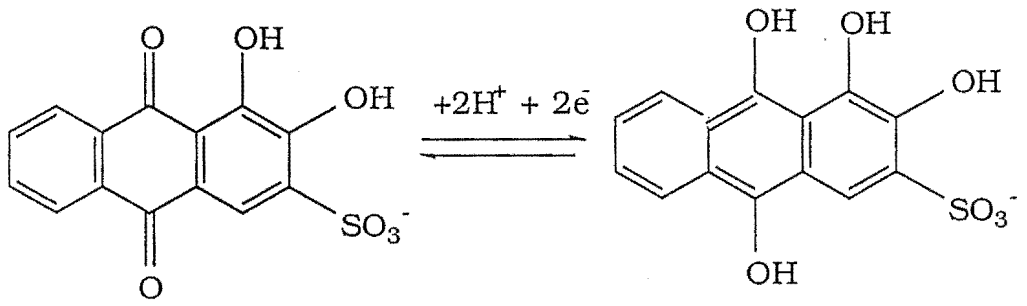

[1] [2]

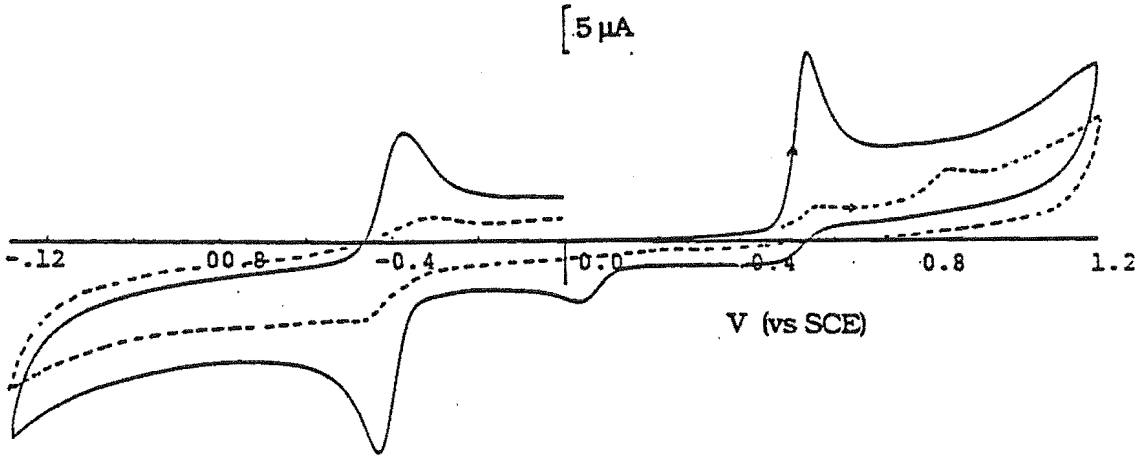

Figure 3.5. Cyclic voltammograms (100 mV s^{-1}) of DASA (1 x 10^{-3} M) in sodium acetate-acetic acid buffer, pH 4.5, at glassy carbon electrode: (solid line) absence of aluminium(III) and (dashed line) addition of 1 x 10^{-4} M aluminium(III).

Aluminium(III) is bound through the phenolic oxygens. It is assumed that the stabilities of the aluminium(III) complex with the reduced (structure [2]) and oxidised ligand (structure [1]) are very similar and hence there is no measurable shift in potential. The decrease in peak height may be due to either the smaller diffusion coefficient for the complex compared to the free ligand or slower electron transfer kinetics for the complex.

For oxidation of the ligand, there is a shift in potential on complexation. The oxidation process is described by:

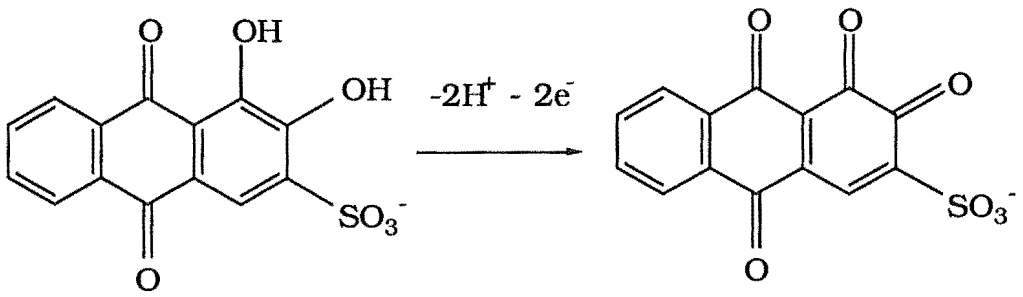

[1] [3]

Aluminium(III) is bound through the phenolic oxygens in the reduced form (structure [1]) of the ligand and is most likely not complexed by the oxidised ligand (structure [3]). For this case the shift in oxidation potential is expected to be related to the stability constant of the complex.

3.3.3. Chromotrope 2R (Ch-2R)

Ch-2R reacts rapidly with aluminium(III) in acetate buffer, pH 4.5, undergoing a colour change from orange to purple. The ligand exhibits an irreversible reduction peak, which is unchanged in the presence of aluminium(III). There are no oxidation processes. Reduction involves the azo group which is not positioned for significant

interaction with the metal bound to the phenolic groups and hence little change in stability constant would be expected on reduction of the ligand. Oxidation of the azo group must occur at a potential more positive than the solvent limit. This is in agreement with previous work on azo compounds which demonstrated that strongly electron donating groups must be present before oxidation can be observed[97].

3.3.4. 1,2-dihydroxynaphthalene-4-sulphonate (1,2-DHNS) and 2,3-dihydroxynaphthalene-6-sulphonate (2,3-DHNS)

1,2-dihydroxynaphthalene-4-sulphonate was generated coulometrically from 1,2-naphthoquinone-4-sulphonate. It has been reported that in the aluminium(III)-(1,2-naphthoquinone-4-sulphonate) system, complexes do not form, whereas in the aluminium(III)-(1,2-dihydroxynaphthalene-4-sulphonate) system, stable aluminium(III) complexes are formed[92,93]. This ligand shows reversible electrochemistry. In preliminary experiments changes occurred in the UV-visible spectrum when aluminium(III) was added to the ligand solution (a shoulder appeared at λ = 370 nm) but there was no change in the electrochemistry under the same conditions (acetate buffer, pH 5.1). These results appear inconsistent with the reported stability constants, and this system was not investigated further.

The electrochemical behaviour of 2,3-dihydroxynaphthalene-6-sulphonate (2,3-DHNS) in the absence and presence of aluminium(III) was studied. Its cyclic voltammograms show instability of the oxidised form at all pH values studied (4.5, 7.0 and 8.6). With added aluminium(III) there was no change in the electrochemistry.

3.3.5. Chrome azurol S (CAS)

The electrochemistry of CAS was investigated and its cyclic voltammogram shows a reversible redox process which can reasonably be assigned to the process:

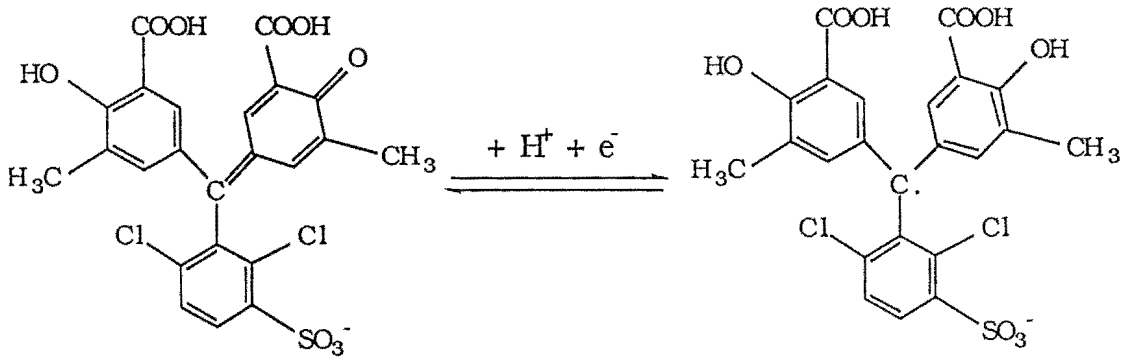

This assignment is consistent with that proposed in a detailed electrochemical study of some closely related sulphonephthalein compounds[98,99]. In the presence of aluminium(III) there was no change in the electrochemistry, although a colour change from amber to red-purple indicated formation of an aluminium(III) complex.

3.3.6. Pyrocatechol violet (PCV)

Figure 3.6 shows cyclic voltammograms of pyrocatechol violet (PCV) and its aluminium(III) complex in acetate buffer, pH 4.5. There is a reversible reduction process which is assigned to the reaction:

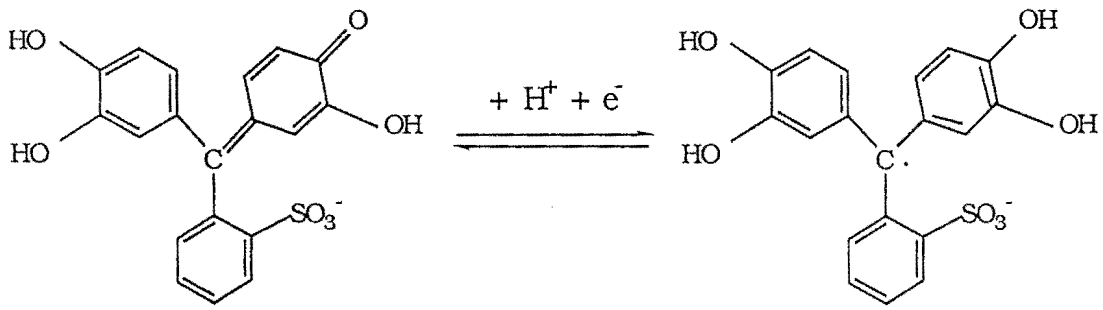

There is no change in the reduction process in the presence of aluminium(III). There is an irreversible oxidation process which is assigned to:

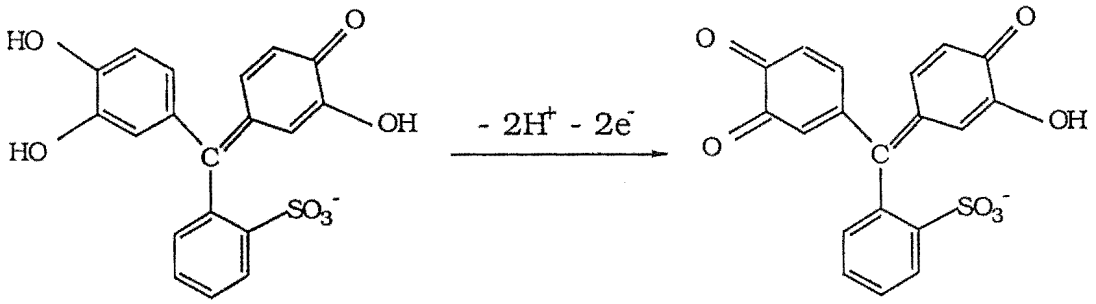

In the presence of aluminium(III) there is a new oxidation peak. At a higher pH (pH 6.5), the peak due to complexed PCV is larger indicating more complex formation.

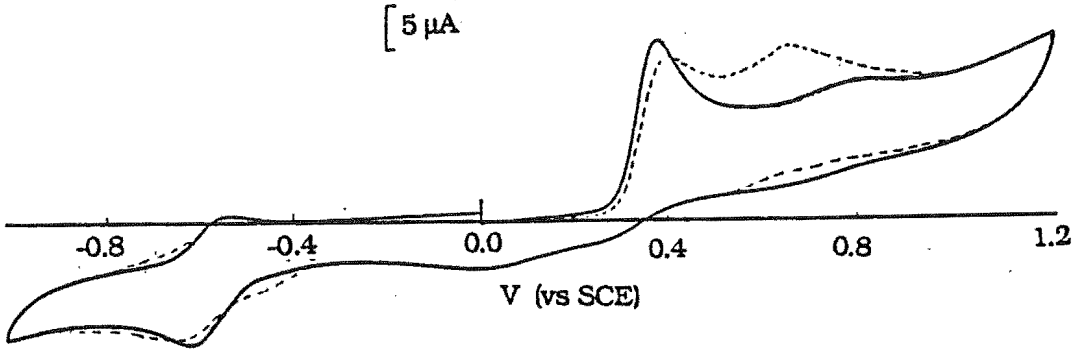

Figure 3.6. Cyclic voltammograms (50 mV s^{-1}) of PCV (1 x 10^{-3} M) in sodium acetate-acetic acid buffer, pH 4.5, at glassy carbon: (solid line) absence of aluminium(III) and (dashed line) presence of 1 x 10^{-4} M aluminium(III).

3.3.7. Catechol, tiron and 4-nitrocatechol

The electrochemistry of catechol was discussed in detail in Chapter One. However, the electrochemistry of aluminium(III)-catechol complexes has not been reported. The electrochemistry of catechol in the presence of aluminium(III) at a range of pH values was studied using cyclic voltammetry. Figure 3.7 shows the voltammograms of catechol and its aluminium(III) complexes in sodium acetate-acetic acid buffer (pH 4.5) and in ammonia-ammonium chloride buffer (pH 8.5) on glassy carbon. In acidic solution the electrochemical reversibility of catechol is greater than in basic solution; this is in agreement the dependence of oxidation rate on proton concentration. At pH 4.5, addition of aluminium(III) to catechol leads to a small decrease in peak currents but no shift in peak potentials. This indicates formation of a complex with a smaller diffusion coefficient than that of catechol itself, but with low stability, hence no shift in potential is observed. The electrochemistry of catechol and aluminium(III)-catechol in the pH range of 8 to 10 was studied in detail. A separate oxidation process due to an aluminium(III) complex is observed and the influence of pH on potential shift, ΔE_p^a ($\Delta E_p^a = |E_p^a{}_{ligand} - E_p^a{}_{complex}|$), is shown in Figure 3.8.

Tiron and 4-nitrocatechol have similar electrochemistry to catechol. Figure 3.9 shows the cyclic voltammograms of 4-nitrocatechol. Both ligands exhibit irreversible redox processes at basic pH. On the addition of aluminium(III), aluminium(III)-tiron and aluminium(III)-(4-nitrocatechol) complexes yield oxidation peaks at more positive potentials than the ligand itself.

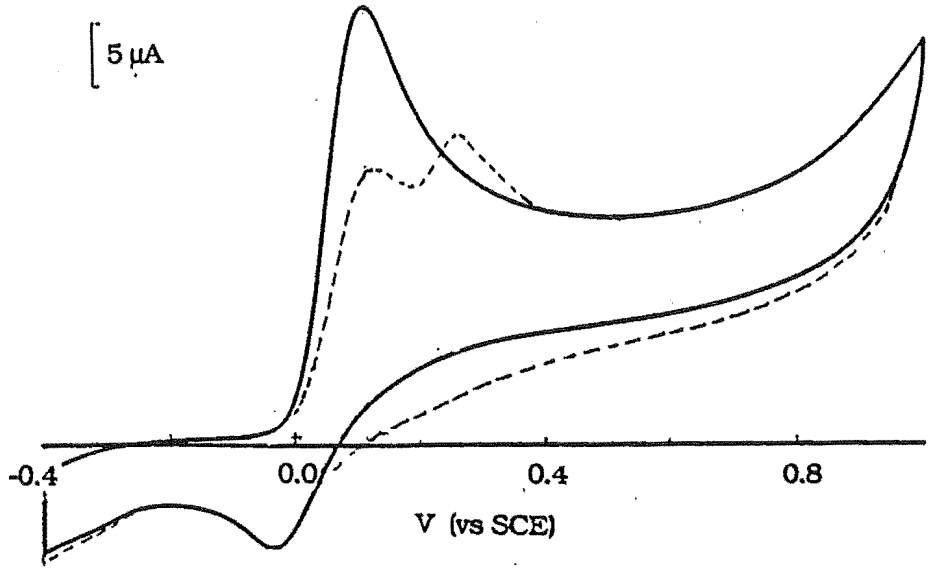

Figure 3.7. Cyclic voltammograms (100 mV s^{-1}) of catechol (1 x 10^{-3} M) (solid line) in the absence of aluminium(III) and (dashed line) presence of 1 x 10^{-4} M aluminium(III) in ammonium chloride-ammonia buffer (pH 8.5) at glassy carbon.

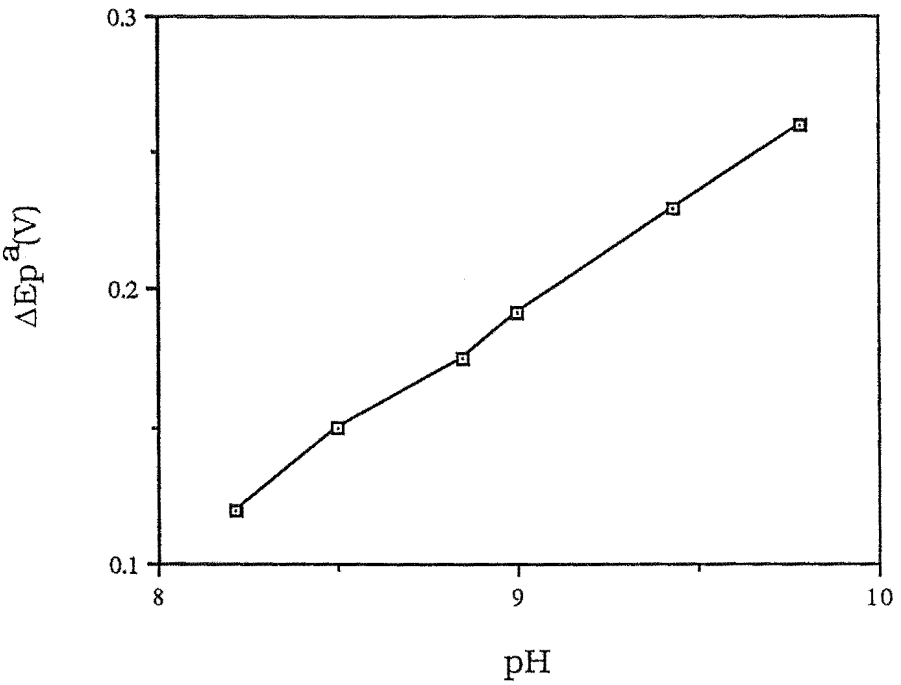

Figure 3.8. Effect of pH on ΔE_p (difference in oxidation potentials between catechol and aluminium(III)-catechol complex).

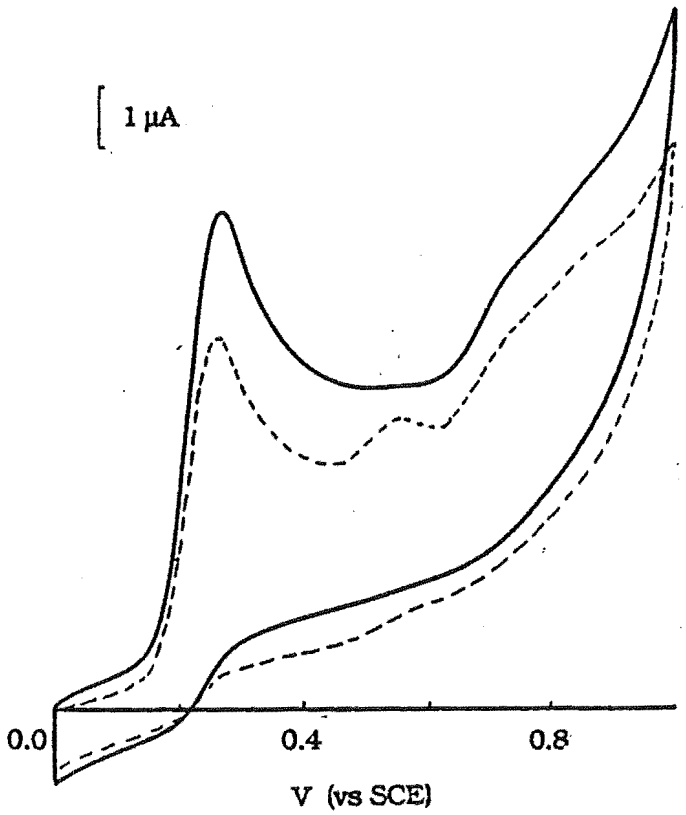

Figure 3.9. Cyclic voltammograms (100 mV s^{-1}) of (solid line) 4-nitrocatechol (2 x 10^{-4}M) and (dashed line) its aluminium(III) complexes in ammonium chloride-ammonia buffer (pH 8.5) at glassy carbon.

3.4. POLYXYLYLVIOLOGEN MODIFIED ELECTRODES

Viologen polyers have received considerable attention recently. Various types of viologen polymers have been prepared which have a viologen structure as a pendant group or in the main chain. An example of the later type is polyxylylviologen (PXV) as shown below[100].

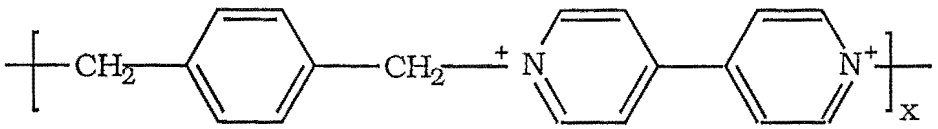

They have been used in chemically modified electrodes as anion-exchange polymers. The coating employed can be used to provide a surface that is capable of efficient pre-concentration. Polyxylylviologen was chosen as the ion-exchange medium in this work because of its charge density, the ease of preparation and deposition and because its redox response occurs at considerably more negative potentials than the oxidation processes of the ligands described above.

3.4.1. Preparation and characterisation of PXV electrodes

Coating PXV on the glassy carbon electrode

The synthesis of the polymer is straightforward and is described in section 3.2.

Several methods have been used to adsorb PXV on glassy carbon electrodes[101]. Adsorption from aqueous solution may be accomplished in two ways: either by a static "dip coating" or a "dynamic electrochemically assisted" procedure in which a persistent polymer film is adsorbed during cyclic voltammetric reduction of the soluble polymer. Adsorption from acetonitrile solution is by using a droplet of $(PXV)(PF_6)_2$ in acetonitrile.

Two methods were used to coat PXV onto glassy carbon electrodes in this work: (1) $(PXV)(PF_6)_2$ droplet: A PXV film was adsorbed on the electrode surface by pipetting 1-3 μL of an acetonitrile solution of $(PXV)(PF_6)_2$ onto the electrode and allowing the solvent to evaporate at room temperature. This method was easy and rapid and the coverage of the electrode was controlled by solution volume and concentration. (2) Electrochemically assisted: PXV film deposition on the glassy carbon electrode was accomplished by voltammetric cycling

of the soluble viologen polymer $(PXV)Cl_2$ in 0.1 M KCl through both the V^{2+}/V^{+} and V^{+}/V^{0} waves. Using this method, the thickness of PXV film can be controlled by controlling the scan time (about 5 minutes) and scan rate (50 mV s^{-1}). These films show good reproducibility.

Voltammetry of PXV and PXV coated electrodes

The voltammetric behaviour of 1 x 10^{-3} M $(PXV)Cl_2$ at a glassy carbon electrode in 0.1 M KCl solution shows two redox processes, $E_p^{a,1}$ = -0.37 V, $E_p^{c,1}$ = -0.38 V, $E_p^{a,2}$ = -0.77 V and $E_p^{c,2}$ = -0.94 V vs SCE (scan rate = 50 mV s^{-1}).

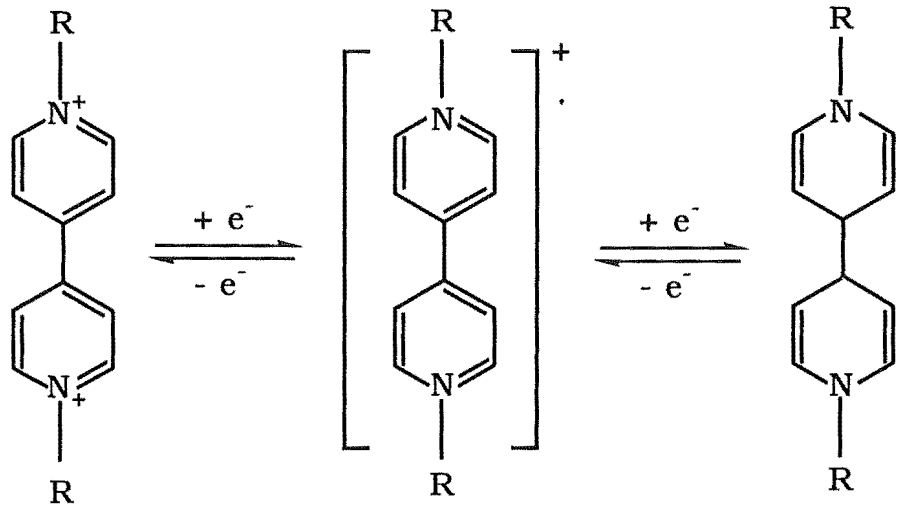

R = C_6H_4-CH_2

Figure 3.10 (a) shows the formation of an irreversibly adsorbed film on glassy carbon during voltammetric cycling of the $(PXV)Cl_2$ through the two redox processes. A narrow shoulder begins to grow on the side of the V^{2+}/V^{+} peak on continued cycling through the V^{+}/V^{0} couple. The maximum adsorption was usually reached within 15-20 scans (about 5 minutes). Figure 3.10 (b) shows repetitive

voltammograms at a scan rate of 50 mV s^{-1} in 0.1 M KCl solution of the resultant PXV coated electrode.

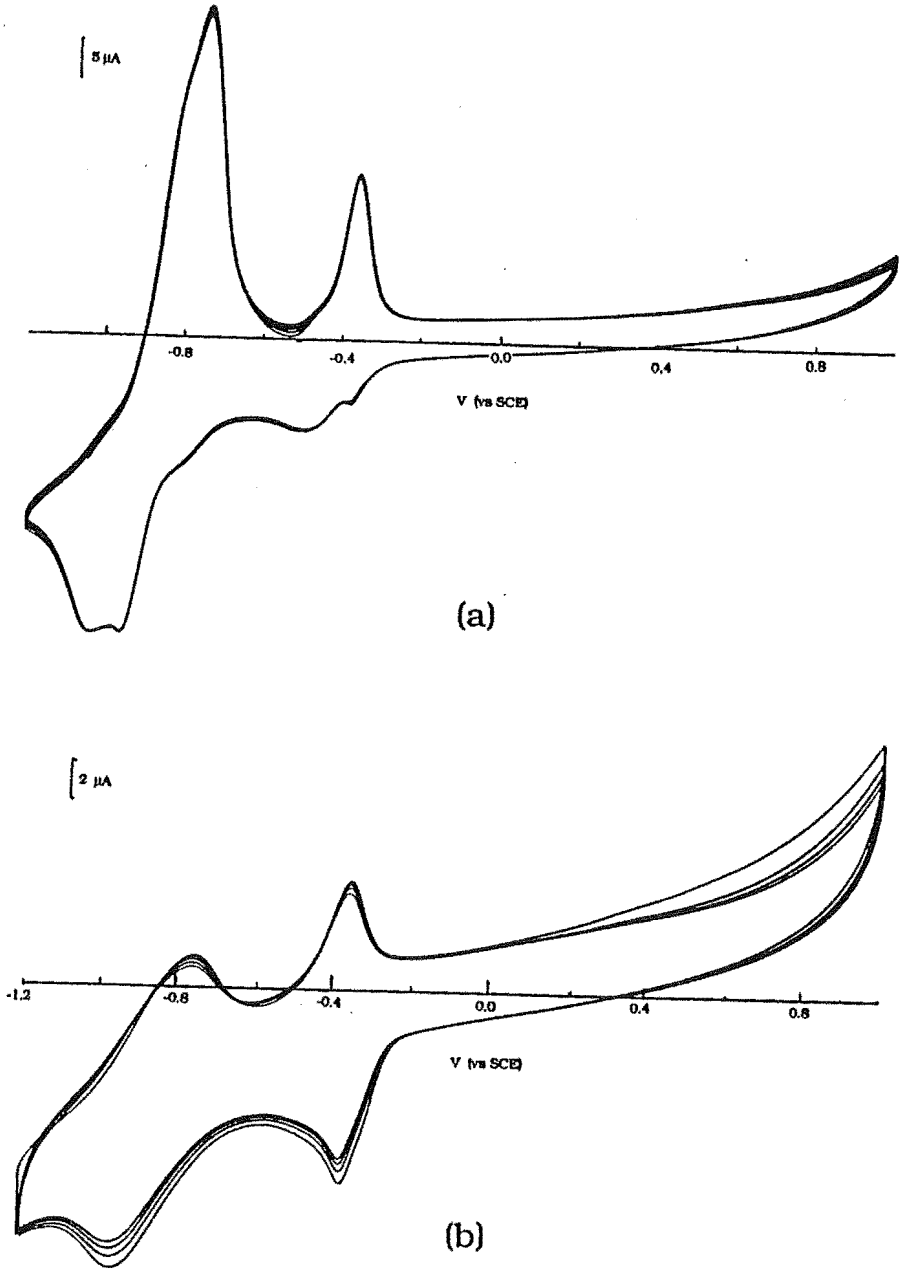

Figure 3.10. (a) cyclic voltammograms (50 mV s^{-1}) of $(PXV)Cl_2$ (1 x 10^{-3} M) in 0.1 M KCl solution at glassy carbon and (b) cyclic voltammograms of PXV coated electrode in 0.1 M KCl solution.

Much larger surface coverages could be achieved using the drop coating method, however dip-coating from a 1 x 10^{-3} M solution of $(PXV)Cl_2$ gave very low coverages even after 6 hours of soaking. This latter method was not used for electrode preparation.

The surface coverages of electrodes were determined by recording a CV at 10 mV s^{-1} and measuring the charge, Q, associated with the reduction step:

$$V^{2+} \xrightarrow{+ e^-} V^+$$

The surface coverage in moles of viologen groups per cm^2 is given by:

$$\Gamma = Q/nFA$$

3.5. INCORPORATION OF LIGANDS AND METAL COMPLEXES INTO PXV MODIFIED ELECTRODES

3.5.1. Incorporation of anionic ligands

Several methods were employed to incorporate ligands in PXV films: (1) the electrode with a PXV coating was soaked in a 1 x 10^{-3} M ligand solution for times ranging from several minutes to several hours; (2) the PXV coated electrode was scanned in 1 x 10^{-3} M ligand solution; (3) aqueous ligand solution was dropped onto the PXV coated electrode surface. After each of these treatments, the electrode was rinsed with distilled water and transferred to the ammonium acetate-ammonia buffer solution, pH 8.5.

PCV, SVRS and DASA were incorporated into a PXV film using method (1). Soaking the PXV-ligand electrode in buffer solution for times ranging from 1 to 10 minutes, followed by an oxidative scan, indicated that ligand is continuously lost from the electrode during soaking. Repetitive cyclic voltammograms in the buffer solution of the PXV-ligand electrodes also showed a continuous decrease in oxidation peak currents. Repeat scans over the same time periods as above, resulted in a greater loss in signal than that observed after simply soaking the electrode. Figure 3.11 shows the response for DASA. The decrease in peak current must result from diffusion of ligand out of the PXV film and/or loss of PXV film from the electrode and decomposition of ligand following oxidation.

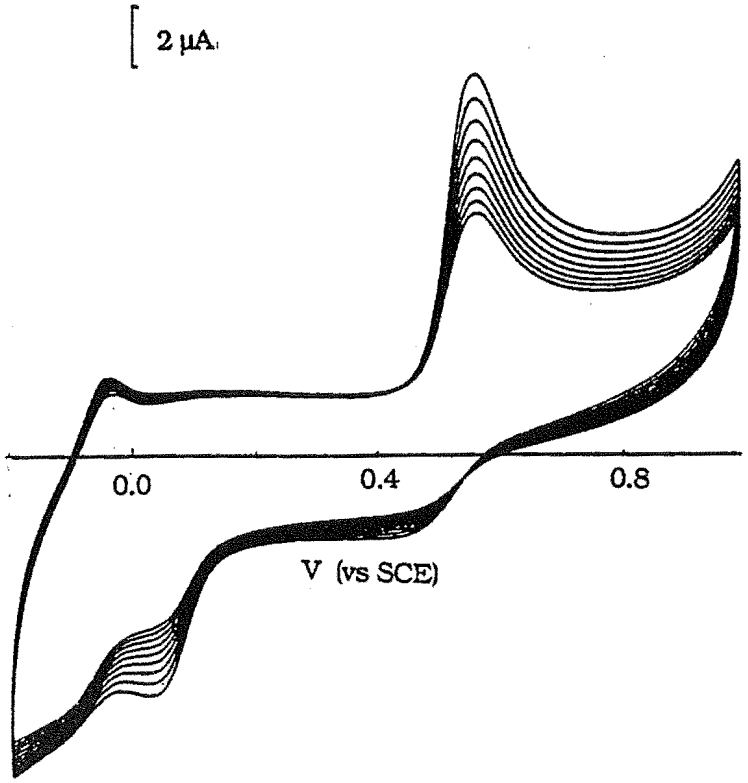

Figure 3.11. Cyclic voltammograms (100 mV s^{-1}) of DASA in the PXV film electrode in acetate buffer (pH 4.5).

The PXV-DASA electrode was soaked in ammonium chloride-ammonia buffer (pH 8.5) in the presence of aluminium(III). No new oxidation peak due to an aluminium(III)-DASA complex was observed. This result and the observed instability of the ligand response make the proposed method for determination of aluminium(III) impractical. This work was not continued.

3.5.2. Incorporation of aluminium(III)-ligand complexes

These experiments were based on the adsorption of anionic aluminium(III)-ligand complexes on the PXV polymer.

Two methods were used in these experiments. (1) The PXV coated electrode at open circuit was soaked in a stirred solution of metal complex for the required time, followed by a 30 second rest period. A cyclic voltammogram or differential pulse voltammogram was then recorded in the same solution. (2) After the soaking and rest period described above, the electrode was rinsed with distilled water and transferred to a buffer solution for analysis by cyclic voltammetry or differential pulse voltammetry.

Adsorption of tiron and catechol and their aluminium(III) complexes on the PXV coated electrodes

The adsorption of catechol, tiron and their aluminium(III) complexes on the PXV coated electrodes was tested. Figure 3.12 shows cyclic voltammograms for the ligands and their aluminium(III) complexes at coated (solid line) and bare (dotted line) glassy carbon electrodes in ammonium actetate-ammonia buffer, pH 8.5. As can be seen in Figure 3.12(a) the cationic PXV film effectively adsorbs the anionic ligand, tiron; the peak height is 4-5 times higher than that on the bare glassy carbon electrode. For the neutral catechol, however, there is no evidence of adsorption. In contrast, aluminium(III)-catechol complexes show strong adsorption on the PXV electrode. The adsorbed complexes must be negatively charged and calculations using the program SIAS and stability constants reported by Kennedy and Powell[102] indicate that for 1 x 10^{-5} M aluminium(III) and 1 x 10^{-4} M catechol at pH 8.5 the distribution of complexes is: $Al(catechol)^{+}$: 0.004%; $Al(catechol)_2^{-}$: 26.82%; Al(catechol)OH: 10.96% and $Al(catechol)(OH)_2^{-}$: 58.67%. Aluminium(III)-tiron complexes exhibit no response on the PXV electrode. This suggests that the aluminium(III)-tiron complexes are not able to enter the film or do not reach the

glassy carbon electrode surface or can not compete with charged ligands for the adsorption sites. This may be due to the large size of the complexes or to crosslinking in the outer part of the film by sulphonate groups which blocks further accumulation of complex.

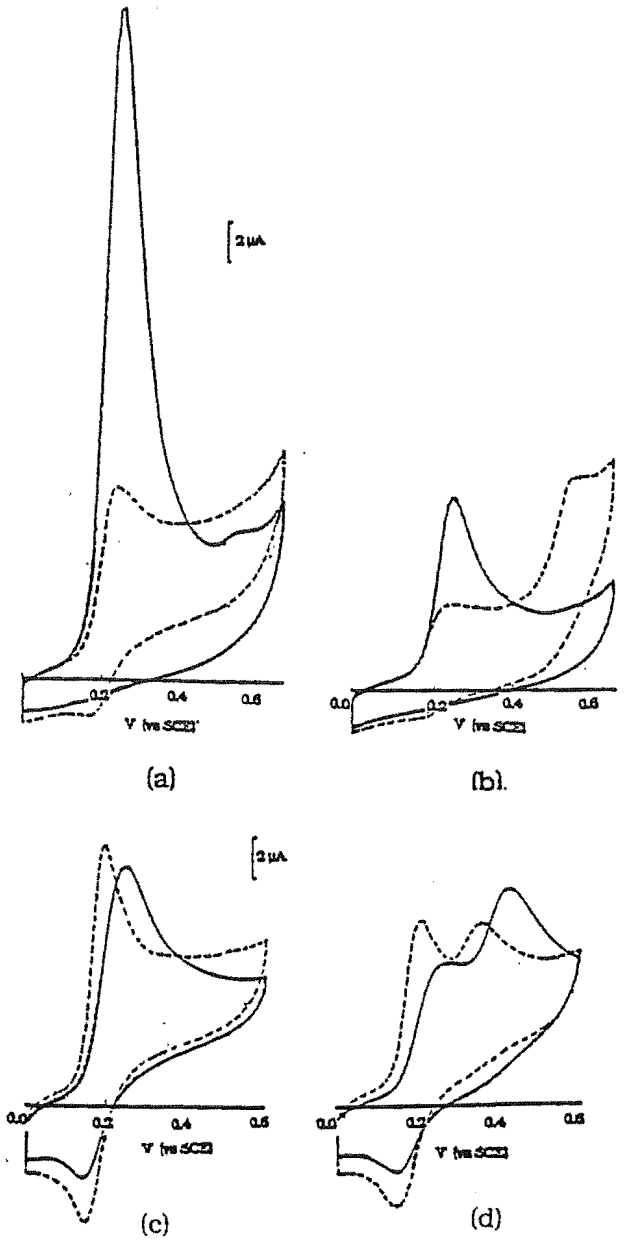

Figure 3.12. Cyclic voltammograms (50 mV s^{-1}) of (a) 4 x 10^{-4} M tiron and (b) 4 x 10^{-4} M tiron and 8 x 10^{-5} M aluminium(III); (c) 4 x 10^{-4} M catechol and (d) 4 x 10^{-4} M catechol and 8 x 10^{-5} M aluminium(III) in ammonium acetate-ammonia buffer at PXV coated (solid lines) and bare (dashed lines) glassy carbon electrodes.

Aluminium(III) on PXV as the catechol complex

Since aluminium(III)-catechol complexes adsorb strongly on the PXV film, the PXV coated electrode can be used for the analysis of aluminium(III).

Each coated electrode can only be used once (see below) therefore reproducible preparation of the PXV film is required. Using 1.5 μL of a 0.025 M $(PXV)(PF_6)_2$ solution in acetonitrile, the drop-coating procedure for preparation of the CME gave a reproducible surface coverage of 1.5×10^{-8} mol cm^{-2} based on the geometric area of the glassy carbon electrode. The sensitivity was dependent on the PXV concentration and volume of solution (Figure 3.13). A 1.5 μL aliquot of 0.025 M PXV solution gave good sensitivity and reproducibility.

For determination of adsorbed aluminium(III) complex, the cyclic voltammetric (CV) mode was found to give greater sensitivity than differential pulse voltammetric mode and a scan rate of 50 mV s^{-1} was used in cyclic voltammetric measurements. The peak height for the complex increased with accumulation time (Figure 3.14) and 2 minutes was chosen as the standard time. Deoxygenation of solutions in the electrochemical cell prior to analysis had no effect on measurements.

A catechol concentration of 1×10^{-5} M was used in these experiments. Higher concentrations of ligand increase the concentration of complex but also make the measurement of the complex peak more difficult. The best compromise was achieved with 1×10^{-5} M catechol.

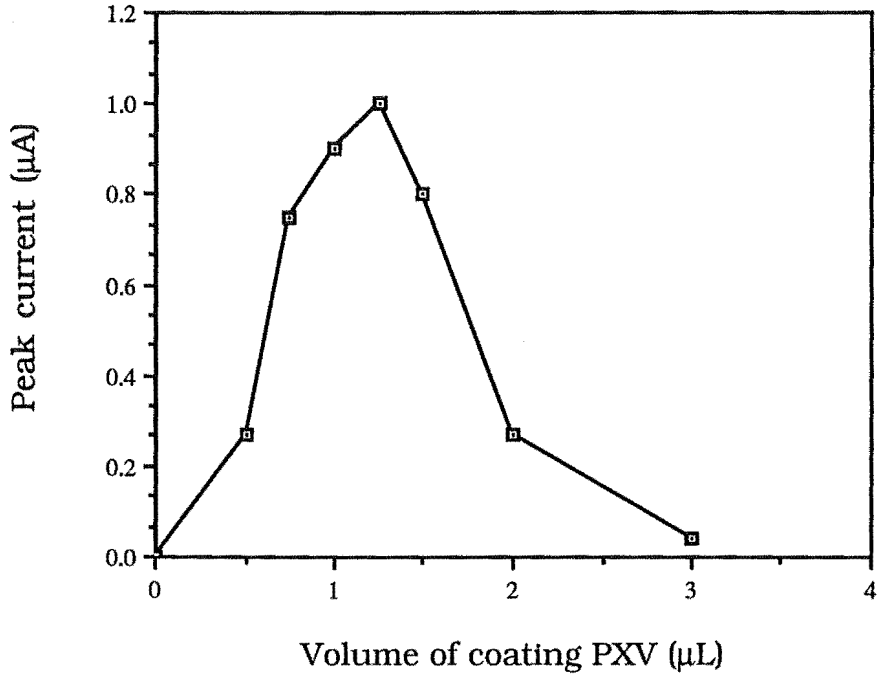

Figure 3.13. Dependence of aluminium(III)-catechol peak current (CV) on volume of PXV coating solutions. [catechol]: 1 x 10^{-5} M; [aluminium(III)]: 4 x 10^{-6} M; [$(PXV)(PF_6)_2$]: 0.025 M.

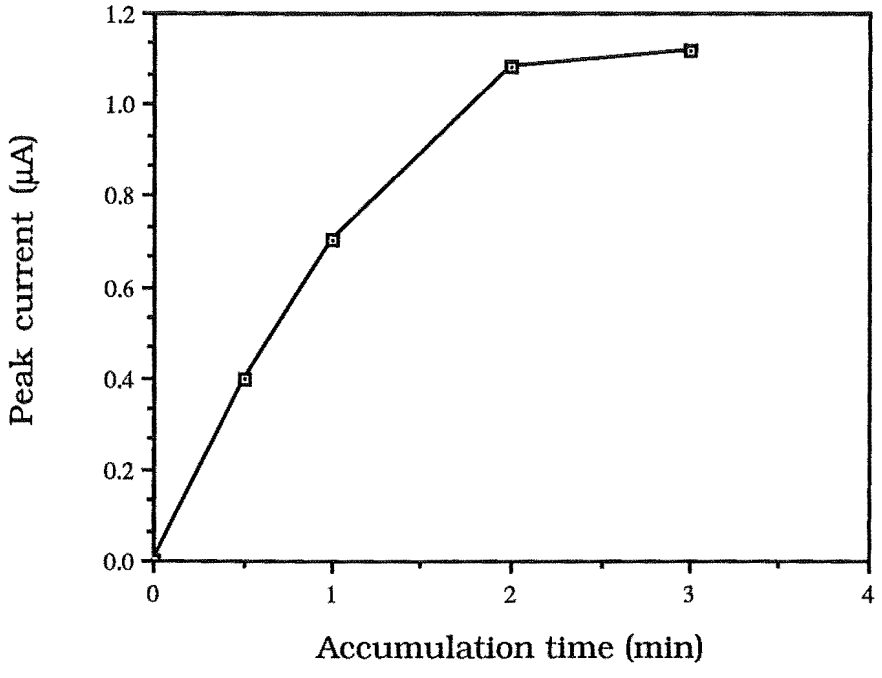

Figure 3.14. Effect of accumulation time on aluminium(III)-catechol peak current. [catechol]: 1 x 10^{-5} M; [aluminium(III)]: 4 x 10^{-6}M.

Figure 3.15 shows the variation of i_p (CV) for the complex with aluminium(III) concentration in the range 2 x 10^{-6} - 8 x 10^{-6} M. Below a concentration of 1.0 x 10^{-6} aluminium(III) the effect of preconcentration is not significant. The concentration of aluminium(III)-catechol complexes formed under these conditions was calculated with the program SIAS. The results in Table 3.3 show that less than 10% of total aluminium(III) is complexed by catechol giving a total complex concentration of less than 8.2 x 10^{-8} M.

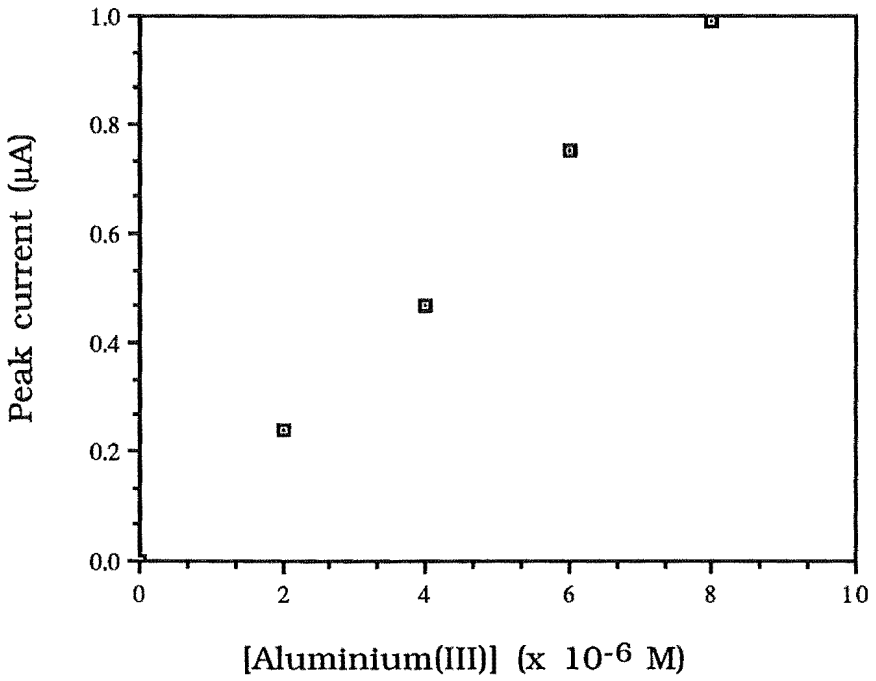

Figure 3.15. The dependent of peak current (CV) for aluminium(III)-catechol complexes with aluminium(III) concentration.

These experiments demonstrate the principle of using a ligand and complex with different charges (neutral and anionic respectively) to selectively preconcentrate the complex for analysis. However, the

relatively low stability of the catechol complexes gives a low sensitivity for aluminium(III) and limits the use of this system.

Table 3.3. Formation of aluminium(III) complexes for 1 x 10^{-5} M catechol and 1 x 10^{-6} M aluminium(III) at pH 8.5 calculated by SIAS program

Complexes	% reaction	Concentration
Al-catechol^{+}	3.3 x 10^{-3}	3.3 x 10^{-11}
Al-(catechol)$_2^{-}$	2.6	2.6 x 10^{-8}
Al-catechol-OH	8.8 x 10^{-1}	8.8 x 10^{-9}
Al-catechol-(OH)$_2^{-}$	5.6	5.6 x 10^{-8}

Adsorption of aluminium(III)-(4-nitrocatechol) complex on the PXV coated electrodes

It is expected that 4-nitrocatechol may form more stable aluminium(III) complexes than catechol due to the electron-withdrawing nitro group. Using the same experimental conditions (buffer, pH, ligand concentration, PXV surface coverage and accumulation time) as described above for catechol, 4-nitrocatechol did indeed show a significantly greater sensitivity for aluminium(III). Further experiments were carried out to optimise the sensitivity.

The effects of PXV film preparation method and pretreatment of the coated electrode were examined. When determining low concentrations of aluminium(III) it was noticed that repeat measurements in the same aluminium(III)-ligand solution gave a decreasing response. This was found to be due to loss of PXV from the

electrode into solution where it binds aluminium(III)-ligand complexes. Thus, deliberate addition of PXV solution to the aluminium(III)-ligand solution also gave a decreased response. Soaking the freshly prepared PXV coated electrode in stirred buffer solution before transfer to the aluminium(III)-ligand solution overcame this problem. The stabilities of the PXV films prepared by different methods were compared. The PXV coverage of the electrode which was made by the method of drop coating decreased from $\Gamma = 1.5 \times 10^{-8}$ mol cm^{-2} to $\Gamma = 2.0 \times 10^{-10}$ mol cm^{-2} after soaking in a stirred buffer solution. The electrode which was made using the electrochemically assisted method showed a more stable PXV film, but surface coverage still decreased from $\Gamma = 3.4 \times 10^{-9}$ mol cm^{-2} to $\Gamma = 6.0 \times 10^{-10}$ mol cm^{-2} after soaking. Since electrochemical preparation is more complex than drop coating, for the standard procedure the electrodes were made by drop coating, followed by soaking in a buffer solution for 2 minutes.

A 4-nitrocatechol concentration of 2×10^{-5} M represented the best compromise between amount of complex formation and ease of measurement of peak currents. A standard accumulation time of 2 minutes at open circuit was used.

Figure 3.16 shows the variation of i_p for oxidation of the 4-nitrocatechol-aluminium(III) complex with aluminium(III) concentration in the range of 2.5×10^{-7} - 5.0×10^{-6} M on a drop coated electrode. The linear range is 2.5×10^{-7} - 3.0×10^{-6} M. On a PXV coating prepared by the electrochemically assisted method, the linear range is 2.5×10^{-7} - 7.0×10^{-6} M aluminium(III).

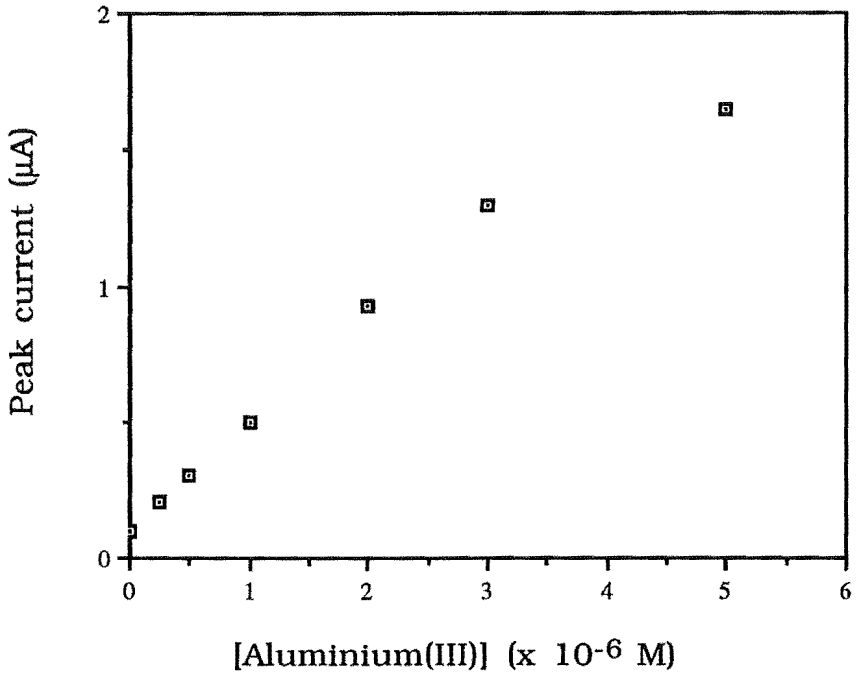

Figure 3.16. The variation of peak current (CV) for oxidation of the 4-nitrocatechol-aluminium(III) complex with aluminium(III) concentration.

Re-use of electrodes

Complexation by 4-nitrocatechol and accumulation at the PXV coated electrodes offers a sensitive method for aluminium(III) determination. A disadvantage of the method is that each modified electrode can only be used for one measurement. Hence the possibility of multiple use of the electrode was investigated in further experiments. After the first measurement, the PXV coated electrode was washed with distilled water and soaked in a stirred buffer solution for 2 to 5 minutes, then the measurement was repeated. The height of the peak due to the aluminium(III) complex was always lower than in the first measurement. This situation is assumed to occur not only due to loss of polymer, but also due to oxidation products fouling the electrode. Several methods were tried to limit the decrease in the

peak height resulting from the latter effect: a narrow potential range was applied during measurement of the peak height and the electrode was held at a negative potential to reduce the oxidized products formed during analysis. In each case, the results were still not satisfactory. Therefore, the PXV film coated electrodes can only be used once.

Problems due to loss of the polymer layer arise because the layer is only weakly bound to the surface of the carbon substrate by chemisorption. Several methods have been reported by other workers for improving the stability of polymer layers on electrodes[103,104]. However, as the problem of surface fouling by oxidation products could not be overcome in this work, further investigations on the problem of polymer loss were not made.

3.5.3. Conclusion

The method of exploiting the different charges on ligand and aluminium(III)-ligand complexes works well. PXV coated electrodes can selectively preconcentrate the complexes. The linear range using 4-nitrocatechol is suitable for determination of aluminium(III) in environmental samples.

The limitation of the method is that the PXV coated electrode can only be used once. Two factors lead to single use: loss of polymer coating and the irreversibility of the 4-nitrocatechol oxidation. Polymer loss might be less with a different polymer, for example, QPVP. Use of a ligand which shows reversible electrochemistry and large stability constants for aluminium(III) complexation might overcome the second problem.

3.6. POLYPYRROLE MODIFIED ELECTRODES

Electropolymerisation of pyrrole gives conducting, oxidised films (PPy) which incorporate an anion from the electrolyte. When PPy is reduced, doping anions, such as NO_3^- and Cl^- are ejected from PPy to maintain charge neutrality.

The general procedure used in these experiments was to incorporate the anionic ligand in the oxidised PPy film during polymerisation. It was anticipated that on reduction of the film, the ligand would be unable to leave the polymer (due to the large size of the ligands) and cations from the electrolyte would enter the film to maintain charge neutrality.

$$PPy^+ / L^- \underset{-\ M^{n+} - e^-}{\overset{+\ M^{n+} + e^-}{\rightleftharpoons}} PPy^0 / L^- / M^{n+}$$

Similar behaviour has been observed for other large anions. Thus $Fe(CN)_6^{3-}$[105], 1-pentanesulphonate and benzenesulphate[106] have been incorporated in PPy films during polymerisation and were found to remain in the films during reduction.

3.6.1. Preparation and characterisation of the PPy/Ligand film coated electrodes

SVRS and DASA were incorporated in PPy films during electropolymerisation of 0.1 M pyrrole in 0.01 M SVRS and DASA solutions. The amount of charge passed during the polymerisation at +0.8 V vs SCE, was monitored to control the thickness of PPy/ligand film. The electrochemistry of the PPy/SVRS and PPy/DASA films was

examined in acetate buffer, pH 4.5, at a scan rate of 50 mV s^{-1}. Cyclic voltammograms of the films (polymerisate charge: 288 mC cm^{-2}) and of PPy/NO_3^- are shown in Figure 3.17.

The electrochemical response of the PPy/ligand films is not a simple superpositioning of the PPy/NO_3^- and ligand electrochemistries (refer Figures 3.4 and 3.5). Clearly each component influences the response of the other. This effect has been noted by other workers[106].

The response of the ligands in the films showed poor reproducibility for replicate film preparations. Preparation of PPy films incorporating small anions generally show good reproducibility, hence the difficulties here may arise from the large anion size. If initiation of polymer growth is difficult, the electrode surface condition may have a significant effect on yield of polymer. A second feature of the PPy/ligand films was loss of response and shifts of peak potentials on continued scans. This may be due to structure changes in the polymer and to either ligand leaving the polymer or to decomposition of ligand after oxidation.

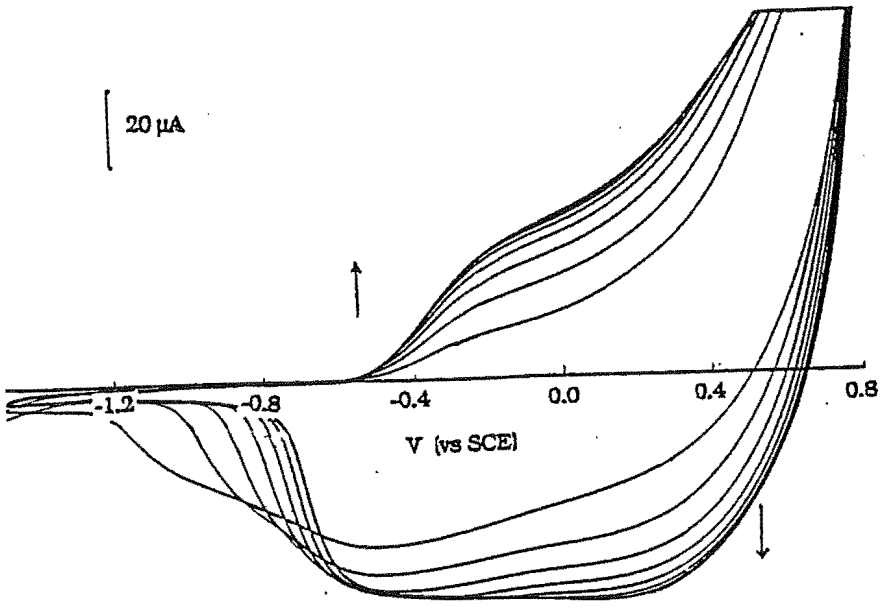

(a)

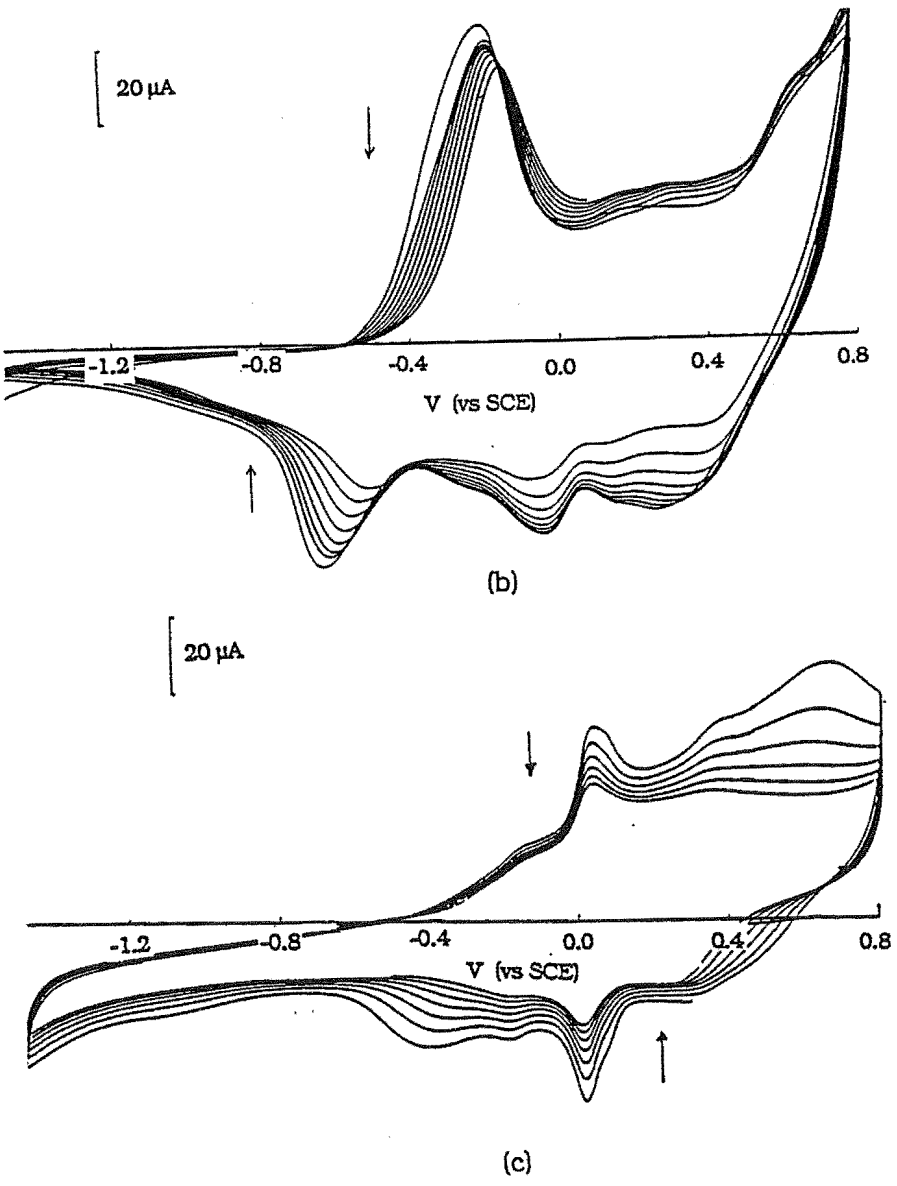

Figure 3.17. Cyclic voltammograms (50 mV s^{-1}) of (a) PPy/NO_3^- (b) PPy/DASA and (c) PPy/SVRS on glassy carbon in acetate buffer, pH 4.5.

The effect of the polymerisation charge on these problems was examined. By controlling the polymerisation time or the quantity of charge passed during polymerisation, different thickness PPy/ligand

films may be obtained. It has been shown that a polymerisation charge of 24 mC cm^{-2} leads to a film thickness of approximately 0.1 μm for a PPy/BF_4^- film[107]. For the PPy/catecholate films, oxidation of ligand must occur simultaneously with pyrrole oxidation, hence this relationship will not be valid for these films. PPy/ligand films with polymerisation charge of 19 mC cm^{-2} to 576 mC cm^{-2} were prepared. As expected, the peak height of the ligand increased with polymerisation charge. Films of different polymerisation charge were assessed for reproducibility of replicate preparations and stability of ligand response. PPy/DASA films prepared using a polymerisation charge of 288 mC cm^{-2} exhibited the best reproducibility of film coating, however, as shown in Figure 3.17(b), repeat scans lead to continuous changes in response. Similar behaviour was observed for PPy/SVRS films as shown in Figure 3.17(c). In order to prevent ligand ions from leaving the PPy film and to improve the stability of PPy/ligand electrodes, the influence of the potential scan range on film response was studied. Assuming that ligand loss occurs when the PPy is reduced, minimising reduction of the film is expected to minimise ligand loss. Secondly, changes in conductivity of the film should be minimise by limiting the amount of oxidation and reduction of the film. Repeat scans recorded over the limited potential range -0.6 to +0.4 V showed no significant improvement. Over-coating the PPy/ligand film with a layer of Nafion or PVP was also investigated as a means of preventing ligand loss. When Nafion was drop-coated onto the PPy/SVRS film surface the red colour of SVRS appeared in the Nafion. This indicates that SVRS was extracted from the PPy/SVRS film. The voltammograms of the Nafion coated PPy/SVRS film electrodes were the same as those of uncoated PPy/ligand films. Coating PVP onto PPY/ligand films also gave no improvement in response.

3.6.2. Reaction of PPy/ligand film coated electrode with aluminium(III)

Polypyrrole films undergo irreversible changes at potentials more positive than 1.0 V vs SCE[70]. Thus, the PPy/ligand electrodes were scanned only to 1.0 V. No peaks due to aluminium(III)-ligand complexes were observed within this potential limit. The decrease in the peak height of the free ligand could in principle be monitored. However, because of the poor reproducibility of film coating and changes on repeat scans, it is difficult to calibrate the electrode response and hence it is impossible to determine the decrease in the ligand peak height with sufficient precision.

3.6.3. Conclusion

Both of the PPy/ligand film-coated electrodes have the same problems. Firstly, there is a loss of signal from ligand in the PPy film indicated by a decrease in ligand peak height during continued scans. This may be due to either ligand leaving the polymer or to decomposition of ligand after oxidation. Secondly, there is poor reproducibility of film thickness although the glassy carbon electrode was treated consistently and the polymerisation charge was controlled as closely as possible. These problems make application of the electrodes to the analysis of aluminium(III) impossible.

CHAPTER FOUR

VOLTAMMETRIC METHODS USING DIP COATED ELECTRODES

4.1. INTRODUCTION

The determination of aluminium(III) in environmental and biological systems is of current interest. In these determinations chemically modified electrodes (CMEs) can play an important role. In principle CMEs offer the opportunity of developing simple and portable methods for routine environmental monitoring. In Chapter Three the use of CMEs for accumulation of aluminium(III)-ligand complexes is described. An alternative mode of use for CMEs is to modify the surface with the complexing ligand and to react this electrode with solution aluminium(III) species.

Alizarin, 1,2-dihydroxyanthraquinone, is the non-sulphonated analogue of DASA and has been used for the polarographic determination of aluminium(III)[108]. Due to its similarity to DASA, it was expected that alizarin would also exhibit an oxidation process, the potential of which would shift on binding to aluminium(III). Its solubility in organic solvents suggested that a simple dip-coating method might be used for CME preparation.

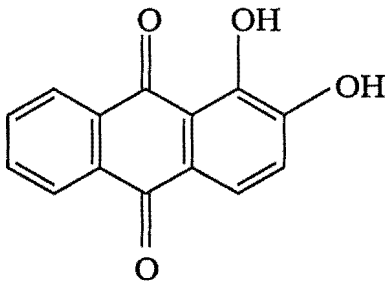

Alizarin

In this work, the fabrication and characterization of a single-use alizarin-modified graphite electrode was studied. The electrode was simply prepared by dip-coating a high-density graphite electrode in an N,N-dimethylformamide (DMF) solution of alizarin. Optimum experimental conditions for aluminium(III) determinations were identified. Determination of exchangeable (1.0 M potassium chloride extractable) aluminium(III) in soil samples with the chemically modified electrode was achieved.

The preparation and use of an electrode modified with 9,10-phenanthrenequinone and 1,2-naphthoquinone was also examined. In contrast to alizarin, these species exhibit chemically reversible electrochemistry and hence the development of a re-usable electrode was investigated.

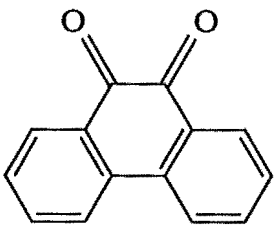

9,10-phenanthrenequinone

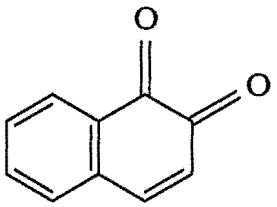

1,2-naphthoquinone

4.2. THE ALIZARIN MODIFIED ELECTRODE FOR ANALYSIS OF ALUMINIUM(III)

4.2.1. Experimental

Cyclic voltammograms were measured using a PAR 173 potentiostat coupled to a PAR 175 universal programmer. Differential pulse voltammograms were obtained with a PAR 174 polarographic analyser. A standard three-electrode 10 mL cell was used, consisting of the CME as working electrode, a platinum wire counter electrode and a saturated calomel reference electrode (SCE). The SCE was placed in a compartment containing buffer and separated from the analyte solution by a Vycor tip (see Figure 2.1).

Soil samples (1.0 g) were extracted with 1.0 M potassium chloride solution (10 mL) by the rapid (5 minutes) extraction method[63] followed by filtration and centrifugation. Fe(III) in the soil extracts was measured spectrophotometrically after reduction with ascorbic acid, followed by stabilization of Fe(II) as the 2,2'-bipyridyl complex[109,110].

Standard analytical procedures

In the standard procedure for electrode preparation, a high-density graphite disk of geometric area 0.28 cm^2 sealed in Teflon was pretreated as described in Chapter Two. For each preparation of the CME, the electrode was dipped in a 2 x 10^{-2} M solution of alizarin in DMF and rinsed with doubly distilled water. A new CME was prepared for each measurement.

Solutions for analysis were prepared by adding an aliquot (5 - 200 μL) of the standard, test extract or standard plus interferent to 5

mL of 0.2 M ammonium chloride-ammonia buffer and diluting to 10 mL with doubly distilled water in a volumetric flask (to give a final pH of 8.4 ± 0.2). Solutions were allowed to stand for 10 minutes at room temperature prior to transfer to the electrochemical cell. The CME was contacted with the stirred solution for an accumulation time of 1 minute at open circuit and the electrode was scanned over the potential range 0.2 - 0.9 V using the DPV mode at a scan rate of 10 mV s^{-1}, with a pulse amplitude of 25 mV and a pulse rate of 2 s^{-1} (pulse width 57 ms). The height of the aluminium(III)-alizarin complex peak at E_p^a = 0.70 V was measured relative to the tangent.

4.2.2. Preparation and characterisation of the electrode

The immobilisation of alizarin onto the electrode depends on the electrode material and electrode surface condition, and on the solvent and the concentration of alizarin used in the dip-coating solution. Ethanol, acetonitrile and DMF were tested for the dip-coating solution. The higher solubility of alizarin in DMF compared to the other solvents gave a larger sensitivity to aluminium(III). DMF was therefore used in all standard preparation procedures. The surface coverage of the electrode was independent of the dipping time but increased with the concentration of the dipping solution, according to their responses to aluminium(III), as shown in Figure 4.1 for a graphite electrode. A concentration of 2 x 10^{-2} M alizarin gave the best sensitivity with satisfactory reproducibility. Reproducibility depends on electrode surface pretreatment and careful polishing and cleaning of the electrode was most important.

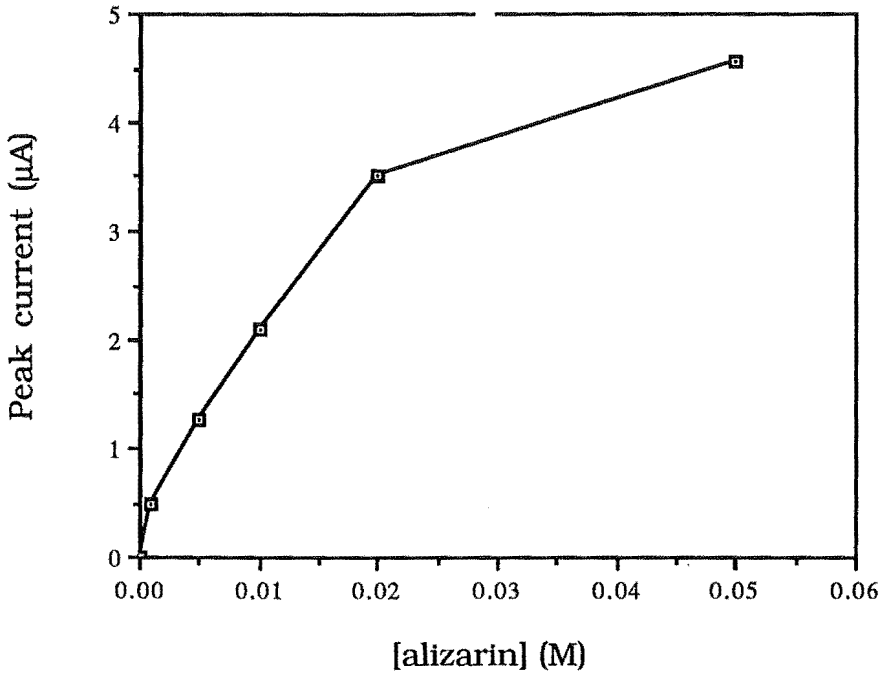

Figure 4.1. Dependence of the differential pulse peak height for the aluminium(III) complex on alizarin concentration in the dip-coating solution. Ammonium chloride-ammonia buffer (pH 8.4); stirred solution; 1 x 10^{-5} M aluminium(III). Accumulation time: 1 minute, at open circuit.

Using a 2 x 10^{-2} M alizarin-DMF solution and a graphite electrode, the dip-coating procedure for preparation of the CME gave a reproducible surface coverage of (11.0 ± 0.1) x 10^{-10} mol cm^{-2} based on the geometric area of the electrode. This value was determined by measuring the charge associated with the reversible two-electron reduction of alizarin at $E^{o}_{surface}$ = -0.31 V, pH 1, from a cyclic voltammogram recorded at 10 mV s^{-1}. The reduction waves are distorted at pH 8.4, hence the cyclic voltammogram was recorded in 0.1 M sulphuric acid after soaking of the CME in ammonium chloride-ammonia buffer for 1 minute. By the same method the surface coverage of alizarin on a glassy carbon electrode was (4.8 ± 0.1) x 10^{-10} mol cm^{-2}. The graphite electrode therefore affords greater sensitivity to

aluminium(III) and this electrode was used in all measurements. The surface coverages suggest that close to a monolayer of alizarin is coated on the electrode. The higher apparent surface coverage of alizarin on graphite than on glassy carbon may arise from the more pitted or porous surface features of the graphite electrode.

4.2.3. Cyclic voltammetry and differential pulse voltammetry of the alizarin modified electrode in the presence of and absence of aluminium(III)

Figure 4.2(a) shows cyclic voltammograms recorded at 100 mV s^{-1} in ammonium chloride-ammonia buffer, pH 8.4, for the alizarin CME after soaking in the buffer for 1 minute in the absence and presence of 1 x 10^{-5} M aluminium(III). In the absence of aluminium(III), an oxidation peak due to alizarin appears at E_p = 0.35 V, and a reversible reduction process is found with E_p^c = -0.75 V and E_p^a = -0.70 V. In the presence of aluminium(III) a new oxidation peak due to aluminium(III)-complexed alizarin appears at E_p = 0.75 V and the peak heights of the uncomplexed alizarin at E_p = 0.35 V and -0.75 V decrease.

Repeat cyclic voltammograms in the absence of aluminium(III) show a dramatic decrease in peak height for alizarin (see Figure 4.2(b)). In the presence of aluminium(III), continued scans recorded after soaking in aluminium(III) solution for 1 minute show a progressive loss of sensitivity to aluminium(III) (not shown). The decrease in peak heights on repeat scans is the expected consequence of the chemically irreversible oxidation of alizarin. This feature of the electrochemistry permits only one scan (i.e. one analysis) for each electrode coating.

The same oxidative behaviour is seen using differential pulse voltammetry. Figure 4.3 shows differential pulse voltammograms

recorded at 10 mV s^{-1} over the potential range 0.4 - 0.9 V after soaking in the buffer for 1 minute in the presence of 0, 2.0 x 10^{-6}, 5 x 10^{-6} and 7.4 x 10^{-6} M aluminium(III). Each scan is recorded on a new electrode coating. The peak height (i_p) for the aluminium(III) complex at E_p = 0.70 V is proportional to aluminium(III) concentration and thus measurement of this peak forms the basis of the analysis.

As shown in Figures 4.2 and 4.3, DPV gives greater sensitivity than CV. The effect of scan rate on peak height (DPV) is shown in Figure 4.4. A scan rate of 10 mV s^{-1} for DPV minimized measurement time while giving sufficient peak resolution and was used for the standard procedure.

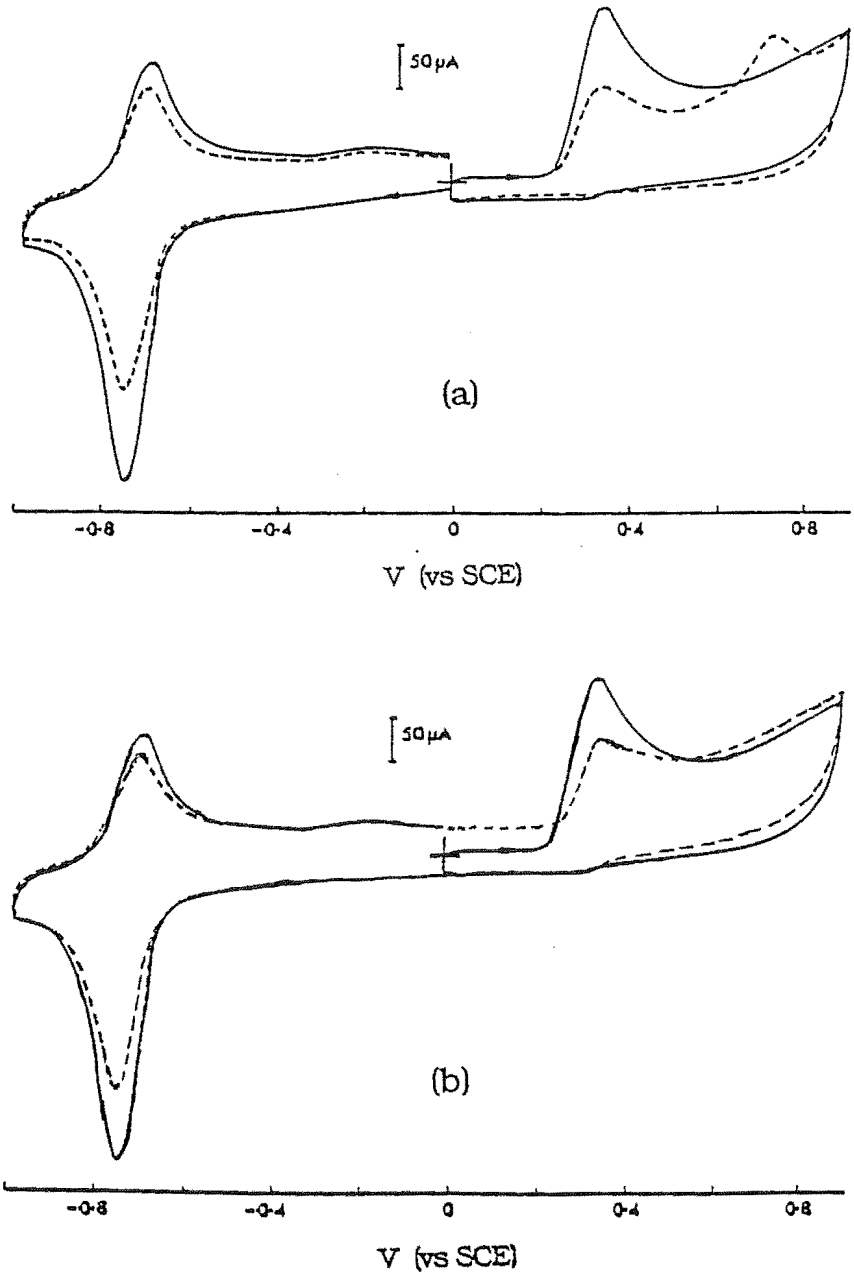

Figure 4.2. (a) Cyclic voltammograms (100 mV s^{-1}) of the alizarin CME in ammonium chloride-ammonia buffer, pH 8.4, after soaking for 1 minute in the buffer in the absence (solid lines) and presence (dashed lines) of 1 x 10^{-5} M aluminium(III). (b) Cyclic voltammograms (100 mV s^{-1}) of the alizarin CME in ammonium chloride-ammonia buffer, pH 8.4, after soaking for 1 minute in the buffer in the absence of aluminium(III); first scan (solid lines) and second scan (dashed lines).

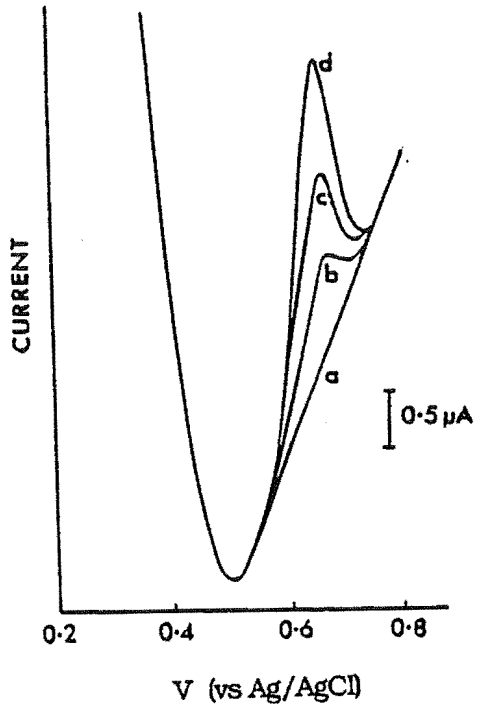

Figure 4.3. Differential pulse voltammograms of the alizarin CME in ammonium chloride-ammonia buffer, pH 8.4, after soaking for 1 minute in the buffer in the presence of (a) 0, (b) 2.0×10^{-6} (c) 5.0×10^{-6} and (d) 7.5×10^{-6} M aluminium(III).

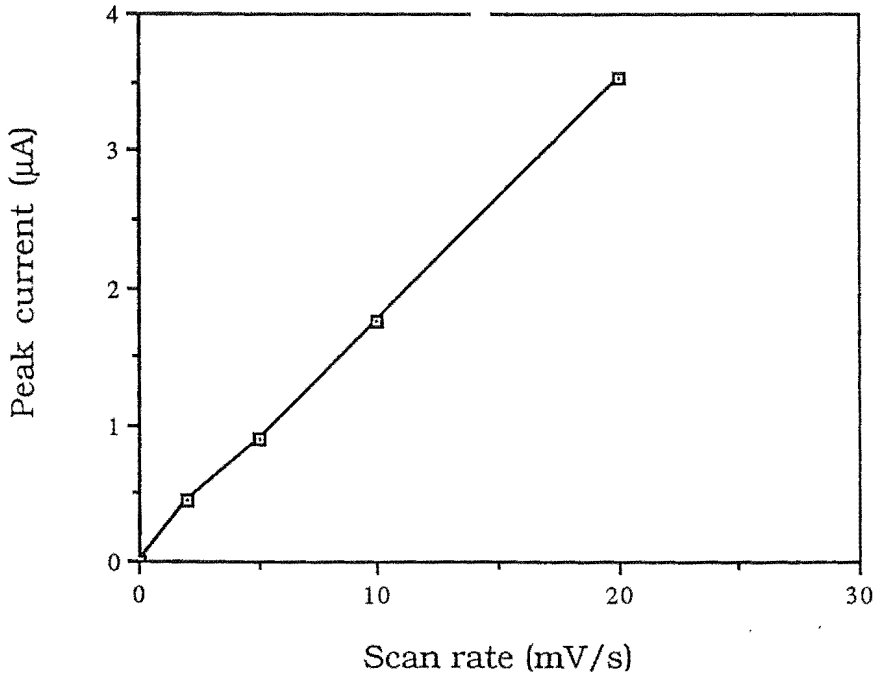

Figure 4.4. Effect of scan rate on the peak current (DPV) of the aluminium(III)-alizarin complex. After soaking for 1 minute in the buffer in presence of 5×10^{-6}M aluminium(III).

The influence of accumulation potential and accumulation time were investigated. The sensitivity for aluminium(III) did not depend on accumulation potential (in the range of -0.20 V to +0.40 V) and accumulation at open circuit was used for all measurements. For a solution of 5 x 10^{-6} M aluminium(III), the peak height of the complex increased with accumulation time (see Figure 4.5). One minute was chosen as the standard time giving good sensitivity with rapid analysis. Deoxygenation of solution in the electrochemical cell prior to analysis had no effect on measurements.

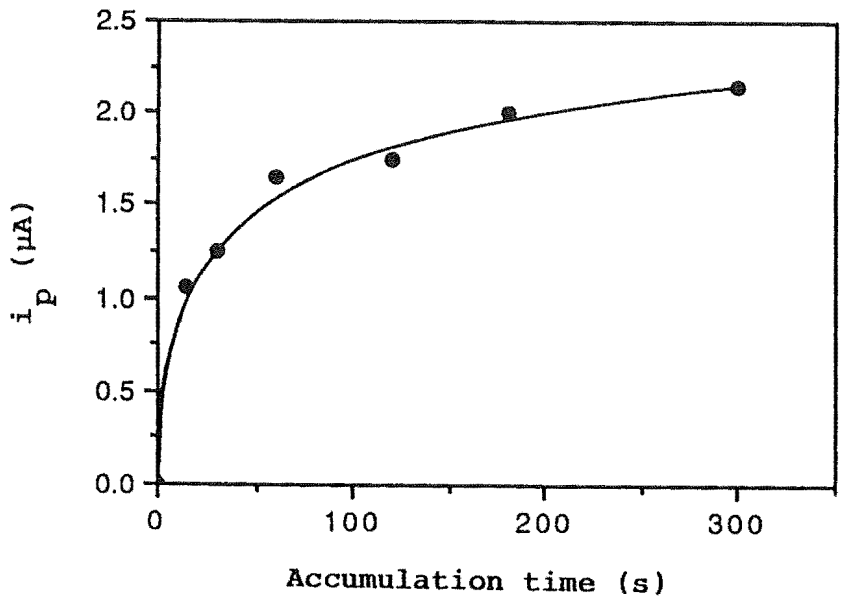

Figure 4.5. Dependence of the differential pulse peak height for the aluminium(III) complex on accumulation time. Ammonium chloride-ammonia buffer, pH 8.4; stirred solution; 5 x 10^{-6} M aluminium(III).

4.2.4. Reaction of the CME with aluminium(III) and solution chemistry

The response of the CME in the absence and presence of aluminium(III) was strongly pH dependent. Most importantly, the height of the aluminium(III)-alizarin peak was pH dependent. Figure 4.6 shows the results of measurements made in the pH range 4.5 - 9.6 using the buffers sodium acetate-acetic acid (pH 4.5 - 6.0) and ammonium chloride-ammonia (pH 7.0 - 9.6). These results indicate that pH 8.4 gives the greatest sensitivity to aluminium(III). The increase in the amount of complex formation with pH is expected for a di-*o*-hydrxyaryl ligand. The decrease after pH 8.5 may be due to an increase in the solubility of alizarin, to a decrease in stability of alizarin or due to formation of $Al(OH)_4^-$.

The potentials of the alizarin peak and the complex peak depend on pH. Figure 4.7 shows the oxidation peak potential of alizarin and the oxidation peak potential of the aluminium(III)-alizarin complex as functions of pH. Oxidation of the aluminium(III)-alizarin complex does not involve a proton change and is therefore pH independent. At pH 8.4, the separation between the oxidation peaks is 0.38 V giving satisfactory resolution.

The magnitude of the blank also depended on pH. In the absence of aluminium(III), several very small oxidation peaks contribute to the blank. Use of ammonium chloride-ammonia at pH 8.4 minimised these peaks. The origin of small peaks was investigated. They are not from (1) buffer solution (2) other metal ions (3) impurity of alizarin and (4) solvent for coating solution. They arise from the oxidation of alizarin in a higher pH solution.

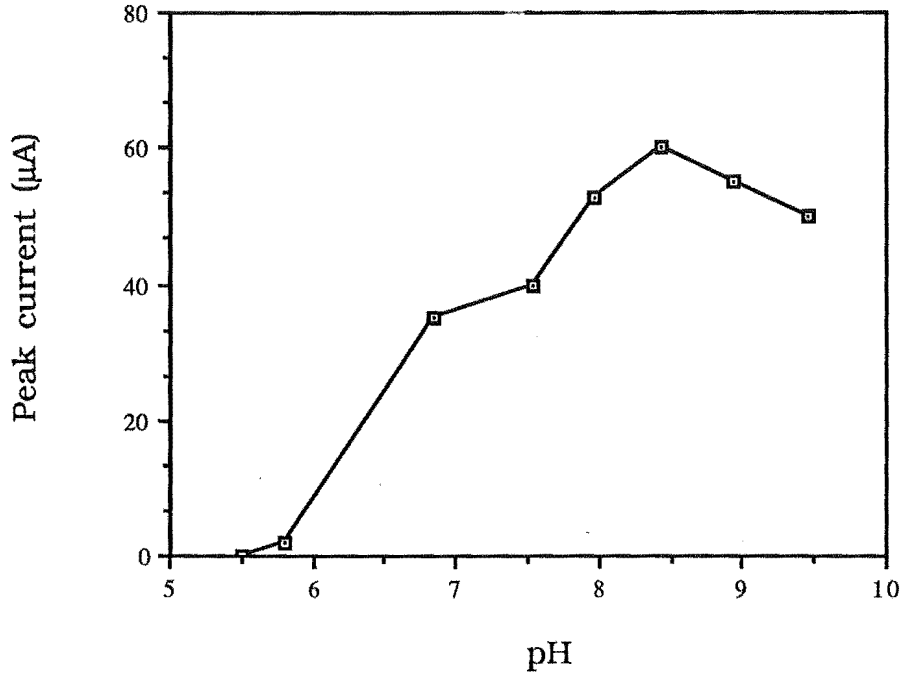

Figure 4.6. Dependence of peak current (CV) of the aluminium(III)-alizarin complex on pH. The CVs (100 mV s^{-1}) of the alizarin CME were recorded after soaking for 1 minute in the buffer in the presence of aluminium(III) (1 x 10^{-5} M).

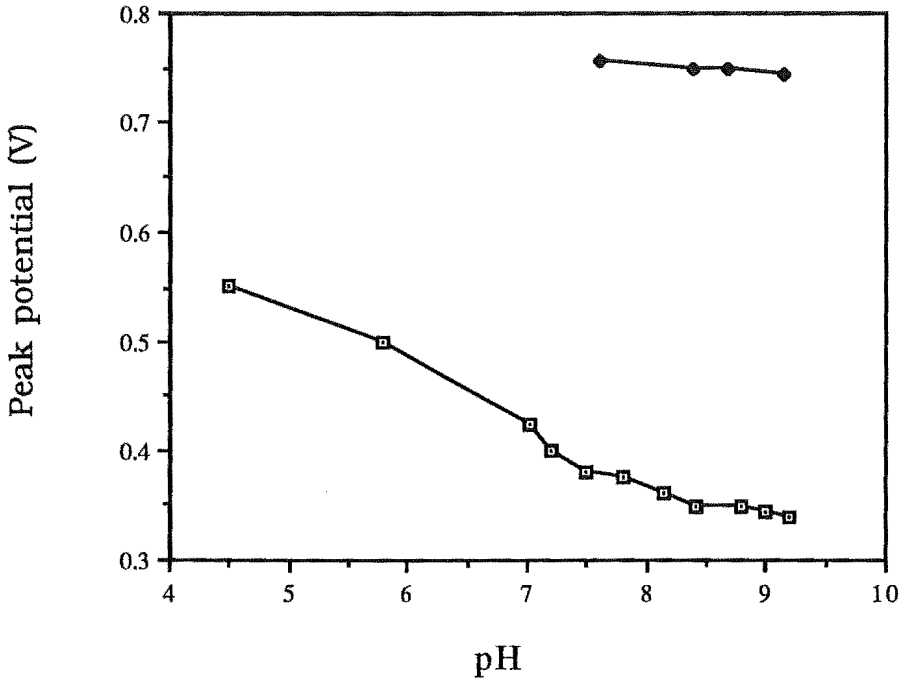

Figure 4.7. Effect of pH on (▫) the oxidation peak potential of alizarin and (•) the oxidation peak potential for aluminium(III)-alizarin on the alizarin coated electrode.

The peak height of the aluminium(III) complex was dependent on the time between preparation of the analyte solution and its analysis. This was most marked in the presence of interferent anions; there was a small (≤ 10%) increase in peak height during the first 10 minutes after preparation and hence a standing time of 10 minutes was adopted for all solutions. The reaction between the test solution and the buffer at pH 8.4 can be represented by Equation 4.1 in which X and Y refer to inorganic and organic ligands, respectively:

$$[Al^{3+} + Al_x(OH)_y + AlX + AlY] + OH^- \rightarrow Al(OH)_4^- \qquad (4.1)$$

For test solutions containing competing organic or inorganic ligands, this reaction was not spontaneous. The reaction presumably proceeds via (partial) formation of non-labile polymeric or hydroxy-ligand species which slowly react or dissolve in the buffer medium.

4.2.5. Detection limit and working range

Using the conditions described above, Figure 4.8 shows the variation of i_p for the aluminium(III)-alizarin complex (DPV) with aluminium(III) concentration in the range 0.05 x 10^{-5} - 2 x 10^{-5} M in the presence of 0 and 1 x 10^{-2} M potassium chloride (see below). Acceptable linearity is shown up to 1.0 x 10^{-5} M and 1.5 x 10^{-5} M aluminium(III), respectively. The limit of detection, calculated as three times the standard deviation (n = 10) for the blank (buffer solution) ($S.D._b$) was 1.5 x 10^{-7} M, giving a working range of 7.5 x 10^{-7} - 1.5 x 10^{-5} M aluminium(III) in 1 x 10^{-2} M potassium chloride. The R.S.D. at 7.5 x10^{-6} M aluminium(III) was 3.8% (n = 4).

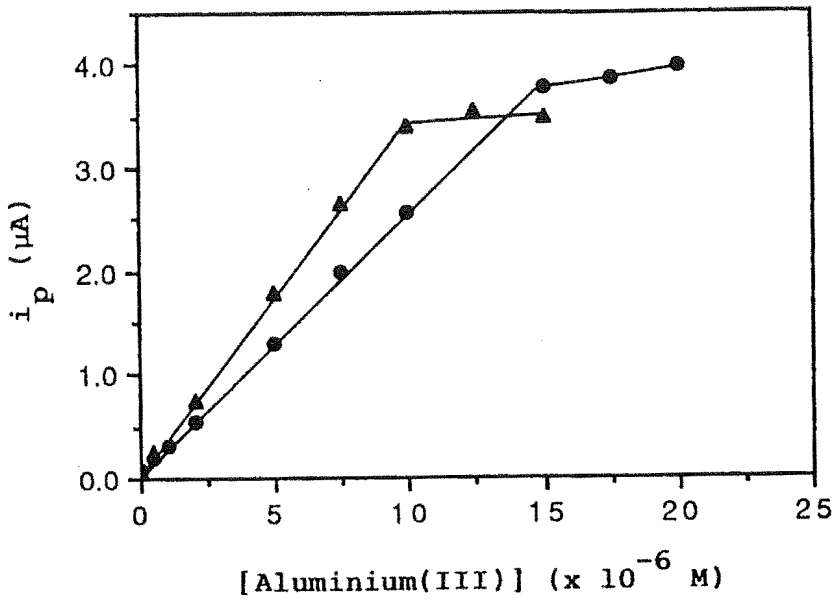

Figure 4.8. Dependence of the differential pulse peak height for the aluminium(III) complex on aluminium(III) concentration in the absence (▲) and presence (●) of 1 x 10^{-2} M KCl. Other conditions as in Figure 4.3.

4.2.6. Interferences

The interferences arising from cations and anions, including those dominant in soil extracts, were assessed for 5 x 10^{-6} M aluminium(III). In Table 4.1 are listed the concentrations of interferents that result in a 20% reduction in the peak height of the aluminium(III) complex. The effect of added malonate (0.1 x 10^{-3} - 1.0 x 10^{-3} M) on the peak height of the aluminium(III) complex is shown in Figure 4.9; all other interferences, with the exception of fulvic acid, led to a qualitatively similar response. Fulvic acid[111] increased the peak height of the aluminium(III) complex to a maximum of 12% at 12 mg kg^{-1} added acid (see Figure 4.10).

Table 4.1. Concentration of interferents causing a 20% decrease in the peak height of the aluminium(III) complex[a]

cation	Concentration (M)	Anion	Concentration (M)
Ca^{2+}	2.5×10^{-4}	F^-	7.5×10^{-4}
Cu^{2+}	7.0×10^{-7}	PO_4^{3-}	5.6×10^{-5}
Fe^{3+}	7.0×10^{-6}	SO_4^{2-}	1.0×10^{-3}
K^+	8.0×10^{-3}	Citrate	1.0×10^{-3}
La^{3+}	8.0×10^{-7}	Malonate	1.2×10^{-4}
Mg^{2+}	5.5×10^{-5}	NTA[b]	3.0×10^{-6}
Na^+	5.4×10^{-3}	Oxalate	5.5×10^{-4}

[a] 5.0×10^{-6} M Al(III). [b] Nitrilotriacetate.

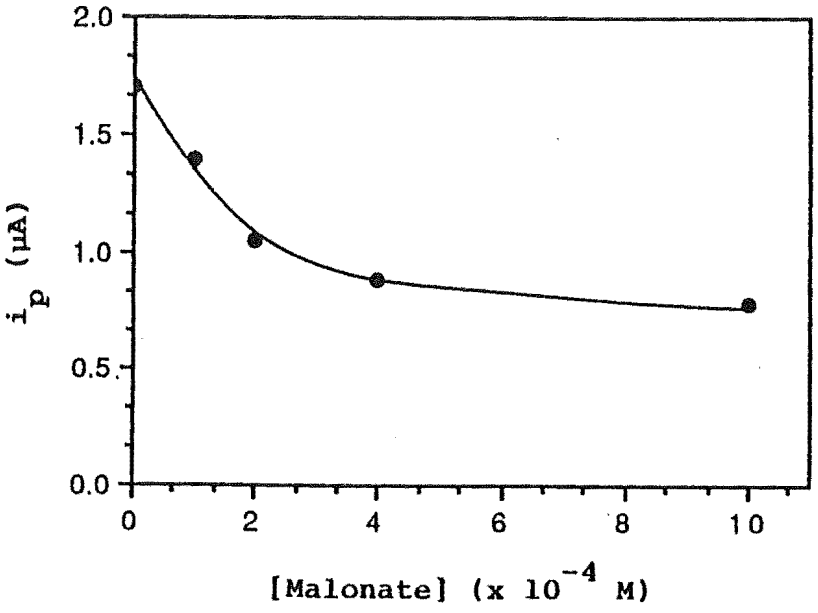

Figure 4.9. Dependence of the differential pulse peak height for the aluminium(III) complex [5×10^{-6} M aluminium(III)] on malonate concentration. Other conditions as in Figure 4.3.

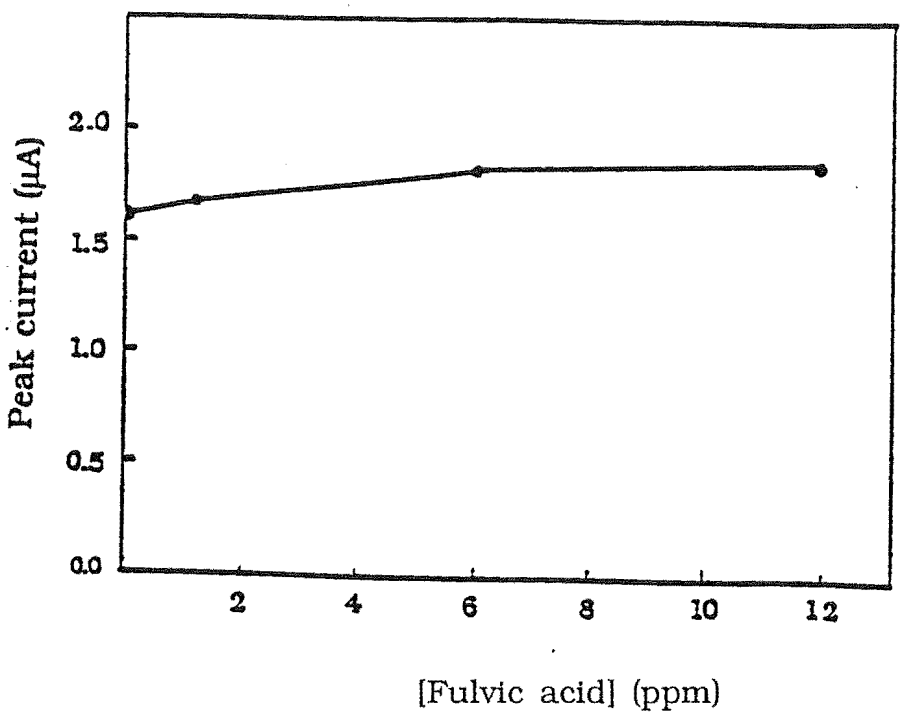

Figure 4.10. Dependence of the differential pulse peak height for the aluminium(III) complex [5 x 10^{-6} M aluminium(III)] on fulvic acid concentration. Other conditions as in Figure 4.3.

The results in Table 4.1 indicate that interferences from F^-, SO_4^{2-}, citrate, malonate and oxalate are minimal. This is to be expected because the hydroxide (OH^-) ion is a stronger complexing agent toward aluminium(III) than F^-, SO_4^{2-} and the majority of simple polycarboxylic and hydroxy carboxylic acids[23,24]. Ligands that compete strongly against OH^- and alizarin, e.g. polyphenols, should lead to a negative interference; the condensed tannins afford an example of this reaction.

In the investigation of anionic interferents, the dominant interferences were shown by nitrilotriacetic acid (NTA), and PO_4^{3-}. NTA is used widely in domestic detergents and is a likely component of polluted waters. Although PO_4^{3-} interferes fairly strongly, the concentration giving rise to a 20% reduction in aluminium response at

5 x 10^{-6} M aluminium(III), ca. 1.8 mg kg^{-1} PO_4^{3-}-P, is significantly higher than would be present in most natural waters, unless highly polluted, and in potassium chloride extracts of soil samples after dilution for analysis (a minimum Al : PO_4^{3-}-P ratio of 10 : 1 was observed in a series of potassium chloride soil extracts)[112]. Chinese quince tannin, an epicatechin polymer, interfered strongly by virtue of its strong complexation of Al^{3+} [112]; a 20% suppression of the peak height of the aluminium(III) complex was observed for a 1.3 mg kg^{-1} solution (ca. 4.6 x 10^{-7} M) and 5.0 x 10^{-6} M aluminium(III).

For fulvic acid, which is essentially aliphatic carboxylate ligand[111], a positive interference was observed, i.e., 12% at 12 mg kg^{-1}; this could not be ascribed to aluminium impurities in the fulvic acid (0.03%), which would give a maximum error of 2%. This may, however, indicate the importance of kinetic (as well as thermodynamic) factors in determining the extent of reaction 4.1.

Interferences may also arise due to reactions at the electrode surface. These may be in the form of competitive adsorption, which displaces or overlays the alizarin coating, or competitive complexation of surface-adsorbed alizarin by strongly binding metal ions (such as Cu^{2+}, La^{3+} or Fe^{3+}) which diminish the degree of surface uptake of Al^{3+}.

Interferences arising from the complexation of Cu^{2+} and La^{3+} with alizarin were almost quantitative, indicating strong competition for the adsorbed alizarin. Interference by iron(III) was ca. ten times lower; this is ascribed to its low solubility in the buffer medium. These three cations will, however, be minor interferents in soil extracts (and in natural waters), except for iron in field moist anaerobic soils (and anoxic waters). Determinations of iron(III) in the potassium chloride extracts of the soils given in Table 2 established that the amounts of iron(III) in these soils were small ([Fe(III):[Al(III)] $\leq$ 0.015). Masking of iron(III) in test solutions was attempted by reduction (ascorbic acid)

and complexation of iron(II) with 2,2'-dipyridyl. This was not successful. Formation of the complex was slow in alkaline solution and in the presence of alizarin $Fe(bp)_3^{2+}$ was oxidized to the iron(III)-alizarin complex at the analytical voltage (+0.70 V). Further, at high concentrations of iron(III) it was observed that precipitation of $Fe(OH)_3$ led to loss of aluminium(III), possibly due to formation of surface ≡Fe-O-$Al(OH)_2$ complexes as described by Lövgren[113].

4.2.7. Determination of aluminium(III) in soil extracts

Application of the alizarin coated electrode was demonstrated by the determination of exchangeable (1.0 M potassium chloride-exchangeable) aluminium(III) in a range of drier soils (yellow grey earths, yge) and moister soils (yellow brown earths ybe) (Table 4.2). Preparation of soil extracts is described in the Experimental section. Sample dilution was necessary (ca. 100 μL to 10 mL) to match the working range for the electrode. Measurements were effected both against standards in 1 x 10^{-2} M potassium chloride and by the method of standard additions (see Figure 4.11). The agreement between the two results (Table 4.2) indicates minimum interference from co-extracted species. The results are compared with those for "chrome azurol S (CAS)-reactive aluminium" (a method proposed for a quick field test for "exchangeable aluminium"[63]) and total aluminium determined by AAS. It is evident that "alizarin-reactive aluminium" approximated to the total extracted aluminium for these soils. Small differences can arise from the contribution of interferent species to the alizarin value and from sample variability.

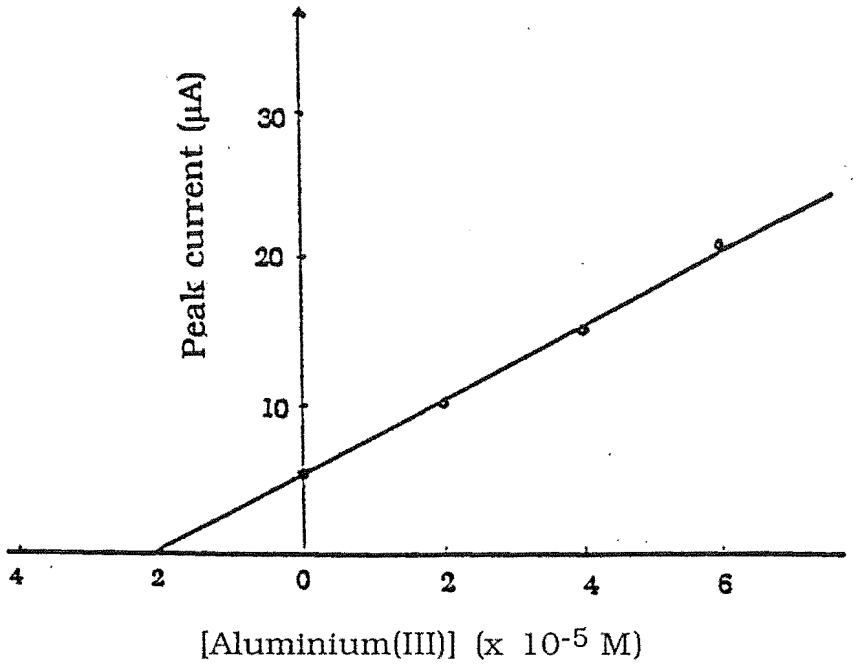

Figure 4.11. The method of standard additions for determination of aluminium(III).

Table 4.2 Exchangeable (1 M KCl extractable) aluminium in soils

Soil type	Description[a]	Depth(cm)	Aluminium (mg kg^{-1})		
			Alizarin-modified electrode[b]	CAS [c]	AAS[d]
Takahe	Silt loam; yge	0-26	81 (65)	94	104
Takahe	Silt loam; yge	26-50	118 (121)	89	76
Takahe	Silt loam; yge	>90	197 (200)	260	225
Summit	Silt loam; ybe	15-30	145 (157)	195	190
Waikari	Clay; ybe	17-39	1210 (1310)	-	1215
Waikiwi	Silty clay loam; ybe	55-92	119 (110)	-	117

[a] yge = yellow-grey earth; ybe = yellow-brown earth. [b] 5 minutes extraction[63]; Values from method of additions; values in parentheses from calibration graph. [c] Chrome Azurol S method, 5-minutes extraction[63]. [d] 16-h extraction; Data supplied by DSIR (NZ) Land Resources.

4.2.8. Conclusion

The alizarin CME, although for single use, is constructed of inexpensive material (high-density graphite) and is very quickly regenerated by polishing and dip-coating. Each electrode coating can be used for only one determination due to the irreversible oxidation of alizarin. Calibration of the electrode before use is therefore not possible but is not necessary. The reproducibility of electrode preparation and of its reaction with aluminium(III) is evidenced by the low R.S.D.(3.8%) achieved for replicate electrode preparations.

The working range is 7.5×10^{-7} - 1.5×10^{-5} M aluminium(III) (0.02 - 0.40 mg kg^{-1}). With sample dilution the electrode can be used for determination of soluble and exchangeable aluminium(III) in soils. A series of soil samples were analysed for exchangeable aluminium(III), and results approximated to total extracted aluminium(III). The working range is too high for pristine waters but is appropriate for monitoring aluminium(III) concentrations in acidified natural waters (e.g., acid rain catchments).

4.3. PHENANTHRENEQUINONE MODIFIED ELECTRODES

An improvement on the alizarin CME would be a re-usable CME for aluminium(III) determination. This requires a ligand with chemically reversible electrochemistry, thus permitting multiple potential scans. The ligands 9,10-phenanthrenequinone[114] and 1,2-naphthoquinone[115] show reversible electrochemistry and it was expected that the reduced hydroquinone form will react with aluminium(III). Hence, use of these ligands suggested the possibility of

constructing re-usable probes for aluminium(III). In these experiments, 9,10-phenanthrenequinone and 1,2-naphthoquinone were coated on graphite and glassy carbon electrodes and their electrochemistry in the presence and absence of aluminium(III) was examined.

4.3.1. Preparation of the CMEs

When a glassy carbon electrode is scanned in a perchloric acid solution of 9,10-phenanthrenequinone the redox peaks of the ligand increase on repeat scans indicating that 9,10-phenanthrenequinone adsorbs irreversibly on glassy carbon[114,116]. Hence, the electroadsorption method was used to immobilise 9,10-phenanthrenequinone onto the electrode. A graphite or glassy carbon electrode was pretreated as described in Chapter Two, followed by scanning in a 1 x 10^{-3} M 9,10-phenanthrenequinone solution in 0.1 M perchloric acid from -0.5 to +0.7 V for 5 minutes. The coated electrode was then placed in a stirred ammonium chloride-ammonia solution and held at -0.5 V for 2 minutes, and its surface coverage was measured. Using a graphite electrode, the electrochemical procedure for preparation of the CMEs gave a surface coverage of 4.6 x 10^{-10} mol cm^{-2} based on the geometric area of the electrode. This value was determined by measuring the charge associated with the reversible two-electron reduction of 9,10-phenanthrenequinone at $E_{surface}$ = - 0.31 V.

The dip-coating procedure was also investigated for CME preparation. Using the same method as described for the alizarin CME, a 1 x 10^{-2} M 9,10-phenanthrenequinone in DMF solution gave a reproducible surface coverage of 4.3 x 10^{-10} mol cm^{-2} on a graphite electrode. This coverage is very similar to that achieved by

electroadsorption and since the latter procedure was more simple, the dip-coating method was used in all measurements.

4.3.2. Cyclic voltammetry of the CMEs

Figure 4.12 shows cyclic voltammograms (100 mV s^{-1}) of the 9,10-phenanthrenequinone coated graphite electrode after potentiostatting at -0.5 V for 1 minute in deoxygenated ammonium chloride-ammonia buffer, pH 8.5. There is a reversible redox process of 9,10-phenanthrenequinone at E_p^c = -0.31 and E_p^a = -0.28 V vs SCE. Repeat cyclic voltammograms (not shown) exhibit no change in peak heights for 9,10-phenanthrenequinone as expected for a chemically reversible redox couple.

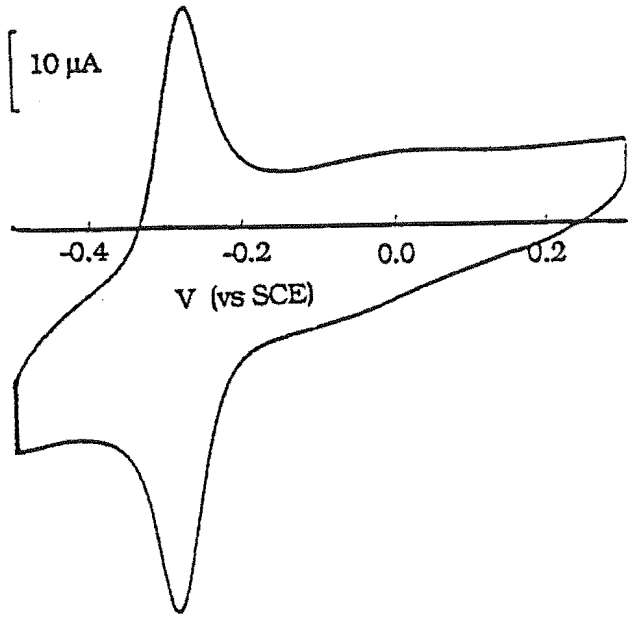

Figure 4.12. Cyclic voltammogram (100 mV s^{-1}) for the 9,10-phenanthrenequinone modified electrode after potentiostatting at -0.5 V for 1 minute in ammonium chloride-ammonia buffer, pH 8.5.

4.3.3. Reaction with aluminium(III)

For reaction with aluminium(III), a potential at which reduction to the di-*o*-hydroxy form occurs must be applied to the CME. In the presence of aluminium(III) in ammonium chloride-ammonia buffer (pH 8.4), potentials of -0.7, -0.5 and -0.4 V were applied to the CME for times ranging from 1 to 10 minutes. The CME was then scanned from the accumulation potential to +0.8 V. No new peaks arising from aluminium(III) complexation were observed in any experiment. In all cases, however, there was a decrease in the height of the ligand oxidation peak. Figure 4.13 compares the response for a CME potentiostated at -0.5 V for 5 minutes in the absence and presence of 2 x 10^{-5} M of aluminium(III). The decrease in height of the ligand peak in the presence of aluminium(III) may indicate loss of ligand from the surface of the CME due to an increase in solubility of the ligand following coordination to aluminium(III). The Figures also demonstrate that in the absence of aluminium(III), the peak height for oxidation of the ligand decreases with soaking time (compare Figure 4.12 with Figure 4.13 (solid line)). This decrease may be due to solubility and instability of 9,10-phenanthrenequinone at high pH.

The decrease in the ligand peak could be used in determination of aluminium(III), but overall the electrode is less satisfactory than the alizarin CMEs. Loss of ligand on repeated soaking necessitates electrode calibration; the accumulation procedure is more complex than that for the alizarin CME and solutions for analysis must be deoxygenated owing to the instability of the reduced quinone in the presence of oxygen.

Preliminary studies were also undertaken with a dip-coated 1,2-naphthoquinone electrode. Reduction of this ligand occurs at E_p^c = -0.19 V, E_p^a = -0.17 V in ammonium chloride-ammonia buffer, pH 8.5.

Again, deoxygenation of solutions was necessary. In the presence of aluminium(III), a new oxidation peak was not observed and hence this ligand appears to offer no advantage over 9,10-phenanthrenequinone for aluminium(III) determination.

In conclusion, the principle of a re-usable probe has been demonstrated but use of the electrode is more time-consuming and experimentally complex than use of the alizarin CME.

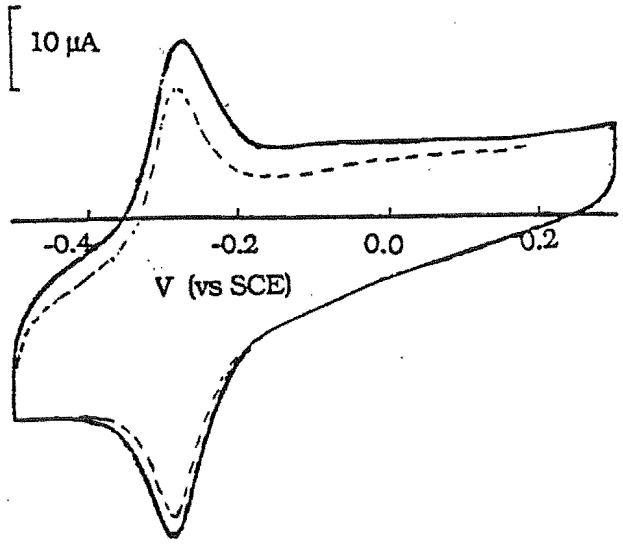

Figure 4.13. Cyclic voltammogram (100 mV s^{-1}) for the 9,10-phenanthrenequinone modified electrode after potentiostatting at -0.5 V for 5 minutes (solid line) in the absence of aluminium(III) and (dashed line) in the presence of 2 x 10^{-5}M aluminium(III) in ammonium chloride-ammonia buffer, pH 8.5.

CHAPTER FIVE

MODIFIED CARBON PASTE AND GRAPHITE EPOXY ELECTRODES

5.1. INTRODUCTION

The work described in Chapters Three and Four concerns modification of the electrode surface by coating with a layer of polymer or ligand. An alternative method of fabricating modified electrodes is to incorporate active species in the electrode material. Carbon paste and graphite epoxy are suitable electrode materials.

The use of carbon paste electrodes has the advantages of ease of electrode preparation and regeneration as well as low background currents. Incorporation of ligands which exhibit rapid reactions with analytes is very simple. A number of studies on the use of modified carbon paste electrodes have been reported. For example, a dimethylglyoxime-containing carbon paste electrode was used for differential pulse voltammetric determination of nickel[117], 2,9-dimethyl-1,10-phenanthroline was incorporated into carbon paste for the determination of copper[118] and 2,2-bipyridyl was applied for the determination of cobalt[119].

In a similar way, ion-exchange resins can be incorporated directly into the paste mixture. Such incorporation results in an alternative approach for the accumulation of ions. For example, if a cation-exchange resin in the hydrogen ion form is used the preconcentration reaction is given by

$nRSO_3^-H^+ + M^{n+} = (RSO_3^-)_nM^{n+} + nH^+$

Applications of carbon paste electrodes containing cation-exchangers or anion-exchangers in analysis have been reported. Cation-exchange resin (Dowex 50W-X8) was modified into carbon paste for the determination of cadmium[120] and anion-exchange resins were used for the determination of iodide[121] and gold (as $AuCl_4^-$)[122].

An epoxy-bonded graphite resin provides a better mechanical strength than carbon paste. The modification scheme is simple and fast and electrodes are readily renewed by standard polishing procedures. Several applications of these electrodes in analysis have been reported[123-125].

In this work, carbon paste electrodes modified with anion exchange resins and ligand were used for aluminium(III) determination. For one procedure, anionic ligands which strongly complex aluminium(III) were incorporated by ion-exchange. The modified electrodes were then reacted with aluminium(III). In a second method anionic aluminium(III) complexes were directly preconcentrated into the electrode by ion-exchange. Alizarin was also mixed into carbon paste and the electrode was examined for determination of aluminium(III). In further experiments, 4-nitrocatechol and 1,2-naphthoquinone were incorporated into graphite epoxy electrodes. These modified electrodes were applied in analysis of aluminium(III).

5.2. EXPERIMENTAL

Electrode preparation

(1) Carbon paste electrodes

The electrodes (Figure 5.1) were prepared in the following manner. Carbon paste was made by thoroughly mixing 1.0 g of graphite powder (UCP-1M Ultra Microcrystal Grade) and 0.4 g of Nujol oil. The body of the electrode was made from a Teflon rod (10 mm o.d.) with a hole (7 mm diameter) bored at one end for the carbon paste filling. Contact was made with a brass rod which was moveable. The carbon paste was packed in and smoothed with a filter paper. Between each measurement the paste was extruded and a small length cut off. This was followed by smoothing of the electrode surface.

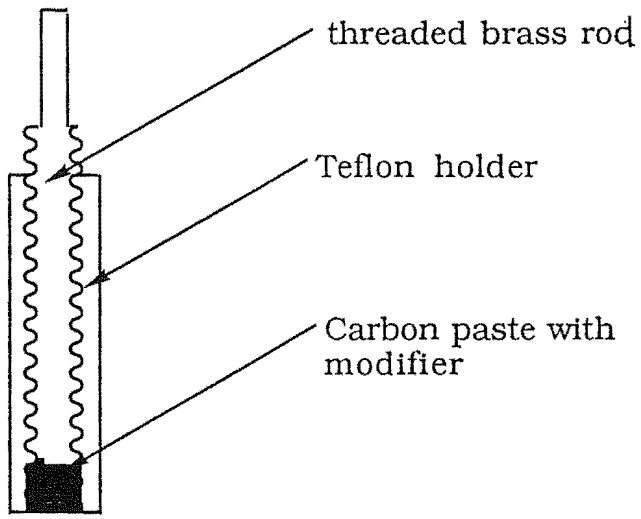

Figure 5.1. Diagram of renewable carbon paste electrode

(2) Graphite epoxy electrodes

Preparation of the electrodes

The electrodes were prepared by thoroughly mixing 2 parts of the epoxy-bonded graphite resin and 1.1 part of the accelerator (Grade RX, Dylon, Cleveland, OH) for 5 minutes. A portion of the electrode material was packed into the end of a 4-mm i.d. glass tube. Electrical contact was established via a copper wire. The electrode was then cured at 60 °C overnight.

Treatment of the electrodes

The electrode surface was polished with a silicon carbide paper and then with 9, 6, 3 and 1 μm diamond paste and rinsed with acetone and doubly distilled water. Prior to use, the electrode was sonicated for 5 minutes in doubly-distilled water.

Maintenance of the electrodes

Between measurements the graphite epoxy electrodes were soaked in doubly distilled water.

(3) Modified carbon paste and graphite epoxy electrodes

Before use the anionic exchange resins Amberlite IRA 400 (BDH) and 900 (BDH) were purified and converted to the H^+ form by successive washes with 0.1 mol L^{-1} NaOH, methanol and 1 mol L^{-1} HCl. After washing with water the purified resins were stored as neutral suspensions in doubly distilled water (100 mg resin/10 mL). For grinding, Amberlite IRA 400 and 900 were dried at 40 °C, ground using a mortar and pestle followed by sifting with a 165 μm sieve.

The modified carbon paste electrodes were made by mixing 0.05 g ground (maximum particle size: 165 μm) or unground Amberlite IRA 400 or Amberlite IRA 900 or 70 μL of liquid ion-exchanger (Amberlite LA 2) (BDH) with 0.1 g graphite carbon powder and 0.04 g Nujol oil.

To prepare alizarin modified carbon paste electrode, alizarin (10% w/w) was dissolved in ethanol (0.02 M) was mixed with carbon powder. Ethanol was evaporated at 60 ^{o}C overnight and the dried powder was then mixed with Nujol oil to make CMEs.

Modified graphite epoxy electrodes were prepared by hand mixing 5, 7.5 and 10% w/w of 4-nitrocatechol and 10% w/w of 1,2-naphthoquinone with graphite epoxy and followed by packing, curing and polishing as described above.

Analytical procedure

For the incorporation of ligand, the anion-exchange resin modified electrode was soaked in stirred anionic ligand solution for 5 to 10 minutes. The electrode was then removed into an aluminium(III) solution. Ligand modified carbon paste and graphite epoxy electrodes were also soaked in aluminium(III) solutions for various reaction times.

For the preconcentration of anionic aluminium(III) complexes, the anion exchange resin modified carbon paste electrode was immersed in a stirred solution of the complex for a given period of time. The electrode was then removed from the preconcentration cell, briefly rinsed with doubly distilled water, and placed in an electrochemical cell containing the same buffer solution. In all cases, the preconcentration step was carried out at open circuit. Unless stated otherwise, the concentration of the ammonium chloride-ammonia buffer was 0.1 M.

5.3. MODIFIED CARBON PASTE ELECTRODES

5.3.1. Ion-exchange resin modified carbon paste electrodes

Amberlite IRA 400, 900 and liquid resin modified carbon paste electrodes were soaked in stirred 1 x 10^{-3} M DASA solution. Figure 5.2 (solid line) shows the differential pulse voltammogram for a ground Amberlite IRA 400 modified electrode in ammonium chloride-ammonia buffer solution (pH 8.5) after soaking in 1 x 10^{-3} M DASA solution for 5 minutes. The electrode exhibits strong preconcentration of DASA indicated by the large oxidation peak for DASA. High background current arising from the ion exchange resin was observed. Similar results were obtained for ground Amberlite IRA 900 and liquid resin modified electrodes. Each DPV measurement was made on a freshly renewed surface and four replicate electrode preparations gave 8% variability in DASA peak height. The voltammograms of unground resin modified electrodes showed poor conductivity and low sensitivity.

The DASA adsorbed ion-exchanger electrode was placed in aluminium(III) solution (1 x 10^{-4} M). The differential pulse voltammogram of the electrode after soaking 5 minutes exhibits a significant decrease in the oxidation peak of DASA but no new peaks due to aluminium(III) complexes (Figure 5.2 (dashed line)). When an electrode prepared by the same method is soaked in buffer for 5 minutes, there is also a decrease in the peak current for DASA which is about 1/3 of the decrease above. Thus, the decrease in the DASA peak arises in part from loss of DASA from resin and also from reaction with aluminium(III). The absence of a peak for aluminium(III)-ligand complexes may be due to the high background current or low concentration of aluminium-ligand complexes.

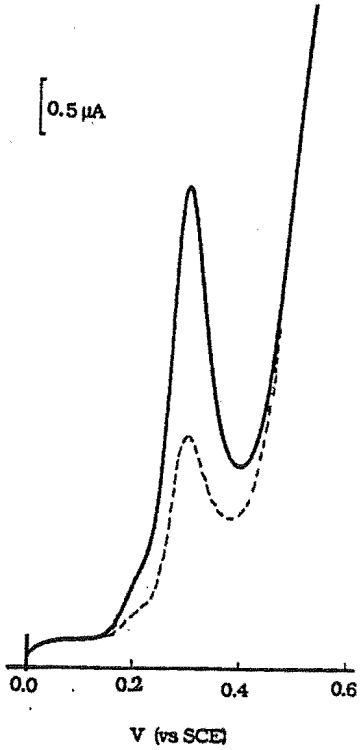

Figure 5.2. Differential pulse voltammograms (5 mV s^{-1}) in ammonium chloride-ammonia solution (pH 8.5) for DASA preconcentrated at a ground Amberlite IRA 400 modified electrode and soaked in the buffer solution in the absence (solid line) and presence (dashed line) of 1 x 10^{-4} M aluminium(III). Accumulation time: 5 minutes.

Spectrophotometric measurements were made to examine the effect of buffer concentrations on the loss of DASA; the resins holding DASA were soaked in different concentrations (0.05 to 1.0 M) of ammonium chloride-ammonia buffer solutions for 30 minutes. The DASA released from the resin was measured spectrophotometrically (λ= 526 nm). Figure 5.3 shows that the amount of DASA released from the resin depends on buffer concentration but even at 0.05 M, DASA is still released from the resin. Because of loss of ligand on soaking and the poor reproducibility of CME preparation further application of the electrodes was not attempted.

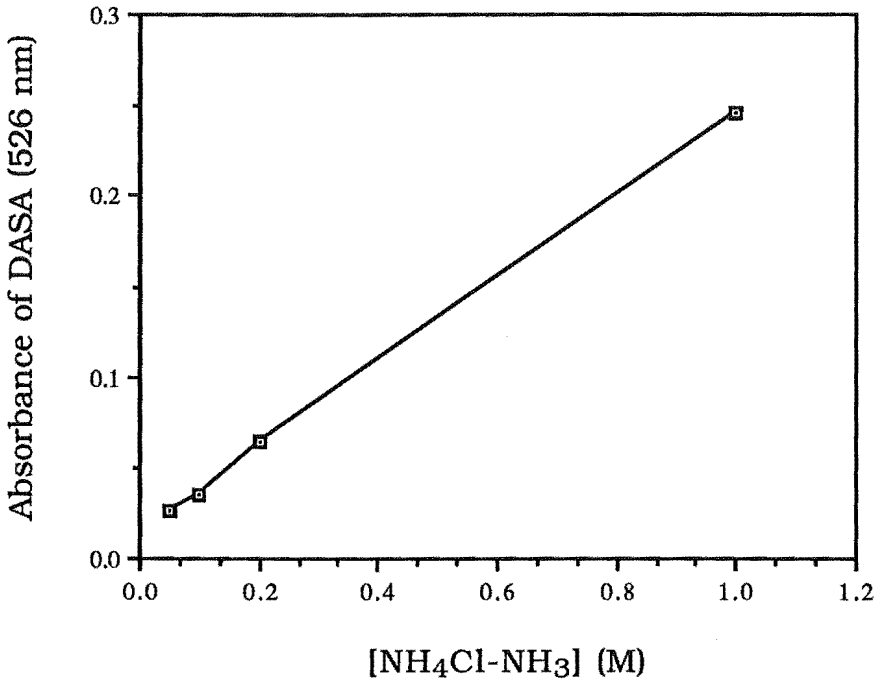

Figure 5.3. Release of DASA from anion exchange resin (Amberlite IRA 400) in different concentrations of ammonium chloride-ammonia buffer solutions using spectrophotometric measurements. Soaking time: 30 minutes.

An alternative strategy using anion exchanger modified carbon paste is to preconcentrate pre-formed aluminium(III)-ligand complexes. In contrast to the strong adsorption of DASA, however, there was no evidence of adsorption of aluminium(III)-ligand complexes on the electrode. The anion exchange resin modified electrode was soaked in 1 x 10^{-4} M aluminium(III) and 1 x 10^{-4} M DASA solution for 5 minutes. Only a small peak due to DASA was found. The absence of a peak due to an aluminium complex may be due to high background current or it may be due to slow uptake of complexes in the resin.

Amberlite IRA 400 has a larger pore size than the 900 resin, however no differences in behaviour were observed.

None of the experiments using ion exchange CMEs gave useful results. Since no aluminium(III) complex peak was detected and there was poor reproducibility for electrode surface renewal, these electrodes were unsuitable for use in the analysis of aluminium(III).

5.3.2. Ligand modified carbon paste electrodes

Alizarin modified carbon paste electrodes

The carbon paste electrode containing alizarin was soaked in ammonium chloride-ammonia buffer solution (pH 8.5) in the absence and presence of 5×10^{-4} M aluminium(III). Figure 5.4 shows the cyclic voltammograms of these electrodes after soaking in the above solutions for 2 minutes. The reaction of the alizarin modified electrode with aluminium(III) gave a significant decrease in the peak of the ligand and a new peak due to the aluminium(III)-ligand complex.

The electrode surface can be renewed by extruding a small length of carbon paste and cutting and smoothing the surface. However, the reproducibility was poor compared with chemisorbed alizarin electrodes (Chapter Four). Additionally, the procedure for renewing the carbon paste electrode was more complex than making new chemisorbed alizarin electrodes. For these reasons, further application of alizarin modified carbon paste electrodes in the determination of aluminium(III) was not investigated.

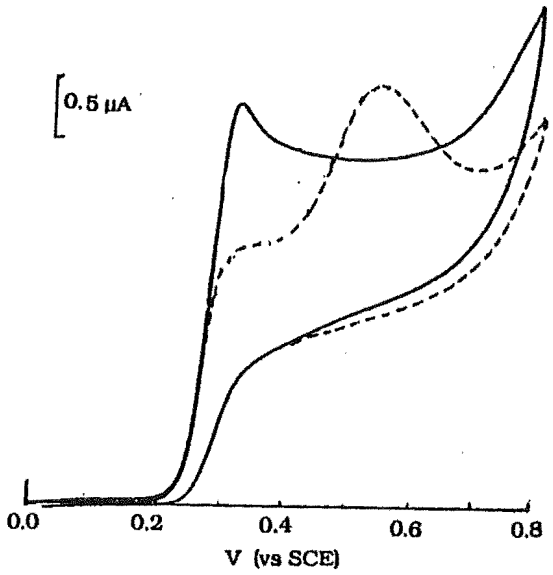

Figure 5.4. Cyclic voltammograms (100 mV s^{-1}) of alizarin modified carbon paste electrodes in ammonium chloride-ammonia buffer solution in the absence (solid line) and presence (dashed line) of 5 x 10^{-4} M aluminium(III). Accumulation time: 2 minutes at open circuit.

5.4. MODIFIED GRAPHITE EPOXY ELECTRODES

5.4.1. 4-nitrocatechol modified graphite epoxy electrodes

Three different concentrations of 4-nitrocatechol were incorporated in graphite epoxy: 5, 7.5 and 10% w/w. The higher the concentration of 4-nitrocatechol incorporated in the electrode the higher the sensitivity for aluminium(III) obtained. Proportions of ligand greater than 10% w/w gave less satisfactory results, however, because of the difficulty of preparing a homogeneous graphite-epoxy-ligand mixture with a large amount of ligand. Figure 5.5 shows the differential pulse voltammograms of the electrode (containing 7.5% 4-

nitrocatechol) after soaking in ammonium chloride-ammonia buffer solution (pH 8.5) in the absence and presence of 1 x 10^{-4} M aluminium(III). The presence of aluminium results in a decrease in ligand peak and a new peak due to aluminium-4-nitrocatechol complexes. Each experiment is performed on a freshly polished surface.

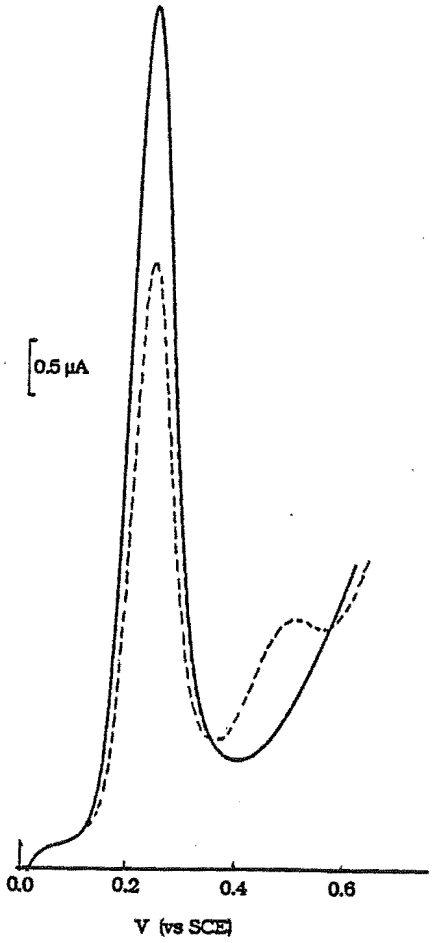

Figure 5.5. Differential pulse voltammograms (5 mV s^{-1}) for the 4-nitrocatechol modified epoxy electrode in ammonium chloride-ammonia buffer solution (pH 8.5) after soaking in the buffer solution in the absence (solid line) and presence (dashed line) of 1 x 10^{-4} M aluminium(III) for 2 minutes.

Accumulation time

The effect of accumulation time on oxidation peak current for the aluminium(III) complex was tested. As shown in Figure 5.6 two minutes accumulation gave a good sensitivity and rapid analysis and two minutes was chosen as the standard time.

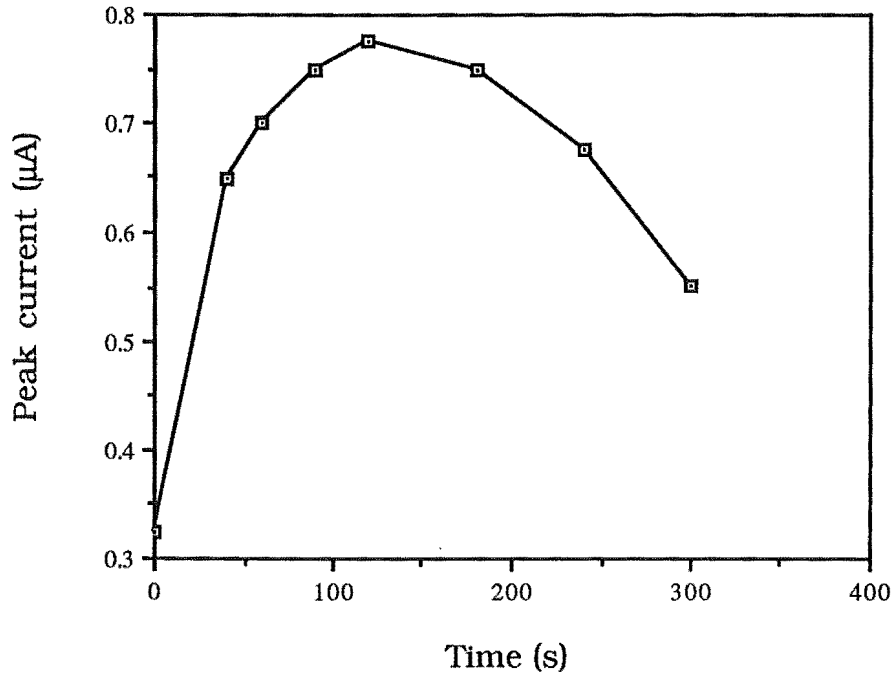

Figure 5.6. Effect of accumulation time on oxidation peak current for the aluminium(III) complex using 7.5% 4-nitrocatechol modified electrode. Concentration of aluminium(III): 1 x 10^{-5} M.

Detection limit and linear working range

Figure 5.7 shows calibration graphs for aluminium(III) using 4-nitrocatechol modified electrodes (7.5% and 10%). For the 7.5% ligand modified electrode, the limit of detection, calculated as three times the

standard deviation (n = 5) for 5 x 10^{-6} M aluminium(III) was 4.8 x 10^{-7} M giving a working range of 2.5 x 10^{-6} - 4 x 10^{-5} M aluminium(III). For the 10% ligand modified electrode, the sensitivity was much higher. The detection limit was 7.2 x 10^{-8} M and there were two linear working ranges: 3.6 x 10^{-7} to 2 x 10^{-6} M and 2.5 x 10^{-6} to 2.5 x 10^{-5} M aluminium(III). Two linear ranges on the calibration graph may indicated a change in stoichiometry from 2 : 1 (ligand : aluminium(III)) to 1 : 1 as the concentration of aluminium(III) increases. The R.S.D. at 5 x 10^{-6} M aluminium(III) was 3.7% (n = 5) for the 7.5% 4-nitrocatechol modified electrode and at 2 x 10^{-6} M aluminium(III) was 1.8% (n = 5) for the 10% 4-nitrocatechol modified electrode. Since the 7.5% w/w ligand electrode gave a longer working range it was used for all further measurements.

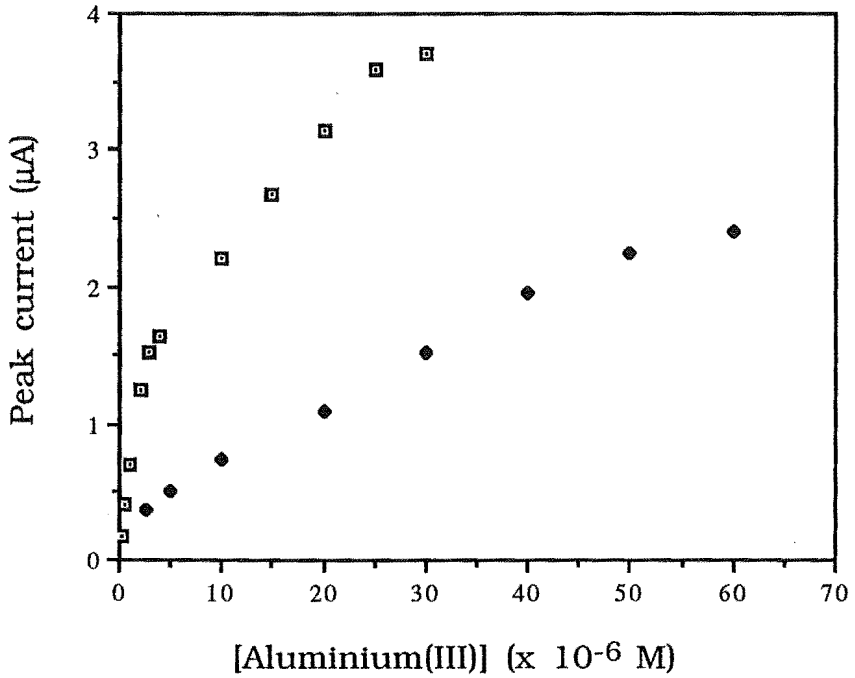

Figure 5.7. Calibration graph for aluminium(III) using (•) 7.5% 4-nitrocatechol modified graphite epoxy electrode and (□) 10% 4-nitrocatechol modified graphite epoxy electrodes.

Interferences

Nitrilotriacetate (NTA) and iron(III) were potentially problematic interferents for the alizarin CME (Chapter Four). The performance of the graphite epoxy CME in the presence of iron(III) and NTA was assessed for 5 x 10^{-6} M aluminium(III) using the 7.5% 4-nitrocatechol modified electrode and compared to that of the chemisorbed alizarin CME. Table 5.1 shows the results.

Table 5.1. Level of interferents causing a 20% decrease in the peak height of the aluminium(III) complex[a]

	4-nitrocatechol CME[b]	Alizarin CME[c]
Fe(III)	1.0 x 10^{-5} M	7.0 x 10^{-6} M
NTA	2.0 x 10^{-6} M	3.0 x 10^{-6} M

[a] 5.0 x 10^{-6} M aluminium(III). [b] 7.5% 4-nitrocatechol modified graphite epoxy electrode. [c] Alizarin dip-coated graphite electrode.

The level of interferents causing a 20% decrease are very similar for both CMEs suggesting that the coordinating abilities of alizarin and 4-nitrocatechol are similar for aluminium(III) and Fe(III). The graphite epoxy CME appears to offer no advantages over the alizarin CME for reducing interferences.

Re-use of the electrodes

Due to the irreversibility of the 4-nitrocatechol oxidation, the second scan in cyclic voltammograms showed a decrease in the peak height of the aluminium(III) complex. Polishing was used to renew the

electrode surface. Between measurements, the electrode was polished using polishing paper, followed by 9, 6, 3 and 1 μm diamond paste. Using this renewal procedure, satisfactory reproducibility was obtained as evidenced by the R.S.D. (3.7%; n = 5) for 5 x 10^{-6} M aluminium(III) using 7.5% 4-nitrocatechol modified graphite epoxy electrode.

5.4.2. 1,2-naphthoquinone modified graphite epoxy electrodes

Since 1,2-naphthoquinone shows chemically reversible redox chemistry, it was expected that loss of sensitivity due to irreversible oxidation might be overcome by use of this modifier. Figure 5.8 shows four consecutive differential pulse scans of a 1,2-naphthoquinone modified graphite epoxy electrode. Scans are initiated at -0.4 V (vs SCE) where the ligand is in the reduced form. There is no loss of signal for the ligand after repeat scans. Figure 5.8 shows the differential pulse voltammograms of the electrode after reducing at -0.4 V while soaking in the buffer in the absence and presence of aluminium(III). A significant decrease in oxidation peak of the ligand was observed after reaction with aluminium(III), however, no new peak due to an aluminium complex was found. After this reaction the electrode was removed, reduced and soaked in buffer solution. The next voltammogram (not shown) indicates a small decrease in peak height for oxidation of ligand (compared to that before reaction with aluminium(III)). This result is consistent with the behaviour of the chemisorbed 9,10-phenathrenquinone and 1,2-naphthoquinone modified electrodes described in Chapter Four. Again, it may be that ligand on the surface of the graphite epoxy CME dissolves from the surface after coordination to aluminium(III). This makes it impossible to reuse the electrode without surface pretreatment. The lack of a new

peak for aluminium(III)-ligand complexes and the need to deoxygenate solutions prior to analysis clearly make this a less satisfactory CME than that incorporating 4-nitrocatechol.

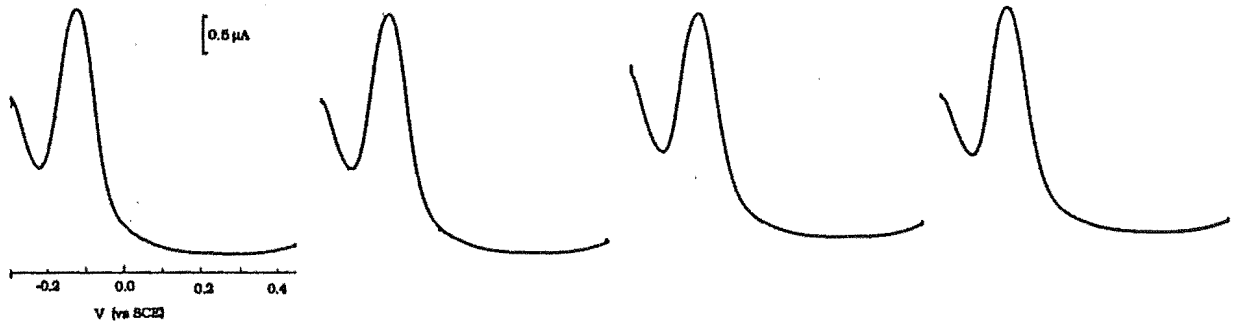

Figure 5.8. Repeat differential pulse voltammograms (5 mV s^{-1}) for a 1,2-naphthoquinone modified epoxy electrode in ammonium chloride-ammonia buffer solution after reducing and soaking in the buffer solution 2 minutes.

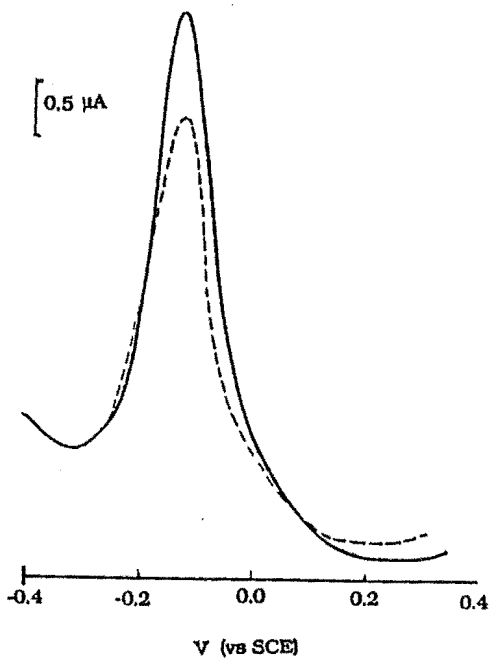

Figure 5.9. Differential pulse voltammograms (5 mV s^{-1}) for a 1,2-naphthoquinone modified epoxy electrode in ammonium chloride-ammonia buffer solution after reducing and soaking in the buffer solution in the absence (solid line) and presence (dashed line) of 1 x 10^{-4} M aluminium(III). Soaking time: 2 minutes at -0.4 V.

5.5. CONCLUSIONS

Graphite epoxy is a convenient material for CME preparation. For multiple-use, polishing gives satisfactory reproducibility. For determination of aluminium(III), the 4-nitrocatechol modified graphite epoxy electrode has similar detection limit, working range and interferences to the chemisorbed alizarin CME. For use in field work, polishing may be a more convenient renewal method than dip-coating. A simplified polishing procedure for graphite epoxy may be found to give satisfactory results.

Carbon paste electrodes do not give satisfactory results for determination of aluminium(III). Previous workers have successfully used similar CMEs to accumulate reducible metal ions, however, the procedure required for aluminium(III) is more complex. Analysis based on ligand-centred electrochemistry cannot be carried out effectively using carbon paste electrodes.

The 1,2-naphthoquinone electrode showed acceptable stability on repeat scans without surface renewal. However, its use for aluminium determination was unsatisfactory, primarily because no new peaks due to aluminium(III)-ligand complex were observed.

CHAPTER SIX

CATHODIC STRIPPING VOLTAMMETRIC ANALYSIS OF ALUMINIUM ON MERCURY

6.1. INTRODUCTION

Solochrome violet RS (SVRS), an electroactive ligand, has been used in indirect electrochemical determination of aluminium(III) for a long time, as described in Chapter Three. Since it was first applied in polarography by Willard and Dean in 1950[32], the use of SVRS for the voltammetric determination of aluminium(III) has been well developed. In this earliest report they stated that in the presence of aluminium(III) the single polarographic reduction wave of SVRS was split into two with the height of the wave at more negative potentials proportional to the aluminium(III) concentration. However, at pH 4.6 equilibration of the aluminium(III)-SVRS solutions required over 4 hours at room temperature, and complex formation was most conveniently achieved by heating at 55 - 70 ^{o} C for 5 minutes.

Subsequently other workers have examined the details of the solution chemistry and the electrochemical response of SVRS and the aluminium(III)-SVRS complex, and they have investigated the analytical utility of this reduction method[54,85-87]. The oxidation of aluminium(III)-SVRS complexes at pyrolytic graphite[97,127] and carbon paste electrodes[128] has also been reported to be useful in the determination of aluminium(III) .

Recently, a very sensitive method based on cathodic stripping voltammetry of the aluminium-SVRS complex at a hanging mercury

drop electrode (HMDE) was reported by Wang et al.[88] They reported that the reduction wave of aluminium(III)-SVRS was enhanced by adsorption of the complex at the mercury electrode. The detection limit was 5.5 x 10^{-9} M and the linear working range for aluminium(III) was 1.85 x 10^{-8} - 1.1 x 10^{-6} M. However, the method as reported has distinct limitations. To effect complete reaction in the acetate buffer (pH 4.5) the solutions must be heated for 10 minutes at 90 ^{o}C then cooled for 15 minutes prior to analysis.

As part of a programme to develop new and improved methods for the indirect electrochemical determination of aluminium(III), a modification the SVRS method of Wang et al., was undertaken. This modification involved optimising the reaction conditions for rapid formation of the aluminium(III)-SVRS complex.

6.2. EXPERIMENTAL

Linear-sweep and stripping voltammograms were obtained using a PAR Model 174A Polarographic Analyzer coupled to a PAR Model 303A static mercury drop electrode and a PAR Model RG0074 X-Y recorder. A standard three-electrode cell was used, consisting of a medium-sized mercury drop working electrode, a platinum wire counter electrode and a Ag/AgCl (saturated KCl) reference electrode. The potential of the reference electrode was checked using the reduction (differential-pulse polarography) of Cd^{2+} in 0.1 M KNO_3. A PAR Model 305 magnetic stirrer was operated at 400 rpm during the accumulation step.

Spectrophotometric measurements were made using a Varian Superscan 3 spectrophotometer.

A 2 x 10^{-4} M SVRS stock solution was prepared daily. The concentration was based on ca. 60% dye content as stated by the supplier. The 1 M ammonium acetate-ammonia buffer was prepared from isopiestically distilled ammonia solution and acetic acid. Aristar-grade sodium acetate and perchloric acid were used.

6.3. METHOD DEVELOPMENT

6.3.1. Effect of pH on complex formation

As mentioned by earlier workers[32,54,85], and discussed in Chapter One, the rate of reaction of aluminium(III) with SVRS increases with pH. The rate of formation of the aluminium(III)-SVRS complex as a function of pH was examined spectrophotometrically at room temperature ([aluminium]: 1 x 10^{-4} M; [SVRS]: 2 x 10^{-4} M). Absorbance changes at 600 nm, where there is the maximum difference in molar absorptivity for SVRS (λ_{max} = 555 nm) and its aluminium(III) complex (λ_{max} = 530 nm), indicated that the reaction is immeasurably slow at pH 4.5 but that the rate increased by a factor of 2.5 over the pH range 7.0 - 9.3.

At low pH, the free ligand may be stabilised by hydrogen bonding.

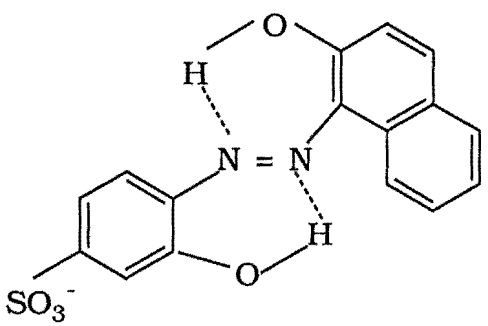

For reaction with aluminium(III), rotation about one N-phenyl bond must occur requiring cleavage of a hydrogen bond.

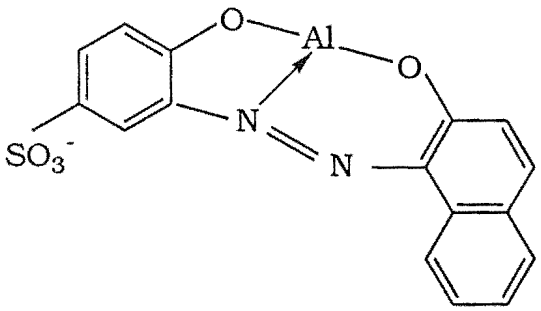

At high pH, SVRS is singly deprotonated thus allowing rapid rotation about an N-phenyl bond and hence reaction with aluminium(III) is facilitated. Similar conformational changes were observed by Chau and Porter[129] for coordination of calcium.

In weakly alkaline solution the rate of reaction of aluminium(III) with SVRS is also dependent on their concentrations. Spectrophotometric studies in ammonium chloride-ammonia (pH 8.8) showed that the formation of complex is rapid (complete reaction in seconds) when the concentrations of both of SVRS and aluminium(III) are relatively large (1.0×10^{-5} and 5.0×10^{-6} M respectively). Similar evidence was obtained from linear scan voltammetry. However, at the lower concentrations of SVRS and aluminium(III) used in the voltammetric analysis the rate of formation of the complex is significantly lower.

In a series of measurements the cathodic current was measured as a function of time after mixing SVRS and aluminium(III). The first measurement, with 60 seconds accumulation time, was made immediately after mixing; each measurement took about 2.5 minutes. For 1.0×10^{-5} M SVRS and 5.0×10^{-6} M aluminium(III), 2×10^{-6} M SVRS and 1.0×10^{-6} M aluminium(III), and 2×10^{-6} M SVRS and 5.0 x

SVRS and 1.0 x 10^{-6} M aluminium(III), and 2 x 10^{-6} M SVRS and 5.0 x 10^{-7} M aluminium(III) the cathodic stripping current increased 0%, 5% and 8% per measurement, respectively. These results indicate that when a low concentration of aluminium(III) reacts with SVRS in a weakly alkaline solution the complete reaction will require a significant period of time. This means that replicate analyses of the accumulated aluminium(III)-SVRS complex can not be made in high pH solution.

In an acetate solution equilibration of the aluminium(III)-SVRS solutions requires over 4 hours at room temperature. Hence, a possible method for determination of aluminium(III) arises from these experiments: aluminium(III) is reacted with SVRS at pH 8.8; the reaction is stopped by lowering the solution pH, then the aluminium(III)-SVRS complex is accumulated on the mercury drop.

6.3.2. Electrochemistry of SVRS and the aluminium(III)- SVRS complex

Cyclic voltammograms of SVRS and the aluminium(III)-SVRS complex in acetate buffer, pH 4.5, on a glassy carbon electrode are shown in Figure 3.3. Their electrochemistry is also discussed in Chapter Three.

Cathodic stripping voltammetry on the mercury electrode involved the reduction processes of SVRS and the aluminium(III)-SVRS complex. The reduction potentials of SVRS and its aluminium(III) complex are pH dependent. The effect of pH on their reduction peak potentials at the hanging mercury drop electrode (HMDE) is shown in Figure 6.1.

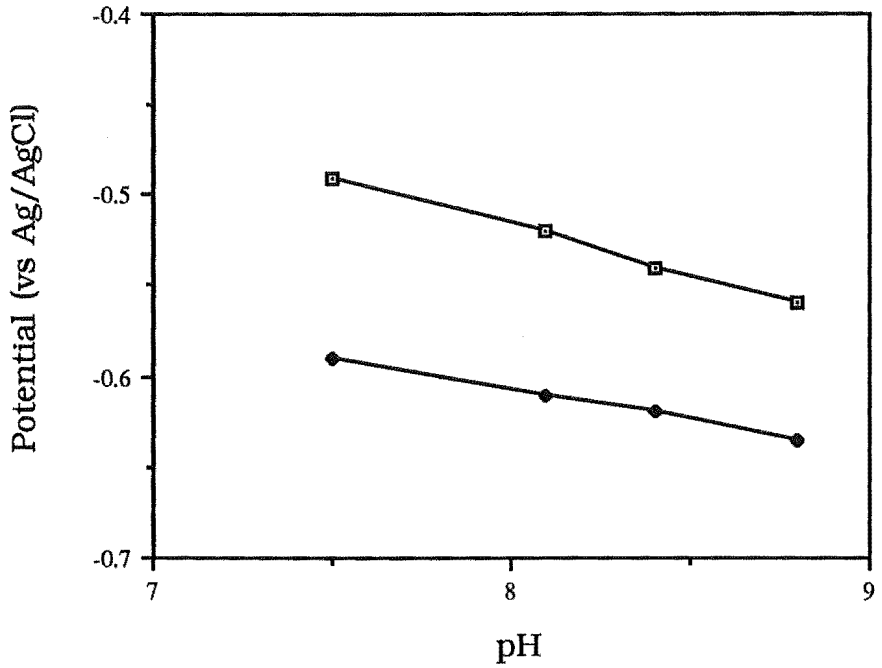

Figure 6.1. Effect of pH on the reduction peak potentials of ( ) SVRS and (•) the aluminium(III)-SVRS complex. Mode: linear scan at an HMDE. [SVRS] = 2×10^{-6} M, [aluminium(III)] = 4×10^{-7} M.

Figure 6.2 shows linear voltage scans for a solution of SVRS (2×10^{-6} M) and aluminium(III) (4×10^{-7} M) after their reaction for 10 minutes at room temperature (pH 8.8). Figure 6.2(A) was recorded at pH 8.8 and Figure 6.2(B) after lowering the pH to 4.6. In each scan the larger peak corresponds to reduction of SVRS and the smaller peak (*) to reduction of SVRS bound to aluminium(III). At pH 4.6 the smaller peak is due to SVRS complexed to aluminium(III). After a 60 second accumulation from stirred solution at -0.47 V, the solution at pH 8.8 gave the stripping peaks shown in Figure 6.2(C) (E_p = -0.60 V). After lowering the pH to 4.6, a 60 second accumulation at -0.20 V gave the stripping peak shown in Figure 6.2(D) (E_p = -0.35 V). In contrast, for a solution of aluminium(III) and SVRS at the same concentrations, reacted for 10 minutes at room temperature and pH 4.5, no peak due

to an aluminium(III)-SVRS complex was observed, even after prolonged accumulation. Hence the rapid room temperature reaction of aluminium(III) with SVRS at pH 8.8 can be used as the basis for cathodic stripping analysis for aluminium(III).

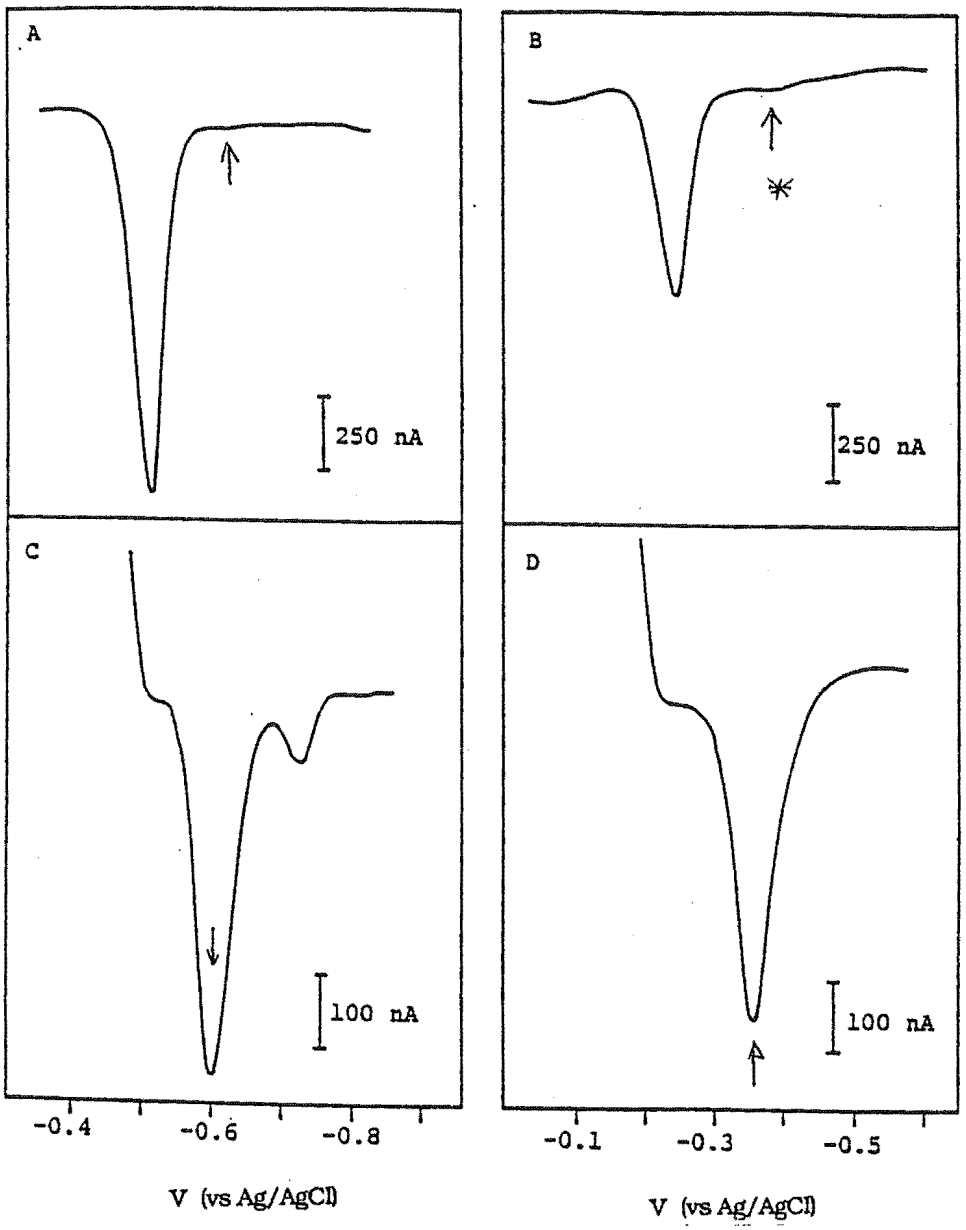

Figure 6.2. Linear scan voltammograms (50 mV s^{-1}) for a solution of SVRS (2 x 10^{-6} M) and aluminium(III) (4 x 10^{-7} M) after a 10 minute degassing and reaction time at room temperature at pH 8.8. (A) pH 8.8, no accumulation; (B) solution pH lowered to 4.6, no accumulation; (C) pH 8.8 after a 60 second accumulation at -0.47 V; (D) pH 4.6 after a 60 second accumulation at -0.20 V.

6.4. RESULTS AND DISCUSSION

6.4.1. Optimum conditions

The method described requires buffering of solutions at pH > 8 (for the complexation reaction) then at pH 4 - 5 (for accumulation) according to the experimental results described above. Ammonium acetate-ammonia was chosen as the buffer because it has good buffer capacity at pH > 8 (ammonium/ammonia buffer) and, after addition of perchloric acid, at pH 4 - 5 (acetate buffer). A solution pH of 8.8 ± 0.1 was most convenient for the standard procedure.

At the concentrations used for analysis, the reaction between aluminium(III) and SVRS was ca. 30% complete after 10 minutes at pH 8.8. Hence there was a continued slow increase in stripping peak current for solutions allowed longer reaction times at this pH. Careful control of the reaction time was required. This was achieved, and the reaction effectively stopped, by lowering the pH to 4.6 by addition of 35 μL of concentrated perchloric acid after a 10-minute degassing and reaction time. The aluminium(III)-SVRS complex was then accumulated from the pH 4.6 solution.

6.4.2. Aluminium(III) analyses

Preparations and measurements of samples were carried out in a Class 100 clean room. Solutions for analysis were prepared by successive addition of 0.5 mL of 1 M ammonium acetate-ammonia buffer (pH 8.8), 1 - 2 mL of stock or diluted stock SVRS solution and 20 - 1000 μL of stock or diluted stock aluminium(III) solution to a 10-mL volumetric flask. Timing was commenced on addition of the

aluminium(III) solution. The solution was immediately transfered to the polarographic cell and N_2 flow commenced. After a total time of 10 minutes 35 μL of concentrated perchloric acid was added. The accumulation potential, -0.20 V, was applied to a fresh mercury drop for 60 seconds while the solution was stirred (400 rpm). Following a 15 second rest period, the stripping voltammogram was recorded by scanning at 50 mV s^{-1} from -0.20 to -0.70 V. The blank was determined by the same procedure, without the addition of aluminium(III) stock solution.

Figure 6.3 shows the variation of stripping peak current with accumulation time at pH 4.6. An accumulation time of 60 seconds provided the best compromise between sensitivity and speed of analysis. The stripping peak current was highly sensitive to the accumulation potential; accumulation at -0.20 V gave the highest sensitivity. The linear-sweep stripping mode afforded greater sensitivity than differential-pulse voltammetry.

The optimum accumulation potential (and accumulation time) determined in this study differ from that reported by Wang et al. We attribute this to different reference electrode potentials. In the present work the reference electrode potential was standardised against $E_{1/2}$ for a Cd^{2+} solution (measured by DPP).

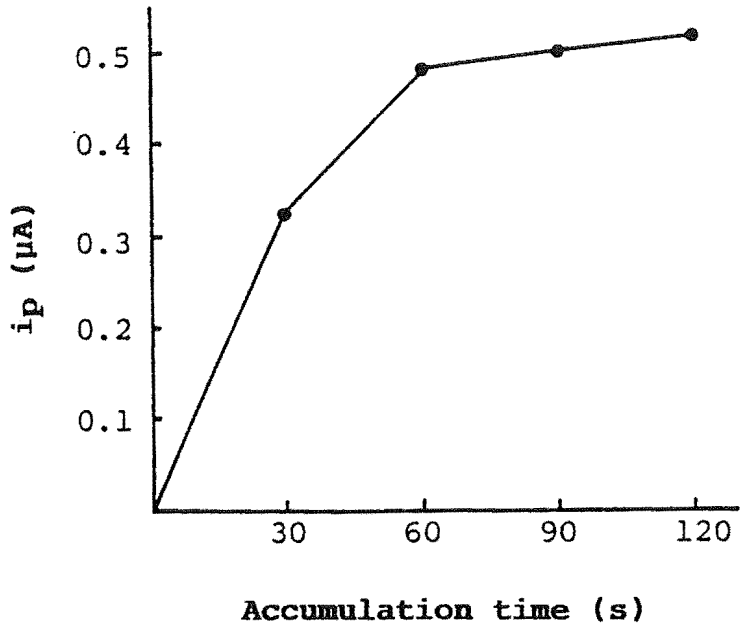

Figure 6.3. Dependence of the stripping peak current (linear scan, 50 mV s^{-1}) on accumulation time for the aluminium(III)-SVRS complex. 2 x 10^{-6} M SVRS; 7 x 10^{-7} M aluminium(III); accumulation at -0.20 V at pH 4.6.

6.4.3. Detection limit and working range

Accumulation in the absence of aluminium(III) established a measurable response for the blank. Experiments in which the concentrations of the buffer and SVRS solutions were varied, and polypropylene reaction cells were substituted for glass cells, indicated that the blank response arose from the SVRS sample. For 1 x 10^{-6} M SVRS, the blank was equivalent to 7 x 10^{-8} M aluminium(III). Hence the minimum distinguishable analytical signal for aluminium(III) determination is dependent on the SVRS concentration.

Figure 6.4 shows the dependence of stripping peak current for the aluminium(III)-SVRS complex on aluminium(III) concentration. For

1 x 10^{-6} M SVRS acceptable linearity is shown up to 2.5 x 10^{-7} M aluminium(III). The slope of the calibration graph was 0.452 A (mol Al)$^{-1}$; R^2 = 0.9999 (n = 6). The detection limit, calculated as 3 σ_b (n = 9) was 4.5 x 10^{-9} M aluminium(III), giving a theoretical working range of ca. 2 x 10^{-8} - 2.5 x 10^{-7} M aluminium(III). The relative standard deviation (R.S.D.) at 2 x 10^{-8} M aluminium(III) added (9 x 10^{-8} M total) was 5% (n = 8). Use of a higher concentration of SVRS extended the upper limit of the linear range.

The detection limit (DL) and R.S.D. reported here are similar to those determined by Wang et al., namely 5.5 x 10^{-9} M and 2% at 3.7 x 10^{-7} M aluminium(III), respectively, but apply to a 1-minute rather than a 10-minute accumulation time. Hence the modified procedure is suitable, and indeed preferred, for similar applications.

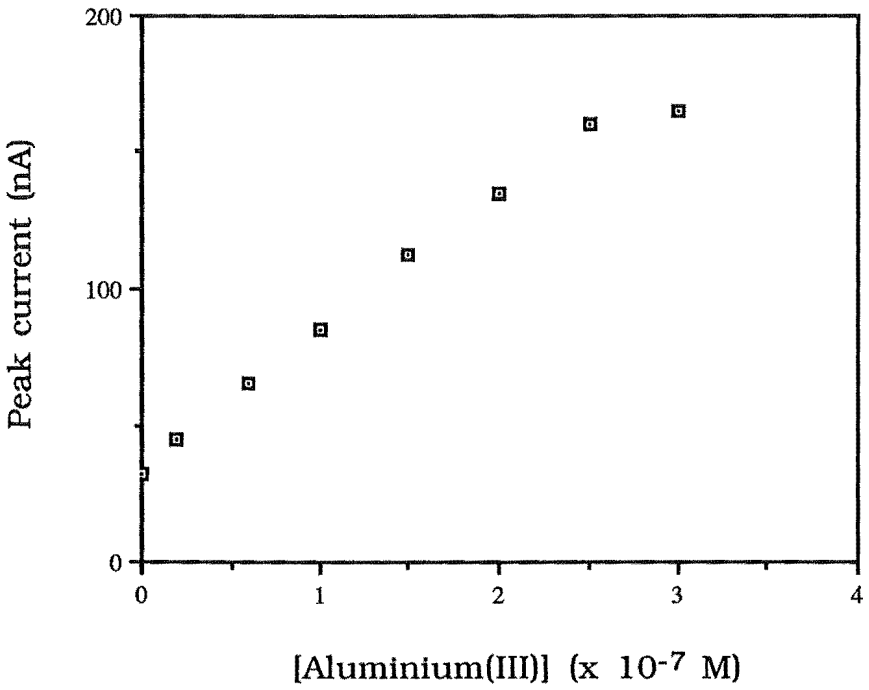

Figure 6.4. Dependence of the CSV differential-pulse peak height for the aluminium(III)-SVRS complex on aluminium(III) concentration. [SVRS]: 1 x 10^{-6} M.

6.5. CONCLUSION

For the cathodic stripping voltammetric determination of aluminium(III) as its SVRS complex, the modifications described here afford a simpler and faster method of analysis. The heating and cooling steps (total time 25 minutes), necessary when working at pH 4.5, are replaced with a 10 minute reaction (effected during degassing) at room temperature at pH 8.8. Control of the reaction time by lowering the solution pH to stop the reaction achieved excellent reproducibility.

CHAPTER SEVEN

AMPEROMETRIC METHODS IN FLOW SYSTEMS: DETERMINATION OF ALUMINIUM(III)

7.1 INTRODUCTION

As described in Chapter One, aluminium(III)(aq) is a toxic element and is harmful to flora and fauna in the environment. Its concentration is an important parameter in the monitoring of drinking water and soil solution.

The determination of aluminium(III) at environmentally or physiologically significant concentrations can be achieved by some electrochemical methods. For example, using a CME modified with a PXV film (Chapter Three) or a CME modified with alizarin (Chapter Four), voltammetry was applied in determination of aluminium(III). It can also be determined by electrothermal atomic absorption spectrometry (ETAAS)[130] or by a variety of convenient spectrophotometric methods[131]. The sensitivity of spectrophotometric techniques may be enhanced by use of surfactants[132,133]. Several colorimetric reagents have been successfully adapted to flow-injection analysis for aluminium(III), e.g. pyrocatechol violet (PCV)[132], eriochrome cyanine R (ECR)[134], xylenol orange[135], chrome azurol S (CAS)[136] and pyrogallol red[133]. However, the wide intrinsic working range accessible by amperometric techniques and the low volume possible in amperometric cells makes the development of electrochemical methods attractive.

For analysis of aluminium(III), flow injection analysis (FIA) has proved to be a suitable tool for rapid, simple analysis with rather inexpensive apparatus. The attainment of steady state conditions, a requirement in continuous flow analysis, is not necessary because of FIA's high reproducibility. The principles of FIA are outlined below.

7.1.1. The principle of flow injection analysis

Flow injection analysis is based on the injection of a liquid sample into a moving stream of reagent(s). The injected sample forms a zone, which disperses with the carrier stream as it is transported toward a detector. The detector continually records the change in absorbance, electrode potential or current, or other physical parameter during the passage of the reaction product through the flow cell[137,138] (see Figure 7.1). The FIA system itself provides reproducible physical conditions arising from three basic factors: reproducible sample injection, controlled dispersion, and reproducible elapsed time from injection to detection. However, as the FIA technique has been developed further, these three basic principles have been modified.

The reproducible elapsed time allows for reproducible physical mixing and dispersion. It is observed that the injected sample zone is always "mixed" with the reagents in the same manner. In other words, reproducible timing controls the dispersion of sample and reagent observed at the detector. Dispersion in a straight tube arises from convection and from diffusion which causes redistribution of reagents and sample in axial and radial directions. To minimise axial dispersion but at the same time achieve good mixing a knitted coil is often included in an FIA manifold; dispersion in the axial direction is much

less in a knitted coil compared to that in a straight tube of the same length and internal diameter.

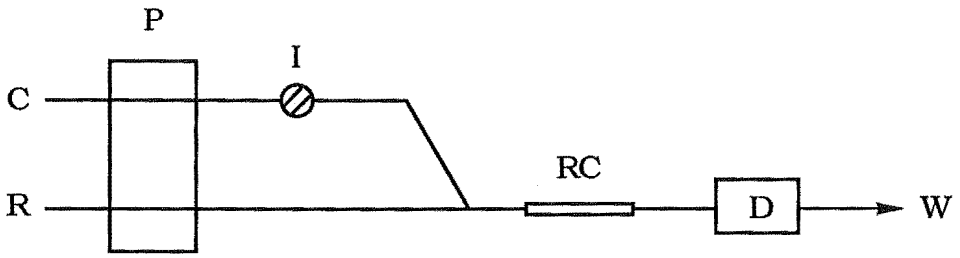

(a)

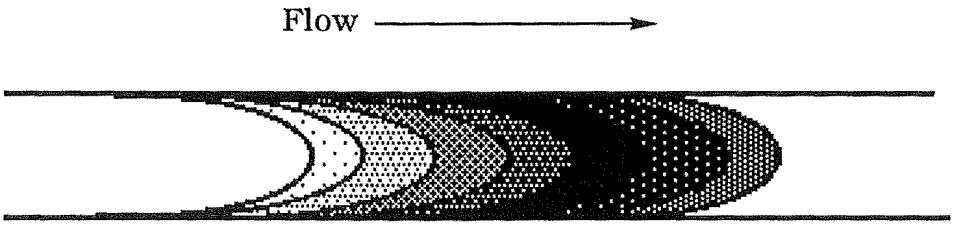

Dispersed sample plug

(b)

Figure 7.1. (a) Simple manifold for flow injection analysis. R, reagent; C, carrier; P, pump; I, injection valve; RC, reaction coil; D, detector. W, waste. (b) Simplified depiction of the sample zone after some dispersion has occurred.

Dispersion is defined experimentally as the amount that the sample concentration is reduced by injecting a sample plug into an FIA system. This is represented mathematically by

$$D_{min} = C^o/C^{max}$$

where D_{min} is the dispersion coefficient at the peak maximum. It may be measured by injection of a non-reactive dye where C^o is the concentration of the undiluted dye, and C^{max} the maximum

concentration of the injected dye as it passes through the spectrophotometric detector.

The dispersion coefficient is a useful parameter that allows comparison of different manifolds. Further, it provides a means of verifying and monitoring the extent of sample dilution resulting from any changes made to the manifold during the method development.

There are two ways that the kinetics of a chemical reaction can be exploited to change the observed FIA signal: by changing the reaction time, and by varying the ratio of reagent to sample. The best way to increase the reaction time is to decrease the flow rate or to stop the flow for a specified period after thorough mixing of sample and reagents. The next best way is to increase the length of the reaction coil.

7.1.2. Scope of present work

The commonly used spectrophotometric and amperometric detection techniques in FIA are both susceptible to fouling, e.g., adsorption of coloured matrix components or substrate on optical fibres or absorption cell windows, or adsorption of redox products on the working electrode surface, respectively. However, the latter can often be rectified in a programmed manner by electrochemical cleaning, as demonstrated in this work.

As part of a project to develop and apply electrochemical sensors for the determination of aluminium(III) a method involving indirect amperometric detection via a redox active ligand was developed for FIA using a micro flow cell. The method used the ligand DASA which binds rapidly with aluminium(III) in weakly alkaline solution (pH 9.0). The oxidation of unbound DASA in the reagent stream was monitored

continuously on a gold electrode at 0.50 V vs Ag/AgCl(0.1 M KCl). The decrease in ligand oxidation current was proportional to the concentration of injected aluminium(III) solution.

7.2. EXPERIMENTAL

A double pumping flow system was used in these experiments; the reasons are discussed below. It consisted of an Alitea C4-XV peristaltic pump (pump 1), an Ismatec IPN-12 peristaltic pump (pump 2) and the flow manifold shown in Figure 7.2.

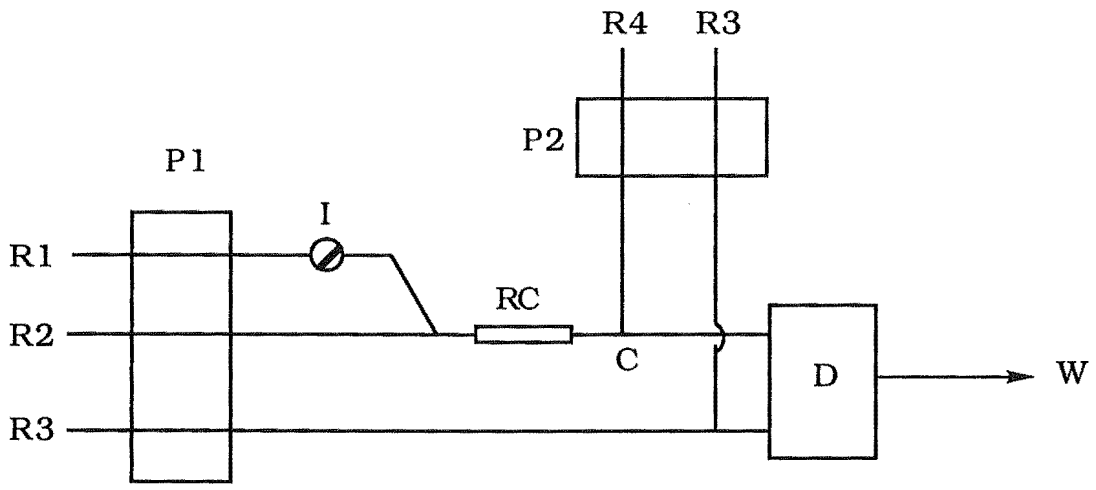

Figure 7.2. Manifold for pulsed flow injection. R1, water; R2, DASA in 0.50 M ammonium acetate-ammonia, pH 9.0; R3, 0.1 M KCl (for reference electrode); R4, 0.50 M ammonium acetate-ammonia, pH 9.0; I, sample injection (25 μL); D, detector; W, waste; P1, pump 1; P2, pump 2.

The flow-rates used for the carrier (R1 = water), reagent (R2 = DASA in 0.5 M ammonium acetate-0.5 M ammonia, pH 9.0), reference

electrode electrolyte (R3 = 0.1 M KCl), and wash solution (R4 = 0.5 M ammonium acetate-ammonia, pH 9.0) were 0.76, 1.19, 0.16 and 1.19 mL minute^{-1} respectively.

The six-port rotary injection valve of the type described by Karlery[138] was connected as shown in Figure 7.3. The sample loop size (25 μL, 50 μL, 100 μL or 250 μL) was defined by the length of microline tubing, and was easily varied. The rotary injection valve in this work had a 25 μL sample loop.

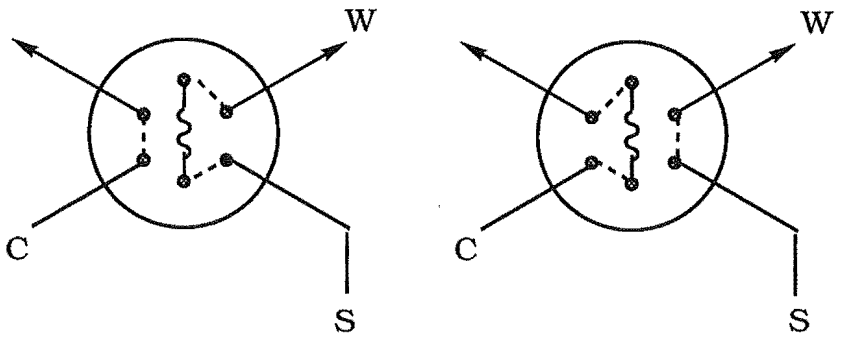

(a) Loading (b) Injection

Figure 7.3. Diagram of injection valve (a) Filling of sample loop, (b) Sample injection into flow system. C, carrier. S, sample. W, waste.

The reaction coil used in this work consisted of 100 cm x 0.51 mm or 50 cm x 0.51 mm i.d. knitted microline tubing (Cole-Palmer). For the merging of the carrier and reagent streams glass connectors illustrated in Figure 7.4 were used (1.0 mm i.d.). They were joined to the microline tubing by a short length of silicone tubing (1.3 mm i.d.). Connectors with this configuration are reported to achieve maximum dispersion of carrier and reagent streams[138].

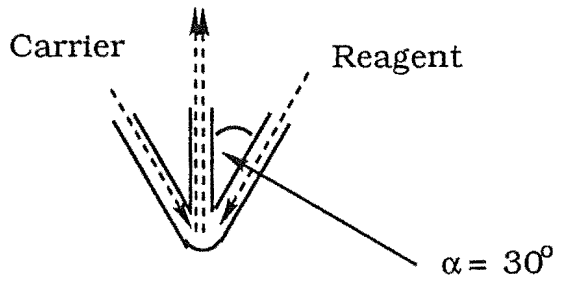

Figure 7.4. Diagram of tubing connection in flow system.

The dispersion coefficient for the injected solution was measured by comparing the peak current for the electroactive ligand DASA when injected and when pumped through the total manifold. The dispersion coefficient (D) was 5.9. The elapsed time, measured from the merging of the sample and reagent zones to the response at the detector, was 6 seconds.

The home-made detector consisted of a wall-jet microflow cell, shown in Figure 7.5. It was fabricated from two blocks of PVC (10 x 20 x 32 mm) separated by a 0.76 mm Teflon spacer which defined an 11 mm x 2 mm reaction channel (volume 17 μL). Three electrodes mounted in one block made contact with solution in the flow channel. The electrodes were 0.5 mm diameter platinum (auxiliary), 0.55 mm gold or 0.3 cm diameter graphite (working) and 0.6 mm silver wire (Ag/AgCl reference electrode).

For polymer coating, a flow cell with a glassy carbon working electrode was used; this is described in Chapter Eight.

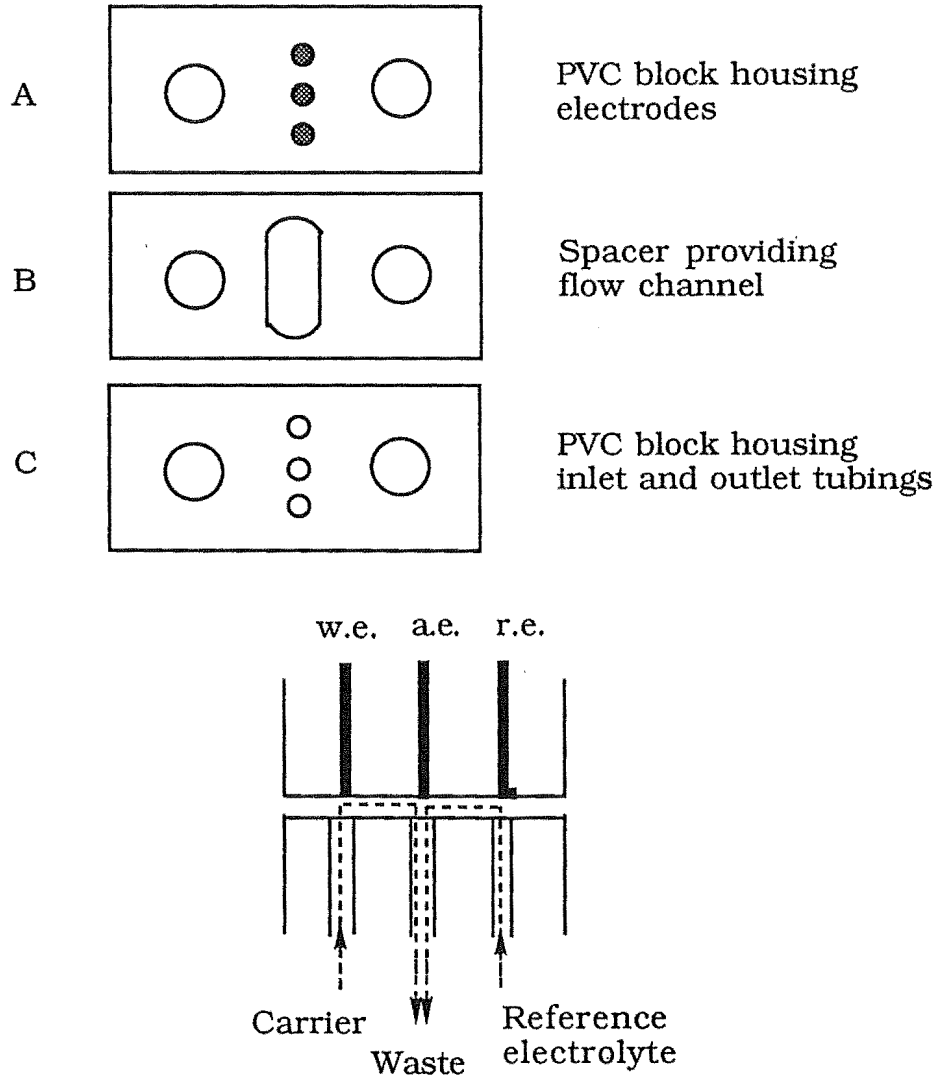

Figure 7.5. Diagram of the wall-jet microflow cell; dimensions of each half=10 x 20 x 32 mm. Large holes for clamping screws.

Amperometric and voltammetric measurements in the flow cell were obtained using a PAR 173 potentiostat coupled to a PAR 175 universal programmer and a Graphtec WX 1200 recorder.

7.3. SOLUTION ELECTROCHEMISTRY OF DASA AND ALUMINIUM(III)-DASA

7.3.1. Cyclic voltammograms

Figure 7.6 gives the cyclic voltammogram for DASA (1 x 10^{-3} M) with and without aluminium(III) (2 x 10^{-4} M) in 0.5 M ammonium acetate-ammonia buffer, pH 8.6, on a glassy carbon electrode. On glassy carbon an oxidation wave of DASA and an oxidation wave of aluminium(III)-DASA complex were observed at +0.38 V and +0.85 V, respectively.

Figure 7.7 shows similar cyclic voltammograms of DASA (2 x10^{-3} M) recorded in the flow cell under stop-flow conditions, in the presence and absence of aluminium(III) (1 x 10^{-3} M) in 0.5 M ammonium acetate-ammonia buffer, pH 9.0. These voltammograms were recorded on gold and graphite electrodes. On the graphite electrode an oxidation wave was observed for DASA at +0.35 V (curve b); this wave diminished in the presence of aluminium(III) (not shown). The gold electrode in buffer only (curve c) showed an oxidation wave at ca. 0.80 V, and the reduction of surface oxides at ca. 0.30 V on the return scan. In the presence of DASA an additional oxidation wave was observed at 0.35 V (curve d). On neither electrode was there evidence for a separate oxidation wave for the aluminium(III)-DASA complex. However, the attenuation of the DASA oxidation wave at ca. 0.35 V in the presence of aluminium(III) could be monitored (curve e). So the decrease of the oxidation current of DASA was the basis of the described method for determination of aluminium(III). +0.5 V was chosen as measuring potential because the highest peak current was obtained at this potential (not shown). Initially gold was chosen as the working electrode because of the ease of reactivation (see below).

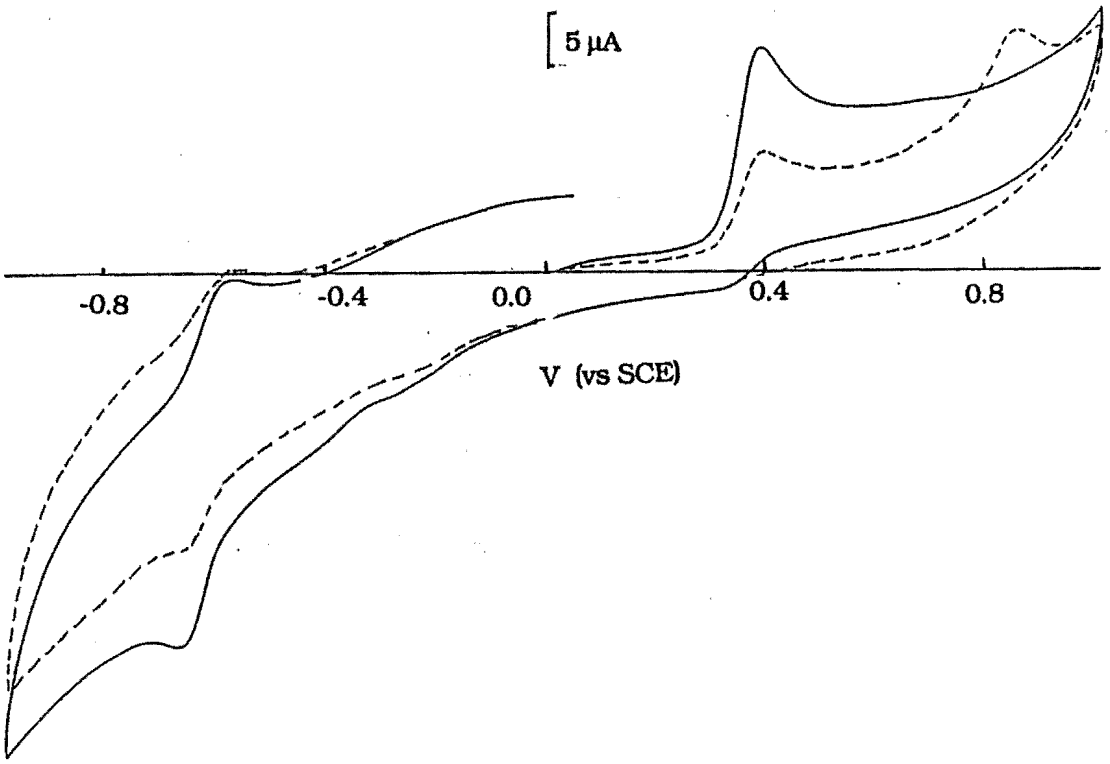

Figure 7.6. Cyclic voltammogram (50 mV s^{-1}) for DASA (1 x 10^{-3} M) (solid line) and DASA (1 x 10^{-3} M) + aluminium(III) (2 x 10^{-4} M) (dashed line) in ammonium acetate-ammonia buffer, pH 8.6, on glassy carbon.

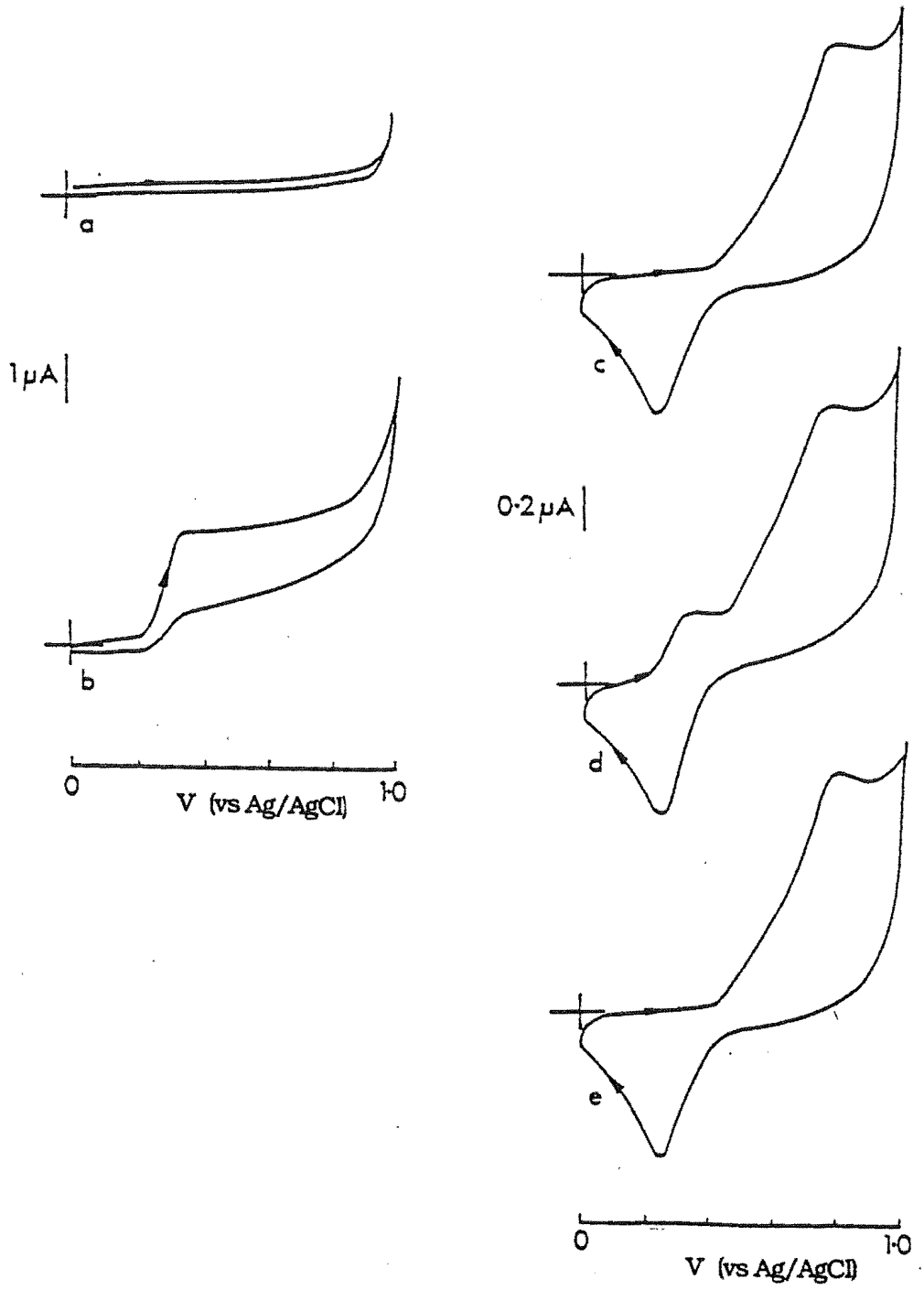

Figure 7.7. Cyclic voltammogram (50 mV s^{-1}) for DASA (2 x 10^{-3} M) and DASA + aluminium(III) (1 x 10^{-3} M) in 0.40 M ammonium acetate-ammonia buffer (pH 8.6) on (a, b) graphite and (c-e) gold electrodes. (a) and (c) buffer only; (b) and (d), DASA; (e) DASA + aluminium(III).

7.4. OPTIMIZATION OF ELECTROCHEMICAL DETECTION AND MANIFOLD DESIGN

7.4.1. Electrode surface renewal

Prior to use the electrodes were hand polished with 1 μm diamond paste. Oxidation of DASA leads to a rapid deactivation of the gold electrode surface, presumably by adsorption of polymerized oxidation products. However, as reported by Johnson and co-workers[139-141], a gold or platinum electrode may be reactivated by voltage pulsing involving an initial oxidative (or reductive) desorption of reaction products (and oxidation, or reduction, of the noble metal surface) followed by reduction (or oxidation) of the catalytic electrode surface. In this study a single cathodic-anodic-cathodic cycle was most effective in retaining electrode activity. The best results were obtained when the electrode was initially activated electrochemically for 10 minutes by voltage cycling, +0.50 V ⇒ + 0.10 V ⇒ +1.00 V ⇒ +0.50 V, at 100 mV s^{-1} as shown in Figure 7.8. For subsequent measurements a single voltage cycle, (+0.50 V ⇒ + 0.10 V ⇒ +1.00 V ⇒ +0.50 V) was used to activate the electrode before the next sample injection. This reactivation is effected under pumping and in the absence of DASA (pump 1 off, 2 on).

Following measurement at 0.5 V, the cathodic-anodic voltage scan traverses the potentials for reduction of the oxidized gold surface, then oxidation of the surface to AuO in the alkaline buffer (Figure 7.7(c)). Desorption of organic oxidation products may be effected by substrate reduction or by reduction of the electrode surface at 0.1 V . After this electrode cleaning, activation is effected by oxidation of the

clean gold surface. This indicates that AuO, rather than gold, is the active surface for DASA oxidation.

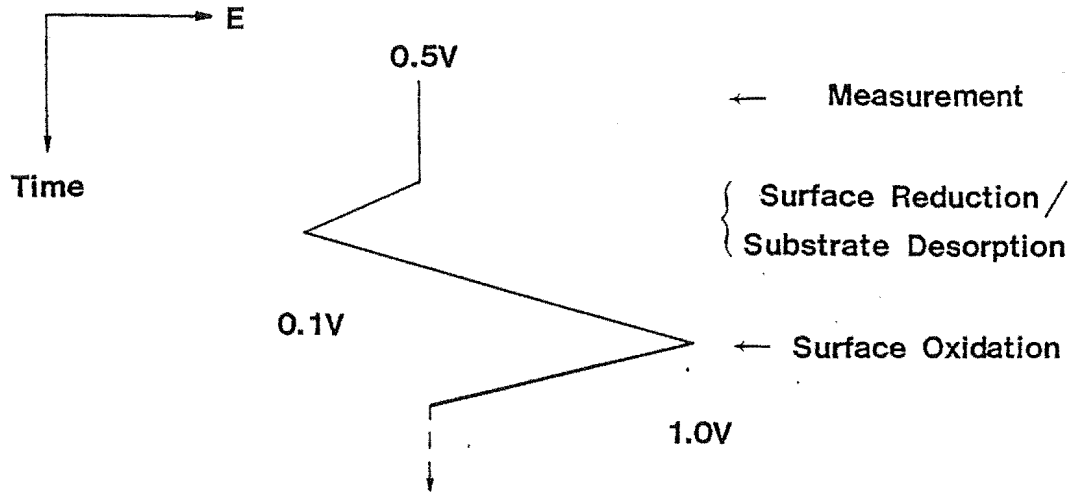

Figure 7.8. Diagrammatic representation of voltage pulsing used for electrode reactivation.

Table 7.1. Effect of voltage cycling on reactivation of electrode

Cycle type (scan rate 100 mV s^{-1})	Effect on activation[a]
+0.50 V ⇒ +0.80 V ⇒ +0.10 V ⇒ +0.50 V	+
+0.50 V ⇒ +0.10 V ⇒ +0.80 V ⇒ +0.50 V	++
+0.50 V ⇒ +0.10 V ⇒ +0.90 V ⇒ +0.50 V	+++
+0.50 V ⇒ +0.10 V ⇒ +1.00 V ⇒ +0.50 V	++++
+0.50 V ⇒ +1.00 V ⇒ +0.50 V	+

a. recovery of sensitivity; + = smallest effect, ++++ = largest effect.

As described in Table 7.1, which shows the effect of different voltage pulsing protocols on electrode activity, the use of lower anodic potentials (0.80 or 0.90 V) was significantly less effective. An anodic-cathodic-anodic cycle was also less effective; the result was similar to the effect of chemical cleaning by injection of NaOH (0.2 M) or flushing (5 minutes) with ammonium acetate (pH 7.0) or ammonium acetate-ammonia (pH 9.0) at open circuit or with an applied potential of 0.50 V.

Figure 7.9 shows the signals for (a) pulsed flow injection of 25 μL of 5 x 10^{-4} M DASA with electrode reactivation (+0.50 V ⇒ +0.10 V ⇒ +1.00 V ⇒ +0.50 V) and (b) normal flow injection without electrode reactivation.

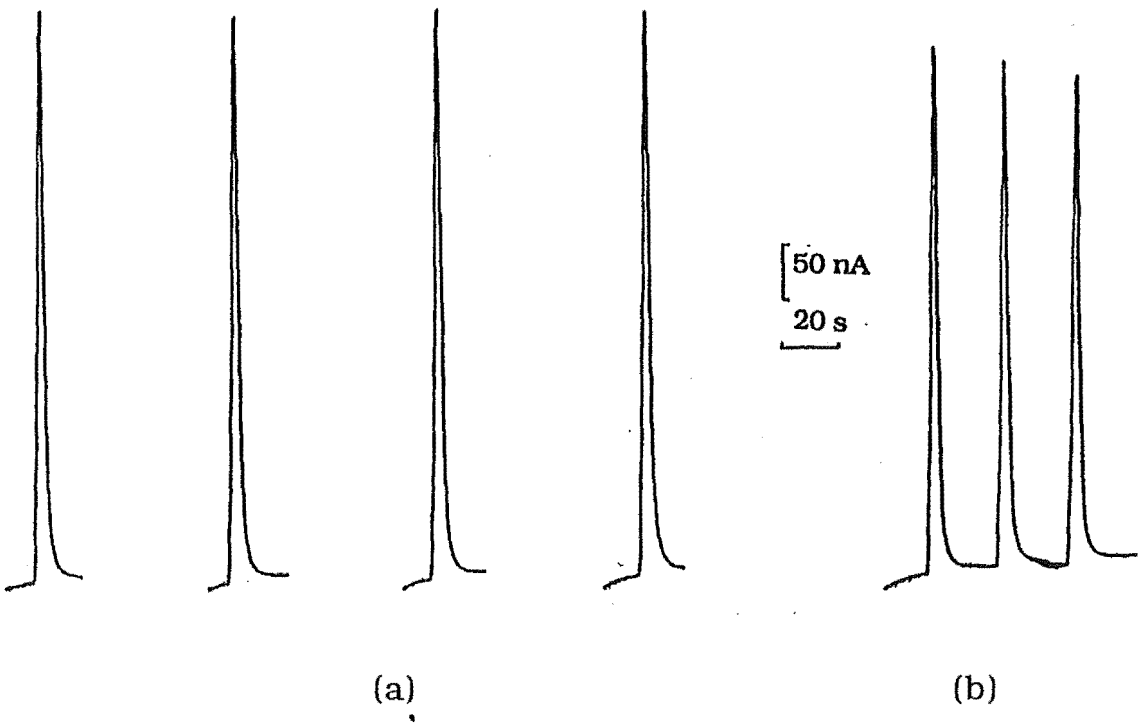

Figure 7.9. The signals for (a) pulsed flow injection of 25 μL of 5 x10^{-4} M DASA with reactivation voltages +0.50 V ⇒ +0.10 V ⇒ +1.00 V ⇒ +0.50 V and (b) normal flow injection without electrode reactivation. Measuring potential = 0.5 V for (a) and (b).

Polishing of the electrode can also renew its surface, but it is inconvenient to remove the flow cell during measurements; also it is difficult to maintain a uniform electrode surface. The use of a "dirty electrode", that is an electrode conditioned by prolonged pumping of DASA, was tested. Sensitivity still decreased on this electrode although its deactivation rate was smaller than that for a newly polished electrode.

7.4.2. Manifold design

In order to minimize contact of DASA with the working electrode, which results in the loss of sensitivity of the electrode, an alternative procedure was adopted. It involved the use of double injection with the manifold shown in Figure 7.10; 250 μL of aluminium(III) solution was injected in line R1 (carrier = water) and 25 μL of DASA was injected in line R2 (carrier = buffer). Electrode activation was as described above, but pump 2 was not required. The flow-rates for the carrier (R1 = water), buffer (R2 = 0.5 M ammonium acetate-ammonia, pH 9.0) and reference electrode electrolyte (R3 = 0.1 M KCl) were 1.19, 1.19 and 0.16 mL minute^{-1} respectively. Injection valve 1 which contained 25 μL of DASA in buffer solution was turned on 6 seconds after injection valve 2 which contained 250 μL of aluminium(III) standard or sample solution. This timing ensured that the reagent was enveloped by aluminium(III) at the merging zone. The current measured at the electrode arose from the non-complexed DASA. Figure 7.11 shows the calibration graph for determination of aluminium(III) using double injection [injection valve 1, 25 μL of DASA (5×10^{-4} M); injection valve 2, 250 μL of Al(III) (varied concentrations)]. However, a narrower linear working range was achieved and a systematic decrease in electrode sensitivity was

observed across replicate measurements. Loss of electrode activity resulting from injection of DASA only was easily reactified by voltage pulsing. However, when aluminium(III) solution was also injected to give a small zone of DASA nested in a larger zone of aluminium(III), there was a progressive loss of electrode activity (ca. 2% per injection). This was ascribed to a slow build-up of polymeric aluminium(III) hydroxy species on the electrode surface, resulting from hydrolysis in the alkaline carrier solution. In contrast, when pulsed flow injection was used (25 μL of aluminium(III) solution) injected into a reagent stream the electrode activity was completely restored by a single voltage cycle.

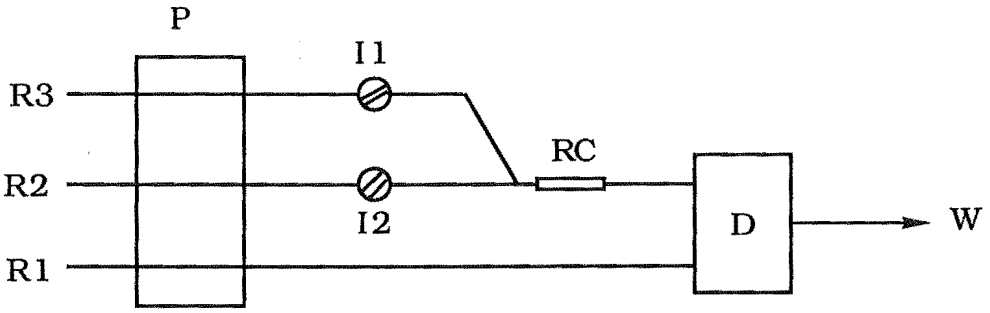

Figure 7.10. Manifold for double injection. R1, 0.1 M KCl; R2, 0.5 M ammonium acetate-ammonia, pH 9.0; R3, water; I1, injection valve 1; I2, injection valve 2; RC, reaction coil; P, pump and D, detector.

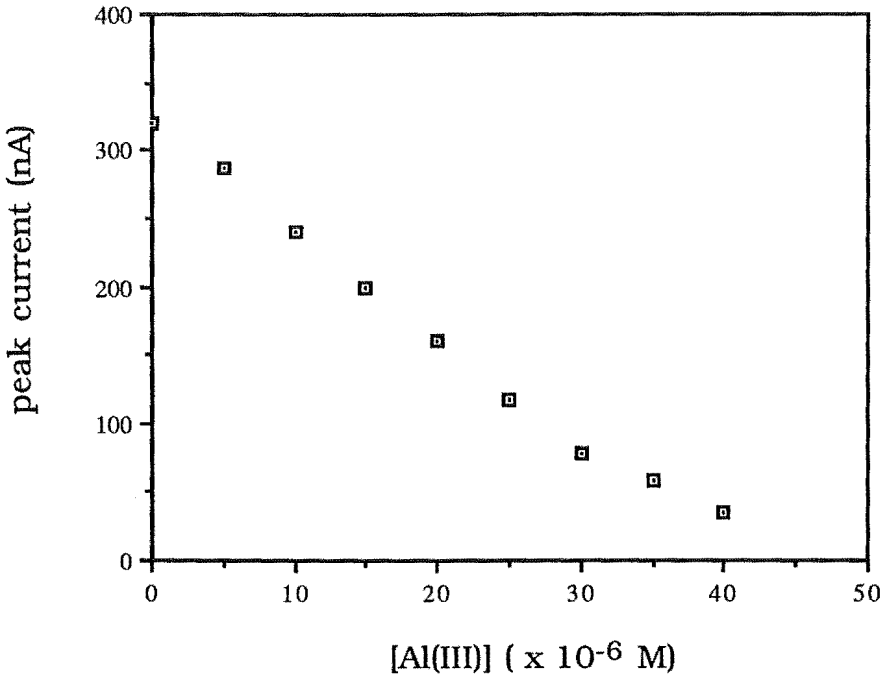

Figure 7.11. Calibration graph for determination of aluminium(III) using double injection with the manifold shown in Figure 7.10: I1, 25 µL of DASA (5 x 10^{-4} M); I2, 250 µL of aluminium(III) (varied concentrations). Measuring potential =0.5 V.

7.4.3. Double pumping

Pulsed flow injection requires use of a double pumping system (the manifold is shown in Figure 7.2). The analytical procedure used in these experiments is described below.

The working electrode in the assembled cell, with pump 2 on (pump 1 off), was initially activated electrochemically for 10 minutes by voltage cycling, 0.50 $\Rightarrow$ 0.10 $\Rightarrow$ 1.00 $\Rightarrow$ 0.50 V, at 100 mV s^{-1}. An individual measurement involved loading 25 μL of Al(III) standard or test solution, switching pump 1 on (pump 2 off) and injecting the sample. When the DASA solution reached the detector after flowing from point C (Figure 7.2), an anodic response was observed, with the current quickly reaching a plateau value. Complexation of DASA by aluminium(III) produced a spike in the current vs. time trace. After 50 seconds, pump 1 was switched off and pump 2 switched on, and a single voltage cycle was used to activate the electrode for the next sample injection. A typical current-time trace is shown in detail in Figure 7.12. Pump 1 was operated only for sample injection in order to minimise the time of DASA contact with the working electrode. Baseline noise (evident in Figure 7.12) arose because no pressure compensation was employed in the manifold during these measurements.

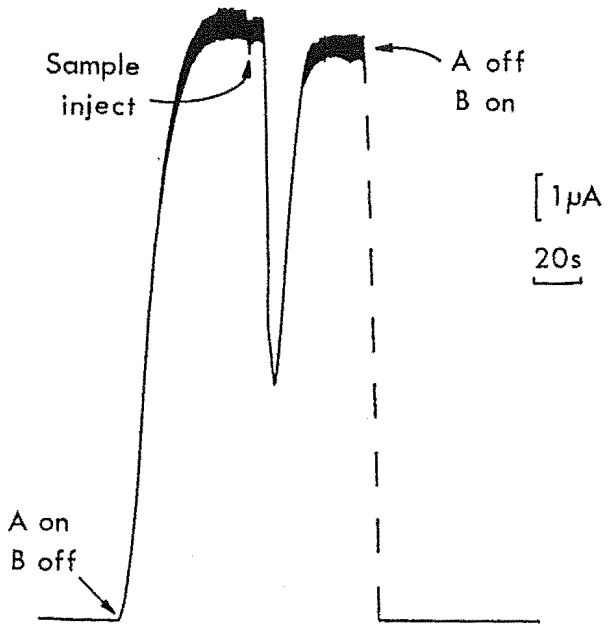

Figure 7.12. Current measured at the gold electrode detector vs. time for one cycle of reagent pulse (pump 1 on) and sample injection. DASA, 5 x 10^{-4} M in pH 9.0 buffer; aluminium(III), 2 x 10^{-4} M, 25 μL. Measuring potential = 0.5 V.

7.5. APPLICATION OF THE DASA-FIA SYSTEM FOR ANALYSIS OF ALUMINIUM(III)

7.5.1. Detection limit and working range

A typical output for pulsed flow injection is shown in Figure 7.13. This involved electrochemical cleaning of the working electrode between each reagent pulse/injection cycle and use of the double pumping system with the manifold shown in Figure 7.2. Figure 7.13 refers to (0.5 - 50) x 10^{-5} M aluminium(III) standards with 5 x 10^{-4} M DASA (dilution factor = 1.64). The linear working ranges (correlation coefficients R ≥ 0.999) for pulsed flow injection are shown

diagrammatically in Figure 7.14. For 2 x 10^{-5} M DASA the detection limit, measured as 2σ for eight replicate measurements for 1 x 10^{-6} M aluminium(III), was 2.5 x 10^{-7} M. For 2 x 10^{-5} M (or 5 x 10^{-4} M) DASA and 9 x 10^{-6} M (or 1 x 10^{-4} M) aluminium(III) the R.S.D.(n = 6) was 4.0% (or < 1%).

Figure 7.15 shows the dependence of cathodic peak height on aluminium(III) concentrations as measured in the double pumping flow system with DASA = 2 x 10^{-4} M.

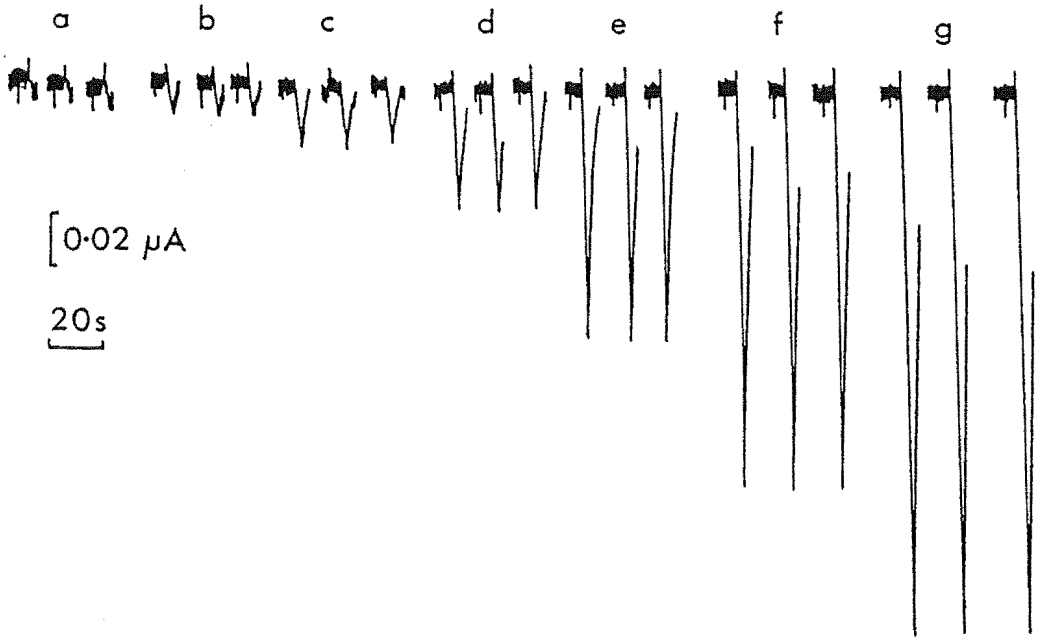

Figure 7.13. Electrode response for pulsed flow injection. 25 μL of aluminium(III) injected into 5 x 10^{-4} M DASA in ammonium acetate-ammonia buffer. [aluminium(III)]: (a) 0.05 x 10^{-4}; (b) 0.10 x 10^{-4}; (c) 0.20 x 10^{-4} ; (d) 0.50 x 10^{-4}; (e) 1.0 x 10^{-4}; (f) 2.0 x 10^{-4}; (g) 5.0 x 10^{-4} M

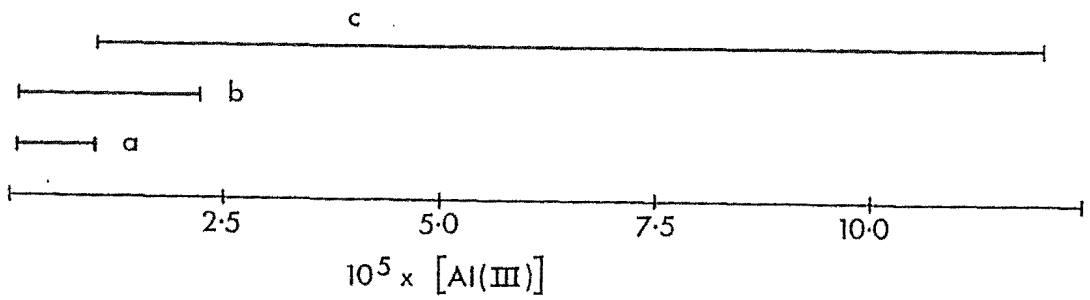

Figure 7.14. Linear working ranges for DASA concentrations of (a) 2 x 10^{-5} M, (b) 5 x 10^{-5} M and (c) 5 x 10^{-4} M.

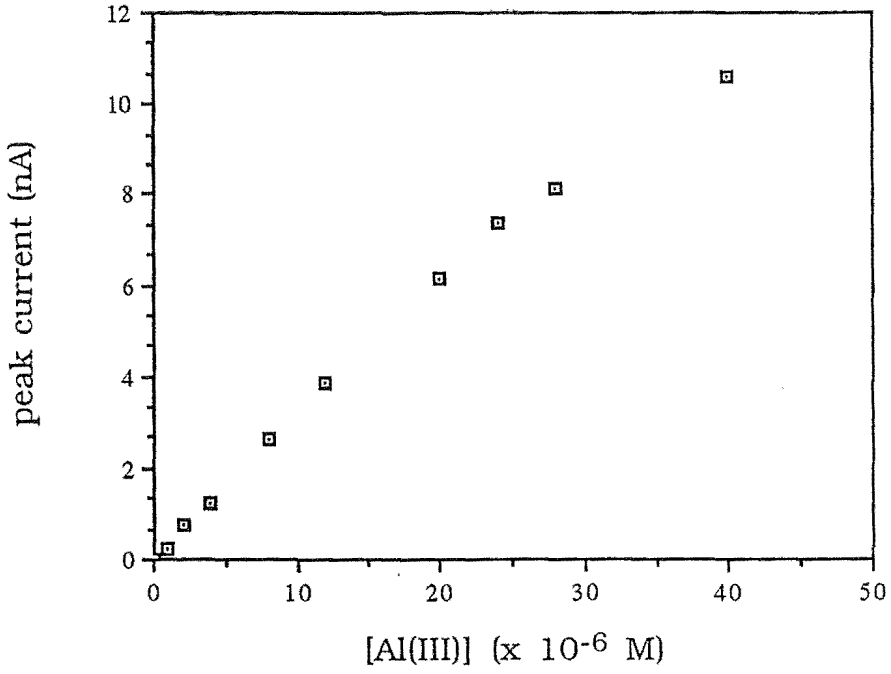

Figure 7.15. Dependence of cathodic peak height on the [aluminium(III)] for injection of 25 μL samples, using the manifold shown in Figure 7.2, DASA: 2 x 10^{-4} M.

7.5.2. Interferences

Interferences were studied after pre-equilibration of an aluminium(III) standard solution (2 x 10^{-5} M) with various concentrations of potential interferents. The DASA concentration was 5 x 10^{-4} M. The manifold for interference experiments is shown in Figure 7.2. In all instances (except for Na^+, K^+, Mg^{2+}, Ca^{2+}, which showed no interference up to 5 x 10^{-3} M), the level of interference was decreased on increasing the pH of the buffer solution (R2) from 7.0 to 9.0. Thus, at pH 8.2 (9.0) the interferences from 2 x 10^{-5} M F^- and citrate were -38% (0%) and -20% (0%), respectively (see Figure 7.16). At pH 9.0, fulvic acid, oxalic acid and PO_4^{3-} did not interfere measurably (up to 25 mg kg^{-1}, 2 x 10^{-4} M and 1 x 10^{-4} M, respectively). The more strongly complexing ligands nitrilotriacetic acid (NTA) and tannin (an epicatechin polymer) gave positive interferences at pH 9.0 (2 x 10^{-5} M, +46%; 25 ppm, +30%, respectively). For Fe(III) (2 x 10^{-5} M) the interference was +63% at pH 9.0.

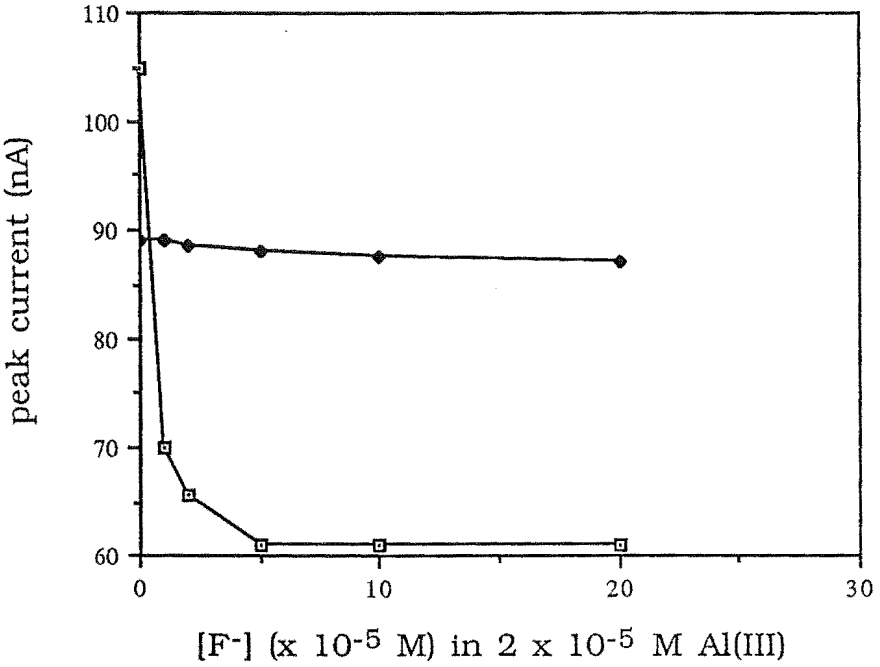

Figure 7.16. Dependence of peak height on concentration of F^-, as a function of pH: (▫) pH 8.18, (♦) pH 9.05.

The high affinity of aluminium(III) ions for OH^- and 1,2-dihydroxyaryl ligands means that these donor groups may compete effectively against many other ligands[24,102,142]. Thus, in the alkaline buffer, OH^- counters possible interference from di- and tricarboxylate ligands, carboxylate polymers (fulvic acid), F^- and PO_4^{3-}. Only the more strongly complexing tannin and NTA ligands interfere. Their competition against OH^- (and the 1,2-dihydroxyaryl ligand DASA) was expected to effect a negative interference. However, positive interferences were observed in each instance. These resulted from direct oxidation of the competing ligand at 0.5 V (established from separate measurements).

Interference from Fe(III) arose from direct complexation with DASA. Attempts to mask this interference by reduction of iron(III)

(with ascorbic acid) and stabilization of iron(II) as the 2,2'-bipyridyl or 1,10-phenanthroline complex were not effective because of oxidation of the Fe(II) complex to the Fe(III)-DASA complex at the measuring potential.

Table 7.2. Concentration of interferents causing a 20% decrease in the measured peak height for aluminium(III)[a]

cation	Concentration (M)	Anion	Concentration (M)
Fe^{3+}	5.0×10^{-6}	F^-	$>2.0 \times 10^{-4}$
Mg^{2+}	$>5.0 \times 10^{-2}$	PO_4^{3-}	$>1.0 \times 10^{-4}$
Ca^{2+}	$>5.0 \times 10^{-2}$	Tannin	20 ppm
K^+	$>5.0 \times 10^{-2}$	Citrate	$>2.0 \times 10^{-4}$
Na^+	$>5.0 \times 10^{-2}$	Fulvate	1.2×10^{-4}
		NTA[b]	1.0×10^{-5}
		Oxalate	$>2.0 \times 10^{-4}$

[a] 2.0×10^{-5} M Al(III). [b] Nitrilotriacetate.

7.6. ANALYSIS OF SOIL EXTRACTS

A series of soil samples provided by DSIR Land Resources was analysed for exchangeable (1 M KCl extractable) aluminium(III). The samples were chosen to provide a wide range of soil type and soil acidity (aluminium toxicity). Soil samples (2.5 g) were extracted with 1.0 M KCl (25 mL) by the rapid (5 minutes) extraction method described by Close and Powell[63], followed by membrane filtration (0.45

μm) and centrifugation. The extract was diluted with buffer (100 - 1000 μL to 10 mL) and the aluminium(III) concentration was determined relative to a standard calibration graph and also by the method of additions.

Since Fe(III) interferes very strongly in the determination of aluminium(III), it was measured separately by the spectrophotometric ascorbic acid - 2,2'-bipyridyl method[109,110]. Table 7.3 shows the concentrations of exchangeable Fe(III) in the soil samples. From these results, it is seen that the amount of Fe(III) in these soils is small and the ratio of [Fe(III)]/[Al(III)] is less than 0.015. Therefore, for these soil extracts the interference from Fe(III) can be ignored in the analysis of aluminium(III).

Results for the ten soil samples are presented in Table 7.4. They are compared with values reported for the alizarin chemically modified electrode (CME) method (described in Chapter Four) and for the 16-hour extraction - AAS method. There is good agreement between these three methods.

The data presented in Table 7.4 indicate that the aluminium(III) concentration measured for soil extracts by the DASA flow-injection method approximates to the "total" aluminium measured by AAS. Interference from Fe(III) was not observed for these air-dried soils (but may be problematic for field-moist anaerobic soils or for anoxic sediments). Small differences between the AAS and DASA values can arise from sample variability, from the contribution of colloidal species to the AAS value and from interference by strongly binding organic ligands in the DASA method. The last effect was expected to be small because of the low solubility of soil organic polymers in the KCl extractant and the low incidence of 1,2-dihydroxyaryl moieties in these polymers[143]. To test this point, a series of high-carbon soils was examined: Bossu, Mangatepopo, Te Rapa and Motomaoho, which

contained 5.9, 9.2, 21 and 24% carbon, respectively. Only for the last soil was the aluminium(III) concentration measured against the calibration graph significantly different from that obtained by the methods of additions.

Table 7.3. Iron(III) and aluminium(III) concentrations in 1 M KCl extracts of soil samples[a]

Sample	depth (cm)	Fe(III)(M)	Al(III)(M)	[Fe(III)] : [Al(III)]
Takahe	(26 - 50)	1.70×10^{-6}	3.73×10^{-4}	0.0046
Takahe	(>90)	5.84×10^{-6}	5.88×10^{-4}	0.0099
Waikiwi	(55 - 92)	2.85×10^{-6}	2.57×10^{-4}	0.0111
Waikari	(17 - 39)	2.40×10^{-6}	4.67×10^{-3}	0.0051
Summit	(15 - 30)	2.93×10^{-6}	6.00×10^{-4}	0.0049
Takahe	(0 - 26)	3.86×10^{-6}	2.57×10^{-4}	0.0150

a. 2.5 g soil; 25 µL diluted extractant (10 - 100 times)

Table 7.4 Exchangeable (1 M KCl extractable) aluminium in soils

Soil type	Description[a]	Depth (cm)	Aluminium (mg kg^{-1}) DASA (flow injection[b])	Alizarin[b,c]	AAS[d]
Takahe	Silt loam; yge	0-26	69	81	104
Takahe	Silt loam; yge	26-50	101	118	76
Takahe	Silt loam; yge	>90	150 (169)	197	225
Summit	Silt loam; ybe	15-30	162	145	190
Waikari	Clay; ybe	17-39	1261	1210	1215
Waikiwi	Silt clay loam; ybe	55-92	89	119	117
Bossu	Silt loam; ybe	0-7.5	272 (292)	-	297
Mangatepopo	Podzolized yb pumice	10-20	100 (103)	-	81
Te Rapa	Peaty silt loam	0-7.5	97 (111)	-	-
Motomaoho	Silty peat	0-7.5	74 (100)	-	-

a. yge = yellow-grey earth; ybe = yellow-brown earth. b. 5 minutes extraction[63]; Values from calibration graph; values in parentheses from the method of additions. c. Chapter Four. d.16-h extraction. Data supplied by DSIR(NZ) Land Resouces.

7.6.1. Comparison of amperometric and spectrophotometric FIA methods

The FIA detection limit of 2.5 x 10^{-7} M aluminium(III) compares favourably with the value reported for pyrocatechol violet (1.1 x 10^{-7} M or 2 x 10^{-7} M)[144,145], CAS (3 x 10^{-7} M)[7], quinolin-8-ol/chloroform (5 x 10^{-7} M)[146] and eriochrome cyanine R (5 x 10^{-6} M)[108]. However, the spectrophotometric detection limit can be lowered by a factor of ca. 10 by use of surfactants[134,147] or by ca. 100 by fluorescence measurement (of the quinolin-8-ol/sulphonate) in the presence of surfactant[148]. The linear working range reported here is similar to that reported for the spectrophotometric flow-injection methods[134,144], but this range is in part a result of the sample loop size and the concentration of complexing agent used.

The major drawbacks of the proposed amperometric-FIA method are the comparatively low sampling rate (ca. 60 h^{-1}) and the inability to mask Fe(III) (which is readily accomplished in spectrophotometric methods by use of hydroxylamine-1,10-phenanthroline[134,144] or ascorbic acid[136,108,109]. An advantage of the method reported here accrues from use of a higher pH; this counters the interference of some competing ligands that interfere in spectrophotometric methods at lower pH (for example, the humic compounds cause significant background absorption (at 581 nm) in flow-injection spectrophotometric determination of aluminium(III)[144]. Further, sample turbidity and colour do not affect the amperometric analysis.

7.7. USE OF ALTERNATIVE LIGANDS AND ELECTRODE SYSTEMS

As described in Chapter Four, the electrochemical properties of several ligands and their aluminium(III) complexes were studied. Their amperometric behaviour in flow systems was also examined. The possible applications of SVRS, PCV and 4-nitrocatechol in FIA are discussed below.

7.7.1. SVRS-FIA system for analysis of aluminium(III)

The reaction of SVRS with aluminium(III) results in a decrease in the oxidation current of free ligand which is similar to that observed for DASA. Therefore SVRS was tested in a flow system with a gold working electrode for analysis of aluminium(III). The manifold is shown in Figure 7.2.

In the commonly used acetate buffer, pH 4.5, the reaction of SVRS with aluminium(III) is slow at room temperature[32,54]. In order to increase the reaction rate a higher pH buffer, ammonium chloride-ammonia (pH 8.6), was used to increase the concentration of deprotonated ligand. Also a STOP-FLOW protocol was adopted; the merged SVRS - aluminium(III) solutions were stopped in a reaction coil held at 40 °C in a water bath for 1 minute. Aluminium(III) was determined by amperometric detection of excess SVRS at +0.5 V vs Ag/AgCl.

Serious electrode fouling problems arose for this ligand. As for DASA this problem was countered by using a double pumping system and by using voltage cycling for electrode activation. Also, the double

injection manifold was tested in this experiment (the analysis procedure is shown in Figure 7.17).

Interference effects were similar to those for FIA-DASA. Fe(III) and tannin again gave strong interferences in aluminium(III) determinations. Figure 7.18 shows calibration graphs for 1 x 10^{-3} M SVRS and 5 x 10^{-4} M SVRS with 0 - 1.2 x 10^{-4} M aluminium(III); these data were obtained using the double injection manifold.

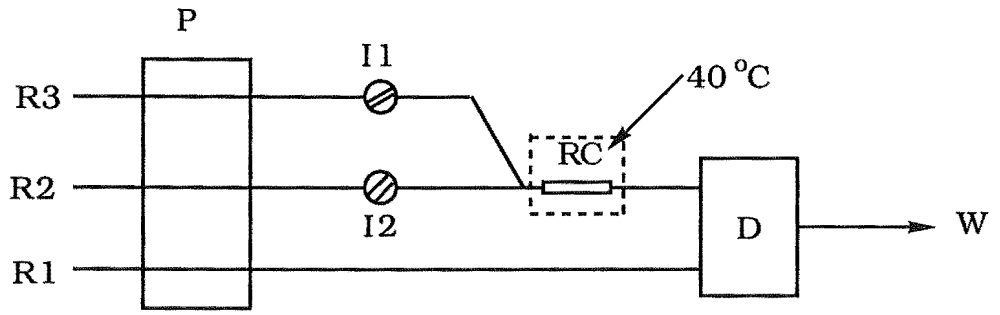

(a)

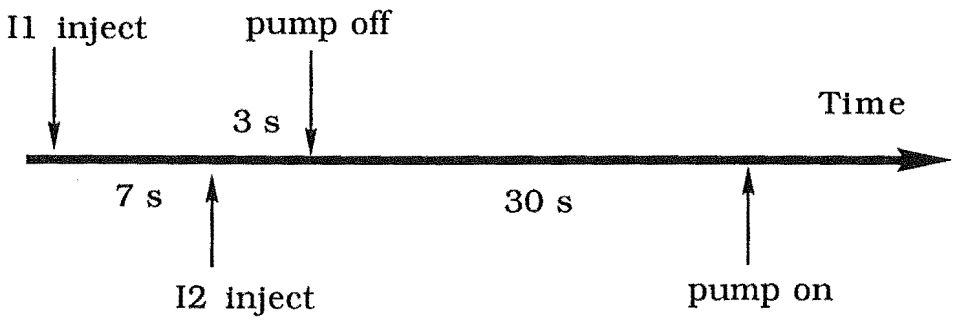

(b)

Figure 7.17. (a) manifold: R1, 0.1 M KCl; R2, 0.5 M ammonium acetate-ammonia, pH 9.0; R3, water; I1, injection valve 1: 25 µL of SVRS; I2, injection valve 2: 250 µL of aluminium(III) and (b) flow diagram of analysis procedure for aluminium(III).

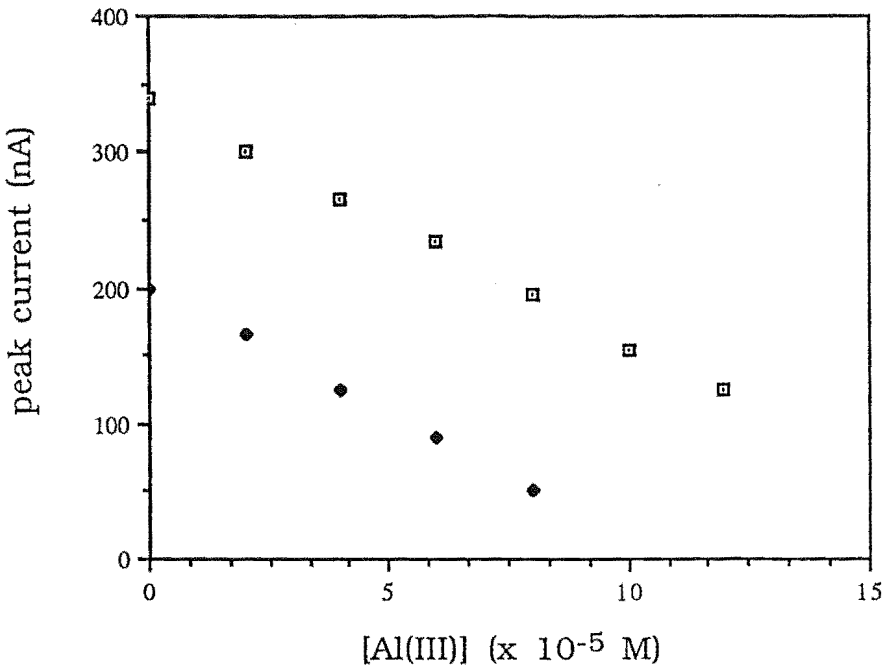

Figure 7.18. Calibration graphs for (▫)1 x 10^{-3} M SVRS, (♦) 5 x 10^{-4} M SVRS with 0.0 - 1.2 x 10^{-4} M aluminium(III).

The results obtained for this system were similar to those for the FIA-DASA system (e.g., the linear working range for 5 x 10^{-4} SVRS was ca. (0.2 - 1.2) x 10^{-4} M aluminium(III) compared with (0.1 - 1.2) x 10^{-4} M aluminium(III) for DASA). However the analysis procedure is more complex, therefore this method was not further applied in analysis of aluminium(III).

While investigating interferences in the FIA-SVRS determination of aluminium(III) it was found that nickel(II) reacts very rapidly and quantitatively with SVRS. This was not investigated further, but using different pH and different reaction temperature to differentiate against other metal ions, analysis of nickel(II) may be possible.

7.7.2. PCV-FIA system for analysis of aluminium(III)

In the flow system PCV gave results similar to those for DASA. Using a glassy carbon electrode aluminium(III) was determined amperometrically at +0.20 V vs Ag/AgCl; analysis was based on the decrease in the oxidation current for non-complexed PCV.

Cyclic voltammograms

Figure 7.19 gives the cyclic voltammogram for PCV (1 x 10^{-3} M) with and without aluminium(III) (3 x 10^{-4} M) in 0.5 M ammonium acetate buffer (pH 6.5) on a glassy carbon electrode. On this electrode, an oxidation wave for PCV and an oxidation wave for the aluminium(III)-PCV complex were observed at +0.25 V and +0.65 V vs SCE, respectively. The attenuation of the PCV oxidation wave at ca. 0.25 V in the presence of aluminium(III) could be monitored. So the decrease in the oxidation current for PCV was the basis of the described method for determination of aluminium(III).

Analysis of aluminium(III)

The flow manifold is shown in Figure 7.20. The flow-rates for reagent (R1 = water; R2 = 2.0 x 10^{-5} M PCV), buffer (R3 = 1 M ammonium acetate-ammonia, pH 8.5) and surfactant (R4 = 0.5% deoxycholic acid) were 1.19 mL $minute^{-1}$, while that for the reference electrode electrolyte (R5 = 0.1 M KCl) was 0.16 mL $minute^{-1}$. RC1 and RC2 were 100 cm knitted coils of microline tubing. Several surfactants were tested in this system to overcome electrode fouling. Deoxycholic acid showed the best results.

A typical output for flow injection is shown in Figure 7.21. These data were obtained using the surfactant deoxychlolic acid and the manifold shown in Figure 7.21. For 1 x 10^{-5} M aluminium(III) with 2 x 10^{-5} M PCV, the R.S.D. (n = 8) was 0.8%. For 2.5 x 10^{-6} M aluminium(III) with 2 x 10^{-5} M PCV, the R.S.D. (n = 8) was 1.4%. For 2 x 10^{-5} M PCV the detection limit, measured as 2σ for eight replicate measurements for 1 x 10^{-6} M aluminium(III), was 1.0 x 10^{-7} M. Linear working range for 2 x 10^{-5} M PCV was (0.05 - 1.0) x 10^{-5} M. Figure 7.22 shows a dependence of decrease in the peak height for 2 x 10^{-5} M PCV on aluminium(III) concentrations (0.0 - 1.0 x 10^{-5} M).

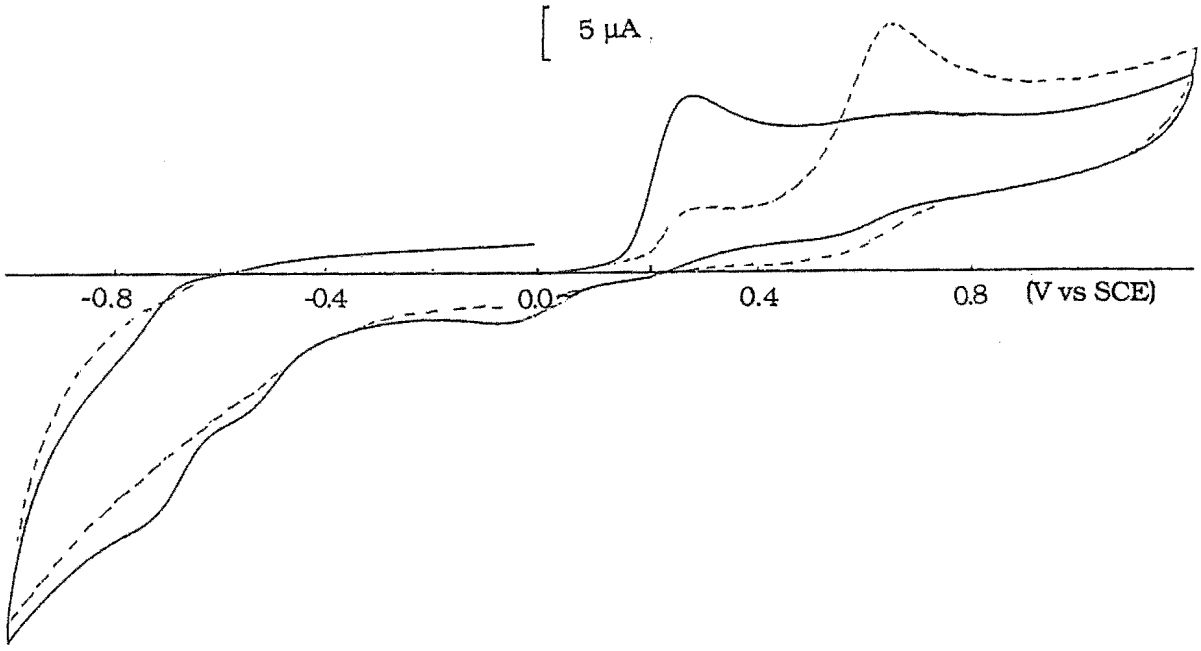

Figure 7.19. Cyclic voltammogram (50 mV s^{-1}) for PCV (1 x 10^{-3} M) (solid line) and PCV (1 x 10^{-3} M) + aluminium(III) (3 x 10^{-4} M) (dashed line) in ammonium acetate buffer, pH 6.5, on glassy carbon.

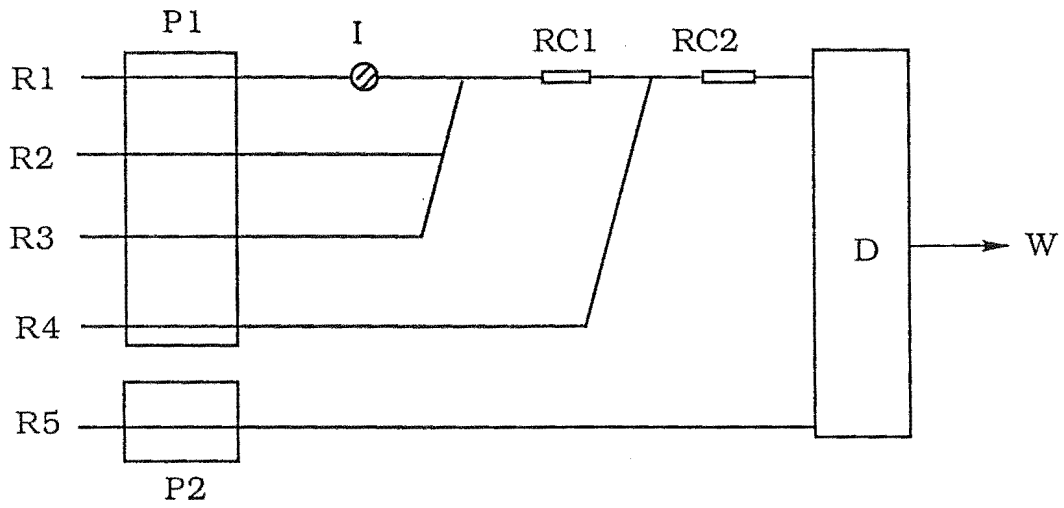

Figure 7.20. Manifold for PCV-FIA measurements. R1, water; R2, 2 x 10^{-5} M PCV; R3, 1.0 M ammonium acetate-ammonia; R4, 0.5% deoxycholic acid; R5, 0.1 M KCl.

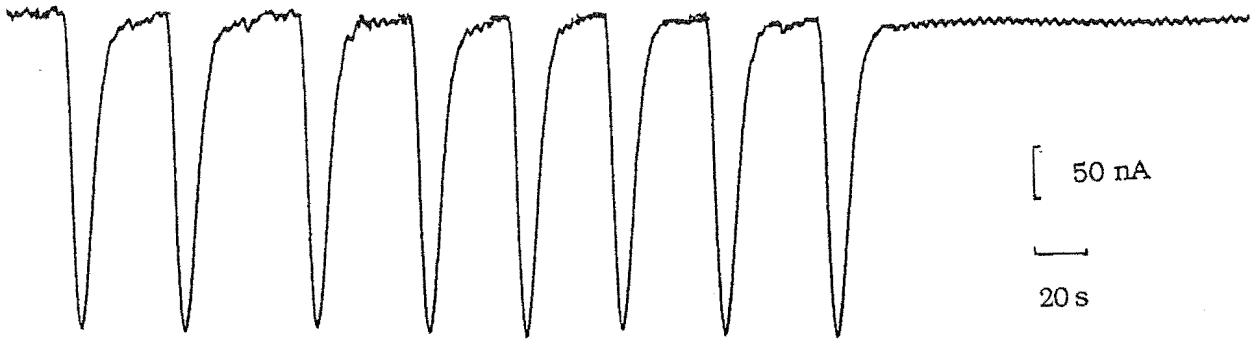

Figure 7.21. Signals for injection of 25 µL of aluminium(III) (1.0 x 10^{-5} M) into 2 x 10^{-5} M PCV.

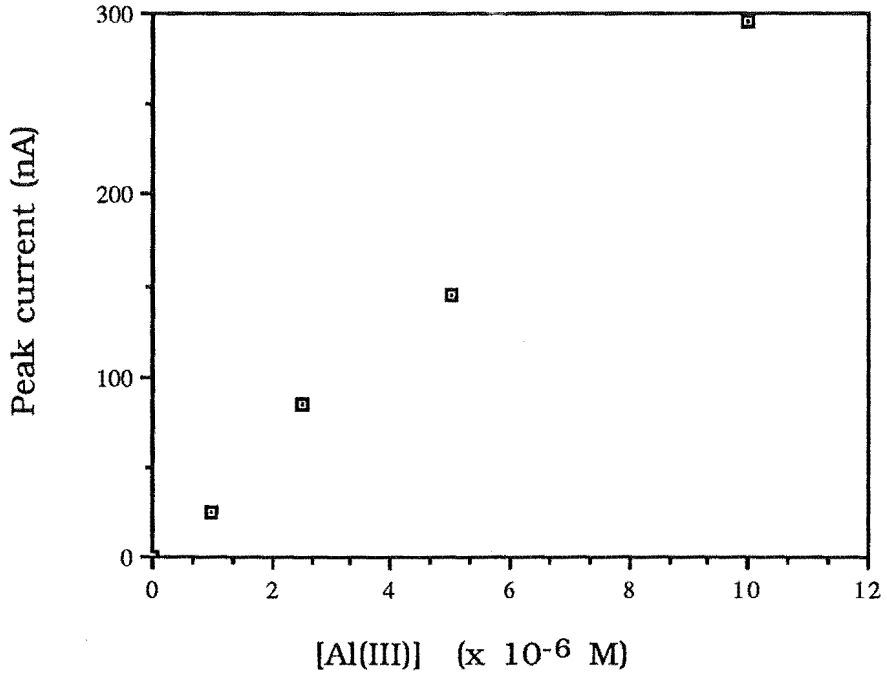

Figure 7.22. Peak current as a function of [aluminium(III)] using manifold shown in Figure 7.19 with [PCV] = 2 x 10^{-5} M.

Compared with the gold electrode, glassy carbon showed less deactivation of the electrode surface. Double pumping was not required when using a surfactant with a glassy carbon electrode. However, the results were similar to those for the FIA-DASA system. Further application of this system in determination of aluminium(III) was not studied.

7.7.3. 4-nitrocatechol-FIA system for analysis of aluminium(III)

Using the manifold shown in Figure 7.20, 4-nitrocatechol was used to analyse aluminium(III) by indirect amperometry at +0.25 V vs Ag/AgCl. The surfactant deoxycholic acid was again used to limit the deactivation of the electrode surface. For 5 x 10^{-5} M 4-nitrocatechol

and 1 x 10^{-5} M aluminium(III) the R.S.D. was 1.3% (n = 6). Further investigations were not made for the reasons described above.

7.8. CONCLUSIONS

Aluminium(III) can be determined in a flow system involving the formation of the Al(III)-DASA complex at pH 9.0 and amperometric measurement of excess DASA at +0.50 V on a gold electrode. Electrode fouling by adsorption of DASA oxidation products was minimized by use of a double pumping system to provide a reagent cycle and a wash cycle.

Other ligands, such as SVRS, PCV and 4-nitrocatechol which were discussed above, can also be used in indirect electrochemical analysis of aluminium(III) in a flow system. These amperometric measurements are based on the (decrease of) current for the oxidation of ligand which remains unbound after addition of aluminium(III). The oxidation of ligands on the electrode surface results in electrode fouling (deactivation). This can be limited by use of a surfactant and by using either a shortened contact time between electrode and ligand solution (e.g., by a double pumping system), or by electrochemical reactivation of the electrode surface.

It is anticipated that each of these flow systems could be applied in the determination of aluminium(III) in environmental and physiological samples.

7.9. POLYPYRROLE AND POLY(3-METHYLTHIOPHENE) MODIFIED ELECTRODES

Wang[151] coated P-3MT onto solid electrodes in FIA systems to prevent electrode fouling. A stable peak due to phenol was obtained when the P-3MT coated electrode was used. The use of PPy and P-3MT films to minimise electrode fouling due to DASA was investigated.

7.9.1. Preparation of the electrodes

The electrochemical polymerisation of P-3MT onto glassy carbon was carried out in deaerated acetonitrile solution containing 0.1 M sodium perchlorate and 0.05 M 3-methylthiophene[84,149,150]. For this purpose the potential was cycled three times between 0.0 V and +1.8 V (vs SCE) at a rate of 20 mV s^{-1}, after which the electrode was held at +0.7 V for 10 minutes. Prior to measurements the modified electrodes were pretreated in the ammonium acetate buffer solution by repetitively scanning the potential between 0.0 and +0.7 V until a stable background was obtained (10 cycles) .

The properties of the P-3MT coating were dependent on the surface of the electrode and the electrode material. P-3MT was readily coated on glassy carbon and platinum electrodes. It was difficult to obtain reproducible properties on graphite because of its poor surface condition. Since a gold electrode will be oxidized at a potential of + 0.60 V, P-3MT coated gold electrodes were not studied.

The preparation of PPy coated glassy carbon electrode is described in Chapter Three.

For coating the glassy carbon electrode in the flow cell, it was found that polymerisation in the flow cell resulted in a non-uniform

coating of polymer. Hence the cell was taken apart and used as the working electrode in a conventional cell.

7.9.2. The characterisation of the electrodes

The PPy coated electrode showed similar electrochemistry to that described in Chapter Three. The characteristics of the P-3MT electrode were compared to those described by Wang[151]. As indicated in Figure 7.23, redox currents obtained for acetaminophen on P-3MT coated electrodes were much larger than those on non-coated electrodes. However, there is also a greatly increased capacitive residual current. These observations were also made by Wang.

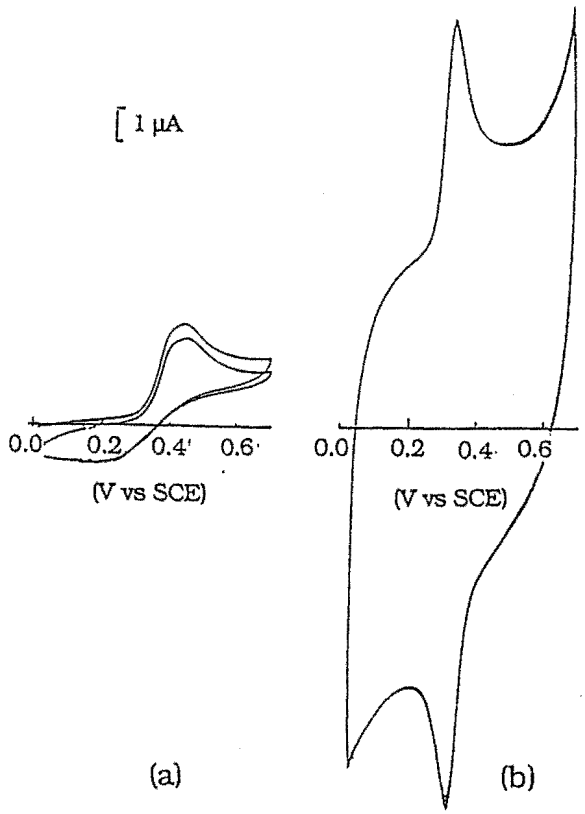

Figure 7.23. Cyclic voltammogram (10 mV s^{-1}) for acetaminophen (1 x 10^{-4} M) in ammonium acetate, pH 7.0, on (a) glassy carbon and (b) P-3MT coated glassy carbon electrode.

7.9.3. Polypyrrole and poly(3-methylthiophene) modified electrodes in FIA

FIA experiments were performed using the flow cell which incorporated a polymer coated glassy carbon electrode. Hydrodynamic voltammograms of DASA on PPy coated electrodes and uncoated electrodes indicated very similar half wave potentials (see Figure 7.24).

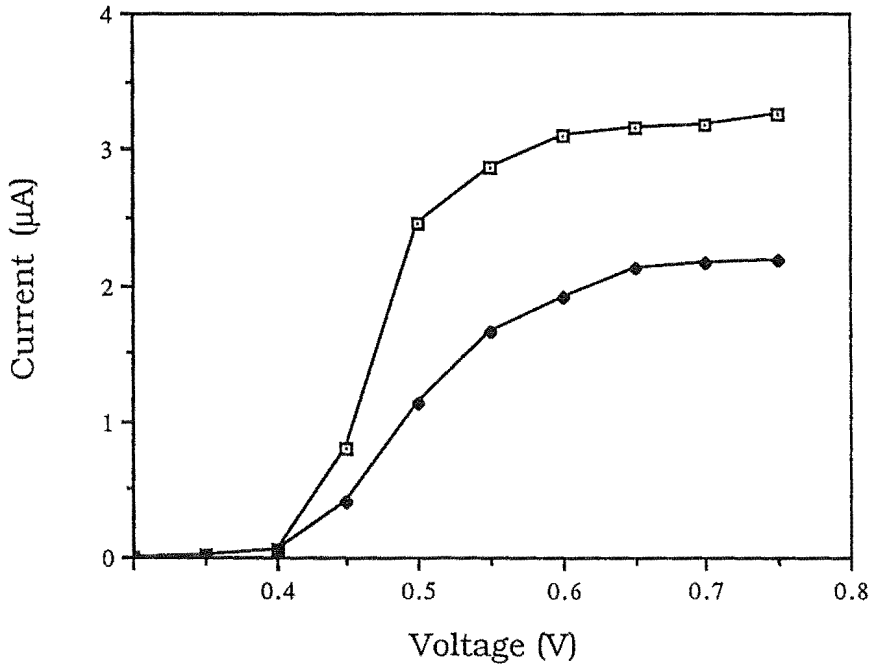

Figure 7.24. Hydrodynamic voltammograms of DASA on (•) PPy film coated electrode and (▣) uncoated electrode.

Deactivation of the polymer coated electrodes was monitored; the sensitivity of the PPy film coated electrode still decreased about 1.2% per injection. For P-3MT, the rate of decrease in peak height on the film coated electrode was slower. Hence for both polymer coatings, the loss of sensitivity occurred at a slower rate than at an uncoated electrode, but results were not considered satisfactory.

CHAPTER EIGHT

AMPEROMETRIC METHODS IN FLOW SYSTEMS: DETERMINATION OF MAGNESIUM

8.1. INTRODUCTION

8.1.1. Environmental significance of magnesium

Man, as well as other vertebrates, requires cations of some metals to facilitate many essential life processes (the heavy metals, e.g. cobalt, zinc; the lighter, and usually more abundant, metals, e.g. calcium, magnesium). Magnesium is an important element for all forms of life. It is taken up by the living cell as a cation. It is concerned with hydrolysis, and with group-transfer; like calcium, it also plays an important part in creating flexible (or rigid) structures and it can trigger a reaction, possibly by effecting a structural change[152]. In bacteria, magnesium is the most abundant bivalent metal. The essential central atom of the chlorophyll molecule is magnesium.

Magnesium is the second most common intracellular cation in humans (whereas calcium is the second most common extracellularly). It is the irreplaceable link that keeps ribosomes intact, and it attaches mRNA to ribosomes[152]. It is a co-factor of all the enzymes that utilize ATP in phosphate transfer, and in many other enzymes concerned with group transfer or hydrolysis. It inhibits release of acetylcholine at the motor end-plate, and in many other ways acts as a reversible antagonist to calcium. The higher incidence of death from heart disease in soft-water areas seems to arise from lack of magnesium[152]. Also, the high

concentration of magnesium(II) present in most aquatic systems dominates over trace metals in the competition for the low concentration of dissolved organics.

The normal range of magnesium in human serum is 15 - 29 mg kg^{-1} (ppm)[153,154], and abnormalities may be indicative of renal failure, diabetic coma, abnormal calcification, or toxaemia in pregnancy (magnesium sulphate is used as a hypertensive agent). Also, magnesium levels are significant in the evolution of certain glandular diseases.

8.1.2. Electrochemistry of magnesium

Standard Potential of magnesium

Like aluminium(III), magnesium(II) is reduced at very negative potentials. Its standard electrode potentials have been calculated from the values of the standard chemical potentials of magnesium(II) compounds and ions[155] (Table 8.1). The standard electrode potential has also been obtained experimentally with the cell Cd, $Cd(OH)_2$, $Mg(OH)_2/MgCl_2/Hg_2Cl_2$, Hg, the potential of which was recorded as a function of the aqueous Mg^{2+} concentration[156].

Table 8.1. Standard potential of magnesium

Reaction	E^o (V vs NHE)
(1) $Mg^{2+} + 2\ e^- = Mg$	-2.363
(2) $Mg(OH)_2 + 2\ e^- = Mg + 2\ OH^-$	-2.689
(3) $Mg^+ + e^- = Mg$	-2.659

Many attempts have been made in analytical electrochemistry to study the polarographic characteristics of magnesium(II). Most of the published results have been obtained with organic solvents; only a few results have been obtained with aqueous solutions. The very negative value of the standard potential of the Mg^{2+}/Mg couple explains the difficulty in observing a polarographic wave in aqueous solutions, since the hydrogen evolution reaction will interfere in most cases.

8.1.3. Analytical methods for magnesium(II)

Magnesium(II) is often determined for environmental and biological monitoring. Titrimetry and atomic absorption spectroscopy[157] are the most frequently used techniques for such determinations. Spectrophotometric determinations for magnesium(II)[158-164], such as that with the eriochrome black T (EBT)[159] complex or calmagite[160] complex are also utilized. Cañete[159] reported an FIA-spectrophotometric method for the simultaneous determination of calcium(II) and magnesium(II) in water. The chemical systems were conventional, murexide-EDTA for calcium(II) and EBT-EDTA for the sum of calcium(II) and magnesium(II), the concentration of the latter being obtained by difference.

Electrochemical methods have also been reported. Kryukova et al. found that magnesium(II) gave a polarographic reduction wave at -2.2 V (vs. SCE) at a dropping mercury electrode in aqueous tetramethylammonium chloride[165]. Indirect polarographic determinations of magnesium(II) are possible after it has reacted with redox active organic ligands. Magnesium(II) forms complexes with a number of easily oxidised (or reduced) chelating ligands for which the complexed ligand and free ligand give oxidation (or reduction)

processes separated by ca 200 mV: for example, *o,o'*-dihydroxyazo compounds (e.g. solochrome violet RS (SVRS)[166] and eriochrome black T (EBT)[167]). Richardson[166] determined magnesium(II) in calcium carbonate samples by polarographically reducing the magnesium(II) complex of solochrome violet RS at pH 11 in a piperidine buffer. Luo and Zhao[168] determined magnesium(II) in hair digests by using the polarographic adsorption wave of the magnesium(II) meso-tetra(4-trimethylammoniumphenyl)porphine complex in a methylamine buffer solution. An et al.[167] reported measurement of the adsorption wave for the magnesium(II)-eriochrome black T complex in aqueous ethylenediamine medium.

The determination of magnesium(II) is frequently included in blood serum analysis, but it has offered a challenge to analysts because of contamination and problems with binding to serum proteins. Seventy-one percent of magnesium(II) in serum is free, twenty-two percent is bound to albumin, and seven percent is bound to globulins[155].

A recent review[169] of methods for the determination of serum magnesium(II) assigned each method to one of eight main classifications and discussed their limitations for use in clinical laboratories; no electroanalytical methods were included. At present, the acknowledged reference method for the determination of serum magnesium(II) is atomic absorption spectrometry; its main disadvantage as a method for clinical analysis is the expense of the equipment.

EBT and magnesium(II)-EBT give polarographic reduction waves at -0.5 and -0.7 V respectively (vs Ag/AgCl). This difference in potentials was used to advantage in a flow system with a potential-scanning electrochemical detector which enabled magnesium(II) determination on blood serum via the reduction of EBT and magnesium(II)-EBT[170].

However, this reduction method required use of a mercury electrode; also deoxygenation (via a thin-film deaerator) was necessary.

As part of a project to develop electroanalytical methods for strongly electropositive elements (e.g. aluminium(III) and magnesium(II)), the goal of this work was to develop a simple flow system for determination of magnesium(II) using an indirect amperometric method.

To counter the limitations described above (including the requirement for a mercury electrode and solution deoxygenation) the present work has utilized the oxidation processes for EBT and magnesium(II)-EBT on a solid electrode. This method is based on complexation of magnesium(II) by EBT, with monitoring of the oxidation current for excess EBT at a fixed-potential on a glassy carbon electrode without solution deoxygenation.

8.2. SOLUTION ELECTROCHEMISTRY OF EBT AND MAGNESIUM(II)-EBT

8.2.1. The cyclic voltammetry of EBT and magnesium(II)-EBT

Eriochrome black T (EBT) is an electroactive ligand. It reacts with magnesium(II) to form a 1:1 complex:

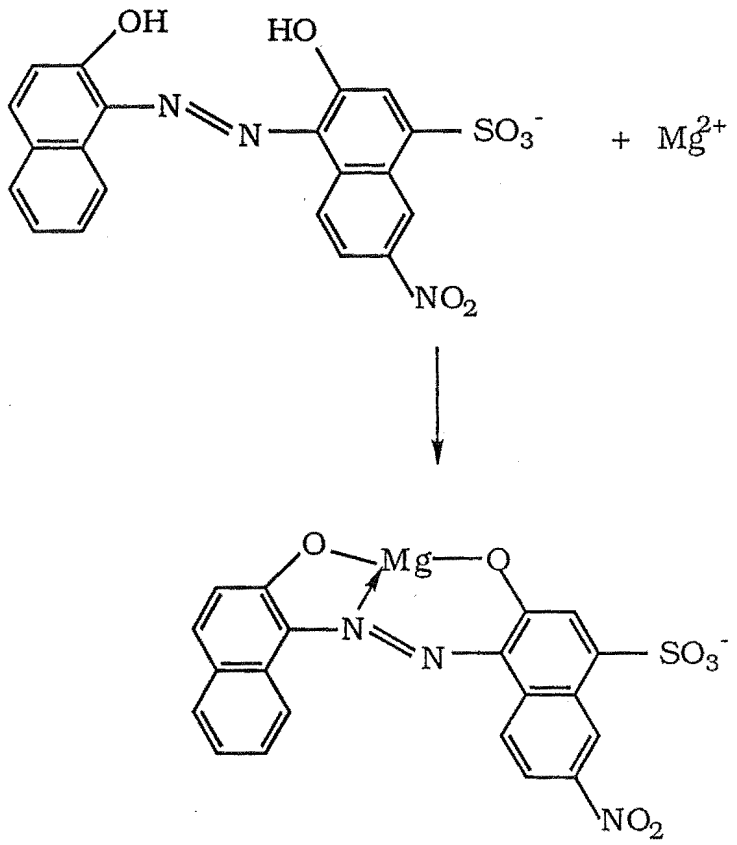

Figure 8.1 gives the cyclic voltammogram for EBT (1 x 10^{-4} M) on a glassy carbon electrode in the 1,2-diaminoethane buffer (5% in 0.1 M KCl) at pH 11.8, in the absence and presence of magnesium(II). The low concentration of EBT (1 x 10^{-4} M) was controlled by the limited solubility of this reagent in water. For EBT the oxidation process was observed at ca. E_p = 0.12 V; on the reverse cycle reduction was observed at E_p = 0.05 V. The oxidation may involve addition of OH to the azo nitrogen atoms. In the presence of 1 x 10^{-4} M magnesium(II) the anodic peak shifted to +0.23 V; on the reverse scan the single reduction peak corresponds to EBT only, indicating that oxidation has promoted metal-ligand dissociation. On addition of calcium(II) (1 x 10^{-4} M) there was no measurable change from the cyclic voltammogram for EBT, consistent with the lower stability of the calcium(II)-EBT complex.

The azo group (and the 2,2'-dihydroxy(aryl) substituents) bonds to the di- and trivalent metals. Formation of a stable or non-labile complex

by the azo group affects the ease of its oxidation/reduction; the observed potential shifts indicate that the redox processes are more difficult for the metal-bound ligand. The concentration of a metal in a system can be established by measuring the height (i_p) of the redox peak for metal-bound ligand (for example, by CSV of aluminium(III)-SVRS as discussed in Chapter Six). Alternatively, in the case of a flow system, it is obtained by measuring the decrease in height of the free ligand peak by poising the voltage between that for the ligand and the metal-ligand peaks (for example, the FIA of aluminium(III)-DASA as discussed in Chapter Seven).

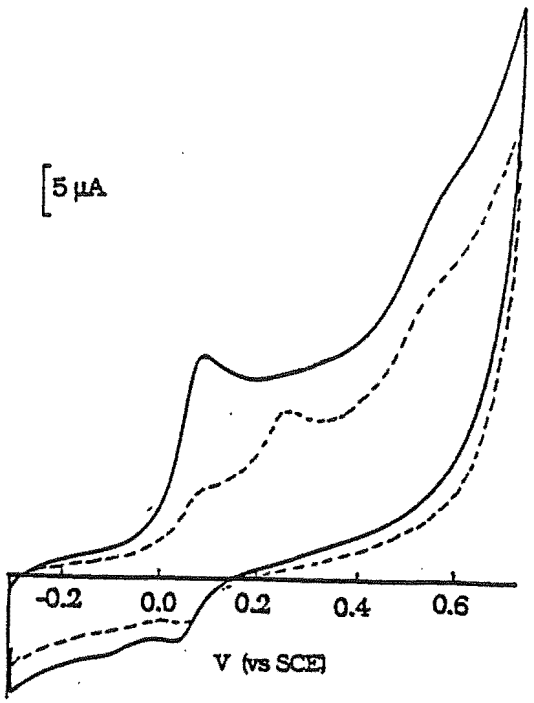

Figure 8.1. Cyclic voltammograms (100 mV s^{-1}) of EBT (1 x 10^{-4} M) in EDA buffer (5% in 0.1 M KCl), pH 11.8. In the absence (solid line) and presence (dashed line) of 2 x 10^{-5} M magnesium(II).

8.2.2. The hydrodynamic voltammetry of EBT, magnesium(II)-EBT and calcium(II)-EBT

A flow system whose manifold is shown in Figure 8.2 was used in this experiment. The microflow cell was a pass-through type with a 3-electrode system as shown in Figure 8.3. It was fabricated from blocks of PVC and had a Teflon spacer. The three electrodes were 0.5 mm diameter platinum (auxiliary electrode), 0.6 mm silver wire (Ag/AgCl reference electrode) and 0.3 cm glassy carbon (working electrode). Other experiment conditions were the same as described in Chapter Seven unless specified otherwise.

Hydrodynamic voltammograms shown in Figure 8.4 were measured by injection of preformed solutions of EBT-buffer or metal-EBT-buffer into the flow system, with and without a surfactant (R4). In the absence of surfactant $E_{1/2}$ values for oxidation of EBT, calcium(II)-EBT and magnesium(II)-EBT were about 0.085, 0.125 and 0.30 V (vs Ag/AgCl; 0.10 M KCl). The greater shift in $E_{1/2}$ for Mg(II) indicated formation of a more stable complex; the decrease in limiting current indicated a lower diffusion coefficient for metal-bound EBT. $E_{1/2}$ values moved anodically in the presence of surfactant (by 0.075, 0.045, and 0.040 V respectively for EBT, calcium(II)-EBT and magnesium(II)-EBT).

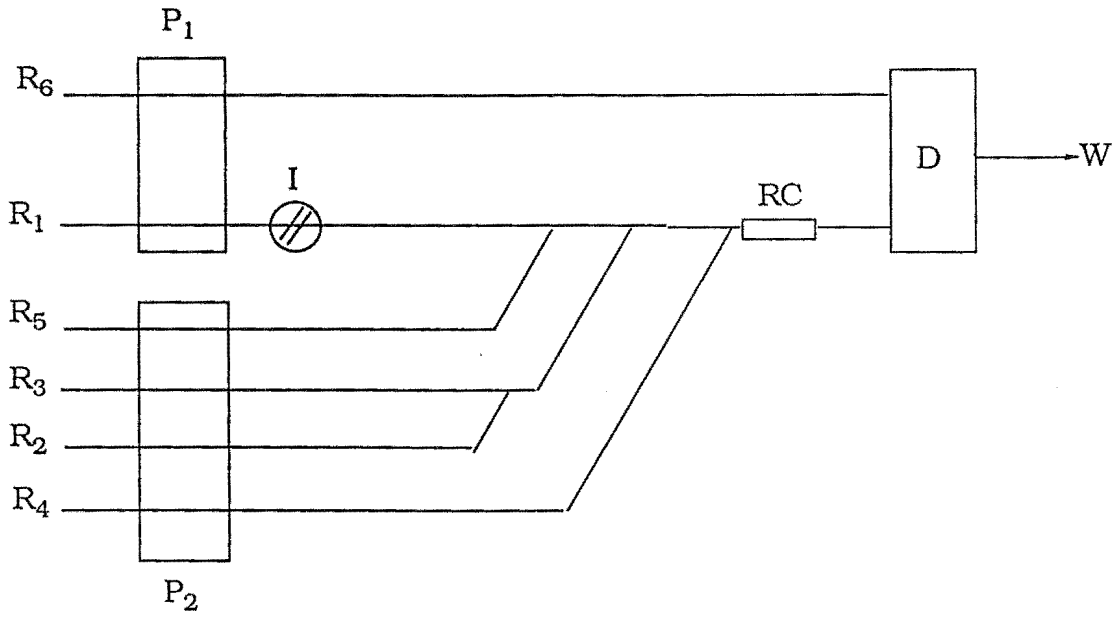

Figure 8.2. The manifold used for hydrodynamic voltammograms of EBT, magnesium(II)-EBT and calcium(II)-EBT and for analysis of magnesium(II) in water. R1, doubly distilled water; R2, 1.5 x 10^{-4} M EBT; R3, 15% 1,2-diaminoethane in 0.3 M KCl, pH 11.5; R4, 0.2% Hostapur SAS 93; R5, 4.5 x 10^{-5} M EGTA, 4 x 10^{-2} M triethanolamine; R6, 0.1 M KCl; I,injection valve (50 μL); D, detector; W, waste; RC, reaction coil; P, peristaltic pumps.

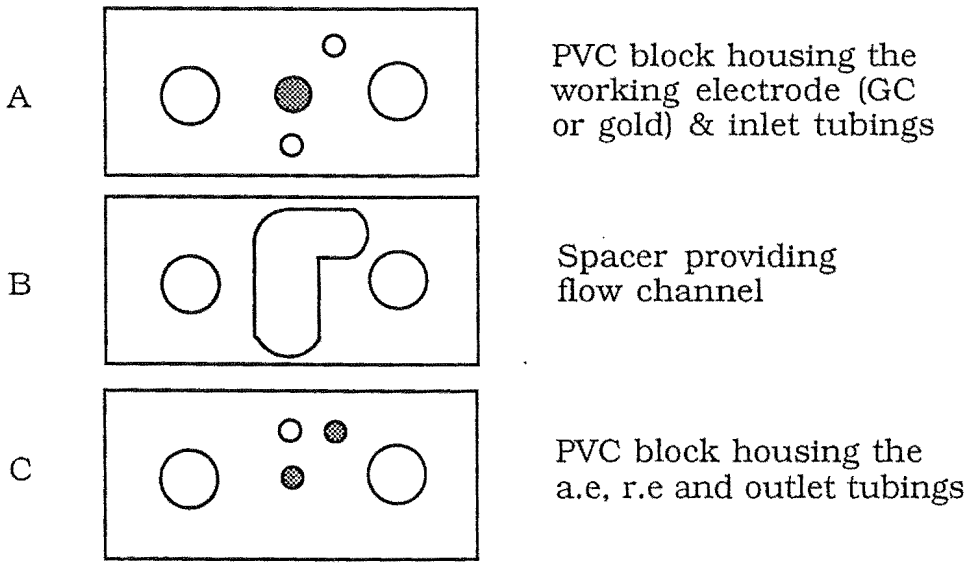

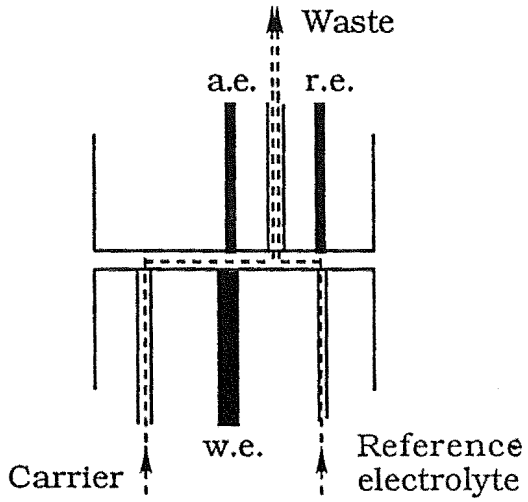

Figure 8.3. Diagrams of the pass-through microflow cell; dimensions each half 10 x 20 x 32 mm. Large holes for clamping screws.

To study the effect of calcium(II) on EBT, quantitative complexation was forced by addition of a 3-fold excess of calcium(II); evidence of the lower stability of this complex is seen by the smaller shift in $E_{1/2}$ (relative to EBT). In the presence of a surfactant the maximum slope of each voltammogram decreased, indicating decreased electrochemical reversibility. However the maximum current for calcium(II)-EBT was greater than that for EBT (the reason is not understood). Consistent with this, the FIA baseline current for oxidation of EBT increased by a small percentage on inclusion of calcium(II) in the carrier stream; however in the presence of magnesium(II), and with no calcium(II) masking agent present, the magnesium(II) peak decreased when calcium(II) at high concentration competed for EBT. Setting the analytical voltage at +0.175 V did not achieve maximum sensitivity for magnesium(II), but minimised (electrochemical) errors associated with calcium(II) binding to EBT (see Figure 8.4).

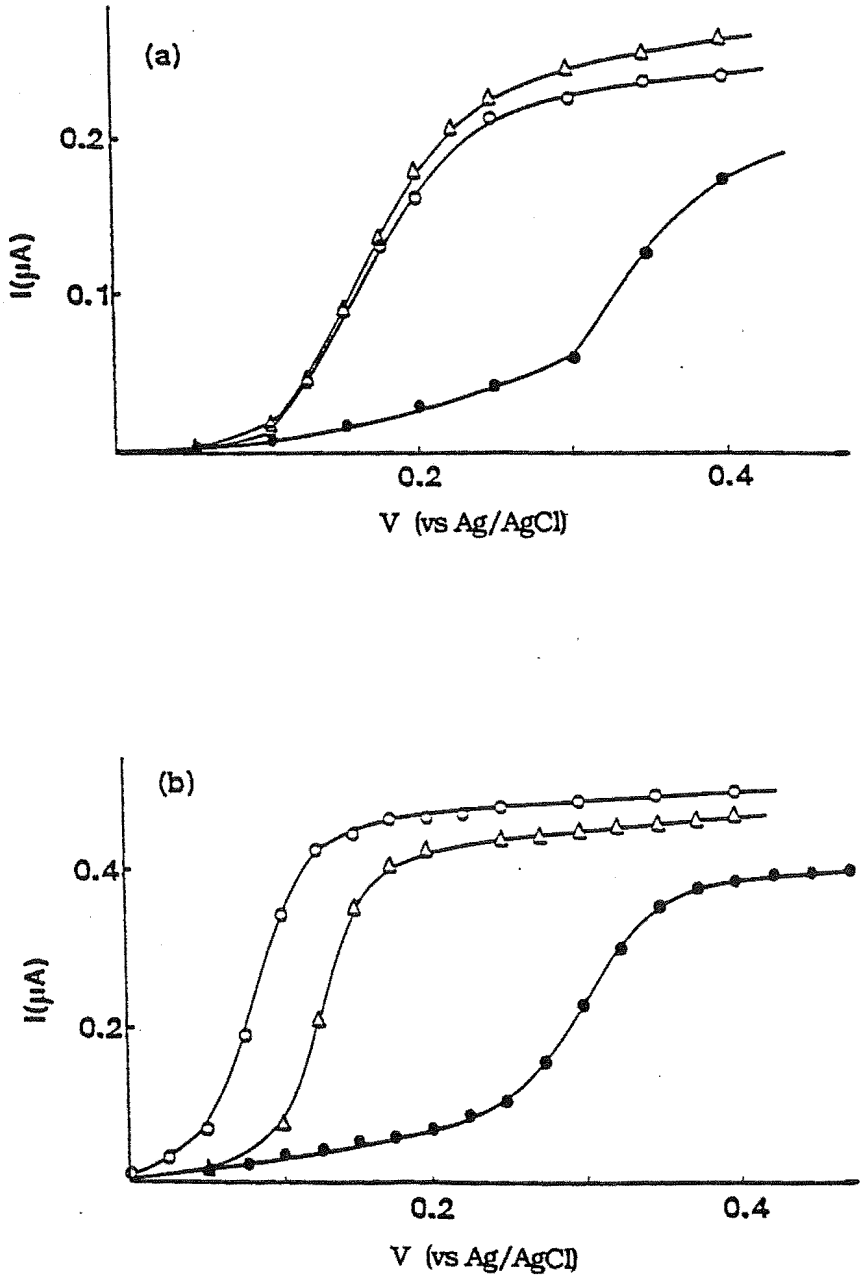

Figure 8.4. Hydrodynamic voltammograms for preformed EBT-buffer and M(II)-EBT-buffer solutions: (a) with surfactant (0.2% Hostapur) and (b) without surfactant; pH 11.5. (o) 2.0×10^{-4} M EBT; (Δ) 2.0×10^{-4} M EBT, 6.0×10^{-4} M calcium(II); (•) 2.0×10^{-4} M EBT, 4.0×10^{-4} M magnesium(II). Manifold as shown in Figure 8.4 with R2 and R5 omitted.

8.2.3. Measurement of magnesium(II)

The hydrodynamic voltammogram identified the oxidation process of EBT at $E_{1/2}$ = +0.175 V. When EBT mixed with buffer, masking reagent and surfactant was passed through the detector set at 0.175 V it resulted in a constant current at the glassy carbon electrode (base line). After magnesium(II) was injected, EBT reacted with magnesium(II) in the reaction coil and only the excess concentration of EBT contributed to the current. Measurement of the decrease in current for the EBT oxidation was the basis of the method described here.

The manifold shown in Figure 8.2 represents the basic design for analysis of magnesium(II). Some modifications were made for different measurements. For analysis of serum samples, pretreatment of samples was carried out on-line before merging the sample zone with EBT. These pretreatments which aimed at separating magnesium(II) from the protein matrix included (1) dilution, and mixing with a surfactant, and (2) on-line dialysis.

Because EBT solution decomposed slowly at pH 11.5, buffering of the EBT from neutral pH was effected on-line in this experiment. The stock solution of EBT was kept in a refrigerator and the diluted working solution was prepared daily.

8.3. OPTIMIZATION OF ELECTROCHEMICAL DETECTION AND MANIFOLD DESIGN

8.3.1. Characterisation and masking of interferences

Since natural water samples contain large amounts of calcium(II), generally in excess of magnesium(II), this would be expected to interfere with the determination of magnesium(II). Although iron and aluminium will be present at much lower concentrations they bind very strongly to *o,o'*-dihydroxyazo ligands and may also interfere. Interferences were generally studied by pre-equilibration of a magnesium(II) standard solution with various concentrations of interferent before injection in the FIA system.

Strong interference was observed for iron(III). On a molar basis the interference was equivalent to 60-90% of the iron(III) concentration; the signal from 1 x 10^{-5} M iron(III) was equal to that for 1.7 x 10^{-5} M magnesium(II) (0.4 ppm). In the FIA analysis of water, samples with high concentrations of iron(III) (≥ 0.5 ppm) gave anomalously high values for magnesium(II). It was established that iron(III) can be effectively masked by triethanolamine as reported[171], but not by EGTA, nor by CN^- (this work).

In the absence of masking reagents, samples with high concentrations of calcium(II) (10 ppm) and a high calcium/magnesium ratio (≥ 12) gave anomalously low results for magnesium(II) by FIA (Table 8.2). EGTA binds calcium(II) quantitatively under the experimental conditions (log K_1 = 11.00)[172]. To adequately mask calcium(II) it was necessary to use excess [EGTA] >[calcium(II)] to ensure that excess calcium(II) did not bind to EBT. However, EGTA also competes weakly for magnesium(II) (log K_1 = 5.20)[172] so a compromise was necessary in terms of EGTA concentration. On the

basis of speciation calculations (which are described in section 8.3.3) and experiments on solutions with different ratios of magnesium(II) : calcium(II) : EGTA it was established that the ratio [EGTA]/[EBT] = 3.0 gave a minimum deviation from magnesium(II) (AAS) values.

Table 8.2 gives evidence of interference from calcium(II) and iron(III) in analysis of water samples, and of the removal of this interference by use of EGTA and triethanolamine as masking reagents. In the presence of EGTA and triethanolamine interference was 0% up to (injection concentration) 5×10^{-4} M PO_4^{3-}, Fe^{3+}, Ca^{2+} or Al^{3+}, or up to 1×10^{-3} M F^- (at 5×10^{-5} M magnesium(II) and 1.5×10^{-4} M EBT).

Table 8.2. Interferences observed in the analysis of natural waters using the FIA-EBT method.

	Reference values[a]				FIA-EBT values of Mg(II)	
	Mg	Ca	Fe	Al	without masking	with masking
sample[b]		(ppm)			(ppm)	(ppm)
V3042	0.6	1.3	0.5	0.10	0.86	0.62
V3041	0.7	2.4	0.2	0.05	0.80	0.80
V3051	0.7	1.4	<0.1	-	0.70	0.70
V2953	1.6	2.0	1.6	-	2.80	1.63
V2967	4.0	2.6	0.6	<0.03	4.45	4.20
V2935	1.2	2.1	<0.1	<0.03	1.19	1.30
V2887	2.4	5.4	0.1	0.06	2.40	2.53
V2994	1.8	22	0.1	0.53	1.40	1.86
V3036	5.2	134	1.9	-	3.53	5.36
V3045	1.5	19.6	0.1	<0.03	1.18	1.54

a. Determined by DSIR, Mg (AAS), Fe (AAS) and Al (FIA eriochrome cycnine R). b. Natural drinking water samples provided by DSIR.

8.3.2. Electrode activity

The deactivation of the electrode mentioned in Chapter Seven occurred in these experiments also. The electrode activity decreased with time, as evidenced by a steady decrease in anodic current for the carrier/reagent stream (EBT-buffer) and a decrease of ca 0.7% per injection in the peak resulting from complexation of EBT with 1.6 ppm magnesium(II).

It is common for oxidation of azo, phenolic or 1,2-dihydroxyaryl systems that oxidation products deactivate the electrode by strong adsorption. For EBT, cyclic voltammograms and amperometric measurements on glassy carbon under hydrodynamic conditions (E = 0.175 V) established significant electrode deactivation with time (cycles) especially at high ligand concentrations. Voltage pulse reactivation of gold, as used for aluminium(III)-DASA in Chapter Seven, was examined; for several voltage patterns tested activation at -0.50 V (60 seconds) was most successful; however this was considered too slow for a flow system[173].

It was established that deactivation of glassy carbon could be minimised by use of a low concentration of EBT (ca. 3.75×10^{-5} M at the detector) and by use of an anionic surfactant in the carrier stream. Several surfactants were tested. All of them caused a concentration dependent decrease in sensitivity for EBT oxidation. This was least and approximately linear for Hostapur SAS 93 (-23% for 1% surfactant pumped) and a proportional change occurred in the FIA peak for magnesium(II), such that $i_{(EBT)}/i_{(Mg)}$ was constant. A 0.2% solution of Hostapur SAS 93 (0.04% in the detector) was used for all subsequent measurements. Baseline (EBT) and peak (magnesium(II)) currents did not change measurably with extended use (1 hour or 20 injections, respectively). Other surfactants studied (e.g. Brij-35, Empigen BB, Empigen OB, Gafac (RM710, RM510 and RS410)) all caused a significant decrease in current sensitivity. Figure 8.5 shows the effect of surfactant type and concentration on apparent [magnesium(II)] measured by FIA.

Thus, deactivation of the glassy carbon electrode was countered by the presence of 0.2% Hostapur SAS 93 in the flow line. Figure 8.6 shows typical output for injections of 1.6 ppm magnesium(II) standard using the manifold in Figure 8.2: R.S.D. = 0.7% (n = 11); for 0.1 ppm

magnesium(II), R.S.D. = 2.5% (n = 9). The detection limit, determined as 2σ for a 0.05 ppm standard, was 0.0055 ppm (n = 11), giving a linear working range of 0.027 - 1.8 ppm (1.0 - 75 x 10^{-6} M) magnesium(II) (see Figure 8.7). Throughput was 90 samples per hour.

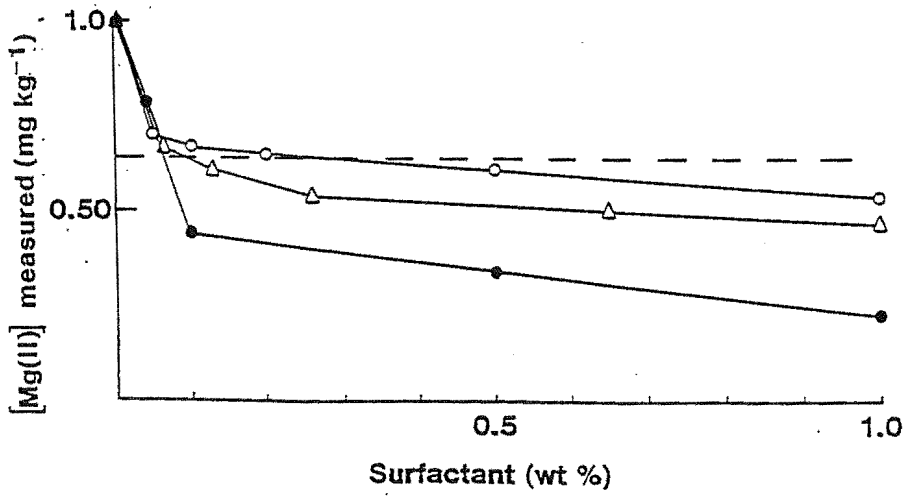

Figure 8.5. Effect of surfactant type and concentration (pumped) on apparent [magnesium(II)] measured by FIA, using the manifold shown in Figure 8.8. (o), Hostapur SAS 93; (Δ), Gafac RM 710; (•), Brij-35. Dashed line represents correct (AAS) value for serum magnesium.

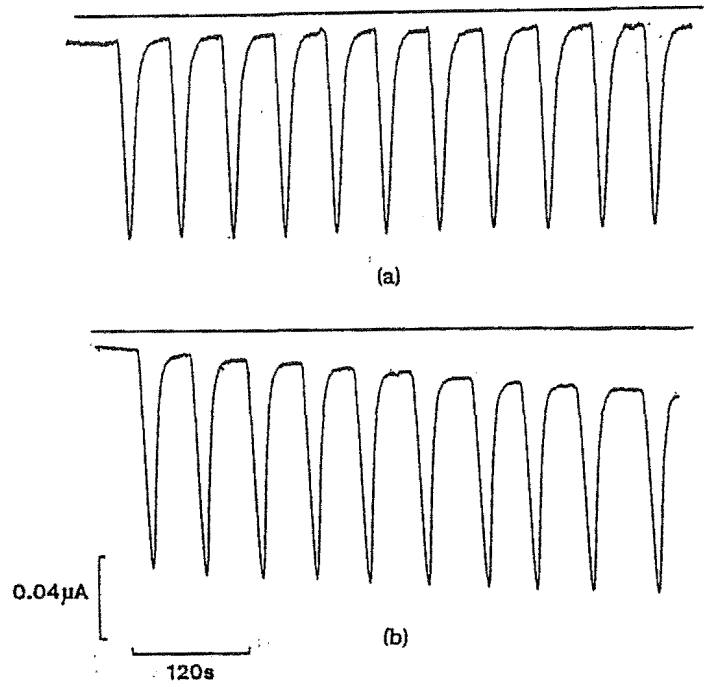

Figure 8.6. Amperometric signals for injection of magnesium(II) standard (1.6 ppm) into EBT (pH 11.5). (a) with surfactant (0.2% Hostapur) and (b) without surfactant; manifold shown in Figure 8.2.

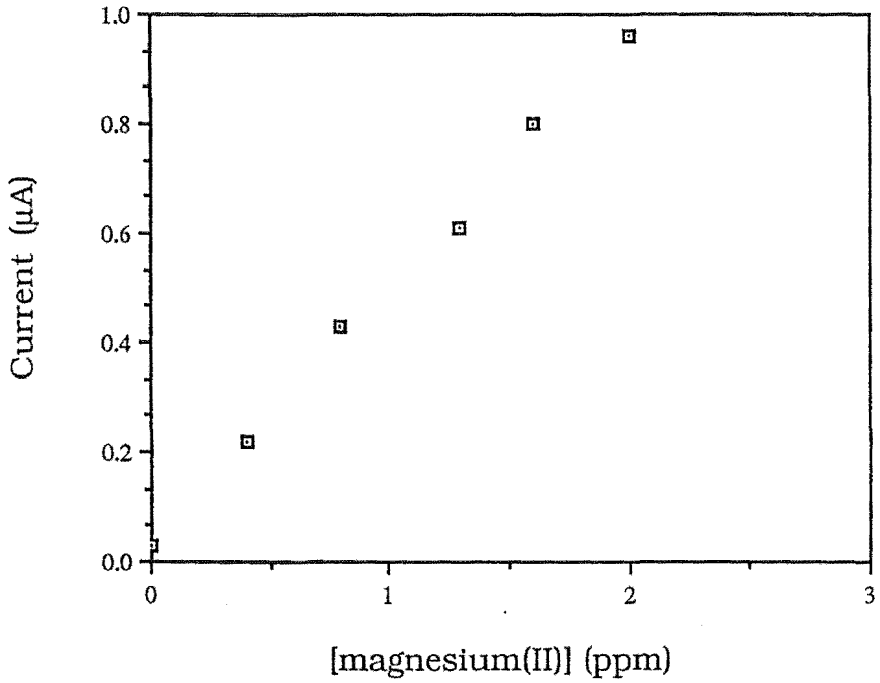

Figure 8.7. Calibration graph for amperometric signals for injection of magnesium(II) with surfactant (0.2% Hostapur) using the manifold shown in Figure 8.2.

8.3.3. Speciation calculations

The objectives of speciation calculations were (1) to determine the optimum pH and minimum [EBT] for quantitative formation of magnesium(II)-EBT in the most dilute environmental samples, and (2) to determine the optimum concentration of EGTA to effectively mask the calcium(II)-EBT reaction without sequestering magnesium(II).

Speciation calculations provide only an approximate measure of solution composition. They are limited by the accuracy and experimental conditions for the stability constants and, in FIA systems, by reaction kinetics. Competing ligands or metals in environmental or biological samples, if omitted from the model, will also limit the validity of the calculations. Calculations were performed with the program SIAS. Protonation and metal-ligand stability constants used were (log values) H_nEBT (K_1 = 11.55, K_2 = 7.00), Mg(II)-EBT (K_1 = 7.00), Ca(II)-EBT (K_1 = 5.30)[174], CaOH (*K_1 = -11.70), MgOH (*K_1 = -11.40)[175]; H_nEGTA (K_1 = 9.54, K_2 = 8.93, K_3 = 2.73, K_4 = 2.08), Mg(II)-EGTA (K_1 = 5.21) and Ca(II)-EGTA (K_1 = 11.00)[172].

For solutions containing magnesium(II) alone formation of magnesium(II)-EBT was calculated to be near quantitative at pH 11.5 and [EBT] $\geq 1 \times 10^{-4}$ M (2×10^{-5} M in detector); for 1×10^{-7} M - 1×10^{-5} M magnesium(II) 98-96% complexation was calculated. Figure 8.8 shows the produced formation of the magnesium(II) complex based on SIAS calculations.

For the chosen concentration of 3.75×10^{-5} M EBT at the detector, formation of magnesium(II)-EBT was calculated to be near quantitative ($\geq$ 96 %) up to 2.0×10^{-5} M magnesium(II) (2.5 ppm injected) but then decreased significantly. This was demonstrated in the calibration curve shown in Figure 8.7 which was linear up to 1.45×10^{-5} M magnesium(II) (1.8 ppm injected).

In the absence of a calcium(II) masking agent the calculated (positive) error associated with binding of EBT to calcium(II) was dependent on the calcium(II)/magnesium(II) ratio. For [EBT] = 3.75 x 10^{-5} M the calcium(II) error increased linearly with [calcium(II)]. Further, for [calcium(II)] = 16 ppm (4.0 x 10^{-4} M), the error relative to zero calcium(II) was +4.0, 4.2, 5.3 and 5.9% for [magnesium(II)] = 3.3 x 10^{-5}, 4.1 x 10^{-5}, 6.6 x 10^{-5} and 8.2 x 10^{-5} M (0.8 - 2.0 ppm) respectively. This established the need to use a masking agent for calcium(II) in environmental samples. Although forming a weaker complex calcium(II), typically present at higher concentration in natural waters, competes effectively for EBT; for 1 x 10^{-5} M magnesium(II) and 4 x 10^{-5} M calcium(II) 98% and 53% M-EBT formed respectively (EBT = 5 x 10^{-5} M).

To model masking of calcium(II) (and magnesium(II)) by EGTA ratios of [EGTA]:[EBT] of 1:1 to 8:1 were considered, with calcium(II):magnesium(II) set at 3:1 and 6:1. It was calculated that EGTA binds calcium(II) quantitatively under the experimental conditions, but at [EGTA]:[EBT] = 8:1, 4:1 and 2:1, and calcium(II):magnesium(II) = 3:1, EGTA also binds 23%, 12% and 4% respectively of magnesium(II).

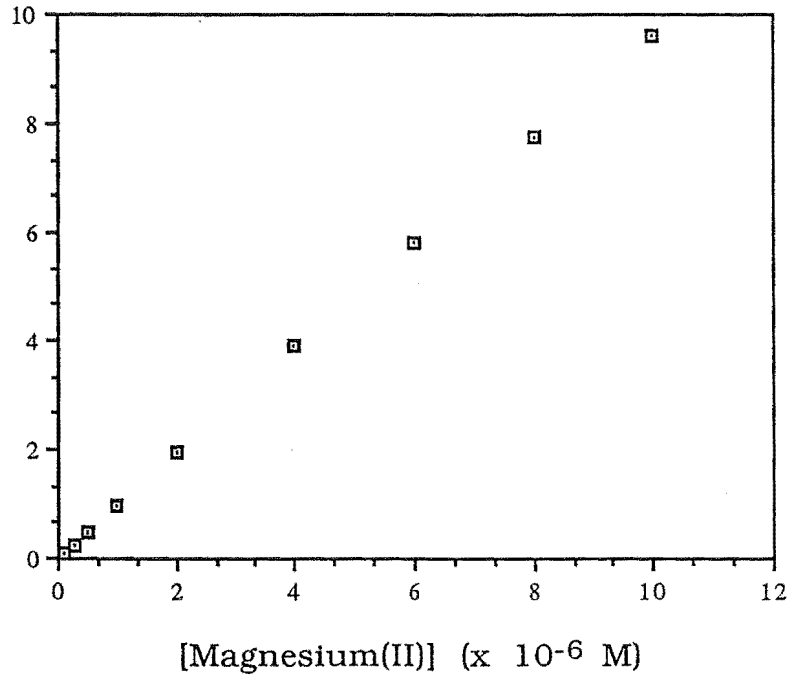

Figure 8.8. The calculated formation of magnesium(II)-EBT complex in pH 11.0. EBT: 2 x 10^{-5} M; magnesium(II): 1 x 10^{-7} M - 1 x 10^{-5} M.

Optimum conditions chosen were [EGTA]:[EBT] = 3:1, which for 2 x 10^{-5} M magnesium(II) and 3.75 x 10^{-5} M EBT (both at detector) and calcium(II)/magnesium(II) = 6, 4, 2 and 1 were calculated to give 100% formation of calcium(II)-EGTA and 92-95% formation of magnesium(II)-EBT.

8.4. APPLICATION OF THE EBT-FIA SYSTEM FOR ANALYSIS OF MAGNESIUM(II) IN WATER

8.4.1. Analysis of environmental samples

For water analysis the flow system consisted of two Alitea C4-XV peristaltic pumps and the flow manifold shown in Figure 8.2. The flow rates were 0.6 mL minute^{-1} (R1 - R5) and 0.2 mL min^{-1} (R6) respectively for the carrier (R1 = water), reagent (R2 = 1.5 x 10^{-4} M EBT), buffer (R3 = 15% 1,2-diaminoethane in 0.3 M KCl, pH 11.5), surfactant (R4 = 0.2% Hostapur SAS 93), masking agents (R5 = 4.5 x 10^{-4} M EGTA; 4 x 10^{-2} M triethanolamine) and for the reference electrode electrolyte (R6 = 0.1 M KCl).

Sixteen water samples received from DSIR (NZ) Chemistry Division were analysed by FIA and AAS. The analysis results are shown in Table 8.3. With use of masking agents the magnesium(II) values determined by FIA and AAS correlated strongly: magnesium(II) (AAS) = 0.990 magnesium(II) (FIA); R^2 = 0.996 (n = 16) (Figure 8.9). Also these results were in good agreement with those determined by DSIR.

Table 8.3. Results for magnesium(II) analysis in water samples using FIA and AAS

	Mg(II) (ppm)		
Sample	FIA	AAS	Reference values[a]
V3042	0.62	0.60	0.6
V3041	0.80	0.79	0.7
V3051	0.71	0.69	0.7
V2935	1.30	1.24	1.2
V2967	4.20	4.05	4.0
V2953	1.63	1.80	1.6
V2887	2.53	2.43	2.4
V2849	4.90	5.05	4.7
V2913	0.62	0.64	0.6
V2994	1.86	1.90	1.8
V3036	5.36	4.75	5.2
V3045	1.54	1.56	1.5
V3064	3.02	3.14	3.0
V3076	2.30	2.24	2.0
V3120	2.47	2.66	2.4
V3160	3.84	2.90	3.7

a. Determined by DSIR; AAS

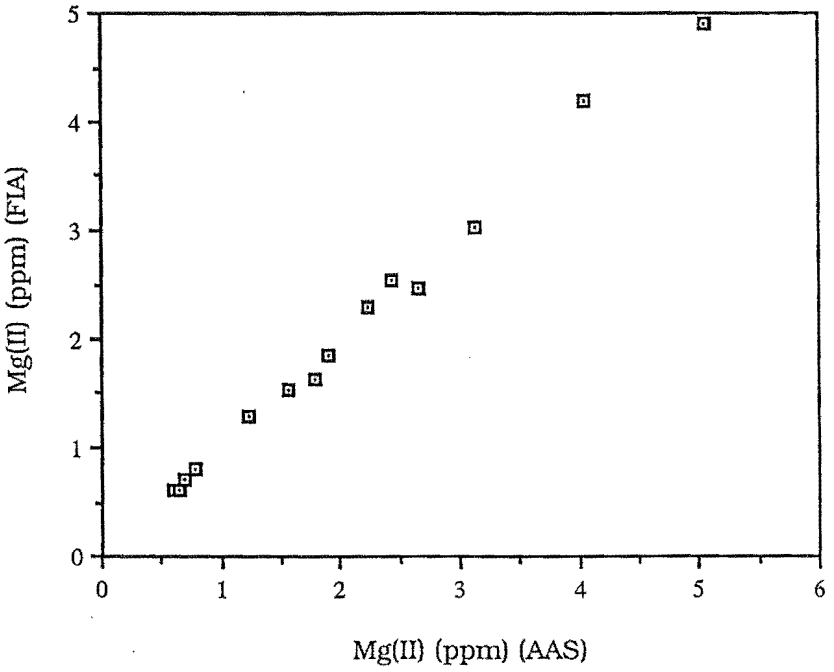

(a)

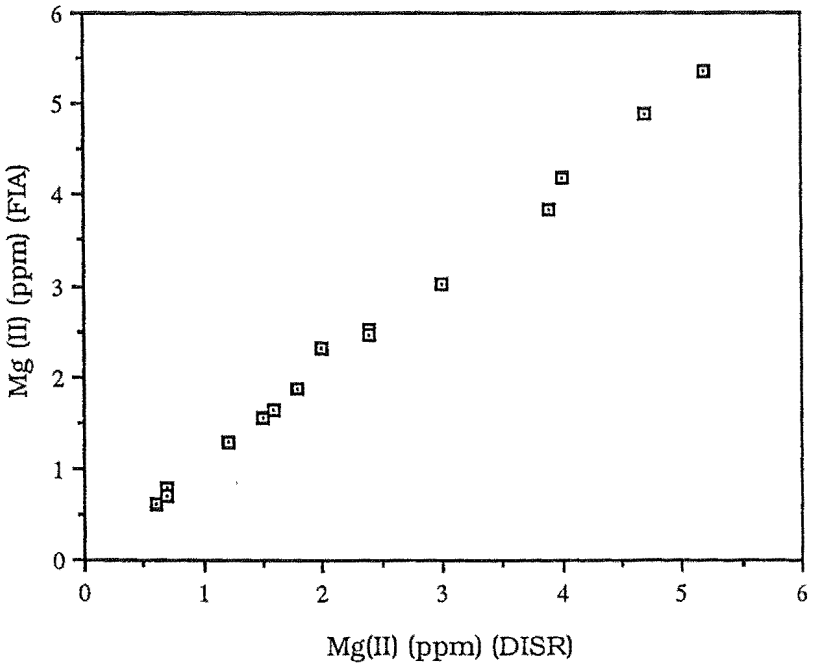

(b)

Figure 8.9. Comparison of results obtained with different methods (a): FIA and AAS (this work), (b): FIA and AAS(DSIR).

8.5. APPLICATION OF THE EBT-FIA SYSTEM FOR ANALYSIS OF MAGNESIUM(II) IN SERUM

8.5.1. Optimization of solution chemistry

Albumin has a propensity to bind dye molecules, either by hydrophobic interaction or by electrostatic attraction between cationic sites on the protein and anionic dye molecules[176]. It was established that EBT binds to serum albumin under the experimental conditions used. This is indicated in hydrodynamic voltammograms of equilibrated EBT-serum samples (see Figure 8.10). Thus serum protein caused a large positive error in the current measured for magnesium(II) in serum. It was established that this ionic association can be masked by addition of anionic surfactants or by use of a dialyser.

For serum samples diluted 20-fold, the concentration of calcium(II) and magnesium(II) expected in the detector are approximately 3.1×10^{-5} M and 7.7×10^{-6} M respectively. Under these conditions the calculated error associated with calcium(II)-EBT formation (no EGTA added) is only -1.5%. So masking reagents were not necessary for direct analysis of diluted serum. The manifold was modified to allow binding of the surfactant to serum protein before merging with the EBT-buffer stream (Figure 8.11).

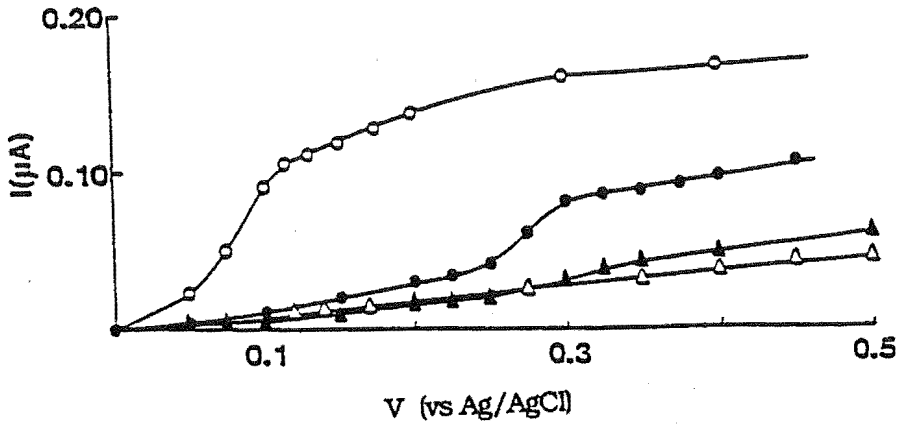

Figure 8.10. Hydrodynamic voltammograms for preformed EBT-buffer, EBT-serum-buffer and M(II)-EBT-serum-buffer solutions, pH 11.5 and 7.5 x 10^{-5} M EBT. (o), EBT; (•) EBT + 1 ppm magnesium(II); (▲) EBT + 1 ppm magnesium(II) + albumin (0.5 g L^{-1}); (Δ) EBT + albumin (0.5 g L^{-1}).

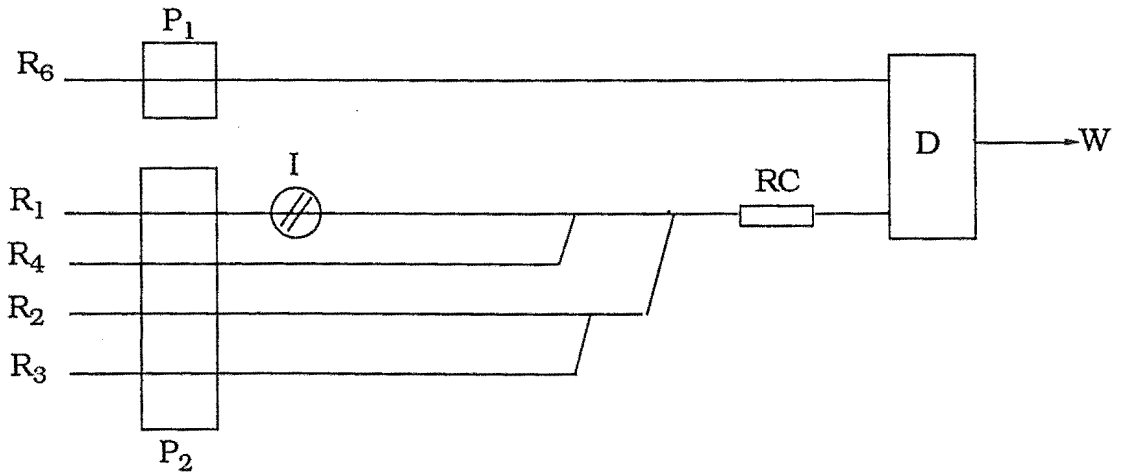

Figure 8.11. Manifold used for direct analysis of magnesium(II) in diluted serum. Reagents as for Figure 8.2; masking agents (R5) not required.

8.5.2. Optimization of dialysis

Dialysis is an important sample pretreatment step whereby particles and large molecules in a sample can be removed[177-181]. The sample is injected into a carrier stream which passes over a dialysis membrane. On the other side of the membrane a recipient stream (distilled water or a reagent) takes up the constituents passing through the membrane. The membrane is placed in a cell working on the same principle as the FIA gas diffusion cell.

The dialysis unit constructed for this work is shown in Figure 8.12. It permitted analysis of serum magnesium(II) in the absence of serum proteins. It consisted of two blocks of acetal (delrin) 120 x 62 x 12 mm with complimentary channels 0.5 x 1.5 x 500 mm separated by 30,000 mwco dialysis membrane. Pretreatment of the membrane involved boiling in 2% Na_2CO_3/0.01 M EDTA solution for 10 minutes then washing with Milli-Q water; the membrane was stored in Milli-Q water.

Analysis of serum by FIA-dialysis used the manifold shown in Figure 8.13. R1, R4 and R6 were as above, R2 = 0.03 M HCl, R3 = 0.01 M HCl, and R5 = EBT (1.0×10^{-4} M) + buffer (15% 1,2-diaminoethane; 0.3 M KCl, pH 11.5). Flow rates for R1 - R6 were 0.6 mL $minute^{-1}$ (R2 - R5) and 0.2 mL $minute^{-1}$ (R1, R6) respectively. Flow was stopped in R1 for 150 seconds after the injected serum sample was contained in the dialyser; during this period the valve V1 was switched to provide stationary solution in contact with the membrane, but also to maintain constant reagent flow through the detector.

For the dialysis experiments protein-bound magnesium(II) was released by initially merging the carrier stream (R1 = H_2O) with 0.03 M HCl (R2); this gave a sample pH of ca. 2.0. Without this acidification results were suppressed by 75 %. For direct FIA analysis of serum, the initial 20-fold dilution of serum sample, plus the effects of dispersion,

were sufficient to release all protein bound magnesium(II) in the presence of EBT. This indicates that the equilibrium constant for the magnesium(II)-protein reaction is comparatively small.

For 30,000 mwco membrane 14% of serum magnesium(II) passed through the membrane in 150 seconds of stop flow. For undiluted serum samples membrane efficiency decreased by ca. 1.1% per injection. Attempts to rectify this problem by washing the membrane on-line with dilute acid, dilute alkali, dilute surfactant or ethanol/water mixtures were not successful. However, this adsorption was effectively countered by a 2-fold dilution before injection. Figure 8.14 shows typical output for replicate analyses of serum samples by FIA-dialysis.

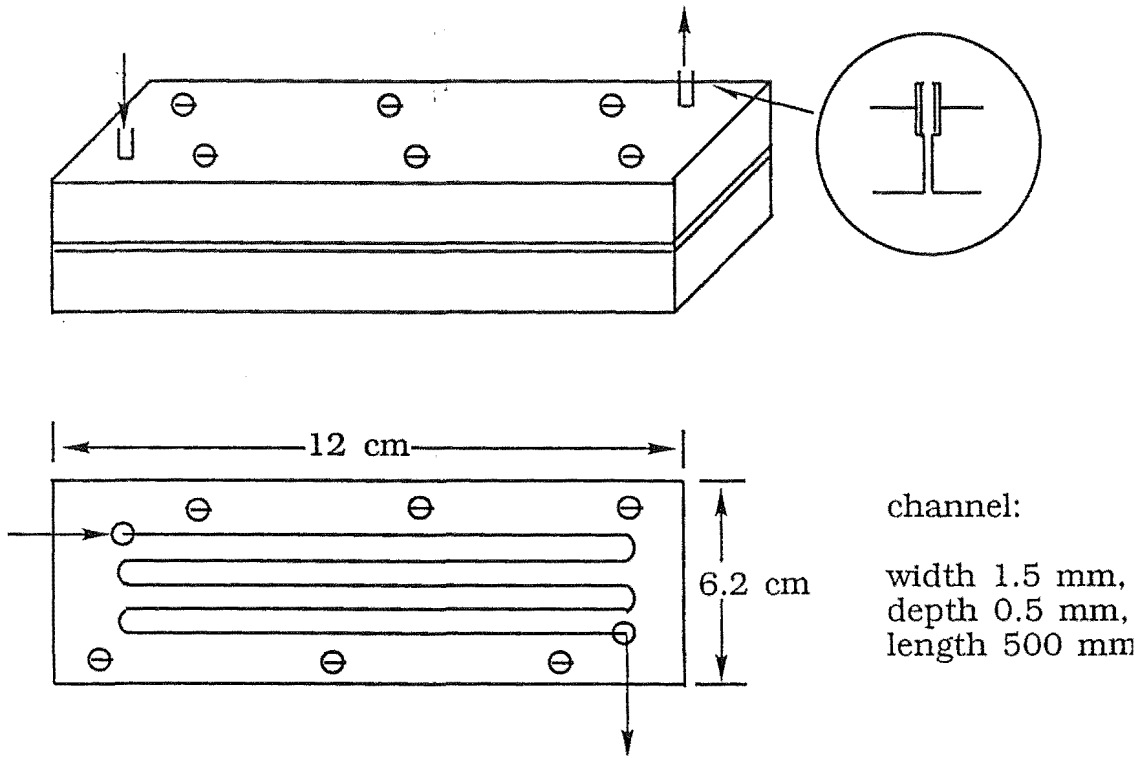

Figure 8.12. Diagram of the dialyser used for analysis of magnesium(II) in serum.

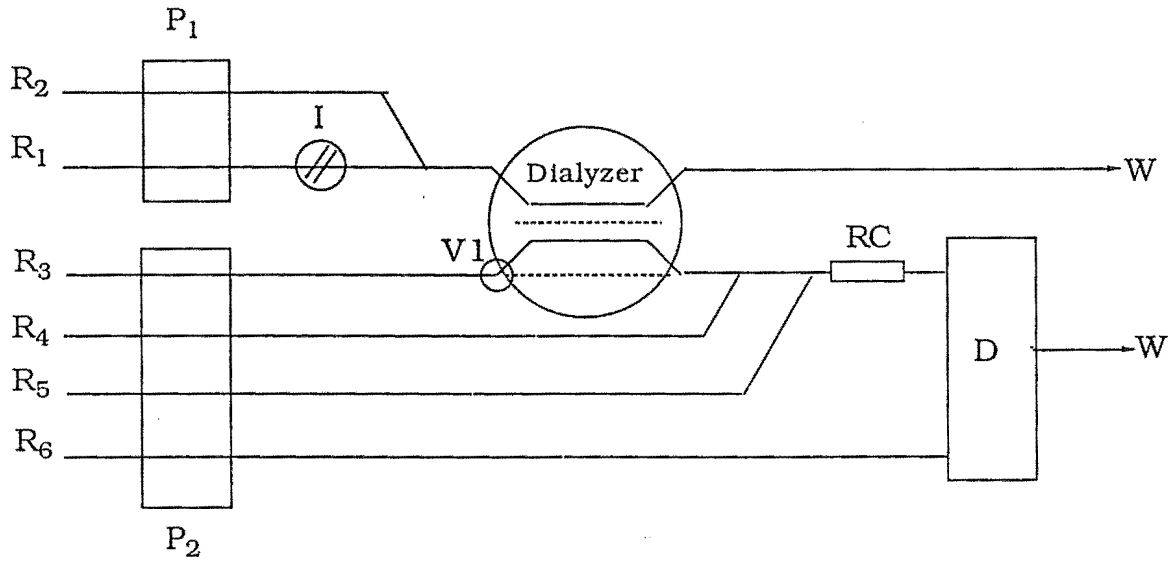

(a)

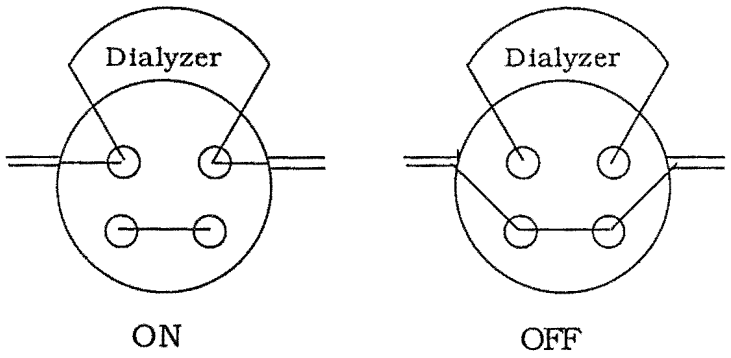

(b)

Figure 8.13. (a) Manifold for analysis of serum following dialysis. R1, R4, R6 as for Figure 8.4. R2, 0.03 M HCl; R5, 1.0 x 10^{-4} M EBT, 15% 1,2-diaminoethane, 0.1 M KCl, pH 11.5; V1, switching valve. (b) Manifold in V1.

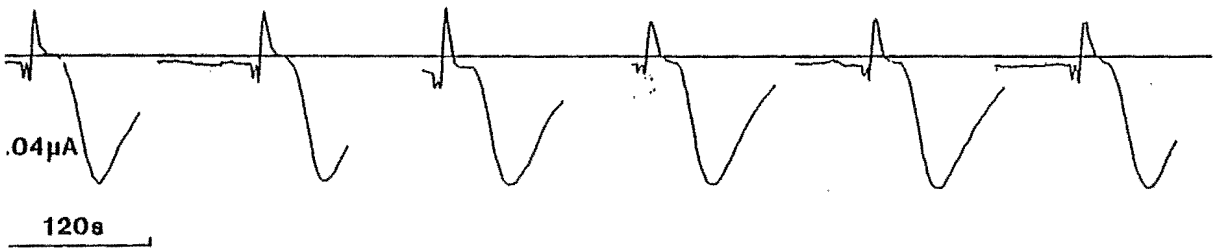

Figure 8.14. Amperometric signals for replicate analyses of serum (diluted 1:1 with distilled water) following dialysis (stop flow 150 s); manifold shown in Figure 8.13.

8.5.3. Analysis of human serum

Hydrodynamic voltammograms shown in Figure 8.10 established a strong interaction between EBT and albumin and between the magnesium(II)-EBT complex and albumin. These interactions were effectively countered by including 0.04% of the n-alkyl sulphonate surfactant Hostapur SAS 93 in the reagent stream. Thus in the absence of surfactant, the "apparent" [magnesium(II)] measured by this amperometric technique was 50% higher than total magnesium(II) by AAS. In the presence of surfactant the FIA amperometric value approached the correct value although excess surfactant lead to negative errors. The surfactant Hostapur SAS 93 was selected because it effected the smallest errors at high concentration; also the smaller slope of the [magnesium(II)] measured vs % surfactant curve (Figure 8.5) gave the widest window of surfactant concentrations which provided close correlation between AAS and FIA values for magnesium(II).

Serum samples were analysed by FIA by direct injection after 20-fold dilution (60 samples h^{-1}) using the manifold shown in Figure 8.11 or by dialysis/FIA (20 samples h^{-1}) (using the manifold shown in Figure 8.12). Figure 8.15 shows amperometric signals for replicate analyses of serum diluted 20-fold with distilled water. Results for the methods are shown in Table 8.4 and compared with analyses by AAS. Samples 1-5 were for serum separated from freshly taken whole blood. Sample 6 was serum from aged blood which had partly lysed, and sample 7 was for reconstituted freeze dried serum (Moni-Trol; Baxter Healthcare Corporation). Analyses of magnesium(II) by AAS were obtained on a Varian 1475 spectrophotometer using the 282.8 nm resonance line.

Serum samples were diluted 20-fold with DDW; samples and standards contained 1500 mg kg^{-1} Sr(II).

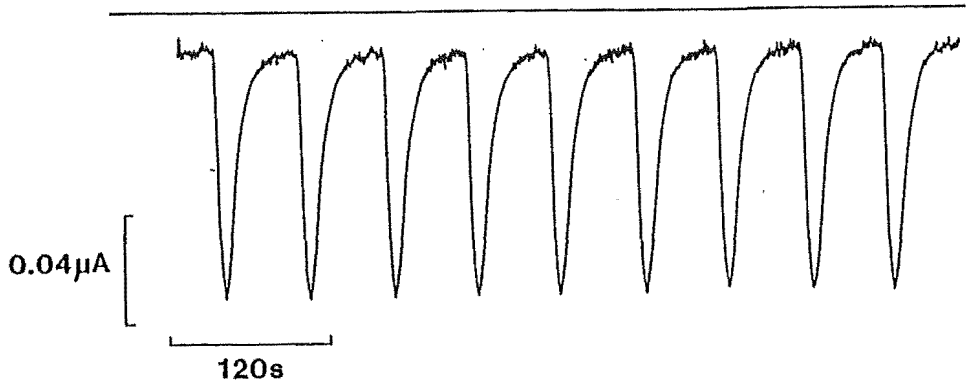

Figure 8.15. Amperometric signals for replicate analyses of serum (diluted 20-fold with distilled water); manifold shown in Figure 8.11.

For the fresh serum samples there was excellent agreement between the measurements by direct FIA, by FIA-dialysis and by AAS (Table 8.4) . However it is evident that serum from an aged blood sample (partly lysed) and from freeze dried serum contained protein constituents which do not pass the dialyser but which interfere with the chemistry or electrochemistry of the magnesium(II)-EBT reaction, or which bind with EBT in the presence of surfactant.

Table 8.4. Analysis of magnesium(II) in serum samples by FIA-dialysis and AAS

	Mg(II) (ppm)		
Sample	FIA	FIA-dialysis	AAS
1	18.4	18.3	18.3
2	18.4	18.7	18.7
3	20.8	20.0	19.5
4	19.7	20.8	19.7
5	18.4	17.9	18.3
6 (freeze dried)	62.8	44.2	44.4
7 (aged)	62.2	35.0	33.4

8.6. CONCLUSIONS

Magnesium(II) can be determined in this flow injection system by formation of the magnesium(II)-EBT complex at pH 11.5 and amperometric measurement of excess EBT at + 0.175 V on a glassy carbon electrode. Interference of iron(III) and calcium(II) were masked with triethanolamine and EGTA respectively. For analysis of natural waters the linear working range was 0 - 1.6 ppm magnesium(II) and the R.S.D. 0.7% at 1.6 ppm magnesium(II) (n = 11); the DL was 0.0055 ppm and sampling rate was 90 samples per hour.

Analysis of human serum samples can be determined by using two methods: (1) direct injection of serum after a 20-fold dilution (surfactant Hostapur SAS 93 countered the association of EBT with

serum albumin) and (2) after dialysis (2.5 minutes) separation of magnesium(II) from acidified serum in the flow system. The linear working range of direct injection was 0 - 1.6 ppm magnesium(II) and R.S.D. = 0.4% (n = 9) at 1.0 ppm magnesium(II).

In this work, the surfactant has two roles, to suppress electrode deactivation and to mask binding of EBT to serum. The masking agents for iron(II) and calcium(II) were not necessary in serum analyses.

For routine analysis of serum, the method of choice is by direct FIA using serum samples diluted twenty-fold. This permits approximately 60 analyses per hour, compared with ca 15 by FIA-dialysis. This throughput is very favourable compared with AAS, and the delay from sample preparation to completed analyses for a single sample is very short compared with the automated calmagite method.

A feature of the present method is its ability to achieve accurate analyses in waters which are high in iron(III) or in aluminium(III). Cañete et al described an FIA-titration method for calcium(II) + magnesium(II) in serum, using EBT-EDTA. However, they made no attempt to characterise or eliminate interferences from iron(III) or aluminium(III).

For each method results were compared with those from flame atomic absorption spectrometry (AAS). The results of the proposed method correlated strongly with those for AAS. The method may be applicable to the analysis of a wider range of natural products.

CHAPTER NINE

CONCLUSION

The development and application of chemically modified electrodes (CMEs) and amperometric determination in flow systems (FIA) for analysis of aluminium(III) have been studied.

For determination of aluminium(III), the primary approach was to use aluminium(III)-specific redox active ligands, either in solution or incorporated in CMEs, as a method for indirect electrochemical analysis of aluminium(III).

In studies of the electrochemistry for several electroactive ligands and the complex formation between these ligands and aluminium(III), two main methods were developed for determination of aluminium(III): (1) use of the increase in peak height for the aluminium(III) complex formed or (2) use of the decrease in peak height due to complexation of free ligand.

The preparations and characterizations of chemically modified electrodes were studied. Three main kinds of CMEs were used in this work: (1) polymer film coated CMEs, (2) chemisorbed CMEs and (3) carbon paste and graphite epoxy CMEs.

Coating of the electrode with a charged polymer followed by incorporation of an anionic ligand or aluminium(III)-ligand complex was studied. Using the PXV films ion-exchange property, the accumulation of aluminium(III) in the electrode as anionic phenolic complexes was investigated. The measurement of aluminium(III)-(4-nitrocatechol) complexes (which have an overall negative charge) after preconcentration at the PXV coated electrode results in a sensitive

method for analysis of aluminium(III). This work also demonstrated how the CMEs can improve the selectivity and sensitivity in analysis by ion exchange.

As one kind of chemisorption CME, an alizarin dip-coated CME was successfully used in analysis of aluminium(III) in soil extracts. Its preparation and use are very simple and the sensitivity and reproducibility in determination of aluminium(III) are good. A more promising aspect is that this CME has the potential to be developed into a cheap, single-use electrode coupled with simple instrumentation for use in field research.

Graphite epoxy is a cheap and convenient material for CME preparation. Polishing the electrode gives satisfactory reproducibility for multiple-use. For determination of aluminium(III) the 4-nitrocatechol modified graphite epoxy electrode has promising results with high sensitivity and reproducibility. For use in field work, polishing may be a more convenient renewal method than other procedures.

It was established that analysis for aluminium(III) based on ligand-centred electrochemistry could not be carried out effectively using carbon paste electrodes. In contrast, for reducible metals it is possible to use these CMEs.

The 1,2-naphthoquinone CME exhibited acceptable stability on repeat scans without surface renewal. Its use for aluminium(III) determination was unsatisfactory primarily because no new peaks due to the aluminium(III)-ligand complex were observed. The absence of a signal due to the complex may be due to dissolution of the charged complex. One possible use for this CME in analysis of aluminium(III) is to add on ion exchanger to the electrode; the charged metal-ligand complex would be adsorped into the ion exchanger instead of dissolving in solution, hence giving a sensitive signal.

The CMEs were evaluated on the basis of factors such as stability, ease of fabrication and detection limits. Fundamental studies, including investigations of the properties of the electrode coating, enabled optimization of CME performance. Also, it was found that the loss of ligand from CMEs due to irreversible oxidation or solubility of the ligand is a major problem in CME studies.

An adsorptive stripping method for analysis of aluminium(III) using a SVRS-aluminium(III) system was developed. The heating step was replaced by allowing the aluminium(III) reaction with SVRS to occur at a higher pH, followed by accumulation in acidified solution. This modification provided good results with high sensitivity and reproducibility and significantly shorter analysis time. In studies of the electrochemistry for the ligands and their aluminium(III) complexes, the aluminium(III)-(4-nitrocatechol) system showed a very sensitive electrochemical signal for aluminium(III) complexes. It is possible that attractive results in analysis of trace aluminium(III) will be obtained using this system by adsorptive stripping voltammetry at a mercury electrode.

An amperometric FIA method for aluminium(III) was developed based on the ligand DASA. Aluminium(III) in soil extracts was determined in the flow injection system by amperometric measurement of excess DASA at +0.50 V on a gold electrode. Electrode fouling by adsorption of ligand oxidation products in flow systems was minimized by use of a double pumping system and cathodic/anodic voltage cycling. Other ligand-FIA systems for analysis of aluminium(III) were investigated. Amongst these, the PCV and 4-nitrocatechol systems showed promising results: smaller deactivation of the electrode and sensitive signals given at a glassy carbon electrode. Because of the high stabilities of aluminium(III)-PCV and aluminium(III)-(4-nitrocatechol) complexes, it is anticipated that these systems could be developed into

methods with appropriate sensitivity for monitoring aluminium(III) in natural waters.

Magnesium(II) in natural waters and serum was determined in a simple flow system. Two methods were effected in analysis of human blood serum samples: (1) direct injection of serum after dilution and (2) after dialysis to effect separation of magnesium(II) from acidified serum proteins in the flow system. Electrode fouling by adsorption of EBT oxidation products and serum in the flow system was minimized by use of several surfactants and the dialyzer.

REFERENCES

1. G. M. Berlyne, Lancet, (1970) 1253.
2. B. O. Rosseland, T. D. Eldhuset and M. Staurnes, Environmental Geochemistry and Health, 12 (1990) 17.
3. F. Adams, Alleviating chemical toxicities: liming acid soils. In G. F. Arkin and H. M. Taylor (Eds.), Modifying the root environment to reduce crop stress. ASAE monograph no. 4. Am. Soc. Agric. Eng., St. Josephs, Mich, (1981) p. 269.
4. C. D. Foy, Effects of aluminium on plant growth. In E. W. Carso (Ed.), The plant root and its environment, University Press of Virginia, Charlottesville. ISBN, (1974) p. 601.
5. T. Wagatsuma and M. Kaneko, Soil Sci. Plant Nutr., 33 (1987) 57.
6. W. J. Horst, A. Wagner and H. Marschner, Z. Pflanzenphysiol, 109 (1983) 95.
7. D. O. Huett and R. C. Menary, Aust. J. Plant Physiol., 7 (1980) 101.
8. D. T. Clarson, Plant and Soil, 27 (1967) 347.
9. D. T. Clarson and J. Sanderson, Planta, 89 (1969) 136.
10. A. Henriksen, O. K. Skogheim and B. O. Rosseland, Vatten, 40 (1984) 255.
11. C. L. Schofied and R. J. Trojnar, Polluted Rain, Plenum Press, New York, (1980).
12. B. O. Rosseland, Effects of acid water on metabolism and gill ventilation in brown trout, Salmo trutta L, and brook trout, Salvelinus fontinalis Mitchill. In D. Drablos and A. Tollan (Eds.), Ecological impacts of acid precipitation, SNSF-project, (1980) p.348.
13. I. S. Parkinson, M. K. Ward, T. G. Feest, R. W. P. Fawcett and D. N.

W. Kerr, Lancet, 1 (1979) 406.

14. E. Nyholm, Environ. Res., 26 (1981) 363.
15. A. Haug, CRC Crit. Rev. Plant Sci., 1 (1984) 219.
16. J. A. Feldrig, Proc. Eur. Dial. Transplant Assoc., 13 (1976) 355.
17. J. A. Kanis, J. Clin. Pathol., 34 (1981) 1295.
18. G. A. Trapp, Journal of Environmental Pathology, Toxicology and Oncology, 6 (1985) 15.
19. J. W. Akitt, J. A. Fransworth and P. Letellier, J. Chem. Soc. Faraday Trans. 1, 81 (1985) 193.
20. D. Langmuir, Techniques of estimating thermodynamic properties for some aqueous complexes of geochemical interest. In E. A. Jenne, (Ed.), Chemical modeling in aqueous systems: speciation, sorption, solubility, and kinetics, ACS Symp. Ser. No. 93, American Chemical Society, Washington, D. C., (1979) p. 353.
21. E. L. King and P. K. Gallagher, J. Phys. Chem., 63 (1959) 1073.
22. B. Behr and H. Wendt, Z. Elektrochem., 66 (1962) 223.
23. D. K. Nordstrom and H. M. May, Aqueous equilibrium data for mononuclear aluminium species. In G. Sposito (Ed.) The environmental chemistry of aluminum, CRC Press, Boca Raton, FL, (1989) p. 29.
24. A. E. Martell, R. J. Motekattis and R. M. Smith, Polyhedron, 9, (1990) 171.
25. W. L. Lindsay, Chemical Equilibria in Soils, John Wiley and Sons, New York, (1979).
26. C. F. Baes and R. E. Mesmer, The Hydrolysis of Cations, John Wiley and Sons, New York, (1976).
27. J. Heyrovsky, J. Chem. Soc., 117 (1920) 27.
28. P. A. Malachesky, Aluminium, In A. J. Bard (Ed.), Encyclopedia of Electrochemistry of elements, Vol. VI, Marcel Dekker, New York, (1976) p. 63.

29. J. Prajzler, Collect. Czech. Chem. Commun., 3 (1931) 407.

30. G. F. Reynolds and T. J. Webber, Anal. Chim. Acta, 19 (1958) 293.

31. M. Galova and V. Szmerekova, Chem. Zvesti, 27 (1973) 437.

32. H. H. Willard and J. A. Dean, Anal. Chem., 22 (1950) 1264.

33. T. M. Florence, Anal. Chem., 34 (1962) 496.

34. D. V. Vukomanovic, J. A. Page and G. W. Vanloon, Can. J. Chem., 69 (1991) 1418.

35. C. M. G. van den Berg, K. Murphy and J. P. Riley, Anal. Chim. Acta, 188 (1986) 177.

36. E. Laviron, J. Electroanal. Chem., 164 (1984) 213.

37. P. Delahay, New Instrumental Methods in Electrochemistry, Interscience, New York, (1954).

38. J. Doskocil, Collect. Czech. Chem. Commun., 15 (1950) 780.

39. G. M. Proudfoot and I. M. Ritchie, Aust. J. Chem., 36 (1983) 885.

40. M. R. Deakin, P. M. Kovach, K. J. Stutts and R. M. Wightman, Anal. Chem., 58 (1986) 1474.

41. S. I. Bailey, F. R. Hewgill and I. M. Ritchie, J. Chem. Soc., Perkin Trans., 2 (1983) 645.

42. M. D. Ryan, A. Yueh and W. Y. Chen, J. Electrochem. Soc., 127, (1980) 1489.

43. A. W. Sternson, R. McCreery, B. Feinberg and R. N. Adams, J. Electroanal. Chem., 46 (1973) 313.

44. F. G. Thomas and K. G. Boto, The electrochemistry of azoxy, azo and hydrazo compounds. In S. Patai (Ed.), The chemistry of the hydrazo, azo and azoxy groups, John Wiley and Sons, London, (1975) p. 443.

45. L. Holleck and G. Holleck, Z. Naturforsch., 19B (1964) 162.

46. L. Holleck and A. M. Shams-el-Din, Electrochim. Acta, 13 (1968) 199.

47. T. M. Florence and G. H. Aylward, Aust. J. Chem., 15 (1962) 416.

48. T. M. Florence, Aust. J. Chem., 18 (1965) 627.

49. A. H. Laitinen and T. J. Kneip, J. Am. Chem. Soc., 78 (1956) 736.

50. L. Holleck and S. Vavricka, Z. Naturforschung, 23B (1968) 748.

51. R. Patzac and M. R. Zaki, Mikrochim. Acta, 21 (1959) 274.

52. B. A. Cooney and J. H. Saylor, Anal. Chim. Acta, 21 (1959) 276.

53. M. Ishibashi, T. Fujinaga and K. Izutsu, J. Electroanal. Chem., 1 (1959) 26.

54. T. M. Florence and W. L. Belew, J. Electroanal. Chem., 21 (1969) 157.

55. J. A. Dean and H. A. Bryan. Anal. Chim. Acta, 16 (1957) 94.

56. E. Coates and B. Bigg, Trans. Faraday Soc., 58 (1962) 88.

57. K. K. Shiu and D. J. Harrison, J. Electroanal. Chem., 260 (1989) 249.

58. K. K. Shiu and D. J. Harrison, J. Electroanal. Chem., 262 (1989) 145.

59. H. D. Abruna, Coord. Chem. Rev., 86 (1988) 135.

60. J. Wang and T. Golden, Anal. Chem., 61 (1989) 1397.

61. A. Merz and A. J. Bard, J. Am. Chem. Soc., 100 (1978) 3222.

62. J. E. Gregor and H. K. J. Powell, J. Soil Sci., 37 (1986) 577.

63. E. A. Close and H. K. J. Powell, Aust. J. Soil Res., 27 (1989) 681.

64. J. J. Fardy and R. N. Sylva, SIAS, a computer program for the generalized calculation of speciation in mixed metal-ligand aqueous systems. Australian Atomic Energy Commission report AAEC/E445, 1978, p. 1.

65. C. K. Chiang, Y. W. Park, A. J. Heeger, H. Shirakawa E. J. Louis and A. G. MacDiarmid, J. Chem. Phys., 69 (1978) 5098.

66. P. J. Nigrey, A. G. MacDiarmid and A. J. Heeger, J. C. S. Chem. Commun., (1979) 594.

67. A. F. Diaz, K. K. Kanazawa and G. P. Gardini, J. C. S. Chem.

Commun., (1979) 635.

68. G. Tourillon and F. Garnier, J. Electroanal. Chem., 135 (1982) 173.

69. R. M. Kannuck, J. M. Bellama and R.A. Durst, Anal. Chem., 60 (1988) 142.

70. J. Heinze, Electronically conducting polymers, Top. Curr. Chem., 152 (Electrochem. 4) (1990) 1.

71. H. Li, J. Roncali and F. Garnier, J. Electroanal. Chem., 263 (1989) 155.

72. A. R. Guadalupe and H. D. Abruna, Anal. Chem., 57 (1985) 142.

73. O. Chastel, J. M. Kauffmann, G. J. Patriarche and G. D. Christian, Anal. Chem., 61 (1989) 170.

74. J. Wang and L. D. Hutchins, Anal. Chem., 57 (1985) 1536.

75. L. D. Hutchins-Kumar, J. Wang and P. Tuzhi, Anal. Chem., 58 (1986) 1019.

76. J. Wang, P. Tuzhi and T. Golden, Anal. Chim. Acta, 194 (1987) 129.

77. H. Shirakawa, E. J. Louis, A. G. MacDiarmid, C. K. Chiang and A. F. Heeger, J. C. S. Chem. Commun., (1977) 578.

78. B. Keita, L. Nadjo and J. P. Haeussler, J. Electroanal. Chem., 243 (1988) 481.

79. M. Delamar, P. C. Lacaze, J. Y. Dumousseau and J. E. Dubois, Electrochim. Acta, 27 (1982) 61.

80. A. G. MacDiarmid, L. S. Yang, W. S. Huang and B. D. Humphrey, Synth. Met., 18 (1987) 393.

81. L. M. Wier, A. R. Guadalupe and H. D. Abruna, Anal. Chem., 57 (1985) 2009.

82. H. C. Hurrell and H. D. Abruna, Anal. Chem., 60 (1988) 254.

83. P. J. Riley and G. G. Wallace, Electroanalysis, 3 (1991) 191.

84. P. R. Teasdale, M. J. Spencer and G. G. Wallace, Electroanalysis, 1

(1989) 541.

85. J. A. Dean and H. A. Bryan, Anal. Chim. Acta, 16 (1957) 87.

86. M. Perkins and G. F. Reynolds, Anal. Chim. Acta, 18 (1958) 616.

87. M. Perkins and G. F. Reynolds, Anal. Chim. Acta, 19 (1958) 54.

88. J. Wang, P. A. M. Farias and J. S. Mahmoud, Anal. Chim. Acta, 172 (1985) 57.

89. V. Stara and M. Kopanica, Collect. Czech. Chem. Commun., 54 (1989) 370.

90. E. Wang and A. Lin, Microchem. J., 43 (1991) 191.

91. M. Pesarento, A. Profumo, C. Riolo and T. Soldi, Analyst, 114 (1989) 623.

92. J. Buffle and A. E. Martell, Inorg. Chem., 16 (1977) 2221.

93. L. O. Ohman, S. Sjoberg and N. Ingri, Acta Chem. Scand., 37 (1983) 561.

94. D. D. Perrin (Ed.). Stability constants of metal ion complexes. Part B. Organic ligands. IUPAC Chemical Data Series, No. 22. Pergamon press Ltd. 1979.

95. A. Factor and G. E. Heinsohn, Polymer Letters, 9 (1971) 289.

96. J. P. Stradins and V. T. Glezer, Encyclopedia of electrochemistry of the elements, Organic Section, In A. J. Bard (Ed.), Marcel Dekker, Inc. New York and Basel.

97. T. M. Florence, F. J. Miller and H. E. Zittel, Anal. Chem., 38 (1966) 1065.

98. P. J. Kudirka and R. S. Nicholson, Anal. Chem., 44 (1972) 1786.

99. J. K. Senne and L. W. Marple, Anal. Chem., 42 (1970) 1147.

100. H. D. Abruna and A. J. Bard, J. Am. Chem. Soc., 103 (1981) 6898.

101. S. E. Creager and M. A. Fox, J. Electroanal. Chem., 258 (1989) 431.

102. J. A. Kennedy and H. K. J. Powell, Aust. J. Chem., 38 (1985) 659.

103. M. Meaney, J. G. Vos, M. R. Smyth and G. G. Wallace, Anal. Proc.

(London), 26 (1989) 15.

104. R. W. Murray, A. G. Ewing and R. A. Durst, Anal. Chem., 59 (1987) 379A.

105. L. L. Miller, B. Zinger and Q. Zhou, J. Am, Chem. Soc., 109 (1987) 2267.

106. T. Shimidzu, A. Ohtani, T. Iyoda and K. Honda, J. Electroanal. Chem., 224 (1987) 123.

107. A. F. Diaz and J. I. Castillo, J. C. S. Chem. Comm., (1980) 397.

108. M. Kapel and D. W. Selby, Talanta, 16 (1969) 915.

109. P. W. Alexander and A. Hidayat, paper presented at the 9th Australian Symposium on Analytical Chemistry, Sydney, 1987.

110. B. F. Reis, H. Bergamin, E. A. G. Zagatto and F. J. Krug, Anal. Chim. Acta, 107 (1979) 309.

111. J. E. Gregor, H. K. J. Powell and R. M. Town, J. Soil Sci., 40 (1989) 661.

112. H. K. J. Powell and A. W. Rate, Aust. J. Chem., 40 (1987) 2015.

113. L. Lovgren, PhD Thesis, University of Umea, 1990.

114. A. P. Brown, C. Koval and F. C. Anson, J. Electroanal. Chem., 72 (1976) 379.

115. A. Vlcek, J. Klima and A. A. Vlcek, Inorg. Chim. Acta, 69 (1983) 191.

116. A. P. Brown and F. C. Anson, Anal. Chem., 49 (1977) 1589.

117. R. P. Baldwin, J. K. Christensen and L. Kryger, Anal. Chem., 58 (1986) 1790.

118. S. V. Prabhu, R. P. Baldwin and L. Kryger, Anal. Chem., 59 (1987) 1074.

119. Z. Gao, G. Wang, P. Li and Z. Zhao, Anal. Chem., 63 (1991) 953.

120. L. Hernandez, J. M. Melguizo, M. H. Blanco and P. Hernandez, Analyst, 114 (1989) 397.

121. K. Kalcher, Fresenins Z. Anal. Chem., 321 (1985) 666.

122. K. Kalcher, Anal. Chim. Acta, 177 (1985) 175.

123. K. Sykut, I. Cukrowski and E. Cukrowska, J. Electroanal. Chem., 115 (1980) 137.

124. J. Wang, Anal. Chem., 53 (1981) 2280.

125. J. Wang, T. Golden, K. Varughese and I. El-Rayes, Anal. Chem., 61 (1989) 508.

126. J. Wang, B. Greene and C. Morgan, Anal. Chim. Acta, 158 (1984) 15.

127. T. M. Florence, F. J. Miller and H. E. Zittel, Anal. Chem., 35 (1963) 1866.

128. H. Specker, H. Monien and B. Lendermann, Chem. Anal. (Warsaw), 17 (1972) 1003.

129. L. Chau and M. D. Porter, Anal. Chem., 62 (1990) 1964.

130. D. C Manning, W. Slavin and G. R. Carnrick, Spectrochim. Acta Part B, 37 (1982) 331.

131. K. L. Cheng, K. Ueno and T. Imamura, Handbook of Organic Analytical; Reagents, CRC, Boca Raton, FL, (1982).

132. O. Røyset, Anal. Chim. Acta, 178 (1985) 223.

133. C. Wyganowski, Microchem. J., 26 (1981) 45.

134. O. Røyset, Anal. Chem., 59 (1987) 899.

135. M. Trojanowicz and J. Szpunar-Lobinska, Anal. Chim. Acta, 230 (1990) 125.

136. D. Zölizer and G. Schwedt, Fresenius' Z. Anal. Chem., 317 (1984) 422.

137. J. Ruzicka and E. H. Hansen, Flow injection analysis, John Wiley & Sons, New York, (1988).

138. B. Karlberg and G. E. Pacey, Flow injection analysis, Elsevier, Amsterdam, (1989).

139. S. Hughes, P. L. Meschi and D. C. Johnson, Anal. Chim. Acta, 132 (1981) 1.

140. D. S. Austin-Harrison and D. C. Johnson, Electroanalysis, 1 (1989) 189.

141. D. C. Johnson and W. R. LaCourse, Anal. Chem., 62 (1990) 589A.

142. R. J. Motekaitis and A. E. Martell, Inorg. Chem., 23 (1984) 18.

143. H. K. J. Powell, unpublished results.

144. O. Royset, Anal. Chim. Acta, 185 (1986) 75.

145. R. L. Benson, P. J. Worsfold and F. W. Sweeting, Anal. Chim. Acta, 238 (1990) 177.

146. H. K. J. Powell and K. L. Shearman, unpublished results.

147. C. Wyganowski, S. Motomizu and K. Toei, Anal. Chim. Acta, 140 (1982) 313.

148. J. I. G. Alonso, A. L. Garcia, A. Sanz-Medel and E. B. Gonzales, Anal. Chim. Acta, 225 (1989) 339.

149. H. S. Li, J. Roncali and F. Garnier, J. Electroanal. Chem., 263 (1989) 155.

150. Z. Xue, A. E. Karagozler and O. Y Ataman, Electroanalysis, 2 (1990) 1.

151. J. Wang and R. Li, Anal. Chem., 61 (1989) 2809.

152. A. Albert: Selective toxicity, ed. 7, Chapman and Hall, Publishers, Inc., New York, 1985.

153. A. T. Haj-Hussein and G. D. Christian, Microchem. J., 34 (1986) 67.

154. R. J. Henry, D. C. Cannon and J. W. Winkelman: Clinical chemistry principles and techniques, Harper and Row, Publishers, Inc., New York, 1974.

155. G. E. Coates, J. Chem. Soc., (1945) 478.

156. B. Jakuszewski and S. Taniewska-Osinska, Zesz. Nauk. Uniw. Lodz, 2 (1961) 195.

157. E. A. G. Zagatto, F. J. Krug, H. Bergamin, S. S. Jorgensen and B. F. Reis, Anal. Chim. Acta, 104 (1979) 279.

158. A. Jensen and E. Riber, In H. Sigel (Ed.), Metal ions in biological systems, Marcel Dekker, New York, (1984).

159. F. Cañete, A. Rios, M. D. Luque de Castro and M. Valcárel, Analyst, 112 (1987) 267.

160. E. M. Gindler and D. A. Heth, Clin. Chem., 17 (1971) 663.

161. J. Alonso, J. Bartroli, J. L. F. C. Lima and A. A. S. C. Machado, Anal. Chim. Acta, 179 (1986) 503.

162. H. Kagenow and A. Jensen, Anal. Chim. Acta, 145 (1983) 125.

163. Y. Yuan, Anal. Chim. Acta, 212 (1988) 291.

164. H. Wada, K. Asakura, G. V. Rattaiah and G. Nakagawa, Anal. Chim. Acta, 214 (1988) 439.

165. T. A. Kryukova, S. I. Sinyakova and T. B. Arefeva, Polarographic Analysis (in Russian), National Chemical Publishers, Moscow, (1959), p. 685.

166. M. L. Richardson, Talanta, 12 (1965) 1009.

167. J. An, J. Zhou and X. Wen, Talanta, 32 (1985) 479.

168. D. Luo and Z. Zhao, J. Wuhan Univ. (Natural Sci, Ed.), (1982) 100.

169. M. R. Wills, F. W. Sunderman and J. Savory, Magnesium, 5 (1986) 317.

170. R. Goldik, C. Yarnitzky and M. Ariel, Anal. Chim. Acta, 234 (1990) 161.

171. H. Wada and G. Nakagawa, Anal. Chim. Acta, 159 (1984) 289.

172. L. G. Sillen, Stability constants of metal-ion complexes, Supplement No. 1. The Chemical Society, London, Spec. Publ. No. 25, (1971).

173. J. B. Hart, unpublished results.

174. G. Schwarzenbach and W. Biederman, Helv. Chim. Acta, 31 (1948) 678.

175. E. Hogfeldt, Stability constants of metal-ion complexes. Part A: Inorganic ligands. IUPAC Chemical Data Series, No. 21.

Pergamon, Oxiford. (1982).

176. M. Pesavento and A Profumo, Talanta, 38 (1991) 1099.

177. J. F. ven Staden, Talanta, 38 (1991) 1033.

178. R. Y. Xie and G. D. Christian, Anal. Chem., 58 (1986) 1806.

179. B. Bernhardsson, E. Martins and G. Johansson, Anal. Chim. Acta, 167 (1985) 111.

180. Q. Chang and M. E. Meyerhoff, Anal. Chim. Acta, 186 (1986) 81.

181. P. E. Macheras and M. A. Koupparis, Anal. Chim. Acta, 185 (1986) 65.